AN ABSTRACT OF THE THESIS OF

Ellen Domaratius Mullen for the degree of Doctor of Philosophy

in Geology presented on March 16, 1983

Title: PETROLOGY AND REGIONAL SETTING OF PERIDOTITE AND GABBRO OF THE CANYON MOUNTAIN COMPLEX, NORTHEAST OREGON

Abstract approved: Redacted for Privacy

William H. Taubeneck

The Canyon Mountain complex (CMC) of northeast Oregon is a fore-arc-related ophiolite. Gabbro intrudes through and is not genetically related to the harzburgite. Transition zone cumulates are derived from fractionating gabbro and the minor injection of Cr and Ni enriched, LREE depleted magma. The gabbro is a differentiated sequence with an olivine, two pyroxene parent represented by pods and dikes within the harzburgite. Succeeding fractionates are two-pyroxene gabbro which crystallized at a higher P_{H_2O}, two pyroxene gabbro with minor olivine, norite, and quartz norite. Orthopyroxene is more abundant in the CMC gabbro than in other ophiolitic gabbros, suggesting an origin by partial melting of a hydrous source. Transition zone rocks and primitive gabbro are tholeiitic. More evolved CMC gabbro is calc-alkaline. The CMC is strongly LREE depleted, with REE abundances similar to other ophiolites.

Plagiogranite and diabase intrude the CMC and pinch out downward in the section. The host gabbro was solid but above temperatures of about 600°C and is partly recrystallized adjacent to plagiogranite

sills. The source of the plagiogranite may have been partial fusion of altered oceanic gabbro into which the CMC gabbro magma was intruded.

The CMC is associated with a Permian to Triassic forearc terrane of greenstones, plutonic ophiolitic fragments, metasediments, and serpentinite melange. Relict clinopyroxene compositions indicate that some greenstones associated with Elkhorn Ridge Argillite cherts are alkalic and represent seamount or transform basalts. These rocks are LREE enriched. Most other basaltic greenstones are calc-alkaline to arc tholeiite and have REE patterns with slight negative Eu anomalies. Their major element data are calc-alkaline and within island arc fields. Gabbros from a disrupted ophiolite in this terrane are tholeiitic with trace element abundances and mineral compositions distinct from the CMC.

The Canyon Mountain complex represents early forearc magmatism generated by hydration and partial melting of depleted upper mantle adjacent to the leading edge of the subducted slab. Forearc ophiolites may be recognized by diapiric harzburgite structure, abundant orthopyroxene, high K_2O, low TiO_2, plagiogranite and diabase sills, rarity of mafic volcanics, and the nature of the surrounding terrane.

Petrology and Regional Setting of Peridotite and Gabbro of the Canyon Mountain Complex, Northeast Oregon

by

Ellen Domaratius Mullen

A THESIS

submitted to

Oregon State University

in partial fulfillment of
the requirements for the
degree of

Doctor of Philosophy

Completed March 16, 1983

Commencement June, 1983

APPROVED:

Redacted for Privacy

Professor of Geology
in charge of major

Redacted for Privacy

Head of Department of Geology

Redacted for Privacy

Dean of Graduate School

Date thesis is presented March 16, 1983

Typed by Marge Bright for Ellen Domaratius Mullen

ACKNOWLEDGMENTS

Investigation of the Canyon Mountain complex and the surrounding terrane has been pursued by the writer with varying degrees of intensity throughout the past seven years. This work has been sustained with the help and countenance of several organizations and many individuals.

Foremost of these is Richard S. Mullen, who never failed to provide moral and financial support, and who has been a constant source of encouragement. Without his concern and sacrifices, this research could not have been accomplished. The writer is deeply grateful for his unflagging help, patience, and understanding.

The long-term interest and support of the writer's parents, William and Laura Ellen Domaratius, is also acknowledged.

Many individuals in eastern Oregon, including Dennis Dall and Clinton P. Haight, Jr., cheerfully allowed the writer access to their property. Special thanks are extended to the Hon. and Mrs. Robert Campbell and Judge Francis Cole for their generosity and companionship.

The interest and suggestions of Dr. Thomas P. Thayer provided much inspiration. The writer's appreciation of the Canyon Mountain complex and its problems has been greatly enhanced through correspondence, discussions, and five days in the field with Dr. Thayer.

Dr. Francoise Boudier and Dr. Maxime Misseri worked with the writer for portions of two field seasons. Joint observations and many discussions on the outcrop were invaluable aids in recognition of significant structural and petrologic features.

Many other scientists contributed toward this research through discussions or help with analyses. Professor Hans Ávé Lallemant and Professor William P. Leeman participated in several interesting conversations, as well as two days in the field in early 1980. Discussions in the field with Howard Brooks and Mark Ferns have also been enlightening. Professor M. Allan Kays of the University of Oregon, and Dr. T. L. Vallier of the U. S. Geological Survey have been sources of helpful suggestions and encouragement.

Professor Peter Hooper of Washington State University provided major element analyses of 20 greenstones collected by the writer, and also performed all major element analyses of Canyon Mountain complex samples. The microprobe at the University of Oregon was made available by Professor Daniel Weill. Analytical work was supervised and standardized by Michael Schaffer, who acted as co-analyst, and who deserves credit for the high quality of the analyses. Trace element analyses on whole rock samples by INAA were conducted at the Oregon State University Radiation Center. Professor Roman Schmitt, Dr. Monty Smith, Dr. Scott Hughes, and Mike Conrady all contributed to learning proper analytical techniques, and made sample preparation and counting equipment available at critical times.

In any scientific endeavor, persistance, independence of thought, and attention to detail in observation, consideration, and writing are of paramount importance. Professor W. H. Taubeneck

has sought to impart these principles to his students through example and suggestion. His careful editing and concern for precise expression substantially improved this dissertation.

Field and analytical work on the Canyon Mountain complex were partly supported by a grant from the Oregon Department of Geology and Mineral Industries and by the Penrose Fund of the Geological Society of America (Grant 2887-81). All microprobe analyses of relict minerals in greenstones and plutonic rocks of the forearc terrane were generously supported by W. J. Bowes Mining.

TABLE OF CONTENTS

LIST OF FIGURES

LIST OF TABLES

LIST OF PLATES
(In pocket)

Plate

1. Petrologic units of the Canyon Mountain complex.

2. Geologic map of the Canyon Mountain complex.

3. Geologic map of Celebration Ridge.

4. Geologic map of Norton basin.

5. Geologic map of Canyon Mountain.

6. Greenstones and related rocks of the northern Blue Mountains, northeast Oregon.

PETROLOGY AND REGIONAL SETTING OF PERIDOTITE AND GABBRO OF THE CANYON MOUNTAIN COMPLEX, NORTHEAST OREGON

INTRODUCTION

The Ophiolite Concept and the Canyon Mountain Complex

The term "ophiolite" is derived from the Greek "ophi", or "serpent", for the common abundance of serpentinite in these distinctive rock assemblages. A complete ophiolite is an orderly rock sequence consisting of peridotite overlain by gabbro which is intruded and re-intruded by basaltic dikes which feed overlying pillow lavas and are capped by pelagic sediments. The concept of an ophiolite as a meaningful, coherent entity was introduced by Steinman (1927) and was defined for present usage by the 1972 Penrose conference on ophiolites. (See Appendix 1.) Ophiolites have been studied intensively because they serve as readily available examples of spreading ridge systems and oceanic crust. Although field, petrologic, structural, and geochemical investigations have resulted in better understanding both of ophiolites and of oceanic and upper mantle systems, we are only beginning to distinguish ophiolites of different petrologic and tectonic settings. Efforts to thoroughly understand these rocks are hampered by limited exposure, missing units, severe deformation, and, more significantly, by the tools available to forge our concepts and construct our working models.

This study focuses on relations between gabbro and peridotite in the Canyon Mountain complex (CMC), a Permian ophiolite of somewhat

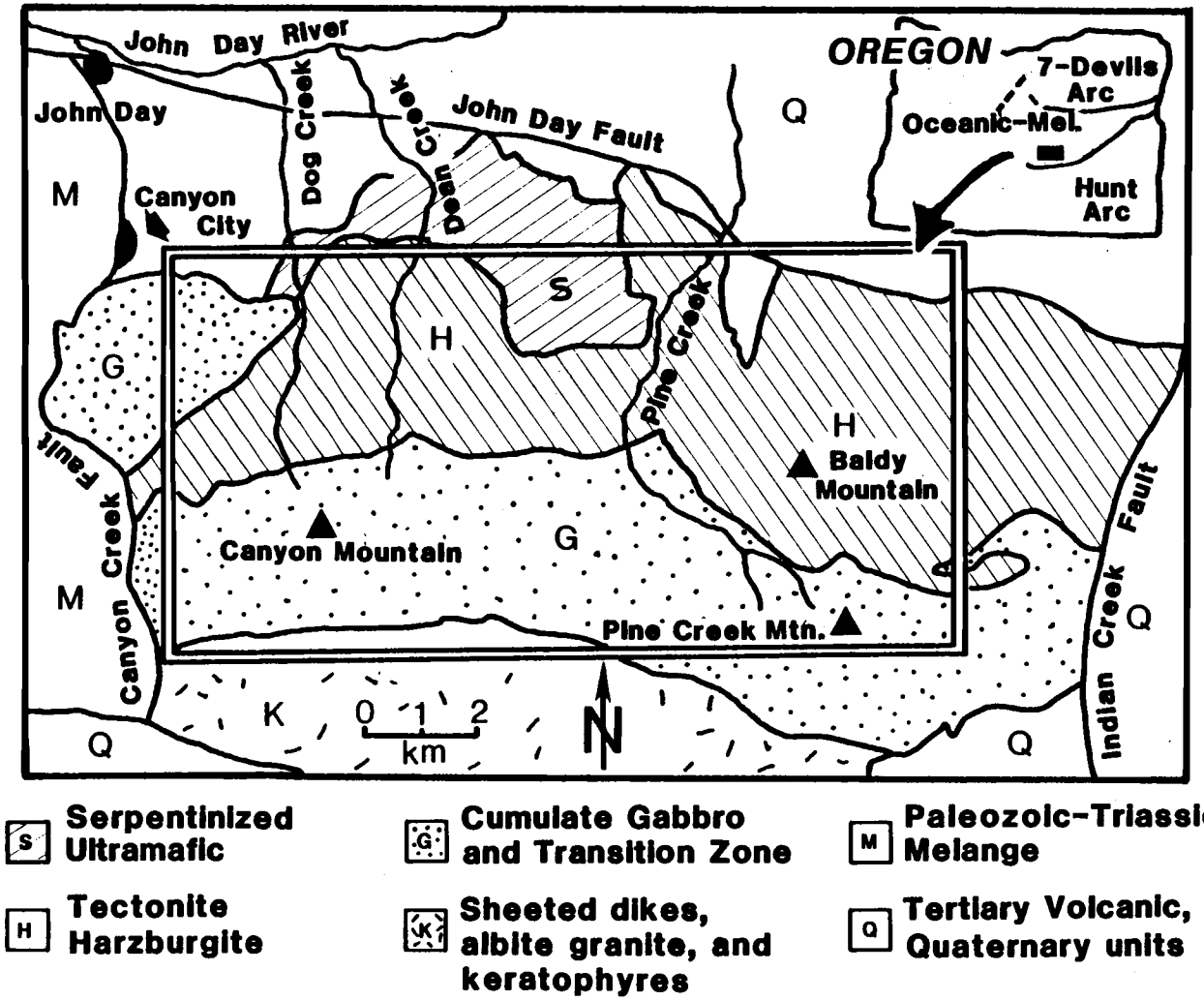

FIGURE 1. General reference map of the Canyon Mountain complex.

anomalous character in northeast Oregon which was visited by the 1972 Penrose Conference participants. (Figure 1). It is spatially and temporally associated with a melange-like terrane which includes cherts, alkalic greenstones, early arc greenstones, and ophiolitic fragments, and has been interpreted as melange (Dickinson, 1979), ocean basin (Brooks and Vallier, 1978), and a forearc region related to the Seven-Devils arc (Mullen, 1982). The silicic character of the upper Canyon Mountin complex has led recent workers (Ave Lallemant, 1976; Himmelberg and Loney, 1980; Gerlach, 1980; Gerlach, et al., 1981) to interpret the CMC as an island-arc related ophiolite. Thus a study of the petrogenesis of these rocks may further our understanding not only of the specific petrology and tectonics of the Canyon Mountain complex, but potentially has broader implications for the understanding of the generation of island arcs and the crust upon which they are built.

This dissertation utilizes field, petrographic and geochemical data to determine genetic relations between gabbro and peridotite, and to determine whether the gabbro and cumulate ultramafic rocks are products of a single or of multiple magmas. Observations pertinent to the origin of diabases and late silicic magmas of the Canyon Mountain complex are included. Finally, the study considers the regional petrologic and tectonic setting of this ophiolite, and combined with conclusions based upon petrologic work, discusses the probable origin and significance of the Canyon Mountain complex, and its possible implications for ophiolites of similar character, as well as the evolution of arc-derived crust.

General Characteristics of Ophiolites

The nearly complete, coherent ophiolites which have been recently investigated via field, petrographic, structural, and geochemical studies include the Samail ophiolite of Oman; Troodos complex, Cyprus; Vourinos complex, Greece; Zambales range, Luzon; Bay of Islands, Newfoundland; Point Sal, California; Josephine Peridotite southwest Oregon and Canyon Mountain complex, northeast Oregon. These are all Phanerozoic tabular masses which vary from five to 475 kilometers in length, and from two to 80 kilometers in width. They contain a basal harzburgite (depleted peridotite) with 70-75 percent modal orthopyroxene (En_{87-95}), 20-25 percent modal olivine (Fo_{88-92}), less than five percent modal diopside (usually Cr-enriched), and Cr-spinel (chromite) of about two percent. These peridotites comprise 20-50 percent of most ophiolites, and are strongly foliated, with a tectonite fabric which seems to indicate deformation by plastic flow in the upper mantle. Bands of orthopyroxene and aligned spinels also define foliation and lineation in outcrop. Thickness of basal harzburgites is generally between two and five kilometers. Overall, the harzburgite sections of ophiolites are too thick to have accumulated *via* differentiation of a basaltic or picritic melt parental to the entire sequence. This, plus their extremely depleted geochemistry and mineralogy, suggest the harzburgite is refractory mantle residue which has undergone two or more episodes of partial melting and is genetically unrelated to the overlying gabbro. Mineralogy and chemical composition of tectonite harzburgite are

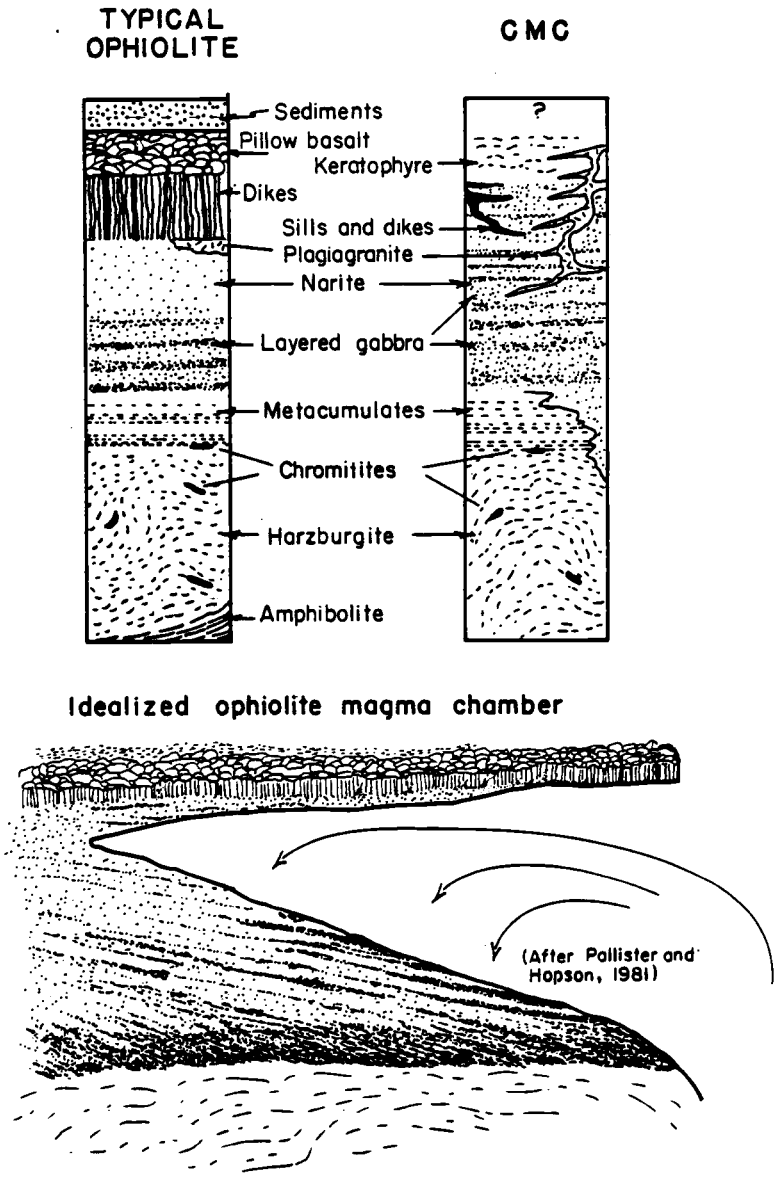

FIGURE 2. General stratigraphy of ophiolites and the Canyon Mountain complex.

generally homogeneous throughout the section, although dunite and lherzolite lenses occur in most harzburgites of ophiolites. The small bodies of dunite may be concordant with structure and be of probable igneous origin or they may be discordant, and may have formed late in the history of the ophiolite via metasomatic reactions (Dungan and Avé Lallemant, 1977) or reaction between gabbro and harzburgite wall rock (Quick, 1982). Structurally concordant and discordant websterite veins and dikes, commonly 10-30 cm wide, mostly represent remobilized fluid from the harzburgite, rather than "exotic" melt.

Podiform chromite bodies with cumulate textures are associated with dunites throughout the harzburgite section. The chromitites are most common at two stratigraphic locations: In the center of the harzburgite and near the top of the tectonite harzburgite section just below the contact with cumulate peridotites and gabbro. Among the podiform chromitites, Cr_2O_3 content, Cr/Cr+Al and Fe/Fe+Mg of chromite vary with stratigraphic position and associated mineralogy, and have a much greater range than in chromitites from stratiform intrusions such as the Bushveld or Stillwater complexes. High Cr_2O_3, Cr/Cr+Al, and low Fe/Fe+Mg are characteristic of deposits within the harzburgite. Low Cr_2O_3 and Cr/Cr+Al more commonly occur in chromitites high in the tectonite ultramafic section near the contact with the gabbro.

Between the tectonite harzburgite and overlying cumulate gabbros, a sequence of cumulate peridotites and mafic gabbros varying

from less than one to greater than three kilometers thick usually occur. They are referred to as the transition zone, or "meta-cumulates", as they display both tectonite fabric and cumulate textures. They include variable amounts of pyroxenite, wehrlite, websterite, lherzolite, with minor troctolite and other feldspathic peridotites which occur as persistant layers (Oman), or as discontinuous lenses (Bay of Islands). Diapiric remobilization (Point Sal) may disrupt the sequence. Gabbros interlayered with the transition zone peridotites are commonly olivine rich; anorthosites also occur. Layers in the transition zone vary from centimeter to meter-wide, both graded bedding and phase layering have been noted in well preserved sections of Oman and Point Sal (Coleman, 1977). Transitions between ultramafic lithologies may be gradual, but boundaries between gabbro and peridotite are usually abrupt. Feldspars are very calcic, An_{90-97}. Clinopyroxene is diopside. The amount of orthopyroxene varies, indicating differences both in magma composition and pressure of crystallization. However, orthopyroxene is seldom abundant, and is absent in the transition zone of the Samail ophiolite.

Textures and compositions of rocks in transition zone cumulates have been interpreted as indicators of conditions within the magma chamber. For example, in the Samail and Bay of Islands ophiolites, uniformly small grain size, adcumulate textures, and the occurrence of slump blocks suggest rapid cooling and accumulation of ultramafic crystal mush, in a possibly turbulent or seismically active wedge-shaped magma chamber (Figure 2).

Cumulate gabbros of ophiolites are commonly layered, and progress from basal olivine-clinopyroxene through orthopyroxene-clinopyroxene to upper-level norite. Layering is common in lower gabbro where it may be traced as continuous sequences for hundreds of meters, although individual layers may persist for no more than 50 meters. Layering is usually rare to absent in the more isotropic (unlayered) hypersthene-bearing upper level gabbro.

Cryptic variation, where it has been investigated (Samail, Point Sal), is evident through the entire cumulate sequence. The influx of new batches of magma similar in composition to earlier magma is indicated by periodic compositional shifts in the cumulate sequence.

A sheeted dike complex which may represent ascendant magmas at the spreading ridge axis commonly intrudes and overlies the gabbro. These dikes are generally several meters wide. Their origin and the timing of their intrusion is not well understood. Generally they are chilled against the gabbro and one another, and crosscut gabbro structure. They are not deformed, but they may be more altered than the gabbro they intrude. Although they demonstratably feed volcanics in Point Sal, Troodos, and Samail, they pinch out downward in the gabbro, and seemingly are not derived from it.

The "normal" ophiolitic sequence as defined by the 1972 Penrose Conference, may include silicic magmas (plagiogranite) such as albite granite, tonalite, trondjhemite, or diorite which are usually intruded into upper gabbros late in the magmatic history of the

ophiolite. These rocks are little deformed, and crosscut gabbro structures, but they are usually not as altered as the mafic dikes.

The geochemistry of ophiolites is relatively uniform, although the data may lead to conflicting conclusions based upon major and trace elements. The content of CaO and Al_2O_3 in whole rocks and minerals is high; TiO_2 is not abundant in the ophiolitic system. No strong iron enrichment trend is evident. In fact, despite the seemingly oceanic affinity, no ophiolite plots on a Skaergaard or Thingmuli tholeiitic trend. Gabbros are strongly depleted in large ion lithophile (LIL) and incompatible elements, and have low overall abundances (0.1 to 2.0 x chondritic) of rare earth elements (REE), with marked depletion of light rare earth elements (LREE). Lower gabbros have positive Eu anomalies, confirming their cumulate origin. Most peridotites have such low abundances of fertile geochemical components (REE, LIL) that gabbros could not be derived from them by partial melting. Similarly, trace element data of the diabases of ophiolites indicate that these rocks and the plagiogranites are not derived directly by fractionation of the gabbroic magma.

Previous Investigations of the Canyon Mountain Complex

The geology of the Canyon Mountain complex (CMC) was first systematically studied by Thayer (1940). His early descriptive and analytical work provided the first clear concept of a predictable relation between chromite composition and stratigraphy in rocks which would later become known as alpine ultramafics. Thayer (1964) later defined the cumulate podiform nature of the chrome bodies, and showed

that the assemblage of rocks (rock succession) of the Canyon Mountain complex was distinctive (1963a). Additional mapping and petrologic studies which focused on the CMC (Thayer 1963b, 1976, 1977; Thayer and Himmelberg, 1968) resulted in correlation between the ophiolitic sequence and rocks of mid-ocean ridges, and the recognition that ophiolites probably are comprised of magmas from more than one source (Thayer, 1977).

Recent investigations of the petrology of the Canyon Mountain complex by Himmelberg and Loney (1980) utilized mineral compositions to determine gabbro-peridotite relations, and concluded that the complex represents a cumulate sequence of gabbros and more leucocratic rocks derived by partial melting of the underlying harzburgite.

Gerlach (1980) studied the origin of leucocratic components of the complex and concluded (Gerlach et al., 1981; Gerlach et al., 1981b) based upon rare earth and trace element data that plagiogranites were derived by partial melting of hydrothermally altered upper-level gabbros. Upper gabbro of the complex has been dated via U/Pb as 278 my (Mattinson and Walker, 1980). $^{40}Ar/^{39}Ar$ dates for the more leucocratic rocks are similar, and slightly younger (268-263 my) (Sutter, in press).

Peridotites of the Canyon Mountain complex have an upper-mantle-derived tectonite fabric. Ave Lallemant (1976) and Misseri and Boudier (pers. comm., 1982) recognize two distinct vertically oriented diapiric structures in the east and west portions of the harzburgite which over-print mantle flow fabrics. Himmelberg and

Loney (1980) have noted a horizontally oriented tectonite fabric in the ultramafic rocks of the transition zone, and have consequently labeled them "metacumulates." They further noted that cumulate gabbro lacks tectonite fabric, and hence crystallized later and under different circumstances than the metacumulate or tectonite harzburgite which have similar fabrics.

Unresolved Problems of the Canyon Mountain Complex

The sequence of rocks at Canyon Mountain, then, is similar to most ophiolites: basal harzburgite overlain by cumulate peridotite and gabbro, and intruded by diabases and plagiogranite. The upper sequence, however, is anomalously silicic with respect to "oceanic" ophiolites, and many problems of the CMC remain to be resolved.

The origin of the tectonite peridotite in the Canyon Mountain complex, and its relation to spatially associated gabbros and more calcium and aluminum-rich cumulates presently is open to debate. As noted previously, the prevalent interpretation of the harzburgite unit of ophiolites is that it represents thoroughly depleted residue from two or more episodes of partial melting (Hopson and Frano, 1977; Dick, 1980; Boudier and Coleman, 1981; Hawkins and Evans, in press). This interpretation is supported by its geochemically depleted character, its refractory mineralogy, and the tectonite fabric noted in these rocks (Den Tex, 1969; Nicholas et al., 1980).

However, other characteristics of the harzburgite noted at Canyon Mountain and elsewhere suggest that the true origin of this

peridotite may not be so straightforward. Although there is a very strong tectonite fabric, textures are seldom so obscured that an overall cumulate fabric is not subtly present in the rocks. In the field, the harzburgite contains feldspars with cuspate textures which may be interpreted in thin section as a late intercumulus phase. The rock on the east side of Baldy Mountain, in the Canyon Mountain complex, seems to grade upward toward dunites and more feldspathic, gabbroic rocks. Furthermore, the peridotites and melagabbro of the transition zone commonly have strongly tectonized fabrics which parallel trends in the harzburgite. Nowhere has a strong structural discordance been noted between transition zone ultramafic and gabbroic rocks and the harzburgite. The basal harzburgite at Tiebaghi, Massif de Sud, New Caledonia has been interpreted by Moutte (1982) to represent a cumulate subjected to later tectonite flow. Thayer (pers. comm., 1982) has suggested a similar origin for the CMC harzburgite.

Further evidence for the cumulate nature of the basal harzburgite is found in the textures and occurrence of the podiform chromites. These rocks which are found throughout the harzburgite section and at the base of the transition zone are clearly cumulate (Thayer, 1964). Local precipitation, or formation as a boundined layer could account for their lateral restrictions and pod-like form. Several mechanisms have been proposed for their occurrence within a tectonite, strongly deformed and depleted harzburgite. Dickey (1975) suggested they were infolded after formation at higher

levels. Lago, et al. (1982) invoked precipitation in a chamber adjacent to a rising dunite or ultramafic magma. Most recently, Hawkins and Evans (in press) called upon plastic refolding of precipitates.

However, each of these alternative models has some objectionable features. Dickey's model is not compatible with observed structure. No lineation or foliation has been reported which is indicative of infolding. Lago, et al.'s model does not explain the variation in Cr/Cr+Al in spinels with stratigraphic height. Feeder pipes of ultramafic magma called for in Lago et al.'s model have never been observed or noted in the field. To further complicate the understanding of harzburgite origin and relation to associated gabbros, there is evidence (presented later in this work) for a link between the abundance of gabbro veins within the harzburgite, and variance in Cr/Cr+Al in chromitites. Hence, the harzburgite may have been in a mushy, hypersolidus state until fairly late in its history.

Harzburgite structure is generally consistant with the presence of a tectonite fabric. However, in the Canyon Mountain complex, structural interpretations of Avé Lallemant (1976) as well as Misseri and Boudier (pers. comm., 1982) indicate that two diapirs are present, rather than a horizontal mantle flow. An additional school of thought links the texture and foliated or banded structure of the harzburgite to igneous lamination (Moutte, 1982; Thayer, in prep.), rather than to tectonite fabric.

Relations between gabbro and peridotites of the Canyon Mountain complex - and of ophiolites in general - are not well understood.

Contacts are obscure and usually gradational through a deformed cumulate ultramafic and mafic sequence. The gabbro of Oman is considered intrusive into the peridotite by Boudier and Coleman (1981). However, textural, mineralogical, and geochemical evidence also has suggested in the Canyon Mountain complex (Himmelberg and Loney, 1980), in New Caledonia (Moutte, 1980; Nicholas et al., 1980) and in the Josephine peridotite (Dick, 1977) that gabbro originates from the underlying peridotite *via* partial melting.

In several respects, the gabbro of the Canyon Mountain complex is anomalous relative to most ophiolitic gabbros, which follow the general succession of olivine + clinopyroxene - then clinopyroxene, and then clinopyroxene + orthopyroxene. Most Canyon Mountain gabbros contain orthopyroxene. Furthermore, the "standard" ophiolitic sequence progresses from layered basal gabbro to isotropic gabbros within about 200 meters. High level gabbros and norites are unlayered. At the Canyon Mountain complex, even the norites contain sporadic but well-defined layering. Hence, compositions or conditions of crystallization allowed the development of pronounced layers through a considerable portion of the magma chamber.

Geochemical evidence is equivocal regarding the tectonic environment of ophiolite origin. Major element AFM plots for ophiolites follow both tholeiitic and calc-alkaline trends. The gabbros and diabases of Samail and Point Sal ophiolites are generally tholeiitic in overall composition and trend. The Canyon Mountain complex is generally calc-alkaline. Other geochemical parameters such as rare

earth elements, or major, minor and trace element discriminant diagrams (Si:FeO*/MgO; $MnO/TiO_2/P_2O_5$; Ti/Cr) yield tholeiitic or ocean ridge affinities for most ophiolites. However, the rocks of the Canyon Mountain complex tend to plot in calc-alkaline fields, substantiating their probable island arc origin.

The principal problem of the Canyon Mountain complex is to reconcile its ophiolitic lithologic sequence with its overall island arc geochemistry. This requires an understanding both of field relations and the precise petrology of ultramafic and mafic rocks. It relates to the question of the origin of early island arc magmas, and the nature and evolution of crust upon which ensimatic arcs are constructed, and is the principal theme addressed in this dissertation.

FIELD RELATIONS AND PETROGRAPHY OF PERIDOTITE AND GABBRO OF THE CANYON MOUNTAIN COMPLEX

The occurrence of good exposure throughout much of the Canyon Mountain complex permits detailed mapping and an improved understanding of field and petrologic relations in this ophiolite. Plate 1 shows the petrologic units mapped at 1:48,000. A 1:12,000 scale map (Plate 2) was made of approximately 23 square miles (60 square kilometers), (Plate 2), which extend in a four-mile (six km) wide strip from Highway 395, eastward about six miles (10 km) to the Ray Mine on the east slope of Baldy Mountain, and on the north approximately from the John Day Fault south beyond the crest of the Strawberry Range approximately to Sheep Rock. Units defined in the field and shown on this map are discussed below. Sample localities of analyzed Canyon Mountain complex specimens are shown on Plate 2.

In addition to the 1:12,000 scale map, three critical areas were mapped at a 1:6,000 scale: Celebration Ridge (Plate 3) for transition zone, the Norton Creek basin for upper gabbro and recrystallized norites (Plate 4), and Canyon Mountain (Plate 5) for gabbro and diabase dikes. These areas will be discussed with the pertinent units.

On the basis of this mapping, the following units are defined, and will be discussed in detail:

1. Harzburgite
2. Transition Zone (metacumulates)
3. Gabbro (olivine-orthopyroxene-clinopyroxne gabbro, two pyroxene gabbro, norite, and quartz norite).

In addition, two zones not recognized in other ophiolites were mapped - a zone of recrystallization within the gabbro, and a zone of infiltration, in which gabbro intrudes through the harzburgite. These zones will also be described and discussed. Throughout this work, horizontal distance will be given in metric units to conform with scientific convention, but elevations are retained in feet for consistancy and ease of reference to available U.S. Geological Survey topographic maps.

Harzburgite Tectonite

The northern third of the Canyon Mountain complex consists of tectonite harzburgite, similar in its overall composition and textures to other ophiolitic basal harzburgites. The rocks have well-developed foliation which is steeply dipping and trends generally east-west. Lineation is expressed primarily by spinels. The unit extends 19 kilometers east-to-west along the strike of its foliation, and 3.2 to 6.4 kilometers in cross-section. Some of the best outcrops of the harzburgite occur in the narrow canyon of upper Dean Creek (el. 5000 to 6600 feet or 1525 to 2000 m) and along Little Indian Creek to its head at a cirque on the north side of Baldy Mountain. The highly magnesian nature of the rock renders its soils unsuitable for vegetation, and the contact between harzburgite and the overlying metacumulate and cumulate may be generally mapped at the boundary between conifer forest and open ridges with juniper.

Mineral compositional data of Himmelberg and Loney (1980) confirm that the mineralogy of harzburgite is uniform. Olivine (Fo_{88-91})

and serpentinized olivine comprise approximately 60 percent of the unit (Table 1). Orthopyroxene (En_{88-90}) is about 25-29 modal percent. Clinopyroxene (usually Cr-diopside) is two to three percent, and Cr-spinel makes up about two percent of the rock.

The amount of serpentinization varies greatly throughout the complex. In the north, the rocks grade into sheared serpentinite and serpentine-matrix melange with no vestige of igneous mineralogy. Alteration similarly affects the ultramafic rocks on the west end of the complex.

Serpentinization and related alteration affects most CMC harzburgite. Clinopyroxene in the rock is not strongly affected. In the west, commonly 30-70 percent of the olivine is altered, and orthopyroxene may be completely bastized. In central portions of the complex north of Baldy Mountain, and along upper Little Indian Creek, the rocks are less than ten percent serpentinized. In all peridotites examined, serpentine is chrysotile-lizardite, indicating hydration at low to moderate temperatures.

In outcrop, orthopyroxene usually occurs as red-brown to greenish brown, resistant, five mm long crystals which impart a knobby texture to weathered surfaces and are usually elongate parallel to foliation. Clinopyroxene is bright chrome green and seldom exceeds three percent of the rock. It is less prominent on weathered surfaces than orthopyroxene. Spinels are black and usually equant.

Foliation is expressed as bands, strings, or tabular concentrations of orthopyroxene which impart a layered appearance to the harzburgite. These bands may be greater than 1 cm wide and usually

persist across an outcrop. Spinels (chromite) are also foliated, and provide the most reliable means for measuring lineation and foliation in the field. Chromite occurs in thin bands which persist for about 0.5 meters.

The intensity of foliation visible in the harzburgite varies, partly due to its less pronounced expression in more altered or serpentinized rocks, and partly due to differences in modal abundance of enstatite, as well as the amount of deformation. In northwest areas at the base of the harzburgite, foliation is generally less apparent in the field. Upwards in the western half of the section, foliation becomes more pronounced, and the rocks develop a banded appearance. This progression is noted best southward along ridges east and west of Dog Creek from the Ward Mine toward the vicinity of the Haggard and New Mine. In the east part of the CMC harzburgite, foliation is most strongly expressed near the Ray Mine, where bands of orthopyroxene from three to five cm wide clearly define foliation planes.

In thin section the mineralogy of the harzburgite is almost as uniform as harzburgite in outcrop. Olivine is deformed, commonly shows glide twins, and is elongate parallel to foliation. Where it is altered substantially to serpentine, mesh structures are usually intact. As noted by Boudier and Coleman (1981), this suggests that deformation occurred prior to serpentinization - or at least prior to the last serpentinization event. Olivine forms small inclusions in some orthopyroxenes, and hence is probably an earlier mineral than the pyroxene.

Table 1. Modal analyses of harzburgite, dunite and pyroxenite.

	Harzburgite 449A	Dunite 563	Pyroxenite 664
Olivine	39.1%	78.4%	7.1%
Orthopyroxene	28.7	1.5	2.6
Clinopyroxene	1.5	--	86.4
Plagioclase	--	--	--
Amphibole	1.2	--	1.1
Serpentine	21.3	14.2	1.1
Chromite	4.6	3.8	1.2
Magnetite	1.5	2.1	0.5
Chlorite	2.1	--	--
Hydrogrossular	--	--	--
	100.0	100.0	100.0

The orthopyroxene is enstatite, En_{88-90} (Himmelberg and Loney, 1980). Schiller structure and exsolution lamellae occur in fairly fresh crystals, and are subtly apparent in altered and bastitic orthopyroxenes. This pyroxene deforms more brittly than olivine. Enstatite is also elongate parallel to foliation, and commonly shows strain effects such as glide twins and wavy extinction. Although orthopyroxene may constitute up to 55 percent of the harzburgite, usually it comprises about 25 percent of the rock.

Clinopyroxene, although deformed, is usually less altered than either orthopyroxene or olivine. The bright green color suggests it is enriched in Cr_2O_3, and the large 2V indicates it is Ca-rich diopside. Crystals vary in size from 0.1 mm to greater than 1 mm, and are unzoned - as are the other minerals of the harzburgite. In many thin sections, clinopyroxene is subhedral to euhedral, and has a blastic appearance. However, it is cut by the same fractures which transect olivine and orthopyroxene, and hence is probably not post deformation or substantially later than either of its associates. Both glide twinning and wavy extinction affect the diopside. Clinopyroxene seldom exceeds three percent, except along parts of Little Indian Creek (elev. 5150'), where some peridotite (sample 284) is lherzolite, rather than harzburgite.

Spinel is subhedral to anhedral, and markedly elongate parallel to foliation. Individual grains seldom exceed two mm, but aggregates may exceed four mm in length. The color of spinel varies with Cr_2O_3 and Fe_2O_3 content, from deep red brown for Cr_2O_3-rich

to golden yellow brown for more iron rich compositions. Modal abundance of spinel in harzburgite varies from more than ten percent in Cr_2O_3-rich rock near the Ward Mine, to less than one percent on southeast slopes of Baldy Mountain.

Alteration of harzburgite is generally rather simple and indicative of low temperature. Olivine transforms to chrysotile and lizardite plus magnetite. Enstatite alters to serpentine minerals, "bastite", and some nontronite. Clinopyroxene is generally unaffected by mineralogical alteration. Spinel goes to magnetite. Alteration mineralogy of the harzburgite is generally uniform throughout and alteration products indicative of high temperatures (above 350°C) such as talc, anthophyllite, or antigorite, are not present. A conscientious search was made for humite minerals, but none were observed in 78 slides of harzburgite and dunite from widely dispersed localities within the harzburgite unit.

Pyroxenite Dikes

Dikes and sills of websterite, clinopyroxenite and orthopyroxerite occur throughout the harzburgite unit of the Canyon Mountain complex. Few exceed four cm in width, although dikes of websterite more than one meter wide occur along Little Indian Creek and on the north face of Baldy Mountain. There are several generations which cannot be distinguished on the basis of either mineralogy or orientation. Early veins - commonly rich in clinopyroxene - are folded along with parallel structure in harzburgite. Others intrude in a sinusoidal fashion. These are crosscut by straight veins.

The majority of pyroxenite dikes are straight, and usually follow joints or fracture systems. Dikes and pyroxenites which parallel foliation are commonly offset along shears or slip-planes which in turn provided pathways for emplacement of more websterite or pyroxenite. Rarely, displaced pyroxenites show drag folds. Usually the rocks appear to have behaved in a brittle manner.

Most dikes and sills are coarse grained. Pyroxenes may reach 1-2 cm in length, and commonly are in the range of 0.5 cm. No pyroxenite dike shows any contact effect. These dikes probably represent, as they do in other complexes, segregation of melt either generated within the harzburgite by stress and heating associated with deformation, or introduction of magma from an outside source (Boudier and Coleman, 1981; Nicholas and Jackson, 1982).

Podiform Chromitites:

Podiform chromitites are a significant feature of the harzburgite tectonite because they are widely dispersed through the unit, and because their compositions and seemingly cumulate textures are difficult to reconcile with the tectonite fabric and depleted nature of the harzburgite.

Chromitite bodies of the Canyon Mountain complex have been studied and described in detail by Thayer (1940, 1969, 1976, 1977). Partly on the basis of these studies, a distinction may be made between chromitites of stratiform intrusions which have low Cr/Cr + Al ratios, high Fe/Mg + Fe ratios, and occur as thin, laterally

extensive layers, and chromitites of alpine ultramafics which are generally higher in Cr/Cr + Al, lower in Fe/Fe + Mg, and occur as oblong pods surrounded by dunite (Jackson and Thayer, 1972).

Chromitites of the CMC are typical of the alpine ultramafic association. They are usually oblong to lensoidal in shape, and range from less than a meter to tens of meters in dimension. They are distributed throughout the harzburgite, and seem concentrated either near the middle of harzburgite or near the contact of harzburgite with gabbro and the transition zone. No chromitites occur in the transition zone. Cr_2O_3 content of spinel in the chromite deposits varies from 35 to 57 percent (Thayer, 1940). High Cr values are generally associated with chromitites near the middle or base of the harzburgite section. Although they are grossly similar in detail, chromitite deposits vary in texture, mineralogy, and composition. For purposes of discussion, the deposits will be considered on the basis of chromite composition and associated silicates, rather than stratigraphic or structural association.

Chromitites which contain only chromite and olivine, or chromite and serpentinized olivine are most abundant in the northern, basal portions of the Canyon Mountain complex harzburgite. They include the Ward, Iron King, and Dry Camp mines, and numerous small, unnamed prospect pits. Farther up in the section, the Haggard and New Mine also has an assemblage of olivine and chromite. Modal proportions of chromite and olivine vary; olivine commonly ranges from 30 to 60 percent in nodular ore, and may be entirely

absent in rare massive chromitite. Leopard ore - large, 1-1 1/2 cm ovoid clots of chromite in an olivine (or olivine and pyroxene) matrix - occurs in most olivine-chromite deposits. The texture is well displayed at the Haggard and New and Ward Mines. Samples from the Ward Mine contain olivine dispersed or enclosed within the chromite aggregate, whereas chromite nodules in leopard ore from the Haggard and New Mine contain only rare olivine.

Microprobe analyses (Table 3) of both enclosed and matrix olivine in sample 82 from the Ward Mine and Sample 410 from the Haggard and New Mine indicate no difference in composition between enclosed and matrix olivines. In these samples, and in Sample 169, Haggard and New, olivine is very magnesian (Fo_{92-96}), is unzoned, and is of uniform composition throughout the probe section as well as in multiple samples from the sample deposit. Its high NiO/Fo ratio suggests early crystallization. Olivine is nearly equigranular, with straight boundaries suggestive of adcumulus growth, possibly with later recrystallization.

Chromite is subhedral to euhedral where present as single grains. In leopard ore, grain boundaries are apparent in the ovoid clusters, unlike textures from Tiebaghi, New Caledonia or Troodos, Cyprus where rapid growth and subsolidus re-equilibration have obliterated traces of individual chromite crystals (Moutte, 1982; Greenbaum, 1977). Chromite is unzoned. Neither stepwise microprobe analyses of individual grains, nor EDS "maps" of Cr_2O_3, Al_2O_3 and FeO* (Figure 3) indicate any compositional variation in these spinels. The composition of chromite in chromite-olivine deposits

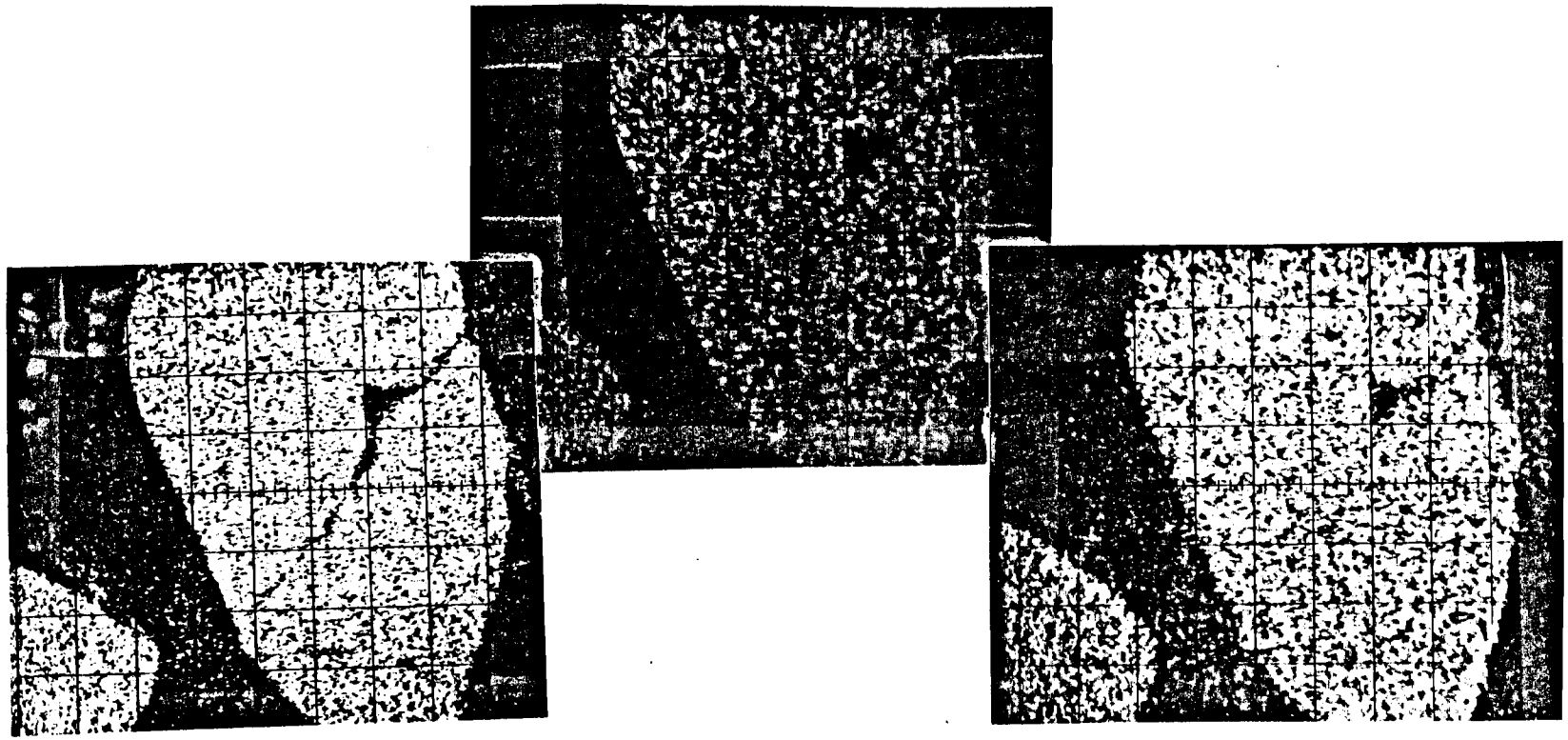

CMC 286 Al_2O_3 CMC 286 Cr_2O_3 CMC 286 Fe *

Figure 3. EDS images of chromite grains

(Table 2) is generally high in Cr_2O_3 (Cr_2O_3 > 50%), and Cr/Cr + Al (> 0.60), and low in Fe/Fe + Mg. However, one sample (667) from a small prospect pit on the east side of Gwynn Creek contained chromite with anomalously low Cr/Cr + Al, which plots in an intermediate position between olivine- and clinopyroxene-associated chromites. This suggests crystallization from a liquid of anomalous composition for stratigraphic height, emplacement from a higher stratigraphic location via deformation, or possible contamination or reequilibration of this chromite with Al-enriched fluids.

Silicate content of chromitites varies (Table 3). Some chromitites contain orthopyroxene + olivine + chromite. Orthopyroxene, where present, is very megnesian (En_{95-92}), usually somewhat altered, and interstitial to both olivine and chromite. It is a late phase in the crystallization of chromitite bodies. The rarity of orthopyroxene within the chromitites contrasts with its abundance in the harzburgite and gabbro of the Canyon Mountain complex. Olivine is slightly less magnesian in these rocks (Fo_{95-92}), and chromites are about equal in chrome content to those in olivine-bearing rocks. No mineral zoning was detected either optically or via microprobe WDS (wave dispersive) and/or EDS (energy dispersive) analyses. The orthopyroxene-bearing chromitites are generally stratigraphically higher in the harzburgite, and include Celebration Mine. They have leopard as well as massive and layered ores. Chromitites enclose olivine but do not enclose orthopyroxene.

TABLE 2. Compositions of chromites

	149 (opx+cpx+ol)					169		(opx+ol)		1	1	74 (ol)		
	1	2	3	4	5	1	2	3	4	rim	core	2	3	4
SiO_2	0.07	0.09	0.13	0.04	0.13	0.12	0.20	0.06	0.17	0.1	0.2	0.07	0.12	0.12
Al_2O_3	18.24	17.90	18.00	18.52	18.05	28.49	28.09	27.13	28.00	14.00	13.67	13.70	13.71	14.09
TiO_2	0.75	0.69	0.67	0.65	0.65	0.29	0.34	0.38	0.37	0.09	0.01	0.04	0.15	0.10
FeO *	17.27	17.67	16.99	17.52	17.71	16.65	16.58	17.19	17.17	14.57	14.28	14.29	13.78	14.47
MnO	0.21	0.21	0.27	0.20	0.21	0.16	0.20	0.18	0.18	0.26	0.24	0.22	0.18	0.24
MgO	14.09	14.16	14.06	14.10	13.94	15.71	15.58	15.44	15.54	15.70	15.95	16.31	15.99	15.95
Cr_2O_3	48.49	48.36	48.25	48.05	48.40	37.25	36.33	37.39	35.85	55.24	55.79	54.59	54.81	56.13
NiO	0.18	0.19	0.19	0.21	0.24	0.09	0.14	0.18	0.13	0.01	0.01	0.00	0.00	0.01
Total	99.32	99.29	98.56	99.28	98.37	98.78	97.47	97.93	97.40	99.97	100.21	99.38	99.74	100.78
Cr/ Cr+Al	72.7	73.0	72.8	72.7	72.8	56.7	56.4	58.0	56.1	79.8	80.3	79.9	80.3	79.9
Mg/ Mg+Fe	44.9	44.5	45.3	44.6	44.0	48.5	48.4	47.3	47.5	51.9	52.8	53.3	53.7	52.4

Table 2 (Continued)

	410 (ol)					82 (ol)							667 (ol)	
SiO_2	0.10	0.13	0.09	0.12	0.13	0.14	0.13	0.10	0.11	0.04	0.21	0.14	0.07	0.01
Al_2O_3	13.21	12.97	12.84	12.64	12.60	13.73	13.38	13.79	14.01	13.84	14.23	14.21	28.75	28.21
TiO_2	0.14	0.16	0.15	0.17	0.14	0.13	0.10	0.15	0.11	0.16	0.15	0.13	0.36	0.06
FeO*	14.27	14.72	14.97	14.31	14.75	14.73	14.82	14.67	14.66	14.71	15.02	14.51	14.46	12.81
MnO	0.23	0.23	0.21	0.22	0.18	0.23	0.24	0.19	0.27	0.32	0.23	0.22	0.20	0.20
MgO	15.01	14.87	14.98	14.73	15.86	14.60	15.02	14.60	15.17	15.22	13.63	14.99	17.01	15.76
Cr_2O_3	56.27	55.31	56.04	56.71	56.13	53.71	53.23	54.54	54.21	55.72	55.03	55.39	38.09	37.16
NiO	0.20	0.14	0.15	0.13	0.22	0.15	0.12	0.06	0.13	0.08	0.00	0.08	0.21	0.01
Total	99.94	98.23	99.10	99.03	99.21	97.41	99.40	98.10	98.68	100.15	98.50	99.70	99.19	97.75
Cr/ Cr+Al	81.0	81.0	81.4	81.8	81.7	79.6	80.5	79.8	79.5	80.1	79.5	79.6	57.0	56.8
Mg/ Mg+Fe	50.4	50.3	50.0	50.7	50.5	49.8	50.3	49.9	50.9	50.9	97.6	50.8	54.1	55.2

TABLE 3. Compositions of silicates in podiform chromitites.

	CMC 90							CMC 286	
	Clinopyroxene			Orthopyroxene		Olivine		Clinopyroxene	
SiO_2	51.89	53.00	53.28	57.11	56.24	40.34	40.33	53.22	53.25
TiO_2	0.35	0.36	0.30	0.10	0.08	0.00	0.00	0.10	0.11
Al_2O_3	2.34	2.47	2.37	2.05	1.75	0.04	0.01	2.28	2.38
FeO*	1.68	1.62	1.61	5.51	5.38	7.21	6.34	1.38	1.49
MnO	0.07	0.02	0.00	0.14	0.07	0.05	0.07	0.06	0.03
MgO	18.62	17.34	18.17	34.47	35.22	52.20	52.58	17.44	16.98
CaO	24.29	24.27	22.28	0.46	0.25	0.00	0.00	23.59	24.05
Na_2O	0.11	0.15	0.16	0.00	0.00	0.00	0.00	0.14	0.19
Cr_2O_3	1.19	1.13	1.15	0.56	0.47	0.00	0.00	0.76	0.80
NiO	0.01	0.01	0.00	0.09	0.13	0.45	0.53	0.11	0.02
	99.32	99.79	99.31	100.50	99.58	100.29	99.92	99.10	99.30
Stoichiometry - 6 oxygens									
Si	1.904	1.929	1.933	1.954	1.942	0.978	0.978	1.944	1.930
Ti	0.009	0.008	0.002	0.002	0.002	0.000	0.000	0.002	0.003
Al	0.106	0.097	0.106	0.080	0.071	0.000	0.000	0.098	0.103
Fe	0.049	0.044	0.046	0.157	0.155	0.146	0.128	0.042	0.045
Mn	0.000	0.000	0.000	0.004	0.001	0.000	0.000	0.001	0.001
Mg	0.948	0.932	0.933	1.758	1.813	1.887	1.902	0.950	0.935
Ca	0.955	0.946	0.917	0.016	0.009	0.000	0.000	0.923	0.951
Na	0.007	0.010	0.007	0.000	0.001	0.000	0.000	0.010	0.013
Cr	0.034	0.032	0.033	0.015	0.003	0.000	0.000	0.021	0.023
Ni	0.000	0.000	0.000	0.002	0.003	0.050	0.050	0.003	0.000
	4.019	4.002	3.999	3.994	4.001	3.002	3.001	3.998	3.995
Fe	0.03	0.02	0.02					0.02	0.01
Mg	0.48	0.49	0.49	93.4	92.1	92.8	93.7	0.50	0.50
Ca	0.49	0.49	0.49					0.48	0.49

Table 3. Continued

	CMC 74		CMC 82		CMC 410		CMC 667	
	Olivine							
SiO_2	41.28	41.97	41.99	41.82	41.83	42.42	42.30	42.05
TiO_2	0.00	0.00	0.00	0.00	0.00	0.00	0.00	0.00
Al_2O_3	0.00	0.00	0.00	0.00	0.00	0.00	0.00	0.00
FeO*	3.12	3.46	3.56	4.11	4.24	4.29	5.09	5.05
MnO	0.00	0.00	0.00	0.00	0.03	0.02	0.07	0.09
MgO	56.41	55.29	54.46	54.36	52.72	52.19	52.48	51.86
CaO	0.00	0.00	0.01	0.00	0.00	0.00	0.00	0.00
Na_2O	0.00	0.00	0.00	0.00	0.00	0.00	0.00	0.00
Cr_2O_3	0.00	0.00	0.00	0.00	0.01	0.01	0.04	0.01
NiO	0.797	0.72	0.61	0.54	0.57	0.65	0.57	0.50
	101.60	101.43	100.64	100.87	99.40	99.58	100.54	99.57
Stoichiometry, 4 oxygens								
Si	0.990	0.973	0.996	0.991	1.005	1.016	1.008	1.010
Ti	0.000	0.000	0.000	0.000	0.000	0.000	0.000	0.000
Al	0.000	0.000	0.000	0.000	0.000	0.000	0.000	0.000
Fe	0.060	0.068	0.070	0.081	0.085	0.086	0.001	0.106
Mn	0.000	0.000	0.000	0.000	0.000	0.000	0.000	0.000
Mg	1.948	1.979	1.930	1.923	1.888	1.864	1.864	1.856
Ca	0.000	0.000	0.000	0.000	0.000	0.000	0.000	0.000
Na	0.000	0.000	0.000	0.000	0.000	0.000	0.000	0.000
Cr	0.000	0.000	0.000	0.000	0.000	0.000	0.000	0.000
Ni	0.013	0.014	0.017	0.015	0.011	0.012	0.011	0.011
	3.020	3.010	2.991	2.995	2.990	2.978	2.985	2.983
Fo	97.0	96.6	96.5	95.9	95.7	95.6	94.9	94.6

Table 3. Continued.

	CMC 149					CMC 169			
	Clinopyroxene		Orthopyroxene		Olivine	Clinopyroxene		Olivine	
SiO_2	53.15	54.36	58.30	57.66	42.02	52.96	53.09	42.27	41.64
TiO_2	0.29	0.22	0.10	0.13	0.00	0.33	0.27	0.00	0.00
Al_2O_3	1.99	1.97	1.19	1.18	0.00	2.69	2.97	0.01	0.00
FeO*	1.18	1.96	4.40	4.15	5.11	1.58	1.73	6.07	5.95
MnO	0.06	0.08	0.08	0.07	0.02	0.04	0.09	0.06	0.05
MgO	17.34	17.38	35.34	35.33	52.17	16.74	16.99	51.72	51.39
CaO	23.60	22.72	0.47	0.46	0.00	23.77	23.48	0.00	0.00
Na_2O	0.16	0.34	0.00	0.00	0.00	0.12	0.17	0.01	0.01
Cr_2O_3	1.03	1.14	0.34	0.46	0.04	1.04	1.14	0.00	0.00
NiO	0.08	0.05	0.07	0.13	0.69	0.01	0.09	0.42	0.41
	98.88	100.19	100.26	99.57	100.05	99.28	100.02	100.56	99.51
Stoichiometry, 6 oxygens									
Si	1.946	1.963	1.985	1.978	0.995	1.934	1.925	1.010	1.006
Ti	0.008	0.006	0.003	0.003	0.000	0.009	0.007	0.000	0.000
Al	0.086	0.084	0.048	0.098	0.000	0.116	0.127	0.000	0.000
Fe	0.036	0.059	0.125	0.119	0.110	0.048	0.052	0.121	0.120
Mn	0.002	0.002	0.002	0.002	0.000	0.001	0.003	0.000	0.000
Mg	0.947	0.935	1.794	1.807	1.886	0.911	0.918	1.930	1.850
Ca	0.926	0.879	0.017	0.017	0.000	0.930	0.912	0.000	0.000
Na	0.011	0.024	0.000	0.000	0.000	0.009	0.012	0.000	0.000
Cr	0.030	0.032	0.009	0.012	0.000	0.030	0.033	0.000	0.000
Ni	0.002	0.001	0.000	0.004	0.080	0.000	0.000	0.030	0.008
	3.991	3.982	3.981	3.987	2.991	3.986	3.986	2.990	2.986
Fe	0.02	0.03				0.03	0.03		
En	0.50	0.50	93.5	93.8	94.1	0.48	0.48	93.8	93.9
Ca	0.48	0.47				0.49	0.49		

Clinopyroxene-bearing chromitites occur primarily in upper sections of the harzburgite, within 500 m of the transition zone contact. They include the Chambers, Bald Eagle, Ray, and Celebration mines investigated in detail for this thesis, and others (U. of O., Ajax, and unnamed pods) studied by Thayer (in prep.). Some (Chambers, Ray, and Bald Eagle) contain olivine, orthopyroxene, and clinopyroxene. Some samples from the Ray Mine contained very little matrix orthopyroxene; several from the Bald Eagle were exclusively clinopyroxene + chromite. As in previous mineralogical types, no zonation of minerals was detected optically or via microprobe.

Olivine in clinopyroxene-bearing chromitite is slightly less magnesian (Fo_{92-95}), and less Ni-rich in general than olivine in clinopyroxene-absent chromitites, suggesting that the magma was slightly more fractionated. Orthopyroxene is En_{94} - not significantly different than in clinopyroxene absent chromitites. However, orthopyroxenes present with clinopyroxenes contain slightly more CaO (average = 0.50%) and NiO (average = 0.14%), and slightly less Al_2O_3 (average = 1.25%) than those without clinopyroxene (average CaO = 0.30%; average NiO = 0.07; average Al_2O_3 = 1.70%) which suggests, conversely, that the magma was less fractionated. Fo/NiO values of olivine in clinopyroxene-bearing chromitites are intermediate to values of clinopyroxene-absent chromitites, indicating that fractionation is not the simple explanation for differences in gangue mineralogy.

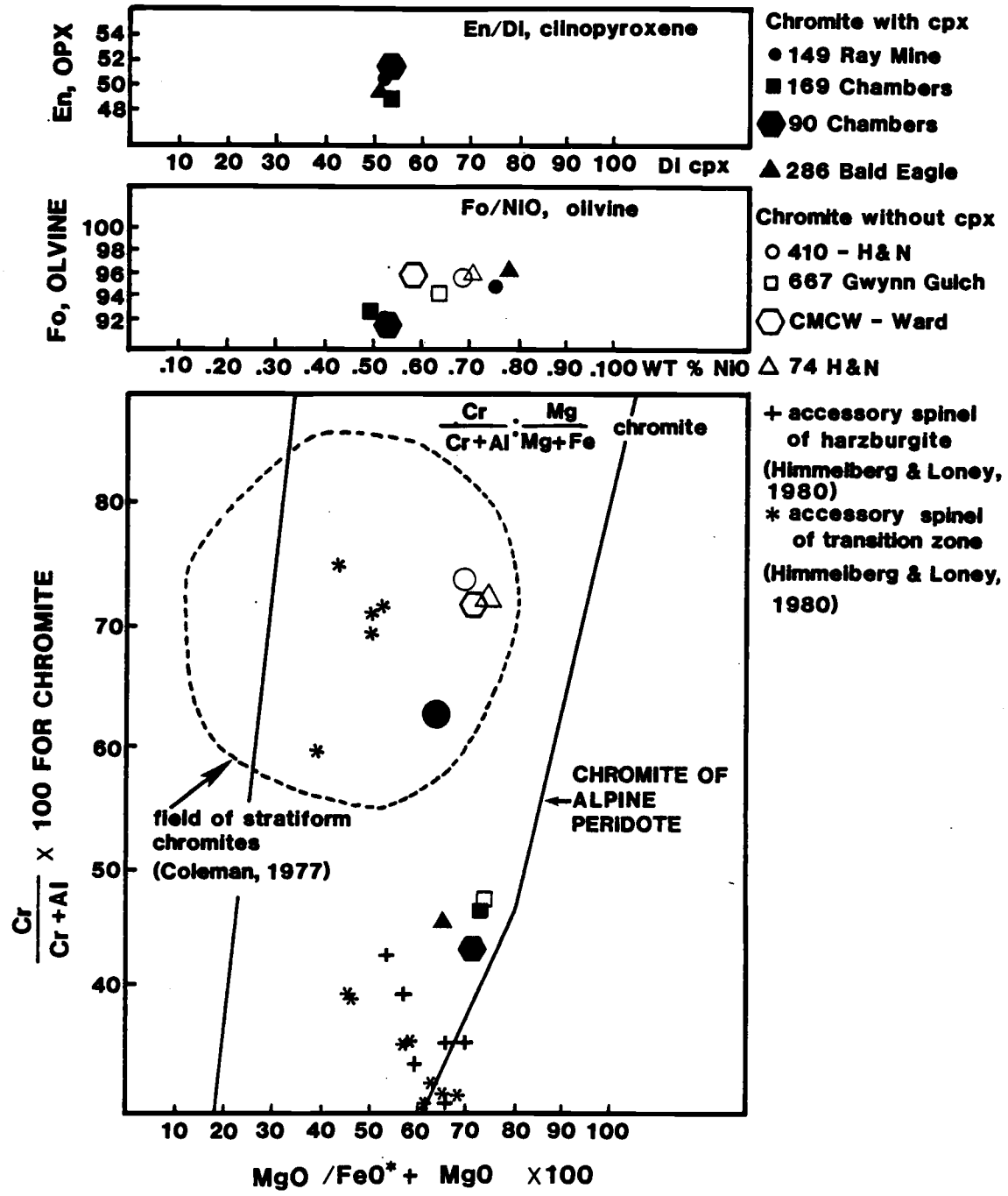

FIGURE 4. Composition of chromite and associated silicates.

All clinopyroxenes have similar compositions, and are in a tight cluster on a plot of En versus Di. They contain one to two percent Cr_2O_3, two-three percent Al_2O_3, 17-18 percent MgO, and 22-24 percent CaO. They are not zoned.

Chromite in clinopyroxene-bearing pods has a lower Cr/Cr + Al ratio than most chromite in olivine or olivine + orthopyroxene pods, and falls mostly outside the field of stratiform chromites on a Cr/Cr + Al: Mg/Fe + Mg diagram (Figure 4). Zoning is not present in chromitites.

In thin section, textures of clinopyroxene-bearing pods are not substantially different than others. Chromite is subhedral-to-euhedral, forms aggregates with visible grain boundaries, and may enclose silicates. Olivine is slightly deformed and euhedral. Clinopyroxene and orthopyroxene have adcumulate textures.

The areal distribution of chromitites, and the variation in compositions of their constituent minerals are important, and will be considered in more detail under conclusions regarding the origin of the Canyon Mountain complex. However, some discussion is pertinent here. Generally, Cr-rich chromite compositions are restricted to the west part of the CMC. East of Pine Creek, Cr/Cr + Al ratios of chromite in podiform deposits are less than about 0.50 (Plate 2). These chromitites commonly contain clinopyroxene, although they are <u>not</u> all clinopyroxene-bearing. The low Cr, clinopyroxene-bearing chromitites occur within zones of harzburgite which are intruded by numerous gabbro dikes (Zone of Infiltration). These gabbros intruded at high temperature, and appear to have infiltrated the

harzburgite during and after its deformation. This coincidence of low-Cr, high Ca podiform chromites with the intruded gabbro is significant, and suggests re-equilibration, or partial re-equilibration of chromitites with gabbroic magma. Straight grain boundaries and tendency for triple-point junctions in some chromitites suggest - but do not prove - that partial re-equilibration and recrystallization may have occurred. To confirm the occurrence of such a process, it is desirable to find a similar change in spinel composition in the host harzburgite. However, no systematic variation in accessory chromite is evident in data of Himmelberg and Loney (1981) (Figure 4) and a concomittent podiform-accessory Cr/Cr + Al change cannot be demonstrated.

There are several hypotheses for the origin of chromitites. Irvine (1965, 1967) suggested contamination of a differentiating magma by either alkalic wall rocks or a more differentiated basalt to drive equilibria back into the Cr-spinel field. Increase in fO_2 (Ulmer, 1969) or decrease in P_T (Cameron, 1979), have also been proposed.

Several explanations have been suggested for the mechanism of introducing podiform cumulate textures into tectonite harzburgite. Dickey (1970) thought podiform chromitites to be the product of partial fusion of lherzolite to release Cr from silicates, and indicated that some other, unspecified, probably cumulate, process is necessary to concentrate Cr sufficiently to form ores. Moutte (1982) considers podiform chromitites of Tiebaghi, New Caledonia

to be primary, cumulate layering, somewhat deformed. Thayer (1964) also attributes podiform deposits of the Canyon Mountain complex and elsewhere to a cumulate origin. More recently, Dickey (1975) considers podiform chromitites to be late-stage introduction which have sunk into harzburgite after precipitation as pods in lower parts of oceanic crust. Greenbaum (1977) attributes the stratigraphic distribution throughout the harzburgite of Troodos to "infolding". Lago et al. (1982) suggest accumulation of chromitite by elutriation and deposition of chromite-olivine in chambers adjacent to conduits, or within the magma pipes themselves. Later, partial melting of mantle peridotite generates olivine-orthopyroxene-chromite residues. Based upon Lago et al.'s model, Cassard et al. (1981) proposed a structural classification of chromite deposits - with structurally discordant as primary, and structurally concordant as more deformed.

The variation in modal mineralogy of the chromitites in the Canyon Mountain complex indicates that liquids varied in composition, or that metasomatic introduction of CaO + Al_2O_3 and re-equilibration similar to that suggested for the Bushveld (Cameron, 1979) was common. CaO-rich chromitites are generally higher in the section, as are Al_2O_3-rich spinels. This fairly straightforward relation suggests that a more fractionated fluid precipitated upper-level chromitites. However, the low Cr/Cr + Al ratio of the Gwynn Gulch sample (667) from the zone of infiltration complicates this simple model, and suggests instead that re-equilibration at least played a role in chromitite history. The adcumulate textures of podiform

chromitites suggest that they originally formed as cumulates and that cumulate texture was preserved through upper mantle deformation by the structural rigidity of chromite-rich rocks. No field evidence supports the conduit model of Lago et al. (1982) for the Canyon Mountain complex. Similarly, no structural trace is present for either in-folding (Greenbaum, 1977) or sinking (Dickey, 1975).

A model of initial in situ precipitation with later hyper- to subsolidus deformation, and some equilibration with infiltrated gabbro is preferred for chromitite of the CMC because: 1) the textures of most podiform chromitites do not preclude re-equilibration with CaO-Al_2O_3-rich fluids at high temperature, 2) gabbroic dikes and infiltrate are present in at least two clinopyroxene-rich deposits, 3) mineralogical fractionation trends are reversed in some Ca-enriched systems from those expected if fractionation was the sole process responsible for harzburgite podiform chromites.

Rocks of the Transition Zone

The transition zone - or metacumulates of Himmelberg and Loney (1980) - extends from the stratigraphic top of the harzburgite near Baldy Mountain and Gand Saddle toward the main ridge less than one kilometer south. It is a sequence of alternating gabbro (20 percent), melagabbro (10 percent) and clinopyroxene-rich peridotite (70 percent). These rocks are not a laterally continuous unit, extending without interruption across the east-west extent of the Canyon Mountain complex. As shown on Plate 1 and Plate 2, instead

they are well exposed on eastern-most ridges, covered by alluvium in intervening valleys, and decrease in abundance westward. The "transition zone" is virtually absent in Norton Creek near the center of the CMC. Layered mafic and ultramafic rocks reappear near the Iron King Mine at the extreme west limit of exposure.

Field Relations

To facilitate discussion of locations within the transition zone, ridges where transition zone rocks occur will be referred to by the numbers shown on Figure 5. Ridges are numbered consecutively from east (1) to west (9). Layers in the rocks are commonly five to ten meters thick, but vary from a few centimeters to 50 meters (Figure 6). Layers are not laterally continuous and may persist only for several meters. The order of rock types, compositions, crystal sizes and abundance varies. No graded bedding, or sedimentary features similar to other ophiolites' transition zones have been noted at the Canyon Mountain complex. Instead, the rocks in the east are strongly deformed, with well defined foliation, and occasional lineation. Tectonism may obscure primary "sedimentary" features. Deformation notable in outcrop decreases westward through the complex, as does the abundance of transition zone rocks. Himmelberg and Loney (1980) designated the transition zone as "meta-cumulates" because the rocks have a tectonite fabric similar to the basal harzburgite.

There is no readily definable contact between the "metacumulate" rocks of the transition zone, the underlying tectonite harzburgite, or the overlying gabbro. Rather than gradation from harzburgite to

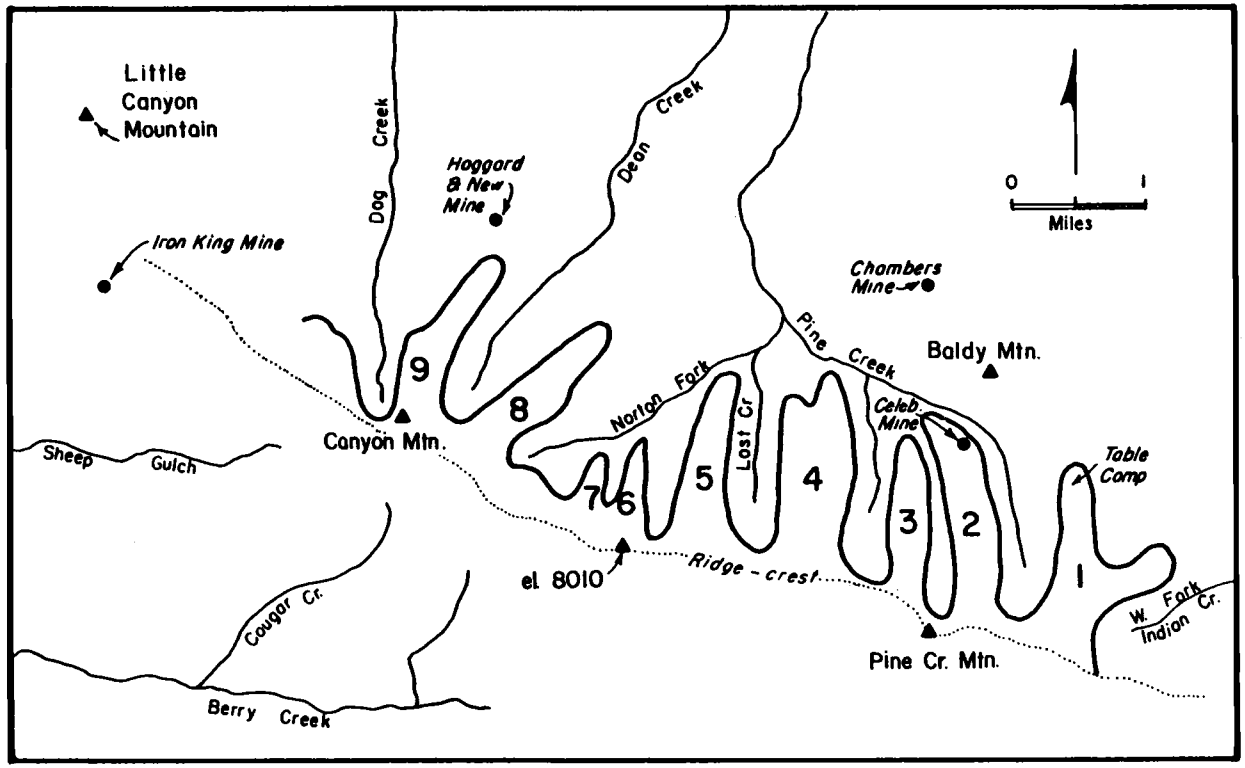

FIGURE 5. Numerical designation of ridges, Canyon Mountain complex.

Transition zone sequence, Ridge 1

Metacumulate gabbro intruded by isotropic gabbro, Ridge 1

FIGURE 6. Lithologies of the transition zone.

ultramafic cumulate, as found in Samail, Bay of Islands, and other ophiolites, gabbro seems to intervene between peridotite and transition zone, and also seems to underlie, surround and intrude the transition zone mafics and ultramafics. Plates 1 and 2, and Figure 6 show that isotropic gabbro crosscuts strongly foliated or lineated gabbros and peridotites of the transition zone in several locations, and gabbro seems to surround isolated pods of transition zone rocks. On ridge tops, contacts between the isotropic gabbro and more structured transition zone rocks are poorly exposed. Where it is visible over considerable extent, such as on the west side of Ridge 4, the isotropic gabbros commonly develop a foliation or layering parallel to the contact which suggests that the gabbro flowed and congealed around a screen or large inclusion. Near Norton Creek (west fork of Pine Creek), five to 30 meter-long screens and large xenoliths of the foliated and lineated transition zone gabbro are enclosed within isotropic gabbros. The foliation of the inclusion is on strike with the transition zone trend, indicating that intrusion was quiet. Farther west, on Green Mountain, foliated ultramafic rocks and melagabbros occur within isotropic and layered clinopyroxene-orthopyroxene cumulate gabbro (see Bear Skull Rim gabbro). Pods and xenoliths of foliated and isotropic ultramafic rock occur in many localities within the upper gabbro, including Norton Basin (Plate 4), Canyon Mountain (Plate 5) and Sheep Rock (Plate 5).

Previous interpretations (Thayer, 1977; Himmelberg and Loney, 1980) have explained these rocks as channel fillings, similar to

exposures of the Skaergaard and the Finneskasset. However, several pods are well foliated, and a thin section of one showed textures and deformation which could be interpreted as a tectonite fabric. An alternative explanation for the pods is that they represent transition zone (metacumulate) xenoliths - or even roof pendants - picked up in CMC gabbro. Two observations support this interpretation: First, the maintenance of uniform strike from ridge to ridge in many large, identifiable pods of transition zone rocks within gabbro as shown on Plate 2 suggests that the transition zone was intruded and enveloped by gabbro. Second, five to 25 cm xenoliths of ultramafic rocks occur in fine-grained gabbro of Norton Basin. If small xenoliths occur, large ones might also occur. Hence, the ultramafic rocks exposed within upper gabbros are interpreted as large xenoliths of the transition zone, rather than as in situ channel fillings.

The width of the transition zone diminishes rapidly westward from Baldy Mountain where the zone is two kilometers wide (Ridge 1), to Yellow Jacket Ridge (Ridge 5) where transition zone ultramafics and lineated gabbro occupy less than 100 meters, and are surrounded by upper level gabbro. The transition zone cannot be mapped as continuous bands due to lack of exposure on ridges, intervening talus, alluvium, and moraine, and lack of recognizable lithic continuity from zone to zone.

On Baldy Ridge (Ridge 1), where the rocks are very strongly foliated (Figure 6), the mafic and ultramafic sequence is generally

lineated gabbro → wehrlite → websterite → lherzolite → gabbro → wehrlite → dunite → pyroxenite. However, this sequence of units is unique, and is not repeated on this, or other, ridges.

Gabbro associated with the transition zone occupies discreet, usually straight, bands within the peridotites. It is rodigized and does not have chilled margins. The transition zone gabbro is parallel to foliation - gabbro which has pronounced structure rarely crosscuts the foliation of ultramafic rocks in the zone.

Significantly, on Celebration Ridge (Ridge 2), as in harzburgite of Baldy Mountain, the mineralogy of the gabbro "layer" may change along strike (for example - from plagioclase and clinopyroxene to a clinopyroxenite). This change of mineralogy along strike may be due to one or more of the following possibilities: Migration of more mafic components into narrow spaces after early crystallization of feldspars; change in equilibrium conditions along strike; lateral filter pressing, change in composition of liquid within the layer as more magma is injected, or metasomatic reactions. Change of liquid composition with the injection of more magma is the most probable explanation.

The layered gabbroic rocks of the transition zone are mostly melagabbro to olivine-clinopyroxene-orthopyroxene gabbro. Modal amounts of minerals vary, but mineral compositions are nearly constant. Melagabbro samples from the base of the sequence on Celebration Ridge, west of the Celebration Mine, have mineralogical compositions nearly identical with those of gabbro and melagabbro at

the uppermost portion of the ridge (Tables 4-8). Gabbros and melagabbros are layered on a scale similar to peridotites.

General Petrography of the Transition Zone

Rocks of the transition zone are dominantly clinopyroxene-olivine rocks, websterite to wehrlite, with gradations in mineralogy from dunite through clinopyroxenite. Clinopyroxene is corroded and recrystallized; olivine is pervasively deformed and recrystallized, and altered partly (15-70 percent) to serpentine minerals. In one thin section from the ridge south of Baldy Mountain (Ridge 1), alteration patterns of clinopyroxene are suggestive of initial zoning. However, minerals in transition zone rocks have not retained zoning, but have re-equilibrated at temperatures of 900-925°C (Himmelberg and Loney, 1980).

Clinopyroxene is Ca-rich diopside, with 2V between 60° and 55°, based upon estimates from optic figures. It commonly is broken, has ragged edges, and displays glide-twins resulting from deformation. Twinning increases up-section, suggesting greater deformation, or more subsolidus brittle deformation with stratigraphic height. In poikilitic rocks, clinopyroxene forms a matrix which encloses fractured olivine. This clinopyroxene is also twinned, and cleavage lamellae are bent.

Orthopyroxene is mostly bronzite, with 2V in the range of 75°-85°. It is commonly more deformed than clinopyroxene, shows exsolution and twinning due to strain, and infrequently forms rims around small olivines. Only one sample (228) contained olivine

within poikiloblastic orthopyroxene. Most orthopyroxene is partly altered to "bastite"; secondary amphibole was not observed in association with orthopyroxene of the transition zone.

A noteworthy characteristic of transition zone metacumulates which contrasts with similar sections of other ophiolites is their more coarse-grained nature. Pyroxenes usually range between one and five mm in size. Many approach 10 mm. This relatively large crystal size indicates slow cooling, substantial adcumulus growth, and possibly late growth during the 900-925° equilibration, rather than conditions of rapid crystallization noted in other ophiolites.

Throughout the transition zone, the sequence of crystallization appears to have been olivine → clinopyroxene, or (olivine + spinel) → clinopyroxene. However, subtleties of texture have been obliterated by deformation. Where plagioclase occurs, it is interstitial, with rounded boundaries suggestive of late reaction with adjacent clinopyroxene, and may be rimmed by pink-to-brown (pargasitic?) amphibole. An contents (An_{92-97}) determined optically are extremely calcic in keeping with the character of other ophiolite transition zones, and a magma rich in CaO. In gabbroic rocks, feldspars are almost completely converted to hydrogrossular and chlorite. Alteration of the feldspar is gradual - analyses of progressively altered plagioclase are given in Table 9. The feldspars of gabbroic rocks tend to be subhedral, rather than lobate, and compositionally overlap feldspars in ultramafic rocks of the transition zone.

Detailed Field Relations of the Transition Zone

Detailed field observations of two well exposed areas of transition zone rocks, Celebration Ridge (Ridge 2) and Ridge 4, were made. These ridges were chosen because both have excellent exposure of transition zone rocks, they are far enough apart to show changes in overall style across the transition zone, and lastly because the contact between rocks of the transition zone and cumulate gabbro of the Canyon Mountain complex is well exposed on the west side of Ridge 4.

Field Relations, Ridge 4

Ridge 4 rises steeply from Pine Creek and consists principally of strongly sheared and altered gabbro from the first outcrops to 100 meters beyond the ridge nose at elevation 7100 feet (2220 m). This gabbro is similar to the gabbro of Bear Skull Rims, and is mapped as part of that unit. Layered gabbro occurs in several locations on the steep part of the ridge. However, most gabbro is isotropic or foliated by late deformation. A layered sequence of dunite, websterite, melagabbro and gabbro occurs on the northeast flank of the ridge. However, the relation of these layered, slightly foliated transition rocks and the gabbro which comprises the north part of Ridge 4 is not apparent.

The ultramafic portion along the crest of Ridge 4 commences at an elevation of 6300 feet (1921 m). These rocks are less foliated than similar lithologies on ridges to the east. Olivine websterite

with large clinopyroxene oikiocrysts occurs 20 meters south of the ridge nose, and appears to be enclosed in nearly isotropic gabbro. Bands of ultramafic rock which vary from dunite to lherzolite to troctolite strike east-west across the ridge and vary from 0.5 to 5.0 meters in width. The ultramafic-gabbro layered sequence continues nearly one kilometer south to an elevation of 7400 feet (2255 m) where it terminates against gabbro and norite of Pine Creek Mountain.

Field relations and textures throughout much of the transition zone do not indicate prevalent turbulent or 'mushy' conditions within the metacumulates, and in this respect are anomalous to most ophiolite transition zones. Subsolidus deformation - noteably folds in gabbro and small slump features - are present in two locations on Ridge 1 and three locations on Ridge 2 (Celebration Ridge). On Ridge 4, there is some evidence of remobilization and perhaps diapiric intrusion of ultramafic layers into mushy gabbro. Gabbroic foliation turns nearly 90° to parallel enclosed large peridotite blocks. Enclosure of foliated gabbro in mushy peridotite is also indicated by field relations on the west flank of the ridge. Hence, some features do suggest that the transition zone persisted as mush, and was locally deformed by slumping or subsolidus movement. However, such occurrences are not a major feature of the transition zone.

Field Relations, Celebration Ridge

Celebration Ridge was mapped at a scale of 1:6,000, or 1 inch = 500 feet (Plate 3). Ten lithologies were identified:

1. Serpentinite (Serpentine minerals > 75%)
2. Dunite
3. Harzburgite
4. Lherzolite (ol → opx → cpx)
5. Olivine websterite (ol → cpx → opx)
6. Websterite (cpx → ol → opx)
7. Plagioclase websterite (cpx → ol + opx → plag)
8. Melagabbro
9. Gabbro
10. Norite

The rock types vary unsystematically along the crest of the ridge, with different lithologies every 5-10 m and layers or bands commonly persisting laterally no more than 10-40 meters. Some banding is very narrow, and even at 1" = 500', all changes in lithology could not be shown. An additional handicap in mapping this ridge is that although exposure at the ridgecrest and to approximately 61 m below the crest is excellent, major portions of the lower ridge, and much rock adjacent to the upper ridge is obscured by talus, glacial moraine, and alluvium.

Celebration Ridge extends approximately 2 km north-south on the east side of upper Pine Creek and provides a cross section from harzburgite on Baldy Mountain to norite at Pine Creek Mountain. The nose of Celebration Ridge rises steeply from Pine Creek. The Celebration Mine occurs in dunite at the north end which persists upward to 6400 feet (1951 m). The dunite is fine-grained, with a slightly

tectonized fabric, and rare, one centimeter wide gabbro veins which crosscut foliation. Although the Celebration Mine chromite body has been largely removed by mining, float of nodular chromitite confirms its cumulate nature. The surrounding dunite is considered similar to dunites in other ophiolites which occur at the top of the harzburgite or between harzburgite and metacumulate section. Unfortunately, the contact bewteen the harzburgite and this dunite is not exposed. The concentration of gabbro dikes on Baldy Mountain west of the ridge and the occurrence of gabbro near Table Camp, east of the ridge, strongly suggest that early cumulate gabbro intervenes between dunite on Celebration Ridge and the main body of harzburgite. However, two large, irregular dunite bodies occur on the south side of Baldy Mountain, and may be related to the dunite body on Celebration Ridge.

West of the dunite, on the northwest side of the ridge, interlayered olivine websterite and plagioclase websterite to melagabbro occur. These rocks are strongly foliated; banding is 10-20 cm thick and strikes slightly oblique to the trend of the ridge.

Orthopyroxenites and clinopyroxenites occur as knockers in dunite matrix from 6200 to 6800 feet (1890-2073 m) along the crest of the ridge. On the north side, a layered outcrop of olivine websterite and lherzolite with oikiocrystic pyroxene occurs. Modal abundance of minerals varies greatly between bands. Irregular patches of dunite are present. Olivine websterite which occurs at the summit of the nose (el. 6800 feet or 2073 m), consists of generally about 60 percent clinopyroxene, 30 percent olivine, and

10 percent orthopyroxene. Dunite adjacent to and between these pyroxene-rich pods is strongly serpentinized. One hundred meters farther up the ridge, layered, foliated gabbro and alternating gabbro and ultramafic rocks occur. The rocks are deformed and possibly folded as hyper- or sub-solidus phases. Identifiable lithologies include dunite, lherzolite, wherlite, websterite, and melagabbro. Southward (up-slope) across the outcrop, orthopyroxene generally decreases and clinopyroxene increases. Contacts between units are gradational; units average about one meter in width. Unfortunately, these zones can be traced no more than five meters due to poor exposure. Layered rocks of similar character were not found on strike below the outcrop. Ultramafics and gabbros of this sequence are relatively unaltered and not strongly serpentinized or rodingized.

Extensive exposures of orthopyroxene-clinopyroxene gabbro occupy the next 400 meters. Some gabbro is layered. Approximate modes are 60 percent plagioclase, 20 percent clinopyroxene, and 20 percent orthopyroxene, with local variations. Orthopyroxene generally increases upward. Gabbro at lower elevations near the layered ultramafics at the ridge nose is Ni-sulphide bearing. Gabbros are altered sporadically along this portion of the ridge, with no predictable pattern of alteration. In thin section, the alteration is usually plagioclase → (hydrogrossular + chlorite). Broad folding and minor (5-10 m) displacement also affect the gabbro. Early subsolidus faults offset gabbro layers two to five meters.

At the contact of gabbro and upper peridotites, elevation 7280 feet, the two-pyroxene gabbro is strongly lineated, but not foliated, and plunges steeply, parallel to the contact. The gabbro is medium grained, 60 percent plagioclase (An_{75}), 20 percent clinopyroxene, and 15 percent orthopyroxene (En_{80}). As is true of all other gabbros in the complex, the gabbro of the central portion of Celebration Ridge is not chilled against the peridotite. The peridotite is severely serpentinized at, and within 20 meters of the contact, possibly because the more competent gabbro acted as a barrier to movement of water during alteration. Diabases are altered and amphibolized here, as well as farther up Celebration Ridge.

Peridotite persists from the contact at 7280 feet (2220 m) to the ridge summit at 7860 feet (2396 m) near Pine Creek Mountain. Sporadic steep lineation suggests localized crumpling of peridotite either as a nearly solid mush or subsolidus prior to substantial cooling. Generally, the layers or bands of different lithologies are not strongly foliated, and mineralogical changes are gradual over one to ten cm, except for interleaved gabbros which do not have gradational contacts with peridotite. Banding or layers vary in width from between 5-10 cm to more than 50 meters, with most in the range of four to eight meters. Banding is more pronounced, lithologic changes are more abrupt, and contrasts between adjacent mineralogies are greater at the top of the ridge, near the contact with gabbro of Pine Creek Mountain.

Rodingized gabbro occurs along the ridge generally as bands less than five meters wide which are not always strongly foliated, and vary in texture from extremely coarse foliated gabbro to medium-grained isotropic gabbro. With one noteable exception described below, their contact with peridotite is sharp. Feldspathic peridotites (including troctolite) are virtually absent from Celebration Ridge. Troctolites are most common as pods within gabbro at the very top of the transition zone sequence.

At the top of the transition zone sequence, lithologies change rapidly and abruptly. Gabbro becomes more abundant. Strongly foliated gabbro alternates with bands of olivine websterite, plagioclase websterite, and dunite in bands 0.3 to 5 meters wide. The rocks at the summit of the Celebration Ridge transition zone sequence have escaped the pervasive serpentinization which effects the rocks below. Bands of very fresh websterite one to five meters wide alternate with dunites and mafic, two-pyroxene gabbro. Changes between lithologies are abrupt; contacts are sharp.

Petrography and Mineral Chemistry of Upper Celebration Ridge

A sequence of interlayered gabbro, melagabbro, websterite, olivine-plagioclase websterite, and wehrlite at the upper limit of the transition zone at 7700 feet (2350 m) elevation on Celebration Ridge (Ridge 2) was chosen for detailed petrographic and microprobe study to determine whether 1) interlayered hypersthene-clinopyroxene gabbro was part of the transition zone or whether

it was intrusive into the transition zone, 2) whether any cryptic variation occurred in transition zone rocks, and 3) whether any subtle mineral zonation was present.

In outcrop this sequence is alternating plagioclase-rich and plagioclase-poor bands five to ten meters wide, with sharp boundaries between layers where contacts are visible. The rocks are strongly foliated, trend nearly east-west, and dip steeply northward, parallel to the general trend within the transition zone. In these exposures on the upper part of the ridge, serpentinization and alteration are not as pervasive as they are below. There is no evidence of recrystallization due to thermal effects, and the small amount of serpentinization may be due to absence of conduits for water in these stronger, more rigid upper rocks.

The location of the sequence analyzed from station 579 is shown on Plate 2, modal analyses are given in Table 4 and microprobe data for olivine, orthopyroxene, clinopyroxene and plagioclase are presented in Tables 5-9. Late amphibole is given in Table 10.

The total interval investigated is 50 meters. Layer A, at the top, is plagioclase-olivine websterite, five meters wide. Layers B and C are five-meter-wide two-pyroxene gabbros. Layer D is plagioclase-bearing olivine websterite four meters wide, with less than one percent plagioclase. Approximately ten meters of olivine-rich lherzolite intervenes between each analyzed layer. Three thin sections of each layer show only minor variations in modal mineralogy.

In thin section, 579A is very fresh, with only three percent alteration to serpentine and hydrogrossular. Texture is equant and

Table 4. Modal analyses of the 579 sequence, Upper Celebration Ridge.

	579A	579B	579C	579D
Olivine	14.5	--	--	14.7
Orthopyroxene	8.3	14.5	17.8	12.9
Clinopyroxene	61.3	20.0	36.5	47.6
Plagioclase	6.1	47.1	31.9	0.2
Amphibole	3.2	12.2	--	2.1
Serpentine	3.2	6.0	--	13.8
Chlorite	--	tr	9.0	6.0
Prehnite	--	--	2.6	--
Oxide	2.2	0.2	0.2	2.5
Sulphide	1.2	--	--	0.2
	100.0	100.0	100.0	100.0

TABLE 5. Olivine of 579.

	579 A					579 D		
SiO_2	39.17	39.14	38.74	37.92	38.92	40.27	39.96	39.53
Al_2O_3	0.00	0.00	0.00	0.00	0.00	0.01	0.02	0.00
TiO_2	0.00	0.00	0.00	0.00	0.00	0.00	0.02	0.00
FeO	22.85	22.51	22.20	22.70	22.87	17.99	18.52	17.88
MnO	0.36	0.37	0.35	0.35	0.32	0.26	0.23	0.26
MgO	38.55	38.35	37.56	38.80	37.86	42.43	42.12	41.84
CaO	0.04	0.06	0.04	0.04	0.05	0.00	0.00	0.04
Na_2O	0.00	0.00	0.00	0.00	0.00	0.02	0.00	0.01
Cr_2O_3	0.02	0.03	0.02	0.02	0.04	0.00	0.00	0.00
NiO	0.17	0.22	0.20	0.21	0.18	0.18	0.17	0.16
	101.15	100.68	99.15	100.03	100.26	101.16	101.01	99.76
Stochiometry - 4 oxygens								
Si	1.00	1.00	1.01	1.07	1.00	1.00	1.00	1.00
Al	0.00	0.00	0.00	0.00	0.00	0.00	0.00	0.00
Ti	0.00	0.00	0.00	0.00	0.00	0.00	0.00	0.00
Fe	0.49	0.49	0.49	0.50	0.50	0.37	0.39	0.38
Mn	0.01	0.01	0.01	0.01	0.00	0.00	0.00	0.38
MgO	1.48	1.48	1.47	1.51	1.47	1.57	1.57	1.57
CaO	0.00	0.00	0.00	0.00	0.00	0.00	0.00	0.00
Na_2O	0.00	0.00	0.00	0.00	0.00	0.00	0.00	0.00
Cr_2O_3	0.00	0.00	0.00	0.00	0.00	0.00	0.00	0.00
NiO	0.00	0.00	0.00	0.01	0.00	0.00	0.01	0.03
	4.01	4.05	2.98	3.09	2.97	2.94	2.96	2.97
Fo	75	75	75	75	75	81	80	80

TABLE 6. Orthopyroxene of 579

	579 A		579 B						579 C				579 D	
SiO_2	54.28	54.35	55.43	54.44	54.53	55.56	55.39	54.70	54.66	54.98	54.80	54.11	55.05	54.65
Al_2O_3	2.25	2.45	1.82	1.77	1.70	1.87	1.80	1.68	2.21	2.21	2.32	2.13	2.26	2.24
TiO_2	0.16	0.15	0.07	0.09	0.03	0.08	0.04	0.04	0.05	0.07	0.00	0.06	0.04	0.04
FeO	14.32	13.91	12.29	12.53	13.40	12.61	12.55	13.15	13.09	12.99	13.17	13.44	11.92	11.89
MnO	0.35	0.32	0.23	0.27	0.24	0.24	0.24	0.30	0.24	0.22	0.23	0.22	0.24	0.22
MgO	26.80	26.80	28.55	28.66	28.81	27.46	28.56	28.19	28.39	27.14	28.14	28.21	29.79	29.50
CaO	0.65	0.92	0.73	0.77	0.63	0.80	0.80	0.67	0.79	0.87	0.58	0.78	0.63	0.64
Na_2O	0.00	0.00	0.00	0.00	0.00	0.00	0.00	0.00	0.00	0.02	0.00	0.02	0.00	0.00
Cr_2O_3	0.16	0.20	0.03	0.77	0.45	0.01	0.11	0.05	0.07	0.10	0.11	0.08	0.22	0.24
NiO	0.12	0.22	0.07	0.04	0.00	0.01	0.00	0.03	0.00	0.12	0.00	0.03	0.04	0.05
	99.08	99.30	99.26	95.63	99.36	98.63	99.50	99.52	99.49	98.72	99.35	99.06	100.18	99.53
Stoichometry - 12 oxygens														
Si	3.92	3.92	3.96	3.92	3.91	3.99	3.95	3.96	3.91	3.96	3.92	3.89	3.89	3.89
Al	0.19	0.21	0.15	0.15	0.14	0.16	0.15	0.15	0.19	0.19	0.20	0.16	0.19	0.19
Ti	0.01	0.01	0.00	0.01	0.00	0.00	0.00	0.00	0.00	0.00	0.00	0.00	0.00	0.00
Fe	0.87	0.84	0.73	0.75	0.80	0.76	0.75	0.78	0.78	0.78	0.78	0.79	0.70	0.71
Mn	0.02	0.02	0.04	0.02	0.14	0.01	0.01	0.01	0.01	0.01	0.01	0.01	0.01	0.01
Mg	2.89	2.87	3.37	3.08	3.08	2.24	3.04	3.01	3.03	2.91	3.00	3.01	3.14	3.13
Ca	0.05	0.07	0.06	0.06	0.05	0.06	0.06	0.06	0.06	0.07	0.04	0.04	0.05	0.05
Na	0.00	0.00	0.00	0.00	0.00	0.00	0.00	0.00	0.00	0.00	0.00	0.00	0.00	0.00
Cr	0.01	0.01	0.01	0.00	0.01	0.00	0.01	0.00	0.00	0.00	0.01	0.00	0.00	0.01
Ni	0.01	0.01	0.00	0.00	0.00	0.00	0.00	0.00	0.00	0.00	0.00	0.00	0.00	0.00
	7.97	7.97	7.96	8.00	8.01	7.93	7.97	7.98	7.99	7.94	7.98	7.99	8.01	8.00
En	77	77	82	80	79	75	80	79	80	75	79	79	82	82

TABLE 7. Clinopyroxene of 579

	579 A									
	1	2	3	4	Core →			5		→ Rim
SiO_2	51.47	51.32	50.30	51.59	51.10	50.49	52.51	51.54	50.78	51.83
Al_2O_3	3.57	3.62	3.71	3.67	3.97	3.70	3.59	3.81	3.48	3.59
TiO_2	0.60	0.54	0.53	0.51	0.61	0.53	0.50	0.56	0.52	0.47
FeO	6.40	5.07	6.01	5.71	5.94	5.95	5.95	6.60	5.44	7.57
MnO	0.18	0.17	0.17	0.22	0.16	0.18	0.17	0.24	0.19	0.23
MgO	14.79	14.64	14.84	14.77	14.92	15.49	14.78	15.26	15.03	16.92
CaO	20.82	22.85	21.63	22.08	22.36	21.98	21.72	21.00	22.27	18.41
NaO	0.28	0.23	0.29	0.29	0.30	0.27	0.26	0.28	0.26	0.20
Cr_2O_3	0.41	0.46	0.40	0.32	0.44	0.42	0.34	0.46	0.39	0.40
NiO	0.08	0.07	0.13	0.05	0.10	0.01	0.11	0.04	0.14	0.11
Total	98.58	98.97	97.99	98.90	99.90	99.01	99.92	99.77	98.50	99.72
Stoichiometry - 12 oxygens										
Si	3.84	3.83	3.79	3.84	3.77	3.76	3.86	3.81	3.80	3.82
Al	0.31	0.32	0.33	0.30	0.35	0.33	0.31	0.33	0.31	0.31
Ti	0.03	0.03	0.03	0.03	0.03	0.03	0.03	0.03	0.03	0.03
Fe	0.40	0.32	0.38	0.36	0.37	0.37	0.37	0.41	0.34	0.47
Mn	0.01	0.01	0.01	0.01	0.01	0.01	0.01	0.01	0.01	0.01
Mn	1.65	1.62	1.67	1.64	1.65	1.72	1.62	1.68	1.68	1.86
Ca	1.66	1.82	1.75	1.76	1.77	1.75	1.71	1.66	1.79	1.45
Na	0.04	0.03	0.04	0.04	0.43	0.04	0.04	0.04	0.04	0.03
Cr	0.02	0.03	0.02	0.02	0.25	0.03	0.02	0.03	0.02	0.02
Ni	0.00	0.00	0.01	0.00	0.01	0.00	0.01	0.00	0.01	0.01
Σ	7.98	8.00	8.03	8.00	8.03	8.05	7.96	8.00	8.02	8.00
Fe	10	8.	10	9	9	9	10	10	8	12
Mg	44	43	43	43	43	44	43	44	44	49
Ca	44	48	4	46	46	45	46	44	46	38

	579 B				579 C						
	1	2	3	4 Rim	Core	Cpx 1	Cpx2	Cpx3	Cpx4	Cpx5	Cpx6
SiO_2	53.32	52.71	53.12	53.42	52.51	50.49	52.55	53.31	52.16	52.82	52.83	52.78
Al_2O_3	2.52	2.54	2.43	2.29	2.46	2.98	2.82	2.92	2.92	2.87	2.82	2.92
TiO_2	0.21	0.17	0.12	0.19	0.19	0.05	0.10	0.15	0.17	0.17	0.21	0.23
FeO	5.39	5.43	5.03	4.72	5.07	5.34	5.29	5.67	5.90	5.08	5.27	4.97
MnO	0.13	0.08	0.13	0.08	0.11	0.09	0.10	0.12	0.16	0.12	0.11	0.12
MgO	15.50	16.03	15.75	15.82	15.56	15.52	15.91	15.42	15.49	15.45	15.32	15.41
CaO	21.62	22.01	22.21	22.48	22.83	21.92	22.01	22.04	20.46	22.50	22.45	22.31
NaO	0.18	0.16	0.15	0.12	0.15	0.21	0.20	0.23	0.20	0.21	0.21	0.22
Cr_2O_3	0.13	0.15	0.15	0.13	0.13	0.18	0.14	0.17	0.18	0.25	0.16	0.23
NiO	0.03	0.06	0.00	0.04	0.00	0.07	0.03	0.00	0.04	0.05	0.13	0.07
Total	99.03	99.33	99.08	99.30	99.00	96.95	99.14	100.03	97.69	99.51	99.50	99.26
	3.94	3.89	3.92	3.93	3.89	3.83	3.88	3.90	3.91	3.89	3.89	3.89
	0.22	0.22	0.21	0.20	0.22	0.27	0.25	0.25	0.26	0.25	0.24	0.24
	0.01	0.01	0.01	0.01	0.01	0.01	0.01	0.01	0.01	0.01	0.01	0.01
	0.33	0.33	0.31	0.29	0.31	0.34	0.33	0.35	0.37	0.31	0.32	0.31
	0.01	0.00	0.01	0.00	0.01	0.01	0.01	0.01	0.01	0.01	0.01	0.01
	1.71	1.76	1.73	1.73	1.72	1.76	1.75	1.68	1.73	1.70	1.68	1.69
	1.71	1.74	1.76	1.77	1.81	1.78	1.74	1.73	1.64	1.77	1.77	1.76
	0.03	0.02	0.02	0.02	0.02	0.03	0.03	0.03	0.03	0.03	0.03	0.03
	0.01	0.01	0.07	0.00	0.01	0.01	0.01	0.01	0.01	0.01	0.01	0.01
	0.00	0.00	0.00	0.00	0.00	0.00	0.01	0.00	0.00	0.00	0.01	0.00
	7.96	8.00	7.98	7.97	8.00	8.04	8.00	7.97	7.97	7.99	7.98	7.98
	08	08	08	08	08	09	08	09	10	08	08	08
	45	46	46	46	46	46	46	45	46	45	45	45
	46	46	46	46	46	46	46	46	44	47	47	47

Table 7. Continued.

579D

	1	2	3	4
SiO_2	52.44	51.98	51.47	52.23
Al_2O_3	3.12	2.97	3.46	3.11
TiO_2	0.32	0.32	0.35	0.31
FeO	4.20	4.88	4.80	4.55
MnO	0.10	0.09	0.12	0.11
MgO	15.66	16.07	15.41	15.59
CaO	21.48	22.08	21.88	21.19
Na_2O	0.12	0.19	0.19	0.15
Cr_2O_3	0.45	0.46	0.54	0.47
NiO	0.07	0.03	0.00	0.43
Total	97.98	99.07	98.22	97.76
Stoichiometry - 12 oxygens				
Si	3.40	3.85	3.88	3.89
Al	0.27	0.26	0.02	0.02
Ti	0.02	0.02	0.30	0.27
FeO	0.26	0.30	0.30	0.28
MnO	0.01	0.01	0.01	0.01
MgO	1.73	1.77	1.71	1.73
CaO	1.71	1.75	1.75	1.69
Na_2O	0.01	0.03	0.03	0.02
Cr_2O_3	0.02	0.03	0.03	0.03
NiO	0.02	0.00	0.00	0.00
Sum	7.95	8.01	7.99	7.95
Fe	07	08	08	08
Mg	47	46	46	46
Ca	46	46	46	46

TABLE 8. Plagioclase of 579.

	579A		579B		579C		579D
SiO_2	44.80	44.71	45.17	44.73	44.71	45.23	No Plagio-
TiO_2	0.00	0.00	0.00	0.00	0.00	0.00	clase
Al_2O_3	36.11	35.88	35.52	36.21	36.32	36.41	analyzed
FeO*	0.30	0.39	0.19	0.20	0.20	0.15	
MnO	0.00	0.00	0.00	0.00	0.00	0.00	
MgO	0.02	0.03	0.02	0.00	0.02	0.01	
CaO	18.71	19.20	19.21	19.11	18.99	18.85	
Na_2O	0.85	0.81	0.66	0.63	0.63	0.62	
	100.79	101.07	100.75	100.89	100.67	101.27	
Stoichiometry - 32 oxygens							
Si	8.24	8.19	8.28	8.19	8.19	8.21	
Ti	0.00	0.00	0.00	0.00	0.00	0.00	
Al	7.81	7.75	7.67	7.81	7.83	7.81	
Fe	0.05	0.13	0.03	0.08	0.08	0.02	
Mn	--	--	--	--	--	--	
Mg	--	--	--	--	--	--	
Ca	3.67	3.77	3.77	3.75	3.70	3.67	
Na	0.30	0.29	0.23	0.22	0.22	0.22	
	20.07	20.13	19.98	20.06	20.02	19.94	
An	92	93	94	94	94	94	

TABLE 9. Alteration of plagioclase to hydrogrossular, 579A

	Plagioclase An_{90}	1	2	3	4	Hydro-grossular
SiO_2	44.80	44.70	38.60	36.70	35.50	37.15
TiO_2	0.00	0.00	0.00	0.00	0.00	0.00
Al_2O_3	36.11	35.9	28.1	27.10	25.10	24.03
FeO*	0.30	0.39	2.52	5.87	6.56	12.65
MnO	0.00	0.00	0.24	0.22	0.23	0.48
MgO	0.21	0.03	2.04	3.41	2.51	3.53
CaO	18.71	19.20	22.9	20.14	20.65	13.59
Na_2O	0.85	0.80	0.02	0.03	0.11	0.01
	100.79	101.80	94.39	93.45	90.64	91.43

Table 10. Accessory phases of the 579 sequence.

	AMPHIBOLE						PREHNITE
	$579A_1$	$579B_2$	$579B_2$	$579C_2$	$579C_3$	$579D_3$	579C
SiO_2	42.78	51.32	51.21	52.17	45.36	45.49	43.17
TiO_2	2.13	0.14	0.10	0.17	1.01	0.74	0.00
Al_2O_3	13.56	7.20	6.85	2.92	12.61	11.96	24.94
FeO*	8.32	6.09	5.79	5.91	8.57	7.03	0.09
MnO	0.08	0.03	0.05	0.16	0.07	0.07	0.01
MgO	14.99	18.25	18.88	15.49	14.85	17.18	0.03
CaO	12.02	12.01	11.57	20.46	11.34	11.22	25.98
Na_2O	2.57	0.87	0.97	0.20	2.04	1.68	0.03
Cr	0.69	0.04	0.02	0.17	0.20	0.43	0.01
Ni	0.04	0.00	0.03	0.04	0.05	0.04	0.00
Sum	97.18	95.95	95.47	97.69	96.10	95.84	94.23

[1]Associated with plagioclase + clinopyroxene.

[2]Associated with orthopyroxene.

[3]Associated with clinopyroxene.

granoblastic, recrystallized from adcumulate. Most clinopyroxene has rounded, lobate borders, indicating late growth and re-equilibration. Plagioclase (An_{90-93}) is intercumulus, comprises about six percent of the rock, is complexly twinned, and shows little evidence of deformation. The feldspar is partly altered to dark brown hydrogrossular and chlorite. This alteration commences at the center of the plagioclase grain, rather than migrating inward from the edges. The alteration (Table 9) progressively depletes feldspar in SiO_2 and Al_2O_3 and enriches it in FeO*, MnO, and MgO until a seemingly uniform end-member hydrogrossular composition is achieved. CaO varies during the alteration process, increasing at intermediate stages.

Olivine (Fo_{75}) is strongly deformed in 579A. Usually it is kneaded into interstitial positions from a probable euhedral configuration. Strain features such as glide twinning are present but not abundant, suggesting that deformation occurred at high temperatures under conditions of plastic flow (Gueguen and Nicholas, 1980).

Orthopyroxene (En_{77}) is nearly euhedral, corroded, and faintly pleochroic. It averages 0.7 mm in diameter. Clinopyroxene is slightly later in crystallization, subhedral, about the same size as orthopyroxene, and is not zoned. Probe traverses and energy dispersive analysis scans (EDS) of clinopyroxenes in 579A indicate that although slight variations in composition are present, no systematic zonation occurs (Table 7).

Amphibole (Table 10) is a clear to light green late magmatic phase, rims some clinopyroxene, and forms boundaries between

clinopyroxene and plagioclase, or between plagioclase and sulphide. The amphibole is a high Al_2O_3 hornblende, with as much as two percent TiO_2, 0.7 percent Cr_2O_3, and 2.6 percent Na_2O.

Primary sulfides constitute 1.1 percent of 579A, but are absent in other layers of this sequence. They contain up to three percent NiO and are a significant phase.

In 579B, overall textures and mineral relations are similar to 579A. The principal difference is the variation in modal abundance between layer A and layer B. In 579B, plagioclase is much more abundant, and the texture is more nearly adcumulate. Plagioclase is very calcic (An_{92-94}), undeformed, and complexly twinned. Its alteration is similar to that in 579A.

Olivine and sulfide are absent in 579B. Orthopyroxene is euhedral and somewhat larger (1.0 mm) than in 579A. It is also slightly more magnesian (En_{75-82}) than in 579A, with an En_{80} average. Clinopyroxene is similar in texture and size to 579A. It is slightly more magnesian and less calcic, and contains substantially less TiO_2.

Amphibole, which forms reaction rims between plagioclase and orthopyroxene in 579B, is an iron-rich tremolite. It is high in SiO_2 (51-52.5 percent), and is post-solidus.

Sample 579C has similar recrystallized adcumulate textures to samples 579A and 579B, and contains no olivine. The grain size is slightly smaller than in other layers, averaging 0.5 mm. Plagioclase (An_{91}) is uniform in composition, complexly twinned, and partly replaced by hydrogrossular and chlorite from the center outward. Orthopyroxene (En_{75-80}), is very noticeably rounded and corroded.

Clinopyroxene is more euhedral in this rock than in others. Its composition is nearly identical with 579B, except for possibly slightly higher Cr_2O_3 and Na_2O. It is unzoned. Amphibole forms as a reaction between clinopyroxene and plagioclase. Its low SiO_2 content (45 percent) and moderate concentrations of Al_2O_3, FeO*, and CaO classify it as a hornblende.

Sample 579D is the most altered and deformed of the sequence. It is an olivine websterite, with less than one percent plagioclase. Plagioclase composition could not be accurately determined due to pervasive alteration. Olivine (Fo_{80-81}) is very strongly deformed. Orthopyroxene (En_{82}) is homogeneous and its more magnesian character is in keeping with the higher Fo content of olivine. Clinopyroxene is less iron-enriched, contains slightly less CaO and slightly more Al_2O_3 than 579B or 579C.

Overall, clinopyroxene of the 579 sequence is more enriched in CaO than clinopyroxene in the Skaergaard trend (Figure 7). Both clinopyroxene and orthopyroxene in the lower two layers of the sequence (579D and 579C) become more iron rich, and ties for pyroxene pairs are nearly parallel. However, pyroxenes of the next layer (579B) reverse this trend, and increase in MgO and CaO. Sample 579A, the top layer, contains pyroxenes which are slightly more enriched in FeO*, and show a return to normal major element fractionation.

Major oxide compositions of olivine, orthopyroxene, clinopyroxene, and plagioclase in the 579 sequence (Figure 8) generally show trends expected in a differentiating magma. Fo of olivine

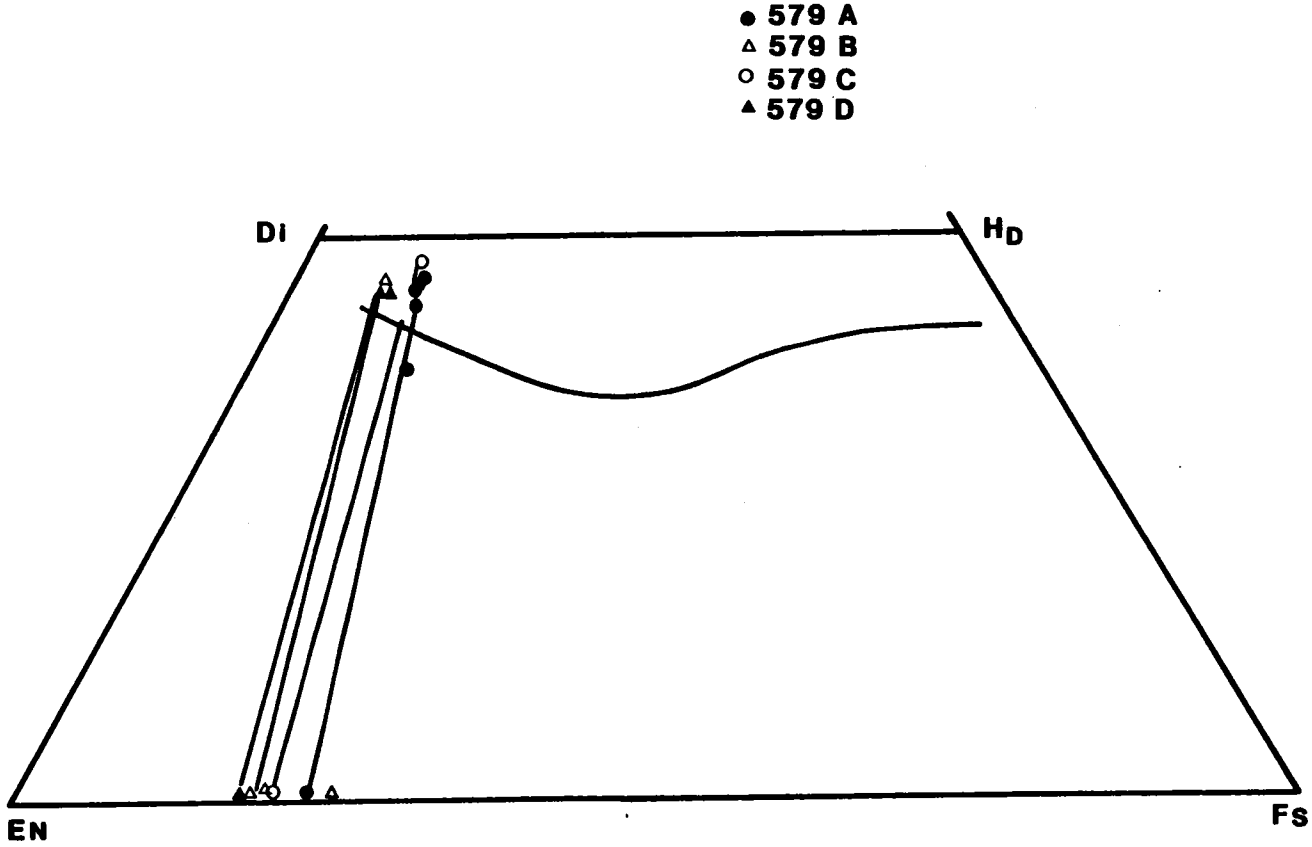

FIGURE 7. Pyroxene quadrilateral of the upper transition zone.

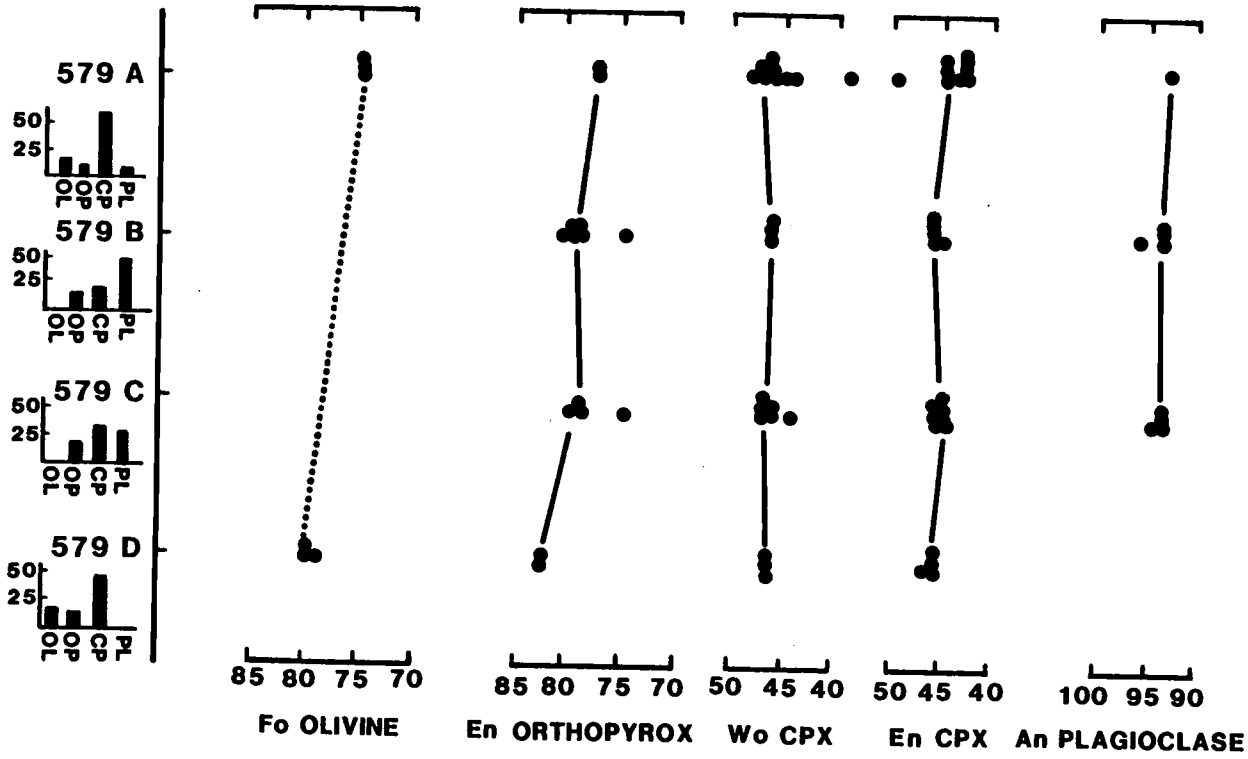

FIGURE 8. Cryptic variation of major constituents in minerals of the upper transition zone, Celebration Ridge.

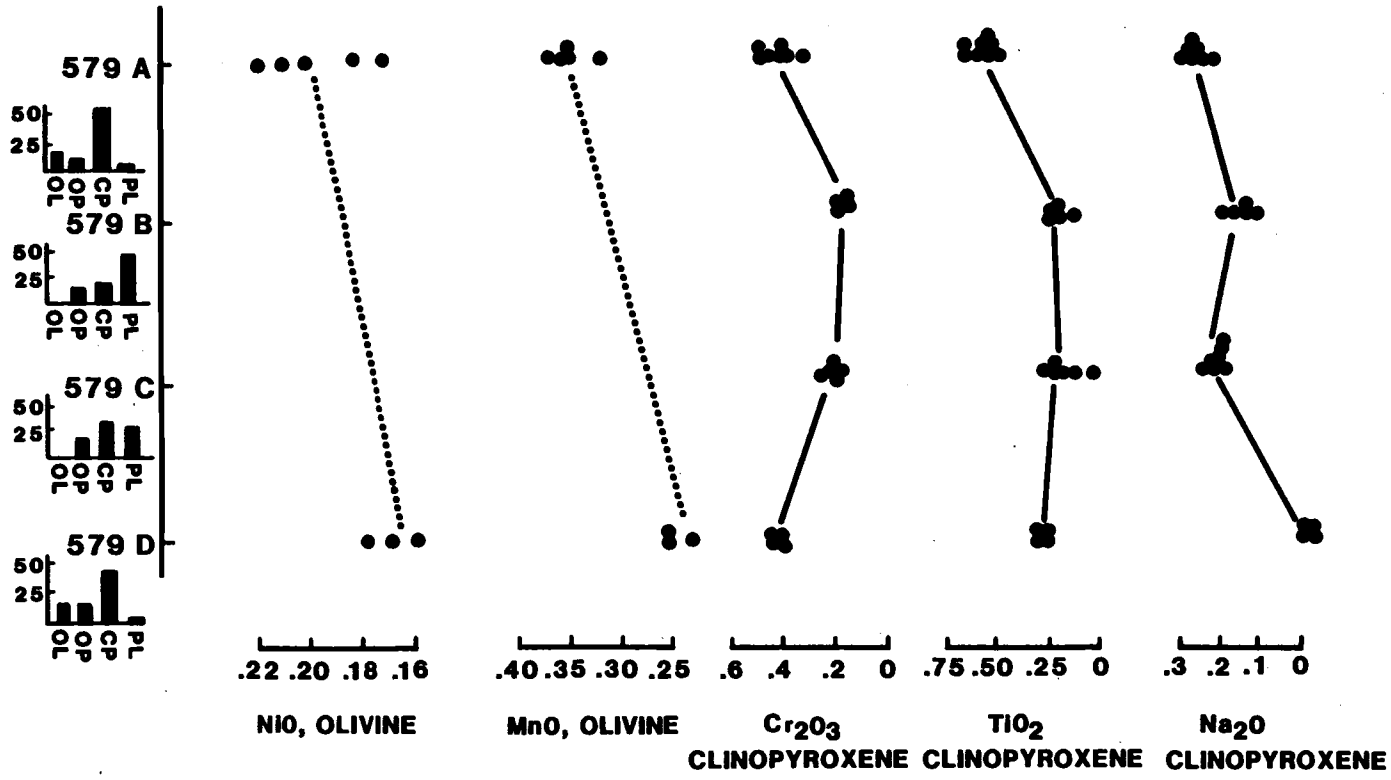

FIGURE 9. Cryptic variation of minor oxides in minerals of the upper transition zone, Celebration Ridge.

increases, En of orthopyroxene decreases, and the An content of plagioclase decreases slightly.

Minor element variation in minerals of the upper transition zone sequence (Figure 9) has seemingly contradictory trends. MnO increases in olivine at the top of the sequence, as would be expected. However, NiO also increases, which is incompatible with simple fractionation. In clinopyroxene, TiO_2 and Cr_2O_3 decrease upward through the lower three units, then increase dramatically in the top olivine websterite. The increases in NiO, Cr_2O_3, and the abrupt increase in TiO_2 for the upper layer are inconsistant with continuous fractionation, and can be best explained by the influx of a more primitive and possibly picritic, magma.

Mineralogical Considerations for Transition Zone Crystallization

In summary, the 569 sequence shows phase and subtle cryptic variation in major and minor constituents over a short stratigraphic distance in keeping with a cumulate origin of all four layers. Variations in modal proportions of minerals and abrupt changes at layer boundaries may be maintained by growth mechanisms such as double diffusive convection (Irvine, 1980), but probably originated due to changes in conditons of crystallization such as increases of P_{H_2O} rather than gradual fractionation. The abrupt change from 579A olivine websterite to the two-pyroxene gabbro of 579B could be accomplished by an increase in P_{H_2O} which would shift equilibria from the olivine-orthopyroxene field to orthopyroxene-diopside crystallization in the olivine-diopside-quartz system (Kushiro, 1969).

Minerals of the transition zone have slight cryptic variation which is compatible with fractionation or precipitation from a liquid of gabbroic composition. In the four layer sequence investigated, with increased stratigraphic height in the first three layers olivine disappears, and the En of orthopyroxene decreases slightly. Plagioclase, however, becomes very slightly more calcic upward, and clinopyroxene of 579C is slightly more enriched in Ca and Mg than in the two layers below. Hence, major oxide variation is not completely regular and suggests that accumulation of the upper transition zone was not a simple process.

Minor elements indicate that a model of continuous, simple, closed system fractionation is incorrect. Although the increase in MnO of the upper, 579A olivine is compatible with its higher stratigraphic position and higher iron content, the increase in NiO of this olivine, and the increase in Cr_2O_3 of 579A clinopyroxene requires replenishment of the magma in these components. Because the entire spectrum of major and minor elements is not reset, and TiO_2 and Na_2O continue to increase in the minerals, fractionation of the magma probably continued with periodic injection and enrichment by small quantities of mafic liquid. A picritic magma, or, more likely, melts of a clinopyroxene-rich source are possibly sources for the observed variations.

The Zone of Infiltration

Previous workers (Thayer, 1977; Dungan and Ave Lallemant, 1977; Himmelberg and Loney, 1980) have noted that gabbro and pyroxenite dikes intrude the tectonite harzburgite. Systematic mapping of gabbro dikes for this thesis has shown that they occur in a zone 3.5 km wide which trends northeast through the central portion of the harzburgite, and includes a pod of gabbro approximately 25 m wide enclosed within the basal harzburgite (the gabbro of Gwynn Gulch). The zone of infiltration is shown on Plates 1 and 2. The distribution and quantity of the dikes and associated feldspathic harzburgite are remarkably symmetrical, and suggest that the zone of infiltration is a significant feature of the Canyon Mountain complex rather than simply the result of random intrusion.

Dikes within this zone vary in width from less than one millimeter to more than two meters. Generally they crosscut the harzburgite fabric, but have no preferred orientation. Where not obscured by rodingization, their mineralogy is nearly identical. They are olivine-two pyroxene gabbro, with clinopyroxene the dominant mafic phase. Their major and minor element geochemistry varies slightly, but indicates that they are relatively unfractionated.

Because overall exposure of bedrock is poor within the zone of infiltration, a quantitative estimate of dike distribution could not be accurately based upon number of dikes per square meter. However, where there is no bedrock exposure, gabbro from dikes or veins is commonly present as float that usually weathers into pieces with

widths approximately the same as the dike from which they originated. Float may be narrower than the dike, but is unlikely to be wider. Hence, instead of the quantity of dikes per unit area, the maximum width of dikes, or float from dikes, was used as an index of gabbro abundance. It should be noted that where wide dikes occur, narrower dikes and veinlets are present also.

Units of the Zone of Infiltration

The sub-zones distinguished in mapping dike distribution are shown on plates 1 and 2. They are:

Zone A. Gabbro, feldspar, and/or clinopyroxenite veinlets less than one cm wide, or feldspathic harzburgite. (Presence of any feldspar or altered feldspar in harzburgite, including isolated individual blobs, was criteria for inclusion of a rock in this zone.)

Zone B. Gabbro veins one to ten cm wide.

Zone C. Gabbro dikes greater than ten cm wide.

Zone D. Gabbro dikes greater than 20 cm wide, forming ten percent or more of the exposures.

Zone A

The outermost zone (Zone A) contains only thin veinlets of gabbro (clinopyroxene + feldspar), feldspar or clinopyroxene. Feldspathic harzburgite, which may contain as much as 35 percent plagioclase, or as little as a single 0.1 mm bleb of feldspar in a square meter of depleted, foliated peridotite, was also mapped as this zone. The

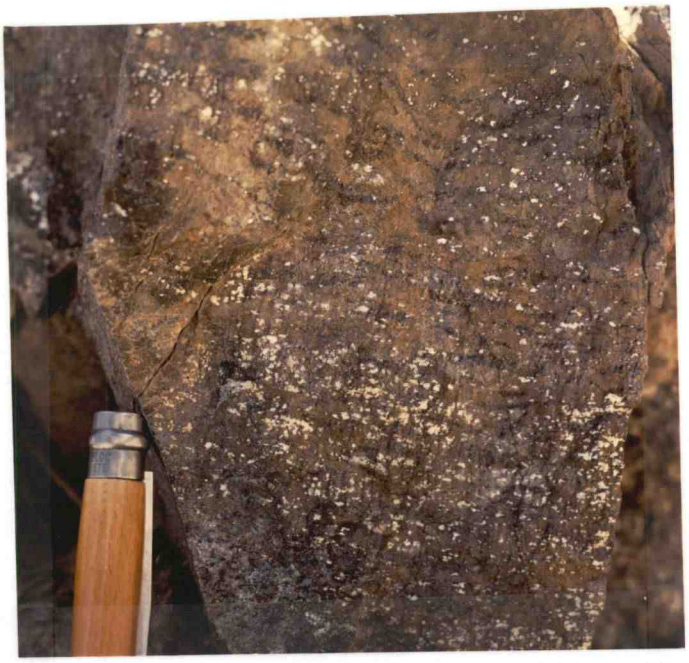

Feldspathic harzburgite, Zone A. East side of Pine Creek

Early and late gabbro veins in harzburgite, Zone B, Baldy Mtn.

FIGURE 10. Lithologies of the Zone of Infiltration.

transition from unaffected harzburgite to zone A is gradual. Blobs of feldspar and thin veins increase slightly in abundance inward from the localities where they were first noted. Significantly, early veins are commonly contorted and may be oblique to peridotite foliation; later veins follow fractures and crosscut early gabbros as well as harzburgite fabric. This relation suggests that early gabbros were present while the harzburgite was mushy or at least behaved in a very plastic manner, and that later gabbros intruded after discrete fractures or cleavages formed in a more solid mass. However, as far as has been determined, there is no significant mineralogical or geochemical difference between early and later gabbro.

Many veins in zone A are discontinuous. They may persist for only a few cm, or may extend, especially where they follow a fracture, across the width of available exposure. Larger veins within this zone have sharp, serpentinized boundaries. Commonly, smaller veins, or early, contorted veins are fringed by feldspars which decrease in abundance away from the vein, and may be elongate either parallel or oblique to harzburgite foliation.

Feldspathic harzburgite is widespread in zone A. Feldspar may occur in broad, layer-like zones, or may be restricted to rare, isolated single lobate blobs (see Figure 10). Where gabbro dikes are large, with straight boundaries, and appear to follow fractures, dispersed feldspar is less common than where gabbro veins are more irregular.

There is a broad range of texture in feldspathic peridotite, from very fine-grained (0.1 mm), evenly dispersed plagioclase, to

irregular, large (> 1 cm) plagioclase and clinopyroxene, which may occur in either harzburgite or dunite. In some dunite, plagioclase and clinopyroxene are intimately associated. Finely dispersed textures are generally confined to bands which may crosscut or parallel foliation, or are adjacent to larger (± 2 cm) gabbro veins.

Plagioclase grains, in outcrop, may trail off along foliation, even where veinlets cross foliation. Smaller plagioclase are aligned with clinopyroxene in discontinuous veinlets, or may form aggregates up to five mm wide. There is no notable "depleted" zone around veins, and very little clinopyroxene in peridotite.

In thin section, the feldspar dispersed in peridotite is lobate and occasionally cuspate, and is pervasively altered to a brown to white isotropic mat of chlorite and hydrogrossular. Twinning is complex, but the plagioclase is not notably deformed. Where composition of feldspar could be determined via Michel-Levy rotation, the plagioclase is An_{91-97}. Feldspars may have thin reaction rims of red-brown to pink amphibole, especially where they are adjacent to orthopyroxene or chrome-spinel. Optically these amphiboles are similar to those described in Gwynn Gulch and other gabbro, and are probably a chrome-rich hornblende.

The dispersed feldspar in tectonite harzburgite, where not strongly altered, shows little evidence of strain. It may follow or crosscut foliation. Although spinel is adjacent to much plagioclase, in none of the thin sections did it core or rim a plagioclase, or seem to be converting from spinel to plagioclase as might be expected if decreasing pressure and consequent phase

transformation were responsible for the generation of plagioclase. Rather, amphibole reaction rims occur at rare contacts of plagioclase and spinel grains in harzburgite.

In contrast to the unstrained but altered isolated feldspar and clinopyroxene crystals within harzburgite, minerals in small gabbro veins are deformed as well as hydrated. Both feldspar and clinopyroxene are granulated and sheared; plagioclase twin lamellae are bent. The veins obviously did not escape deformation during late plastic flow or emplacement of the harzburgite. Plagioclase is altered to hydrogrossular + chlorite, and clinopyroxene is bordered by red-pink amphibole as well as rimmed and replaced by acicular tremolite. Hence, the gabbro veins do not show any contact effects with the host peridotite, and they display effects of fairly high temperature alteration. The veins, as well as individual, isolated crystals were probably hydrated and rodingized at the same time that serpentinization occurred.

Many clinopyroxenite bands and websterite dikes parallel to foliation have a border of depleted, pyroxene-free dunite which may be one centimeter or more wide, and probably represents contribution of the harzburgite to the websterite band. This contrasts markedly with the gabbro veins which do not have a depleted zone adjacent to them. Instead, feldspar and clinopyroxene increase in abundance with proximity to the vein (Figure 10) and may be emplaced from the gabbro <u>into</u> the peridotite. Hence the clinopyroxenite websterite bands and dikes, and the gabbro veins seem to represent different events or episodes of magmatism - the pyroxenites from an early

squeezing out of still slightly fertile peridotite (Nicholas and Jackson, 1982) or cumulate episode (Thayer, 1963), and the gabbro from intrusion into the harzburgite.

Zone B

The width of gabbro dikes generally increases inward from the A zone. Dikes with a width of up to 10 cm were mapped as zone B. The gabbro mineralogy, alteration, and field relations are similar to narrower dikes in zone A. Generally, the dikes tend to follow fractures and have straight boundaries. Feldspathic harzburgite is not as common in zone B as in zone A.

Zone C

Zone C contains rather broad dikes, greater than ten cm wide. The dike mineralogy and textures are similar to those of zones B and A. Deformation is notable in thin sections. The gabbro has been slightly rodingized and hydrated at elevated temperatures.

Dikes in zone C, and some even broader dikes in zone D, are banded, or "layered" parallel to their borders (Figure 11). This banding might be construed as of either cumulate or flow origin. The gabbro in dikes does not have a flow lamination, per se, as do the upper level gabbros of Pine Creek Mountain. Dike texture is essentially deformed adcumulate, rather than hypidiomophic- or panidiomophic-laminar. However, they are constricted in that magma in dikes cannot move or be removed via filter-pressing upward in the same manner as cumulates in larger chambers.

Banded dikes, Zone D, north side of Baldy Mountain

Dikes enclosing harzburgite, Zone D, north side of Baldy Mountain

FIGURE 11. Gabbro dikes in the Zone of Infiltration.

A proposed mechanism for the origin of banding is as follows (Figure 12): 1) flow banding segregated mafic and felsic constituents; 2) the melt stagnated, 3) long, slow cooling within a peridotite at some depth allowed diffusion of last melt to minerals. This mechanism is similar to Irvine's diffusive convection (1980) but occurs on a smaller or more limited scale. Texture and composition of a rock formed in this manner would differ somewhat from a cumulate in a large chamber because melt could not readily be removed or reequilibrated with overlying magma.

An additional possibility is that partly solidified dikes were forcefully injected with more gabbroic magma of similar composition. If this process occurred, some dikes might contain xenoliths of banded gabbro in a more isotropic matrix. Indeed, this process of periodic injection of similar magma will be suggested for the gabbro of Gwynn Gulch. This gabbro does contain autoliths of lineated gabbro in an isotropic matrix. Although smaller scale analogies were not observed in any dikes, this process of continued injection of primitive magma into a mushy, partly solidified dike is another probable mechanism for generation of layered dikes which might account for strain effects evident in larger dikes.

Zone D

In zone D, gabbro occurs in dikes greater than 20 cm wide, and forms more than ten percent of visible outcrops. This zone occurs in two localities: the south side of Baldy Mountain, and in the northwest part of the zone of infiltration, east of Pine Creek. On Baldy

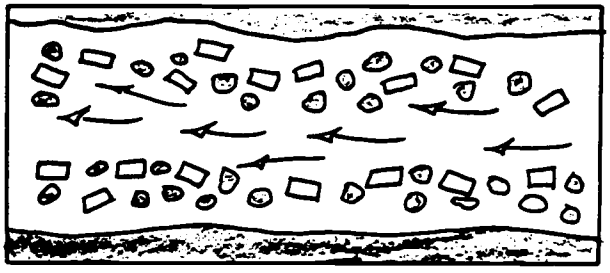

A. Segregation in crystal mush flow.

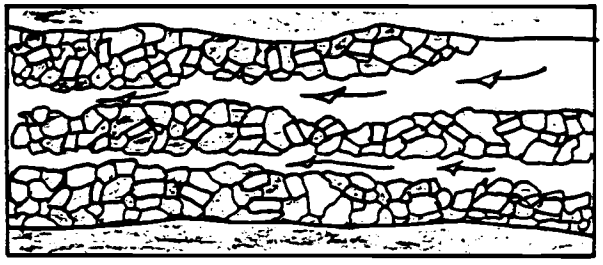

B. Intrusion into mostly solidified gabbro.

FIGURE 12. Mechanisms of layered dike development.

Mountain, dikes crisscross both one another and foliation, and form anastomosing clusters in which gabbro may be more than three meters wide and contain inclusions of harzburgite (Figure 11). Upward, the dikes pinch out. Some gabbro dikes change into pyroxenite along their length. The base of Baldy Mountain and the probable contact of harzburgite and gabbro or transition zone rocks is completely covered with talus - much of which contains gabbro - and the question of whether this zone of dikes originated from a larger body of gabbro cannot be resolved. The D-zone to the east of Pine Creek, however, is not associated with any known, larger gabbro body, and must represent a locus of dike concentration.

Origin and Significance of the Zone of Infiltration:

Gabbro of the zone of infiltration is typically olivine - two pyroxene gabbro with abundant clinopyroxene and little modal orthopyroxene and olivine (Table 11, sample 110G). Plagioclase is very calcic. The layering in wide dikes indicates magmatic flow, and the increasing mafic content along dikes which narrow upward on Baldy Mountain suggests that filter-pressing and forceful injection were operative.

There are at least three, and possibly four generations of gabbro dikes in the tectonite harzburgite.

1. The earliest dikes have irregular boundaries, "bleed" into the surrounding harzburgite, and are plastically deformed. They were probably emplaced into a crystal mush, or highly plastic peridotite.

2. The second generation of dikes have straight boundaries, and were emplaced into fractures which crosscut foliation in the harzburgite. They have mineral foliation which parallels the harzburgite. Boundaries of these dikes may be offset along foliation. They were emplaced into fractures while the harzburgite experienced ductile shear.

3. A third generation of dikes have banding or layering parallel to their straight edges. They were intruded forcefully into fractures in brittle peridotite after deformation ceased, and developed layering by flow segregation or repeated injection of phyric magma.

4. The last intrusives are isotropic gabbro in dikes which crosscut or parallel foliation of the harzburgite. These dikes may be the same generation or later than #3.

This chronology of dike emplacement and similar mineralogy of all gabbro dikes examined indicates that gabbro of very similar composition was emplaced throughout much of the cooling and deformation history of the harzburgite.

The following considerations are germane to understanding the origin of these dikes: 1) There is no zone of depletion around the gabbro dikes, as there is adjacent to very early pyroxenite bands in harzburgite. Instead, feldspar and clinopyroxene are enriched near the edges of early veinlets and deformed dikes, and decrease in abundance with distance from the dike; 2) Veinlets and dikes crosscut tectonite fabric; 3) There are no "fertile" phases in this peridotite except clinopyroxene and plagioclase; 4) Composition of all dikes seems uniform, and similar to gabbro of Gwynn Gulch; 5) Importantly, spinels in chromitites within the zone of

infiltration are high Al_2O_3 varieties. Elsewhere in the Canyon Mountain complex they are chrome-rich.

Structural studies of the Canyon Mountain complex by Misseri and Boudier (pers. comm., 1982) are also important to consideration of the origin of the zone of infiltration. Detailed structural petrography coupled with field work has shown that the Canyon Mountain complex tectonite harzburgite consists of two diapiric structures - one on the east and one on the west - with steep foliation and lineation. Between these areas, and coincident with the infiltration zone mapped on the basis of gabbro dike distribution, the structure of the harzburgite flattens. Consequently, it seems that the intrusion of gabbro may have significantly affected the peridotite- or was channeled by peridotite structure at a very early stage in the history of the Canyon Mountain complex, while the peridotite behaved plastically or as a mush.

Gabbro of the infiltration zone is not considered to originate through partial melting of the harzburgite of the Canyon Mountain complex for the following reasons:

1) No fertile components, or trace of fertile components (e.g., feldspathic harzburgite or pyroxene-feldspar veins) occur in harzburgite east or west of this zone. Pyroxenite bands are present, and probably represent "sweating out" or reorganization of original ultramafic rock. It is considered unlikely that mantle peridotite fertile enough to produce the quantity of gabbro in the zone of infiltration could have all feldspathic melt removed, even by repeated episodes of partial melting.

2) No zone of depletion occurs around gabbro veins to indicate migration out of the peridotite and into the vein as is present at Lanzo (Boudier and Nicholas, 1977) and Ronda (Dickey, 1975), or in early CMC websterite veins. Instead, a "zone of enrichment" is present, suggesting migration of feldspathic components from the dike into host peridotite.

3) In Lanzo (Boudier and Nicholas, 1977; Nicholas and Jackson, 1982) and other fertile massifs where partial melting can be demonstrated - gabbroic melt and veins - especially of early stages of partial melting - are parallel to foliation of the parent peridotite. In contrast, gabbro dikes of the Canyon Mountain complex zone of infiltration commonly cross-cut the harzburgite fabric.

4) Spinel or garnet do not apparently contribute to plagioclase or clinopyroxene. Where Cr-spinel occurs adjacent to plagioclase in the harzburgite the two phases are separated by a reaction rim of Cr-rich amphibole or clinopyroxene. Hence partial melting in not due to phase transformation at lower pressure, as is true of the fertile massifs cited above. The mineralogy of the harzburgite is stable at low pressure.

5) Isolated feldspars are not deformed, and were not greatly effected by plastic flow or deformation in harzburgite, although in some rocks they occupy "pockets" (Himmelberg and Loney, 1980) parallel to foliation.

6) Early, contorted gabbro veins most commonly enrich adjacent peridotite in gabbroic melt (feldspar and clinopyroxene) and intruded mushy or very plastic harzburgite. Larger and later veins which

crosscut them intrude through discrete fractures - which indicates that with time the peridotite cooled and behaved in a more brittle manner, despite the presence of an increased proportion of gabbro. If partial melting was responsible for production of the gabbro, the reverse sequence might be expected - brittle, followed by increasingly plastic behavior as the proportion of melt increased and temperature either increased or, for partial melting at decreasing pressure, remained constant.

Nicholas and Jackson (1982) proposed a three-stage model for sequential intrusion of dikes produced by partial melting of peridotite: 1) dikes emplaced prior to plastic deformation, including pyroxenite dikes; 2) dikes emplaced during shear flow. These would be parallel to the shear flow plane and the foliation; 3) later dikes which crosscut foliation emplaced by hydrofracting of gabbroic magma under pressure.

However, it is questionable whether a peridotite which contained a large amount of partial melt at high temperature would be brittle enough to fracture <u>across</u> a strongly developed foliation.

Waff and Holdren (1981) have shown that grain boundaries in mantle nodules do not contain residual melt, and the lava which transported the nodules to the surface did not penetrate the xenoliths. Dry intergranular surfaces are stable and resist wetting. Hence, intergranular introduction of melt is inhibited. Therefore, a refractory layer in the upper mantle would be impervious to magma injection <u>via</u> grain-boundary wetting, and some mechanism such as the propagation of fractures is necessary for magma transport. Such

fracturing could occur for the model of Nicholas and Jackson (1982) due to hydrofracting during early melt generation, and in the Canyon Mountain complex it could occur in the zone between two rising mantle diapirs, or could be developed by migration of a volatile phase which was an early stage of melt infiltration. Volatiles (H_2O) might account for the occurrence of Cr-rich amphibole and the ubiquitious alteration of feldspar in the ultramafic rocks. If infiltration occurred during serpentinization, volatiles would be abundant, as would strain effects due to harzburgite volumetric increase.

The fact that gabbro from all generations of Canyon Mountain complex gabbro dikes is virtually identical in composition, and does not show any systematic change in major or trace element composition from early to late dikes suggests that the gabbro in the infiltration zone was supplied from a large external source, and not generated by partial melting of this harzburgite.

Field relations shown on Plate 2 and discussed above suggest that the gabbro dikes of the zone of infiltration directly feed and blend into the principal gabbro of the Canyon Mountain complex. Although this relation cannot be unequivocally demonstrated in the field, the absence of a well-defined transition zone stratigraphically above the center of the zone of infiltration, and the apparent envelopment of the limited amount of transition zone rock by gabbro attest to the abundance of gabbro and lack of precipitation in this area. The influx of a primitive magma through this zone would

yield both effects. Primitive gabbro would probably not fractionate immediately, hence there would be a few cumulates or transition zone rocks in the area where the gabbro entered the chamber, and a better developed transition zone farther away. An influx of magma might also envelope whatever precipitates did accumulate.

The mineralogical composition of gabbro within the dikes presented above and the chemical data discussed in subsequent sections of this work also indicate that the gabbro within the dikes is mostly a primitive composition from which the principal CMC gabbro units are derived by fractional crystallization to produce the main CMC gabbro and much of the transition zone cumulates. Thus, the dikes in the zone of infiltration represent conduits or passages through which gabbro entered the CMC magma chamber, rather than downward injections of fractionated magma.

Gabbro of the Canyon Mountain Complex

Cumulate gabbro which lacks identifiable tectonite fabric comprises approximately one-third of the Canyon Mountain complex. The gabbro includes a variety of lithologies: olivine, two-pyroxenes; two-pyroxenes; norite; and quartz norite, a variety of textures from adcumulate to panidiomorphic and flow laminated, and a variety of alterations, from pristine through plagioclase→hydrogrossular, to "epidiorite" (Thayer, 1972) with amphibole replacing pyroxene, and chlorite in plagioclase. Most gabbros contain orthopyroxene, contrary to the majority of ophiolites.

Field evidence was sought for the occurrence of multiple gabbroic magmas. However, no field evidence for separate intrusions of major gabbro units was found. Although four gabbro units are described below, the contacts between them are gradational over a hundred meters or more, and the gabbro represents a single, differentiated sequence. The four units identified on the basis of field and petrographic evidence are discussed below.

Gabbro of Gwynn Gulch

The gabbro which occurs in Gwynn Gulch is very limited in extent (see Plates 1 and 2) but is among the most significant rocks of the complex. This gabbro is best exposed in low logging road cuts on the west side of Gwynn Creek, at an elevation of approximately 4600 feet (1400 m), in the NW 1/4, sec. 7. Small outcrops and float occur along the nearly E-W strike on hills west of this locality, indicating that the gabbro extends in a thin lens, east-west, parallel to harzburgite foliation. The band of gabbro of Gwynn Gulch is at least 25 meters wide and extends for at least 300 meters along strike. This gabbro is "rimmed" by about five meters of coarse clinopyroxenite. Float of interlayered gabbro and peridotite was collected along Gwynn Creek, but no outcrops of this rock were noted. The contact of gabbro, pyroxenite, and layered sequence with the enclosing harzburgite is not exposed.

The gabbro of Gwynn Gulch varies in texture, although its mineralogy (and geochemistry) is uniform. Two types of gabbro

occur: 1) coarse (5-7 mm) lineated gabbro which plunges steeply northeast, and is folated and layered E-W, parallel to the enclosing harzburgite, and 2) medium-grained (0.5-3 mm) isotropic gabbro. This mixture of lineated and isotropic gabbro suggests that deformation occurred prior to solidification and/or final emplacement of all gabbro. Because early gabbros which are deformed (665) have virtually the same composition and geochemistry as later, isotropic gabbro (666) and no differentiation is evident, the magma of Gwynn Gulch must have been replenished by melt of composition similar to the early magma.

The gabbro of Gwynn Gulch is an olivine, two-pyroxene gabbro (Figure 13) with small amounts of early olivine. Textures are adcumulate. The rock contains three to twelve percent olivine (Table 11) up to two mm in diameter, lobate to anhedral, somewhat corroded, and usually interstitial although occasionally enclosed in clinopyroxene. Optic figures suggest a composition of Fo_{75-80}. In unaltered gabbro, olivine is fresh, and shows faint glide twins. Where adjacent to plagioclase, olivine may have thin rims of clinopyroxene.

Orthopyroxene is non-pleochroic, less abundant (four to twelve percent) than olivine or clinopyroxene, interstitial to anhedral, and shows fine, deformed exsolution lamellae. Optic figures suggest that orthopyroxene is bronzite, approximately En_{80}. Orthopyroxene appears to be slightly later than olivine.

Clinopyroxene, comprising 38-48 percent of the Gwynn Gulch gabbro, is anhedral to lobate or cuspate in form, has only limited

Sample 666. Gabbro of Gwynn Gulch
X 20

Sample 540. Gabbro of Table Camp
X 20

FIGURE 13. Olivine, two-pyroxene gabbro of Gwynn Gulch and Table Camp.

Table 11. Modal analyses of gabbro

	GG		BSR		TC		Pine Creek Mountain					Dikes
	666	665	626	629	95	540	708	707	713	714	335	110G
Olivine	12.2	3.1	--	--	4.3	3.8	--	--	--	--	--	1.0
Orthopyroxene	12.6	8.5	2.3	1.3	6.7	7.5	17.8	21.2	19.1	16.9	20.6	3.1
Clinopyroxene	47.1	43.4	31.5	12.4	36.2	39.1	25.7	19.6	17.1	14.7	16.4	29.1
Plagioclase	18.9	4.7	15.7	10.1	41.9	38.7	46.2	51.9	52.4	61.3	59.7	16.9
Hornblende	3.2	3.1	5.8	1.7	1.2	1.6	2.5	3.7	17.2	2.8	1.2	--
Chlorite	--	17.9	12.9	31.6	3.1	6.2	6.2	2.4	2.5	1.9	0.6	28.3
Actinolite	--	5.4	2.9	18.4	--	--	--	--	--	--	--	--
Hydrogrossular	4.2	8.6	28.7	24.5	5.7	3.1	--	--	--	--	--	21.3
Serpentine	1.1	4.1	--	--	--	--	--	--	--	--	--	0.3
Fe-oxide	0.7	1.2	0.2	--	0.9	--	1.4	1.2	1.7	2.1	1.1	tr
Sulfide	--	--	--	--	--	--	0.2	--	tr	--	0.4	--
Apatite	--	--	--	--	tr	tr	tr	tr	tr	0.3	tr	--
Quartz	--	--	--	--	--	--	--	--	--	--	tr	--
TOTAL	100.0	100.0	100.0	100.0	100.0	100.0	100.0	100.0	100.0	100.0	100.0	100.0

exsolution, and is relatively undeformed. It encloses both olivine and orthopyroxene, hence crystallized fairly late. It has a 2V of about 55° based on optic axis figure estimates, suggesting a diopsidic composition.

Plagioclase (An_{85-92}) is strongly and complexly twinned, and subhedral in shape. Zoning was not noted. Plagioclase probably enlarged by adcumulus growth. It occurs between mafic phases. Where two feldspars join, their grain boundaries are straight. The absence of apparent zoning may indicate either that a uniform magma composition was maintained by exchange with crystals near the top of a growing pile, or that pervasive recrystallization re-equilibrated the gabbro of Gwynn Gulch.

Late magmatic amphibole replaces and rims mafic phases (most commonly, clinopyroxene), and also forms interstitial patches between grains. It may completely enclose plagioclase. It has red-pink (α) to cream-pink (β) to very light green (γ) pleochroism, low second order interference colors, extinction angles of 21° to 24°, a 2V of 75-80°, and is optically negative. Hence, the optic data indicate that the amphibole is hornblende. The pronounced reddish coloration may be due to substantial Cr_2O_3 in the mineral. Amphiboles of similar optic characteristics in chromitites whose composition was determined by microprobe contained up to 1.5 weight percent Cr_2O_3 (Table 4).

The pyroxenite and layered peridotite associated with the gabbro of Gwynn Gulch contain varying abundances of clinopyroxene, olivine, and altered pseudomorphs of orthopyroxene. Clinopyroxene

is dominant in sample 664 which contains 86% clinopyroxene, with about seven percent olivine, three percent orthopyroxene, and one percent amphibole, opaque and alteration. Clinopyroxene is the most abundant phase in all ultramafic rocks associated with the gabbro of Gwynn Gulch. Clinopyroxene and orthopyroxene lamallae are bent somewhat by moderate deformation. These ultramafic rocks may represent cumulates from fractionating gabbroic magma or, less likely, a reaction product of gabbro and harzburgite.

As noted, the gabbro of Gwynn Gulch is adcumulate, and of very limited extent. Hence, it is plausible that it might represent a cumulate layer in a sequence of cumulate harzburgite. However, the greater degree of deformation and tectonite fabric of adjacent harzburgite, coupled with presence of isotropic gabbro in Gwynn Gulch, and the lack of equivalent cumulate textures in the nearby harzburgite argues against simple accumulation of a cumulate pile. An alternative explanation is that the Gwynn Gulch gabbro represents trapped melt of magma which intruded along a zone of weakness in the harzburgite and penetrated foliation planes within the ultramafic rocks. Periodic replenishment or replacement of the Gwynn Gulch magma may have occurred as gabbro repeatedly moved upward through the peridotite. The clinopyroxene-rich ultramafic rocks of Gwynn Gulch may represent cumulates from fractionating gabbroic magma - a sort of small transition zone. The extent of these cumulates is not large, but is greater than would probably accumulate from a single pulse of fractionated primitive gabbro.

No rocks more silicic than olivine gabbro are present with or near the Gwynn Gulch gabbro. Such rocks might be found if the gabbro fractionated without replenishment. Their absence is good evidence for replenishment by primitive magma.

Textures and mineral compositions of Gwynn Gulch rocks are similar to rocks of the transition zone. It is possible that the Gwynn Gulch gabbro is infolded transition zone. However, there is no structural evidence to support this hypothesis (Misseri and Boudier, pers. comm., 1982). Also, the association of Gwynn Gulch gabbro with a zone in which many gabbro dikes cut the peridotite (Plates 1 and 2) suggests that Gwynn Gulch served as a way station for passage of gabbro through harzburgite when both were at elevated temperatures. The gabbro of Gwynn Gulch is the most primitive gabbro of the Canyon Mountain complex, and represents trapped melt which was parental to the major gabbro units of the CMC.

Gabbro of Bear Skull Rims

Coarse-grained to medium-grained gabbro in which clinopyroxene is the dominant mafic phase outcrops on east and west sides of Pine Creek (Figure 15 and Plates 1 and 2). These rocks are well exposed along the tops of Bear Skull Rims. Several good outcrops also occur on steep slopes west of Baldy Mountain. Similar clinopyroxene-rich gabbro occurs on east and west sides of Norton Creek, and on lower parts of major north-south ridges. Gabbro merges with, and in places seems to intrude the transition zone sequence of layered gabbro and ultramafic rocks near Gand Saddle.

Sample 629. Gabbro of Bear Skull Rims
X 35

Sample 708. Gabbro of Pine Creek Mountain
X 35

FIGURE 14. Two-pyroxene gabbro of Bear Skull Rims and Pine Creek Mountain.

Layered gabbro of Bear Skull Rim, west of Pine Creek

Layered norite, Norton basin, Intrusive diabase has chilled margin

FIGURE 15. Lithologies of Bear Skull Rim and Pine Creek Mountain gabbro.

Grain size of the gabbro of Bear Skull Rims varies in outcrop; layering is usually present although it may be subtle or not persistant. Layering is commonly developed at a five to ten centimeter scale, although layers varying between three and 30 cm were observed. Phase layering is common, but grain-size layering was not noted and graded layering is very rare. In some locations, such as the northeast side of Bear Skull Rims, layering is contorted, and changes in orientation are very abrupt, suggesting folding or slumping prior to solidification. Melanocratic and ultramafic bands or pods are distributed through the gabbro, especially in the vicinity of the Gand Saddle transition zone rocks (SE 1/4, sec. 15).

The gabbro of Bear Skull Rims persists up the southwest side of Baldy Mountain as major apophyses of gabbro which interfinger with tectonite harzburgite, and blend into a system of dikes which intrude through the harzburgite.

No olivine was observed in gabbro mapped as the Bear Skull Rim unit. Clinopyroxene of Bear Skull Rim gabbro is generally anhedral, and may be corroded or 'squeezed' between grains of plagioclase. The clinopyroxene rarely shows glide twins, but bent exsolution lamellae or wavy extinction are common. Optic figures suggest a composition of very calcic augite to diopside. This inference is supported by microprobe data on an equivalent gabbro (Himmelberg and Loney, 1980).

Orthopyroxene is strongly altered to serpentine + chlorite + amphibole. Where present as relict or pseudomorph, it retains a

euhedral to subhedral form. Compositional data, again from Himmelberg and Loney (1980), indicate that it is bronzite (En_{85}).

Some clear amphibole rims orthopyroxene. Clino- and orthopyroxene are fringed and replaced by amphibole which is light pink-brown to pale green, with 2V suggested by optic figures of about 85°, negative, and maximum 29° extinction angle - a hornblende. This amphibole seems to be late magmatic. Secondary, fibrous actinolite rims and replaces clinopyroxene and also replaces some late hornblende.

Plagioclase is anhedral, and twinned more simply than feldspar in Gwynn Gulch gabbro. Optical measurements of 001 twin extinction angles yield An_{70-75}, in good agreement with Himmelberg and Loney's (1980) determination of An_{72} *via* microprobe analysis. The plagioclase of Bear Skull Rim gabbro is unzoned.

In thin section (Figure 14) the gabbro of Bear Skull Rims is relatively undeformed, with adcumulate to hypidiomophic textures where alteration has not obscured original mineral relations.

All samples of Bear Skull Rims gabbro are at least somewhat altered. Feldspar generally is changed to hydrogrossular + chlorite. Mafic minerals are altered to acicular amphibole (actinolite, cummingtonite). The pervasive alteration may partly account for the absence of olivine and dearth of orthopyroxene in these rocks. However, pseudomorphs were not observed, and the low abundance of olivine and orthopyroxene is probably real.

Gabbro of Table Camp

Olivine-bearing, two pyroxene gabbro occurs on the south and east slopes of Baldy Mountain. This gabbro has a more evolved rare earth element signature (Figure 37) and higher SiO_2 (Table 14) than the gabbro of either Gwynn Gulch or Bear Skull Rims. Hence, although texturally and mineralogically similar to gabbro of Gwynn Gulch (but with substantially less modal olivine), the gabbro of Table Camp is somewhat later, or represents a different batch of magma.

The gabbro of Table Camp is medium-grained, with prominent pyroxenes on weathered surfaces. Layering is usually subtle phase layering in bands five to 20 cm wide which do not persist more than three meters. Foliation in some unlayered rocks may be due to slight flow lamination, but is usually associated with deformation. There is no apparent lineation.

In thin section (Figure 13) the gabbro of Table Camp has an adcumulate texture, with granoblastic recrystallization due to brittle deformation. Pyroxene exsolution lamallae and plagioclase twins are strongly bent; glide twinning occurs in mafic minerals and plagioclase. Embayed and lobate grains of olivine 1.0 mm or less in diameter are interstitial to the other primary phases but may be enclosed in clinopyroxene. Optical data for olivine suggest a composition of Fo_{75-80}.

Orthopyroxene is a very minor but significant component of the gabbro at Table Camp. It is subhedral, usually 1.0-1.5 mm in

maximum dimension, and optically negative with a 2V of about 80° indicating bronzite. Fine exsolution lamellae are well preserved. The crystals are not embayed or resorbed, as are the olivines. However, deformation of Table Camp gabbro obscures many textural details, and the generally brittle behavior of orthopyroxene would obliterate most embayments or apophyses.

Clinopyroxene is anhedral to subhedral, with a moderate 2V which suggests augite. It is usually larger than orthopyroxene, ranging from 0.5 to 3.0 mm in diameter. Exsolution and the development of cleavage are pronounced, and were probably enhanced by strain.

Late magmatic amphibole, similar to amphibole in the Gwynn Gulch gabbro occurs as an interstitial phase, and rims and corrodes mafics-especially clinopyroxene. It is red-brown - to cream-pink - to light green, with a large ($\sim$ 80°) 2V and optically negative, with a maximum extinction angle of about 23°. It is hornblende, probably chrome-enriched.

Plagioclase of the Table Camp gabbro is strongly deformed. Twin lamallae are usually bent. Deformation precluded determination of An content, except in a few properly oriented unstrained feldspars enclosed within larger deformed plagioclase or pyroxene crystals which have taken up the strain. These enclosed grains are An_{92-94}.

In a few locations the gabbro of Table Camp is strongly altered. This alteration post-dates consolidation. Actinolitic amphiboles form uralitic mats of small acicular crystals around clinopyroxene,

and entirely replace orthopyroxene. Plagioclase is altered to prehnite + chlorite.

Gabbro of Pine Creek Mountain

The gabbro of Pine Creek Mountain is gradational with the cumulate gabbro of Table Camp and Bear Skull Rims texturally, mineralogically, and geochemically. In the mapped area (Plate 1 and 2), it extends westward from the top of Celebration Ridge and Pine Creek Mountain along the ridge-crest toward Canyon Mountain. The area of exposure is difficult to determine precisely because contacts with other gabbro units are gradational. However, it represents at least one-third of the total gabbro, and includes at least six square miles (about 15 square kilometers).

In the field, this gabbro is fine-grained, and is the only gabbro in which sulphides (chalcopyrite, pyrite) may be seen in hand specimen. Both phase and grain-size layering occur in the rocks. Grain size layering is present on Yellow Jacket Ridge (Ridge 5) near 6600 ft (2010 m), and is abundant in upper Norton Creek (Figure 21). In the gabbro near Pine Creek Mountain (Figure 15), grain-size layering is uncommon, and most layers are distinguished solely on the basis of the varying modal proportions of mafic minerals and plagioclase. Layers are five to 20 centimeters in width, and may have very marked contrast between adjacent and alternating mafic and leucocratic bands. Some layering is folded gently into broad folds such as those described by Avé Lallemant (1976) as F_2, post magmatic deformation. Alignment of grains

(igneous lamination) can be distinguished in the field. Many layered rocks are finer-grained than isotropic counterparts. Gabbros within a broad zone which extends from Yellow Jacket Ridge to the southeast flank of Canyon Mountain are recrystallized and will be discussed in a separate section (see recrystallized zone).

Microscopic textures of the Pine Creek Mountain gabbro are adcumulate to heteradcumulate (Figure 14). Some upper, well layered gabbro shows striking igneous lamination, with nearly parallel alignment of lath-shaped plagioclase and rectangular hypersthene (Figure 20). Textures of some quartz-free gabbro approach panidiomorphic. Grain size in thin section varies from 0.1 to 0.5 mm.

Olivine is not present in the gabbro of Pine Creek Mountain. Optical data suggest that the rosy-pink to faint green, pleochroic orthopyroxene is hypersthene, approximately En_{65-70}. It ranges from 16 to 21 modal percent of the rock (Table 11). Clinopyroxene (14-26 modal percent) is subhedral, faint green, and non-pleochroic. Pyroxenes are rimmed, corroded, and replaced by late magmatic to subsolidus pale green to light pink-brown amphibole. Clinopyroxene is not strongly altered. Plagioclase is generally about An_{65}, and forms 46 to 65 percent of the rock. In late upper gabbro it is commonly lath-shaped, whereas in early gabbro of Pine Creek Mountain, plagioclase is an adcumulate phase. Adcumulate overgrowth of plagioclase is apparent in some samples due to alteration of rims.

Fine-grained (0.1-0.3 mm) sulphides are interstitial and probably represent a late, immiscible sulphide phase which was concentrated

in upper gabbro of the Canyon Mountain complex. They constitute as much as ten percent of the rock.

Quartz is uncommon, but occurs in several gabbro samples, noteably from the eastern limits of mapped Pine Creek Mountain gabbro and in Norton basin, where it constitutes up to seven percent of the rock. It is interstitial, has wavy extinction and in two samples (335, 355) corrodes some plagioclase. It is mostly a late magmatic phase, but also occurs in small clear, lobate blobs and veins which are post-magmatic and related to albite granite intrusion.

The presence of the Pine Creek Mountain gabbro in the upper stratigraphic levels of the Canyon Mountain complex mafic section is anomalous with respect to most ophiolites because it is well-layered, has cumulate to laminar textures, and the abundance of hypersthene and the occurrence of quartz indicate that it is a late gabbro of the Canyon Mountain complex series. Most of the Pine Creek Mountain unit may properly be termed norite to quartz norite. Norites, as noted earlier, are commonly present in upper sections of ophiolitic gabbro, but are not usually layered.

Summary: Characteristics of the Gabbro Units

Gabbro of Gwynn Gulch: Olivine - two pyroxene gabbro, with large, subhedral olivine. Adcumulate texture. Plagioclase = An_{85-92}.

Gabbro of Bear Skull Rims: Two-pyroxene gabbro. Hydrated and altered. Plagioclase = An_{70-75}, orthopyroxene relatively minor.

Gabbro of Table Camp: Olivine - two pyroxene gabbro. Adcumulate texture with small subhedral olivine $\approx$ five percent. Early plagioclase = An_{92-94}; later plagioclase $\approx$ lower An, possibly An_{70}.

Gabbro of Pine Creek Mountain: Two - pyroxene gabbro and norite, rare quartz norite. Euhedral hypersthene up to 21%. Iron and copper-iron sulphides in upper levels. Plagioclase = An_{65-70}. Flow lamination and hypidiomorphic textures.

Crystallization History of the Gabbro of the Canyon Mountain Complex

The crystallization history of the gabbro inferred from textural and mineralogical evidence is shown in Figures 16 and 17. Crystallization is described below in the Fo-Di-SiO_2 system $\pm$ H_2O (Kushiro, 1969). The sequence of crystallization is: 1) crystallization of Gwynn Gulch gabbro at low P_{H_2O} in the olivine-enstatite field, 2) later crystallization of the clinopyroxene in the Gwynn Gulch gabbro as magma composition moved onto the Di diopside-enstatite cotectic, 3) crystallization of the Bear Skull Rim gabbro under more hydrous conditions, and movement of the magma into the diopside field, 4) decrease in P_{H_2O} and return to olivine crystallization on the olivine-enstatite-diopside join, and lastly, 5) movement of magma and precipitate compositions along the diopside-enstatite join toward increasingly siliceous compositions, with quartz norites as an end product.

Gabbro of Gwynn Gulch contains olivine and orthopyroxene which show some evidence of resorbtion; the rock overall has an adcumulate

texture. Its mineral compositions seem to be the most primitive of the gabbros, and it is interpreted to have crystallized on the Fo-Pr cotectic as composition of the magma moved toward the Fo-Di-Pr invarient point (Figure 16).

The gabbro of Bear Skull Rims contains rather calcic plagioclase, but no olivine and little identifiable orthopyroxene. Its clinopyroxene is substantially altered to early amphibole and its plagioclase is altered to hydrogrossular and chlorite. The absence of olivine, and abundance of hydrous phases suggest that an increase in P_{H_2O} during crystallization moved the magma off the Fo-Di-Pr invarient, and into the Di field. Gradual loss of H_2O, and dehydration, or possibly an enclave which did not experience hydration, resulted in a return to the Fo-Di-En cotectic, and crystallization of the gabbro of Table Camp.

The gabbro of Pine Creek Mountain contains plagioclase of lower An content (65-70), and some upper norite contains quartz, abundant apatite, and even zircon. Olivine is absent. Orthopyroxene and clinopyroxene are texturally similar (subhedral to euhedral) and probably crystallized simultaneously. Therefore, the gabbro of Pine Creek Mountain probably represents continued crystallization of the same, or similar magma, along the Di-En join under hydrated conditions. P_{H_2O} was probably less during crystallization of the Pine Creek Mountain gabbro than during early crystallization of the Bear Skull Rim gabbro, as its pyroxene is mostly very fresh.

The mineralogy of the Canyon Mountain complex gabbro indicates continuous, or nearly continuous, crystallization and fractionation

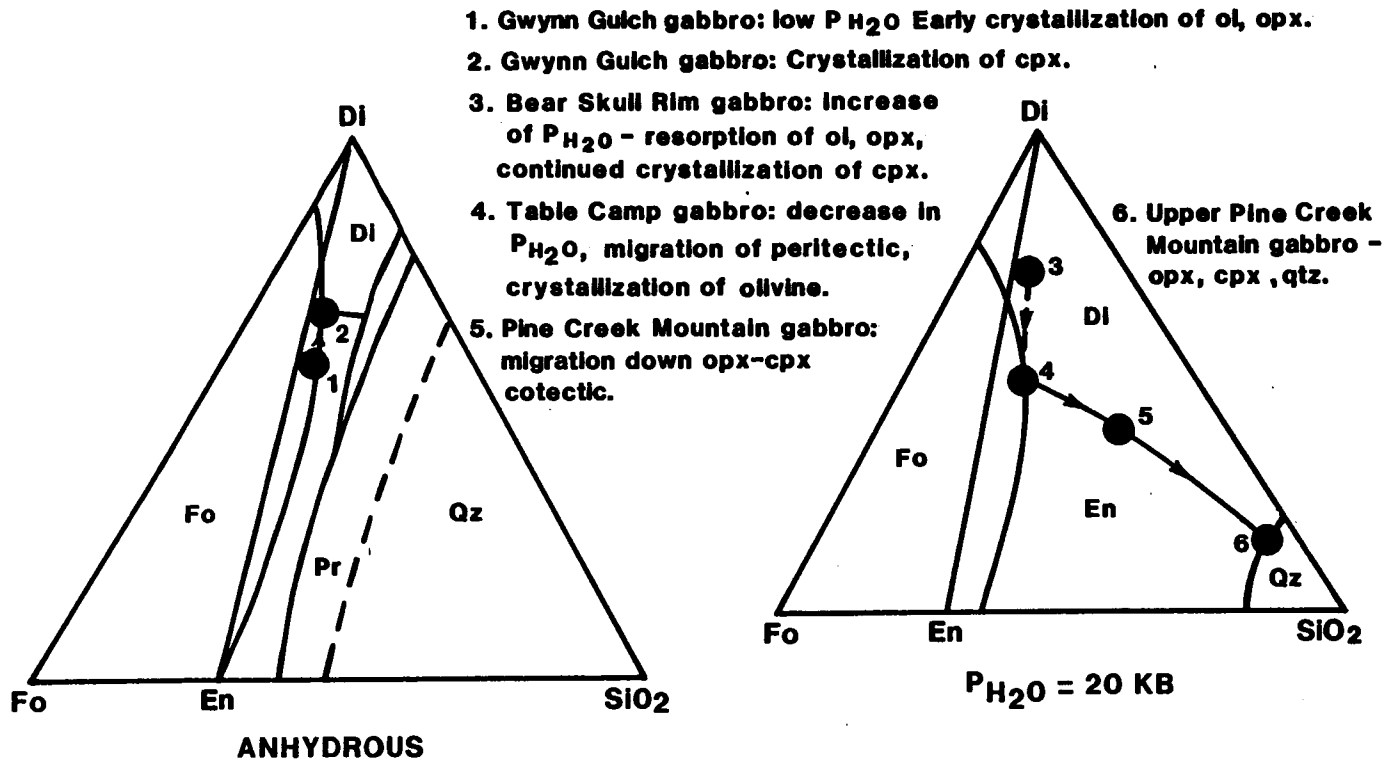

FIGURE 16. Crystallization of the Canyon Mountain complex gabbro in the system forsterite-diopside-silica (after Kushiro, 1969).

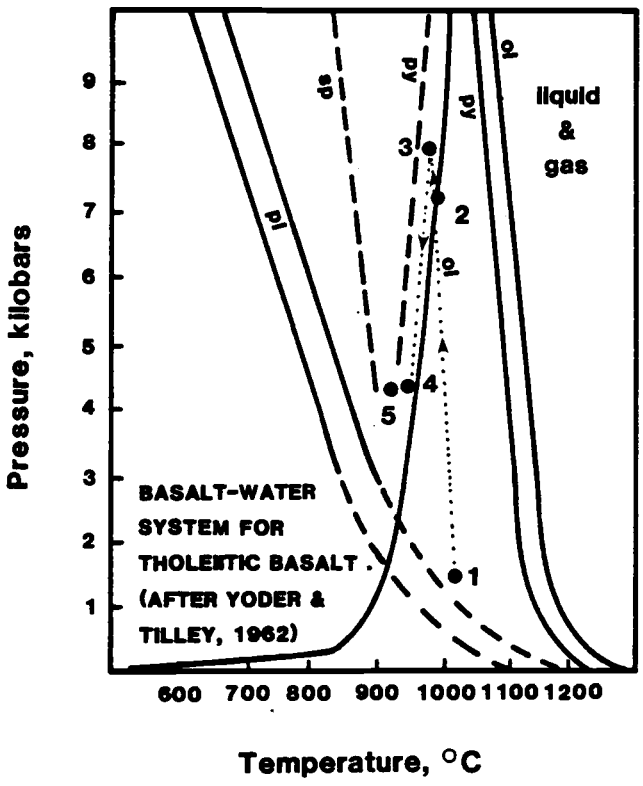

1. Gwynn Gulch gabbro: low P_{H_2O} crystallization of ol, opx cpx
2. Gwynn Gulch gabbro: rise in P_{H_2O}
3. Bear Skull Rim gabbro: Resorbtion of ol, opx, crystallization of cpx
4. Table Camp gabbro: lowered P_{H_2O}, reappearance of olivine
5. Pine Creek Mountain gabbro: No olivine

FIGURE 17. Crystallization of the Canyon Mountain complex gabbro in the basalt-water system.

of a single batch of magma which experienced one major, and probably many minor fluctuations in P_{H_2O}. Because mineral abundances and compositions vary slightly, particularly in the "upper" Pine Creek Mountain gabbro and norite, additions of small batches of magma and/or pressure fluctuations occurred during crystallization.

The presence of well-developed layering with marked flow lamination in the upper gabbro and norite suggests magmatic movement. The absence of features such as cross-bedding, trough-banding, or slump structures reported in other ophiolites and in stratiform intrusions indicates that movement of the magma was not vigorous, and that crystallization occurred in relatively placid conditions.

Abrupt changes in grain size occur between adjacent layers of Pine Creek Mountain gabbro. Although many of these rocks are now recrystallized (see Zone of Recrystallization), the grain-size variation is mostly a primary igneous feature. Thy and Ebenson (1982) attribute similar textures in the Fongen-Hyllingen complex of Norway to differential supercooling and changes in volatile pressure.

Hence, the pronounced layering in the Pine Creek Mountain gabbro may be due to periodic injection of small-but-similar batches of magma and associated changes in P_{H_2O} and thermal equilibrium. The rarity of similar layering in other ophiolites may result from more vigorous movement within the upper CMC chamber and/or a difference in the style, quantity, and composition of late injected magma.

The Zone of Recrystallization

In the glaciated basin of upper Norton Creek (West Fork of Pine Creek), above an elevation of about 6400 feet (1951 m) norites and quartz norites are intruded by numerous diabase sills which have chilled margins against the norite, and by plagiogranites which cross-cut as well as parallel foliation (Plate 4). Along a narrow (100 meter-wide), east-west trending zone of diabase and plagiogranite in the north part of the basin, migmatitic textures are developed in mixed gabbro and intrusives, and norite is recrystallized. Outward from this area, noritic gabbro with large, lineated, black poikiloblastic hornblende occurs in another 100-meter-wide zone. Concentrically outward, "epidiorite" (hydrously altered gabbro with green hornblende and actinolite replacing clinopyroxene - Thayer, 1972) is present. Significantly, altered gabbro, intruded by albite granite along and south of the main ridge crest is not recrystallized, and there is no similar zonation associated with the gabbro-plagiogranite contact although this plagiogranite is much more voluminous than its equivalent in Norton basin. The presence of stress during instrusion of albite granite into Norton basin may have enhanced recrystallization of this gabbro.

Central Zone of Plagiogranite and Migmatite

Gabbroic rocks in the narrow, central zone of abundant albite granite and diorite are intimately mixed with the leucocratic intrusives, and many outcrops have the appearance of migmatites.

Coarse gabbro blends into mafic diorite, which merges texturally and mineralogically with albite granite (Figure 18). Layered norites are plastically deformed into irregular, globular or ellipsoidal mixtures of fine grained and coarse grained, mafic to felsic gneissic rock (Figure 19). Thin hornblende veins transect foliation. Clearly defined veins, sills and dikes of both plagiogranite and diabase occur within the central migmatite zone (Figure 19). Plagiogranite is discussed in greater detail below. It should be noted here, however, that wide plagiogranite sills and dikes in the central zone commonly contain abundant angular gabbro xenoliths. The zone of albite granite in Norton basin also includes diorite with mafic schleiren of diabase, basalt (?) and fine gabbro. The mafic clots and relicts comprise more than half of some rocks, and are especially noteworthy in large talus blocks at the nose of ridge 6, elevation 6600 feet (2060 m).

Thin sections of most gabbro samples from this innermost zone have granoblastic to xenomorphic-granular textures. Triple-point junctions are well developed. Grain sizes in these recrystallized rocks are uniform (0.1-0.5 mm). Hornblende is rare. Acicular amphiboles are absent. The crystal habit indicates static recrystallization.

In some thin sections, hypidiomorphic relicts of plagioclase (An_{65}) or augite are present in a matrix of recrystallized, granoblastic plagioclase (An_{45}) and equant clinopyroxene (Figure 20). Large clinopyroxene crystals commonly reorganize into numerous smaller crystals. Where not recrystallized to an equant or

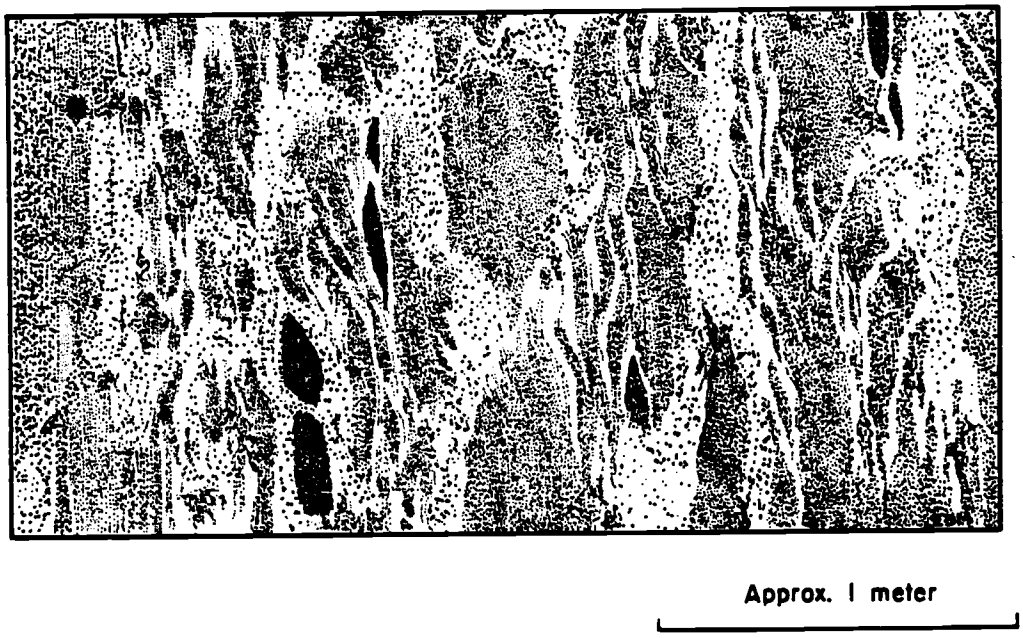

FIGURE 18. Migmatitic textures of Norton basin.

Plagiogranite dike with gabbro xenoliths. Norton basin.

Grain-size variation and deformation in partly recrystallized gabbro. Head of the West Fork, Indian Creek

FIGURE 19. Lithologies of the migmatitic and gneissic zones.

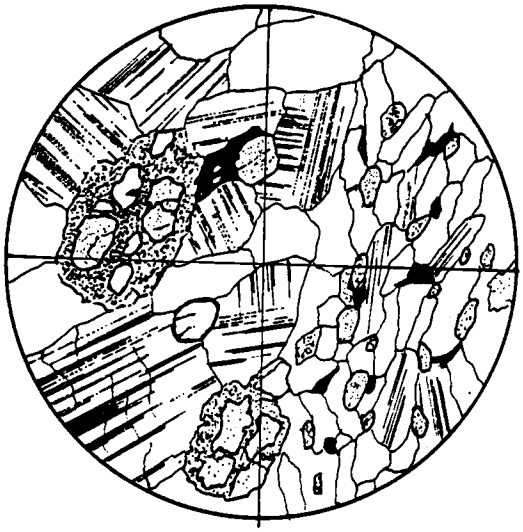

Partly recrystallized, bimodal laminar texture, in sample 468, Norton basin. X40

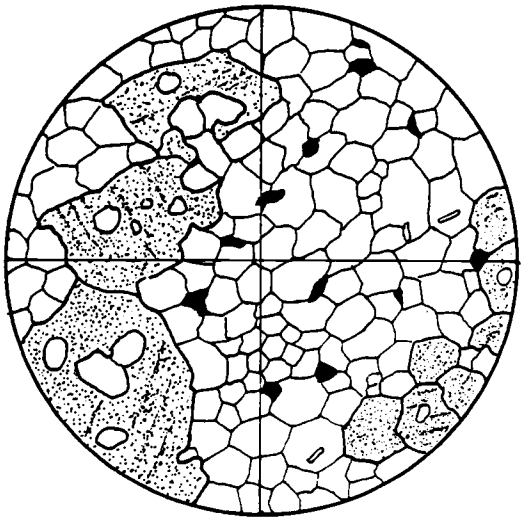

Granoblastic texture-sample 269, Norton basin. X100

FIGURE 20. Petrography of recrystallized gabbro.

xenomorphic habit, clinopyroxene may be poikilitic or develop seive texture enclosing plagioclase. Orthopyroxene is unaffected by recrystallization.

Zone of Partial Recrystallization (Gneissic Zone)

The narrow, migmatitic zone in which albite granite and diorite are common in Norton basin is bordered on the outside by a 100-meter-wide zone of gneissic hypersthene gabbro and partly recrystallized norites. Foliation is pronounced, and parallels igneous layering and lamination. Many norites retain their original banding, but exhibit saccroidal textures. Where complete recrystallization does not occur, the minerals are annealed and dehydrated.

Norites of the gneissic zone have textures in thin section which are hypidiomorphic to allotriomorphic, annealed, and occasionally xenomorphic and xenomorphic granular. Igneous textures indicate flow lamination. A noteworthy characteristic of these rocks is extreme variations in grain size in adjacent, alternating layers (Figures 19-21).

Fine-grained layers contain crystals 0.1-0.3 mm in diameter. Coarser layers contain 1.0-1.5 mm grains. The contact between layers is abrupt. There are no gradationally-sized minerals. Very few grain boundaries are irregular. Most rocks display some preferred orientation. A mosaic texture with straight grain boundaries and a tendency toward triple-point junctions occurs in those which have been slightly recrystallized. These textures are granoblastic polygonal to decussate. Overgrowths are visible on some plagiocalse

Grain-size variation in partly hornblendized gabbro. Norton basin.

Hornblende development in amphibolized gabbro.

FIGURE 21. Lithologies of the poikiloblastic zone.

crystals. Grains in these rocks are clear; few are altered or contain impurities. Significantly, amphibole or other hydrous phases are not abundant in dehydrated rocks.

Poikiloblastic Zone

Hornblendized gabbro, with large poikiloblastic hornblende replacing clinopyroxene occurs in a broad zone outside the gneissic, annealed gabbro (Figure 21). Hornblendes may be as much as three centimeters long, and are strongly lineated, indicating that stress was applied to these rocks during high-temperature hydration.

In thin section, small equant clinopyroxene is replaced by brown-green hornblende which then coalesces into a single amphibole crystal (Figure 21). Hypersthene is unaltered. Plagioclase is annealed and corroded by hornblende, but not substantially altered. Acicular amphiboles and/or uralitic textures do not occur in the poikiloblastic hornblende-bearing zone.

Although this zone is intruded by some albite granites which contain large, angular xenoliths of diorite, diabase, and gabbro, the albite granites do not contain poikiloblastic gabbro. Hence, albite granite pre-dates, or is coeval with, development of this texture.

Diabases and Plagiogranite in the Zone of Recrystallization

The Norton basin diabases vary in width from a few centimeters to 30 meters or more, averaging about two meters. They may be traced along strike for as much as 60 meters before being terminated

by faulting or covered by vegetation and talus. The diabases have textures which range from aphanitic to diabasic. Porphyritic varieties have zoned clinopyroxene and/or plagioclase phenocrysts - a significant feature in light of the annealed, homogeneous compositions of upper-level gabbro. There is no definite age relation between diabases of different widths or textures. All diabases observed had chilled margins against and sharp contacts with gabbro. Where present with plagiogranite, diabase is commonly strongly amphibolized.

The plagiogranites (commonly albite granite) may parallel the diabases, but mostly crosscut them and are in turn crosscut by them. The two magmas seem to have overlapped in time and space, but show no tendency to overlap in composition. There is no apparent "magma mixing" or blending of mafic and felsic magmas to produce an intermediate variety. Instead, diabasic dikes may intrude along the center of an albite granite, and plagiogranites contain xenoliths of diabase.

Four observations are pertinent to understanding the relation of diabase and albite granite to the zone of recrystallization and the Canyon Mountain complex. First, although plagiogranite and diabase are present in the same location, and seem coeval, diabase is much more abundant in the Norton basin area. Plagiogranite on the south side of the Canyon Mountain ridge alternates with, and is equally or more abundant than, diabase. However, on the north side of the ridge, albite granite is subordinant.

Second, in Norton basin, albite granite is mostly confined to two narrow en-echelon zones on the north and east. Diabase is present throughout.

Third, the diabase almost never contains xenoliths, and gives every indication of quiet intrusion. In contrast, plagiogranite intruded vigorously and commonly contains xenoliths of varied lithology and origin, including ultramafics, coarse gabbro norite, and diabase. Many clasts in albite granite are large (up to 0.5 meters) and angular, and occur in dikes no more than four meters wide (Figure 19). Intrusion breccias are associated not only with the albite granites of Norton basin, but are characteristic of all plagiogranites of the Canyon Mountain complex (Gerlach, 1980). Hence, intrusion of most plagiogranite was not placid, but entailed considerable brecciation, especially in lower gabbros.

Lastly, both diabase and plagiogranite pinch out downward in the gabbro and are not appraently fed by the CMC magma. Several diabase dikes were noted in the harzburgite. All were amphibolized, and also appeared to have no contact metamorphic effects on the adjacent peridotite, suggesting that the peridotite was not substantially hydrated and was at an elevated temperature when the diabase dikes were emplaced. Only one occurrence of possible plagiogranite intrusion into the harzburgite was noted, and consisted of plagiogranite float and thermally metamorphosed peridotite containing acicular amphibole near the Bald Eagle Mine on the southwest slope of Baldy Mountain. Thus, available field evidence indicates

without question that the plagiogranite and diabase were intrusive into the CMC gabbro and peridotite, and it is unlikely that they originated in the same magma chamber which produced the CMC gabbro.

Origin and Significance of the Zone of Recrystallization

A zone of recrystallization similar to that of the Canyon Mountain complex has not been reported in any other ophiolite. However, recrystallized and/or annealed textures are described in the Gosse Pile stratiform intrusion central of Australia (Moore, 1973). The gneissic zone of the Gosse Pile intrusion contains orthopyroxene megacrysts and relicts and strained-but-annealed plagioclase and clinopyroxene. The contact between unrecrystallized layer cumulates and gneissic rocks is gradational over several hundred meters. There are no evident hydrated, amphibolized zones associated with the Gosse Pile. Moore (1973) attributes the granoblastic textures of gneissic rocks to strain-enhanced recrystallization at 900°C, 10 kb pressure.

Garnet-bearing, and garnet-absent granulite facies gabbroic rocks are well documented in association with the island-arc basement of the Jijal complex, Pakistan (Jan and Howie, 1981) and the Chilas complex, Pakistan (Jan, pers. comm., 1981). Much of this gabbroic rock is recrystallized or partly recrystallized norite which contains relict unrecrystallized hypersthene. Observations by this writer in the field, and of thin sections indicate that textures of Jijal and Chilas rocks are very similar to the Canyon Mountain complex, although recrystallization of the Pakistan rocks

occurred probably at higher pressures. There is also some similarity on a regional scale: the Jijal and Chilas granulites are rimmed by amphibolite. Garnet-pyroxene geothermometry indicates temperatures of 800-825°C for the Jijal recrystallization (Jan and Howie, 1981).

Fine-grained granular rocks of the Fongen-Hyllingen complex, Norway, are interpreted as being of primary igneous origin by Thy and Esbensen (1982). Grain-size of adjacent layers varies greatly, and changes abruptly from 0.2 mm to 5 mm. There is no optical zonation of minerals in either fine or coarse layers. Fine-grained layers have granoblastic textures with extremely polygonal grains and straight grain boundaries. The variation in grain size, and the granular textures are attributed both to incidental differences in the amount of supercooling and to release of volatile pressure to raise the liquidus temperature and thereby also increase the degree of supercooling.

However, a similar occurrence of alternating fine-grained and coarse-grained layering in the Josephine gabbro and peridotite of southwest Oregon is interpreted as recrystallization of coarse-grained rocks to yield fine-grained rocks (Jorgenson, 1979). Penetrative deformation affects these rocks; minerals are not compositionally zoned. Recrystallization occurred along closely-spaced slip-planes during metamorphism; textural banding was produced by syntectonic recrystallization which accompanied regional metamorphism.

The marked resemblance between adcumulate texture and granulites has been noted and discussed in some detail by Vernon (1970).

Both textures are characterized by fairly straight grain boundaries and triple-point junctions. However, adcumulates tend to have more curved boundaries, rounded inclusions, and lack reaction micro-textures such as orthopyroxene rims of polygonal olivine (O'Hara, 1961). Adcumulates generally contain a larger proportion of elongate grains, some rational grain-boundaries, and inter-cumulus phases. Adcumulate textures are common in lower gabbro of the Canyon Mountain complex, and are present along with flow lamination affects in gabbro of Pine Creek Mountain, and the layered norites of Norton basin.

However, the recrystallized zone is composed of recrystallized adcumulates in which the interstitial phases are absent, lath-like phases (orthopyroxene and some plagioclase) are embayed, and large single clinopyroxene crystals are re-ordered into multiple crystals, possibly due to the application of slight stress during recrystallization. The strong lineation of poikiloblastic amphibole in the zone of recrystallization indicates stress during recrystallization.

The close spatial association of recrystallized gabbro and norite with diabases and plagiogranites suggests that gabbro recrystallization is related to these late magmas. Albite granite is intimately mixed with diorite and gabbro in the inner zone. Textures appear migmatitic. Recrystallization and dehydration are most intense in the inner zone and decrease systematically outward. Recrystallization also seems more closely related to plagiogranite concentration than to diabase. However, of the two magmas (diabase - plagiogranite), the plagiogranite would be generally cooler, and hence would have less thermal effect on country rocks. The greater

thermal effect of the plagiogranite may be related to intrusion throughout a longer time span than the diabases and maintenance of high wall-rock temperature due to continuous flow of granitic magma through dikes or sills.

Significantly, diabases are chilled against gabbro but plagiogranite is not, either in small intrusions of Norton basin, or along the contact of the gabbro and the large albite granite body south of the ridge crest. If the host gabbro was at an elevated temperature at the time of intrusion, it might be cool enough to produce chilled margins in supercooled diabases, and sufficiently warm to avoid chilled textures in plagiogranite.

A precise estimate of gabbro temperature at recrystallization cannot be made here via geothermometry because precise compositional data for Norton basin pyroxenes are not available. Upper level norites sampled by Himmelberg and Loney (1980) yielded temperatures of 900°-925°C which may represent hyper- or subsolidus equilibration, rather than subsolidus recrystallization.

A crude estimate of gabbro temperatures during initial intrusion of diabase and plagiogranite may be made on the basis of textures. Calculations by Corrigan (1982) suggest that for a chilled texture (40u to 60u grain size) to develop in a tholeiitic diabase, cooling must occur at 10°C/hour, whereas for crystal sizes similar to plagiogranites, cooling at 0.5-1.0°C/hour or slower is acceptable. Calculations based upon gabbro thermal conductivity of 481 x 10^5 cal/cm^2 sec for gabbro (Clark, 1965) suggest that a temperature differential of about 500°C would be necessary to achieve sufficiently

rapid cooling of the diabase. This estimate does not allow for either hydrothermal circulation within the gabbro, or for supercooling of the diabase, both of which would decrease the temperature differential cited above. Assuming a temperature of 1100° for diabasic magma, gabbro temperature would have been at least 600°C. This approximation coincides very roughly with Jaeger's (1957) estimate that for chilled margins to develop in a thin sill or dike at 1100-1200°C, adjacent wall rock temperatures would be 708-725°C, and for intrusions of 1000-1100°C into country rock @ 0°C, wall rock temperatures would be elevated to 670-685°C.

For plagiogranites to remain unchilled, ΔT should not exceed 250°C. Assuming a temperature 850°C for plagiogranite intrusion, gabbro wall rock temperature initially should be approximately 600°C. Again, this estimate ignores the possible and probable effects of water in removing heat from gabbro, or of lowering solidus temperature of plagiogranite magma.

Thus, the available constraints on gabbro temperature suggest that in early stages of plagiogranite intrusion, gabbro was at, or slightly higher than 600°C, and was probably in late stages of cooling and solidification.

Two mechanisms may have caused or affected gabbro recrystallization. 1) Heat - from intrusion or from another source - is necessary to achieve granulite facies conditions locally (650°C @ P_{fluid} = 1 kb), although for recrystallization of existing plagioclase and pyroxene which is simply re-organization of existing lattices into smaller

crystals, a lower temperature may be sufficient. Hypersthene is not recrystallized, suggesting that high granulite-facies temperatures of greater than 850°C were not reached for a significant amount of time. Because relict hypersthene occurs in Jijal rocks metamorphosed at 800-825°C, however, temperatures may have risen to 825°. 2) Stress may also cause or enhance recrystallization. The rarity of strain in recrystallized minerals, and in zones adjacent to the inner migmatitic zone suggests that major deformation such as that associated with recrystallization of Josephine gabbros in southwest Oregon (Jorgenson, 1979) did not occur in conjunction with Norton basin recrystallization. However, the well-developed lineation of poikiloblastic hornblende in the outer zone, and the recrystallization of clinopyroxene and plagioclase to finer-grained aggregates suggest that the system was under slight stress during recrystallization.

Gabbro within the inner zone of granulitic textures is very dehydrated, and hydration increases as temperature decreased outward from amphibole veins in the gneissic zone to poikiloblastic hornblende, to "normal" altered gabbro (Thayer's "epidiorite", 1972). The strong dehydration of the inner zone suggests that addition of water was not associated with recrystallization. The abundance of breccias and xenoliths in albite granites of the inner zone indicates that their intrusion either followed faults or was accompanied by volatiles. Considerable strain may have been imposed during plagiogranite intrusion. Because there is little evidence of water in the albite granites (no mica, myrmekite, etc.), the possible volatile phase accompanying albite granite intrusion probably was

not associated with the intrusives, but may have been released from previously altered gabbro. Intrusion of the albite granite as a dry liquid would also require it to be hotter than if it contained much water, which would increase thermal effects upon the gabbro.

Migmatitic textures present in outcrop strongly suggest that some gabbros were heated sufficiently to become plastic and partially fused. Fusion of hydrated gabbro to yield quartz-normative liquid occurs at 700°C, P = 5 kb (Wyllie, 1979). Partial melting affected no more than one to two percent of Norton basin gabbro - an amount insufficient to account for the quantity of plagiogranite within Norton basin, and certainly insufficient to produce the albite granites south of the ridge crest. Much fused material appears to have remained within the recrystallized gabbro, although some probably migrated into, and mixed with the plagiogranite. Similar processes and contamination affect diabases in the recrystallized zone, but not elsewhere in Norton basin.

The zone of recrystallization is principally a result of plagiogranite and diabase intrusion into hot (600°C), hydrated gabbro along probably pre-existing, en-echelon zones of weakness, under slight to moderate stress. Field relations indicate that the sill-like intrusives were injected downward and laterally into the norites; they were not intruded upward through the peridotite.

Trace element modeling (Figure 60) has suggested that diabase and plagiogranites of the Canyon Mountain complex are derived from light rare earth element (LREE) - depleted, altered gabbro (Gerlach et al., 1981). Partial fusion of altered gabbro and contribution of

melt to albite granites does occur in Norton basin, but is probably a result of albite granite intrusion, rather than a major contribution to albite granite genesis. Volumetric considerations, and the absence of any apparent feeder system to the overlying major zone of plagiogranite preclude Norton basin as a major source of plagiogranite.

A possible source of diabase and albite granites which is compatible with trace element requirements (see Figure 60, and Conclusions) is partial melting of overlying altered gabbro of oceanic crust. Clearly the Canyon Mountain complex is plutonic, and most probably it is intrusive into oceanic crust. Although possible country rock is not obviously represented at the CMC, screens of altered gabbro occur in epizonal keratophyre 1-2 km north of the ridge crest (Thayer, pers. comm., 1982). These large xenoliths or screens were neither mapped nor sampled as part of this dissertation, and no data is available regarding their mineralogy or geochemistry.

Strongly altered gabbro of probable oceanic origin does occur within the melange of the forearc (oceanic-melange) terrane. These rocks are discussed in detail later (Igneous association and origin of peridotite and gabbro) and geochemical evidence which supports origin of plagiogranite by partial melting of hydrated ocean floor gabbro is discussed. The presence of probable altered oceanic gabbro does not prove the suggestion that intrusion of arc-related gabbro into oceanic crust generated albite granite via partial melting. However, it does allow this possibility. Further investigation of the screens present in the Canyon Mountain complex, and additional consideration of thermal requirements seem warranted.

MAJOR ELEMENT GEOCHEMISTRY OF PERIDOTITE AND GABBRO OF THE CANYON MOUNTAIN COMPLEX

Major element analyses for ten oxides (SiO_2, Al_2O_3, TiO_2, FeO*, MnO, MgO, CaO, Na_2O, K_2O, and P_2O_5) were obtained for 20 samples representing a variety of lithologies: five depleted tectonite peridotites (one dunite, three harzburgites and one lherzolite), seven peridotites and gabbros of the transition zone, and eight gabbros, with two samples from each of the four principal gabbro subdivisions.

Major Element Abundances in Tectonite Harzburgite

The major element composition of Canyon Mountain complex tectonite peridotites does not depart greatly from abundances reported in other ophiolite tectonite units. Analyses are given in Table 12. Variation of major oxides with SiO_2 is shown in Figure 22. The depleted tectonite peridotites analyzed here are from the zone of infiltration, and had very narrow (< 1 cm wide) feldspar-bearing veins closely adjacent. However, analyzed material was crushed and handpicked to be certain that feldspar was not visibly present in the rocks and that the analyses reflected only peridotite mineralogy.

Compared with the strongly depleted harzburgite of other ophiolites, the peridotites of the infiltration zone are noticeably enriched in Na_2O, CaO, and Al_2O_3. Peridotites in this zone also have detectable amounts of K_2O (0.01%, or between 1000 and 4000 ppm). Significantly, they are low in TiO_2 (0.01-0.02%) which suggests that

TABLE 12. Major element analyses of peridotites of the Canyon Mountain complex.

	218	612	284C	449B	614
SiO_2	42.69	38.05	42.53	44.34	52.44
Al_2O_3	1.50	1.66	1.11	1.84	10.64
TiO_2	0.01	0.02	0.01	0.01	0.50
FeO	8.61	9.70	8.60	8.33	7.50
MnO	0.13	0.14	0.13	0.12	0.21
MgO	33.80	35.89	35.77	32.77	13.19
CaO	1.71	1.29	1.48	1.65	11.22
Na_2O	0.09	0.14	0.25	0.58	1.43
K_2O	0.07	0.06	0.07	0.07	3.06
P_2O_5	0.09	0.00	0.00	0.00	0.04
Σ	95.70	86.95	89.95	89.71	100.23

because TiO_2 is not highly mobile, the LIL and alkali elements were added to the peridotite via metasomatism, possibly simultaneously with the intrusion of melt. No fractionation trend is apparent in the SiO_2 variation plots (Figure 22).

The low TiO_2 content indicates that the tectonite harzburgite is almost entirely depleted. Fertile peridotites such as the lherzolite of Lanzo (Boudier and Nicholas, 1977) or garnet lherzolite of Ronda (Dickey, 1970) contain an order of magnitude greater abundance of TiO_2, (0.10%) and similar or slightly greater alkalis.

Further evidence that infiltration affected peridotite geochemistry is the analysis of 614, a harzburgite which contains veins and large clots of gabbro. This rock has 12 percent paragasitic amphibole which rims pyroxenes and formed as an interstitial, subsolidus phase, and five percent calcic plagioclase (An_{90}) which is altered to hydrogarnet and chlorite. Whole rock analysis of this peridotite which was handpicked to eliminate visible feldspar yielded 10.6 percent Al_2O_3, 11.2 percent CaO, 1.4 percent Na_2O, and 3.1 percent K_2O. This rock has the chemistry of a melagabbro which is very strongly enriched in K_2O.

Major Element Abundances in Rocks of the Transition Zone

Rocks of the transition zone analyzed for their major element content (563, 564, 565, 566, 567, 579, 581) represent a series of dunite, melagabbro, wehrlite, lherzolite, websterite, and gabbro from Celebration Ridge (Ridge 2). Analyses are given in Table 13,

TABLE 13. Major element analyses of the upper transition zone, Celebration Ridge.

	563	564	565	566	567	579A	581A
SiO_2	36.31	51.75	47.35	49.47	49.81	48.27	50.69
Al_2O_3	0.13	1.04	18.97	7.13	24.96	4.63	1.36
TiO_2	0.01	0.02	0.07	0.25	0.12	0.41	0.07
Fe^*O	9.10	4.85	4.12	8.24	3.52	11.05	5.37
MnO	0.14	0.12	0.08	0.15	0.05	0.21	0.10
MgO	35.24	21.85	10.52	17.27	5.06	17.48	21.13
CaO	0.19	13.36	15.18	13.56	13.65	13.40	13.71
Na_2O	0.09	0.79	1.55	0.83	2.74	1.39	1.07
K_2O	0.06	0.05	0.07	0.05	0.07	0.06	0.05
P_2O_5	0.00	0.02	0.01	0.02	0.02	0.01	0.01
TOTAL	81.27	93.85	97.98	96.97	100.00	96.91	93.56

and variation of major oxides with SiO_2 is shown in Figure 23. Major element geochemistry of the transition zone rocks reflects the high CaO content of clinopyroxene and plagioclase, and the varying amounts of each in the rock. The abundance of MgO in gabbros of the transition zone (565 (10.7 percent); 567 (4.9 percent)) indicates a fairly primitive character. On most major element variation plots (Figures 23-29) the transition zone samples fall on a different, and more tholeiitic trend than CMC gabbro. A plot of TiO_2 versus FeO*/MgO (Figure 26) for this series of rocks shows that the main gabbro of Pine Creek Mountain lies on the same trend as gabbro interbanded with peridotite, and on a trend of less TiO_2 enrichment than most gabbro of the Canyon Mountain complex. Two samples (566, a melagabbro, and 579A, an olivine websterite), plot at similar FeO*/MgO ratios, indicating low degrees of melt fractionation, but substantial TiO_2 enrichment. The melagabbro (566) is a gabbroic layer within peridotite cumulates near the base of the ridge, and probably represents an accumulation of fractionated melt as clinopyroxene, orthopyroxene, and olivine crystallized from the magma. Sample 569A, the olivine websterite from the top of Celebration Ridge, also plots far above the general trend, suggesting that it also represents a late fractionation product of cumulate sequence, although its overall mineralogy is rather primitive.

Peridotites of the transition zone on Celebration Ridge generally reflect their modal mineralogy and stratigraphic location in major element analyses. For example, 579A, an olivine websterite from the top of Celebration Ridge is higher in FeO* and lower in MgO than 581A,

an olivine websterite from a lower stratigraphic position. Similarly, a pyroxenite from the bottom of the sequence (564) which may represent an unfractionated composition, is much lower in Al_2O_3, CaO, and FeO, and higher in MgO than either 581A or 579A above. Both TiO_2 and MnO increase in the upper transition zone samples. These findings support the conclusion that overall, the CMC transition zone represents successive cumulates of a fractionating magma.

However, nearly adjacent samples of modally similar gabbro (565, 567) vary significantly in MgO and Al_2O_3, although FeO* and CaO are approximately the same. These discrepancies may be due in part to greater alteration of 565, or may be due to slight fluctuations in composition of the magma, or irregularities in precipitation during crystallization of the transition zone.

Major Element Abundances in Gabbro

Results for the eight gabbroic rocks analyzed (664, 666, 626, 629, 539, 540, 707, and 522) are given in Table 14. Major element abundances are rather uniform throughout the group. Na_2O is the only oxide which varies noteably from concentrations reported in most cumulate gabbros of ophiolites. In Canyon Mountain complex samples, Na_2O varies between 1.2 and 2.5 percent - whereas Na_2O is less than one percent in most ophiolites.

CMC gabbros, overall, are slightly enriched in Al_2O_3 (11.6-19.6 percent), and are low in TiO_2 (0.14-0.29 percent). Through the sequence of gabbro lithologies identified on the basis of field relations, stratigraphic location, and petrography, as SiO_2 increases,

TABLE 14. Major element analyses of gabbro of the Canyon Mountain complex.

	Gwynn Gulch		Bear Skull Rims		Table Camp		Pine Creek Mtn.	
	664	666	626	629	539	540	707	522
SiO_2	54.92	45.70	48.63	48.68	50.28	51.29	50.58	51.44
Al_2O_3	2.15	11.63	19.62	18.59	17.88	18.48	16.64	18.22
TiO_2	0.07	0.19	0.14	0.15	0.19	0.18	0.19	0.29
Fe^*O	4.36	9.90	4.97	5.13	6.56	4.85	8.47	7.86
MnO	0.12	0.16	0.09	0.09	0.11	0.09	0.14	0.11
MgO	15.89	17.28	8.79	10.16	10.68	10.09	8.91	8.39
CaO	17.39	10.32	14.38	13.44	12.24	13.43	12.79	13.22
Na_2O	1.65	1.22	2.33	2.08	2.48	2.49	1.71	2.21
K_2O	0.06	0.06	0.06	0.06	0.07	0.06	0.06	0.06
P_2O5	0.03	0.00	0.03	0.01	0.03	0.02	0.02	0.01
Σ	96.61	96.46	99.04	98.39	100.52	100.98	99.51	101.81

Al_2O_3, CaO and MgO broadly decrease whereas FeO and TiO_2 increase slightly (Figure 22). Changes in abundances are not dramatic, but are broadly consistent with trends expected in a single fractionating chamber which is occasionally replenished with gabbroic magmas similar to the composition of sample 666, the gabbro of Gwynn Gulch.

Major Element Variation in Peridotite and Gabbro of the Canyon Mountain Complex

The variation of major oxides with SiO_2 content for tectonite peridotite and cumulate gabbro is shown in Figure 22. The olivine-two pyroxene gabbro of Gwynn Gulch plots in an intermediate position between gabbro and peridotite on all graphs, indicating that in terms of major element variation it is the least differentiated and most primitive gabbro. The gabbro of Bear Skull Rims occupies an intermediate position between the gabbro of Gwynn Gulch and the Table Camp and Pine Creek Mountain gabbro samples. Trends for TiO_2, FeO*, MgO, CaO, and Na_2O are smooth and indicate regular changes in magma composition with SiO_2 content.

Plots of the major oxides against SiO_2 for the transition zone show less regular variation. In particular, Al_2O_3, FeO* and Na_2O show a broad scatter. Transition zone samples are noteably lower in TiO_2 and Na_2O, and higher in MgO overall than CMC gabbro of equal SiO_2 content. Within the transition zone itself, TiO_2, Al_2O_3, FeO*, and Na_2O increase with decreasing SiO_2, MgO increases slightly with increasing SiO_2 whereas CaO is constant. The seeming reversal

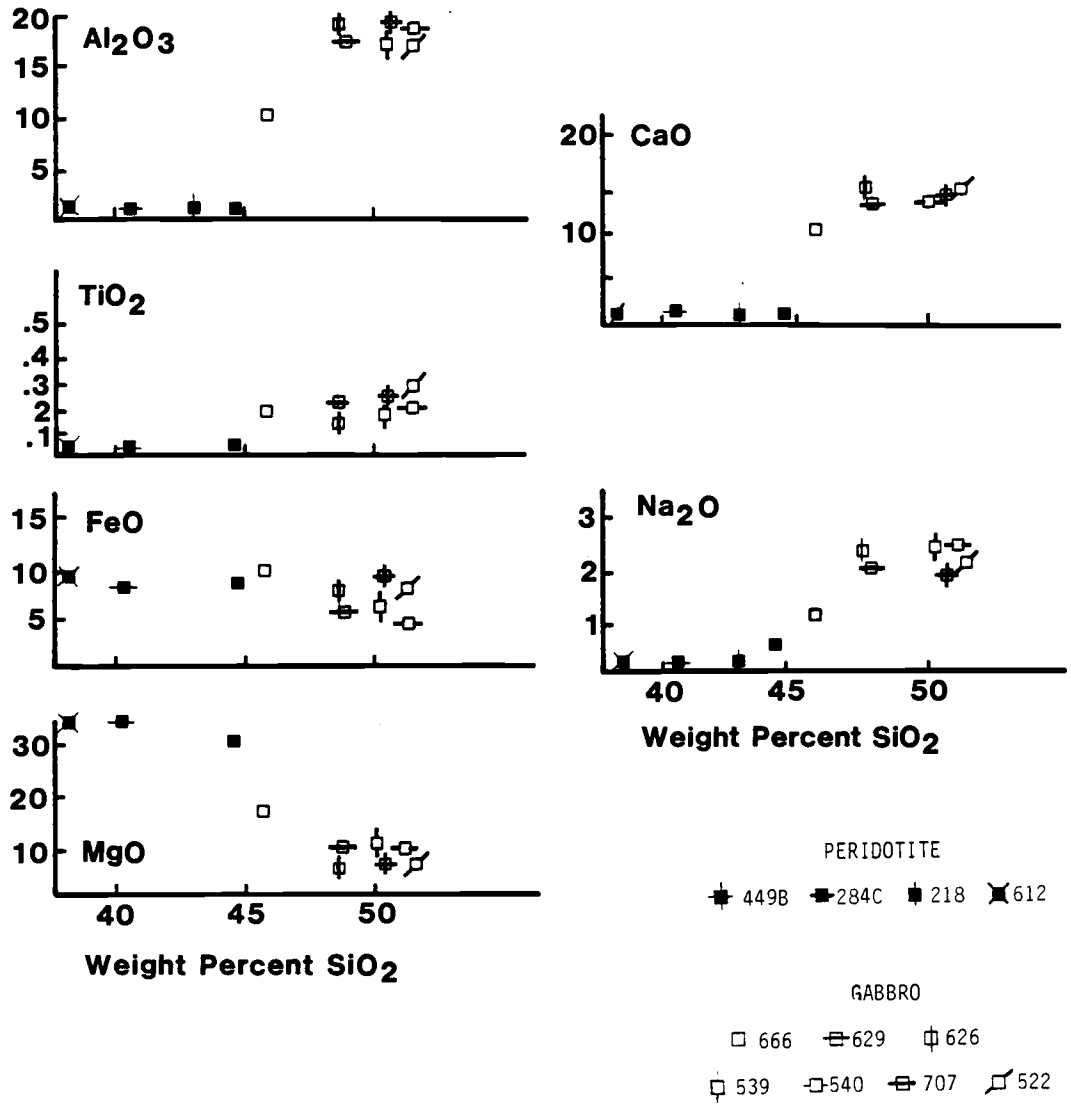

FIGURE 22. SiO_2 variation diagram for tectonite peridotite and cumulate gabbro of the Canyon Mountain complex.

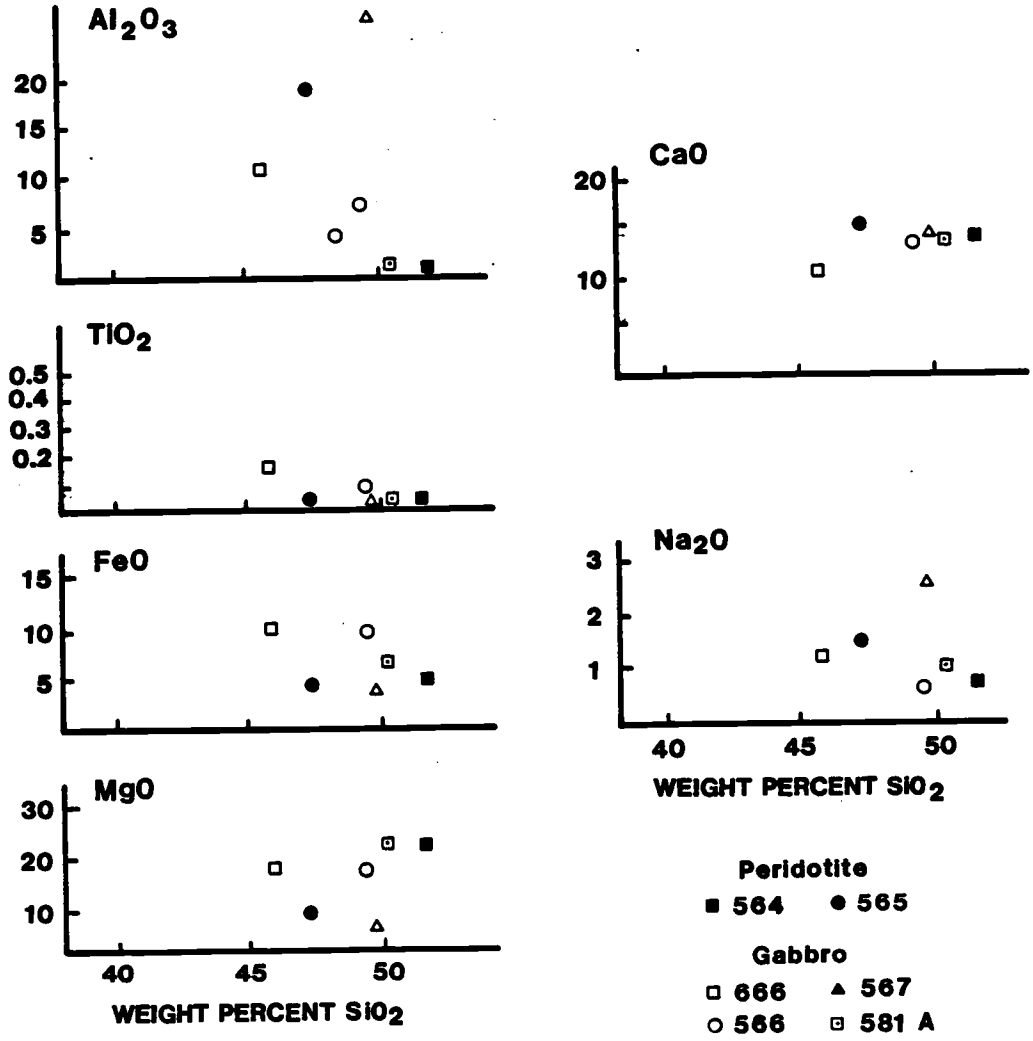

FIGURE 23. SiO_2 variation diagram for rocks of the transition zone of the Canyon Mountain complex.

of normal fractionation trends is partly due to the overall increase in fractionation with stratigraphic height. Ultramafic samples (579, 581) from the upper ridge have more evolved oxide/SiO_2 ratios than a gabbroic sample from near the ridge base (567). However, the reversal in trends cannot be entirely explained on this basis (564, an olivine websterite from the ridge base, for example, is an anomalously 'evolved' rock, with high SiO_2), and probably also indicates periodic influx of fresh magma.

Geochemical Affinity of Canyon Mountain Complex

Tholeiitic, calc-alkaline, or alkaline fractionation trends of magmas may be determined by several criteria. One tool for determining geochemical affinity and fractionation trends is a ternary plot of CaO/Al_2O_3/MgO (Coleman, 1977) (Figure 24). Compositions of Canyon Mountain complex samples fall mostly outside fields for ocean ridge ophiolites such as Samail or Bay of Islands. The transition zone series is more MgO and Al_2O_3 enriched, and has less CaO proportionally, than the gabbro. The cumulate gabbro of the CMC plots at the base of a trend for upper gabbros of the Kiglapait alkalic-calc alkaline intrusion (Morse, 1969). Both the transition zone series and a suite of CMC plagiogranites (Gerlach, 1980) parallel this trend rather than the Skaergaard trend which shows greater overall Al_2O_3 enrichment. The proportionally higher content of MgO, and lower CaO in transition zone rocks and the primitive gabbro of Gwynn Gulch is expected, due to

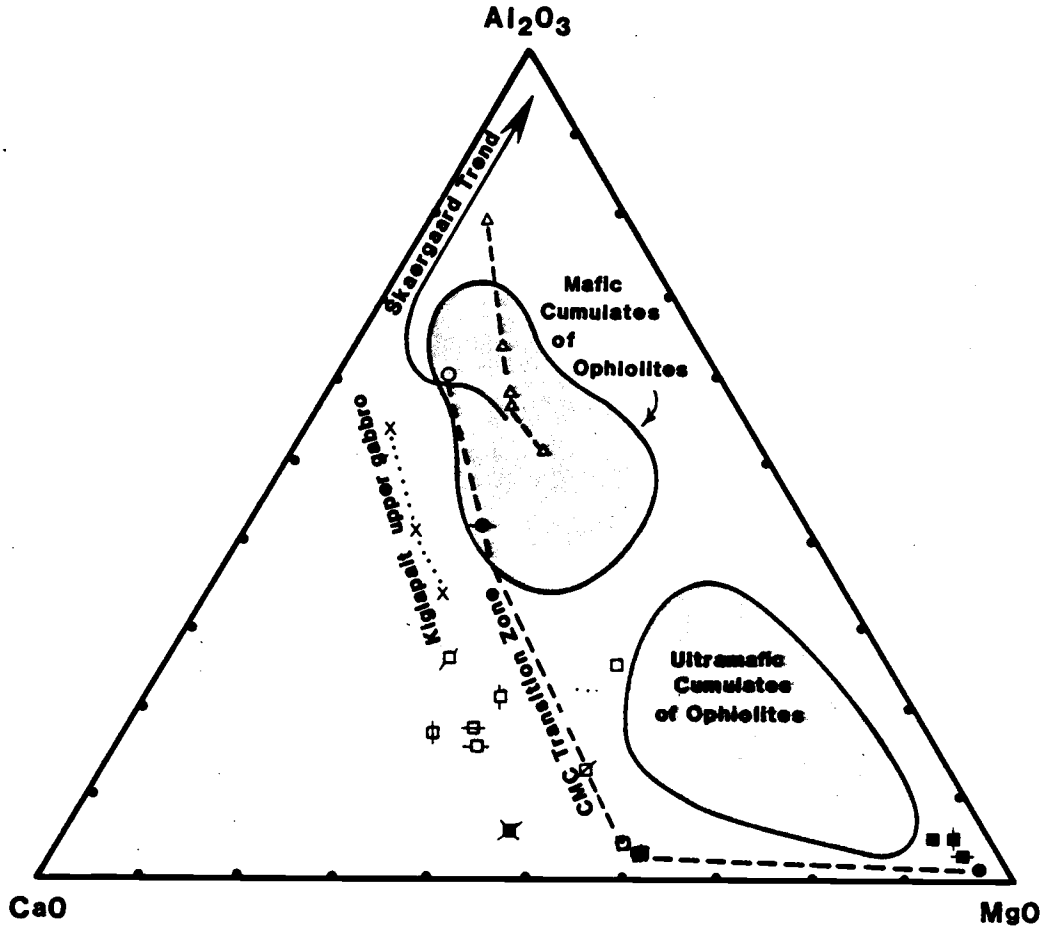

PERIDOTITE

449B 284C 218 612

TRANSITION ZONE

564 565 566 567 581A

GABBRO

666 629 626

539 540 707 522

FIGURE 24. $CaO:Al_2O_3:MgO$ diagram for tectonite peridotite, cumulate gabbro, and rocks of the transition zone, Canyon Mountain complex.

their more mafic character. Significantly, most of these samples plot outside the ophiolite ultramafic cumulate field and indicate CaO enrichment throughout the cumulate sequence.

All analyzed gabbroic and ultramafic components of the Canyon Mountain complex are enriched in K_2O with respect to equivalent components of other ophiolites, although they have low K_2O compared to continentally derived rocks and stratiform complexes (Figure 25). This may partly reflect alteration. However, gabbro pairs with markedly different degrees of alteration (665, 666) have very similar abundances of K_2O and Na_2O and hence the pronounced abundance of both alkalis is considered primary, rather than a function of alteration. Enrichment in alkalis is a characteristic of the alkaline and calc-alkaline, but not the tholeiitic series, and suggests that the Canyon Mountain complex does not represent an ocean ridge environment.

A plot of CMC samples on an SiO_2: FeO*/FeO*+MgO diagram (Figures 28 and 29) indicates high SiO_2 content for a given stage of fractionation. Some rocks of the transition zone, as well as mafic cumulates plot outside fields for most ophiolitic rocks, indicating a lack of pronounced FeO enrichment through the Canyon Mountain complex, and consequently a calc-alkaline trend.

On an AFM diagram (Figure 30) CMC samples fall slightly toward the $Na_2O + K_2O$ apex from the normal oceanic ophiolite, and align well with the generally calc-alkaline trend of low iron-enrichment found by Gerlach (1980) and Thayer (1977) for CMC plagiogranites and diabases.

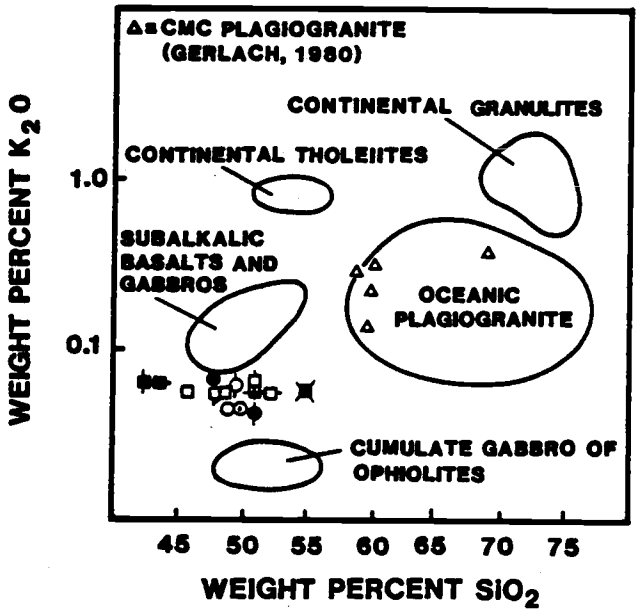

PERIDOTITE

449B 284C 218 612

TRANSITION ZONE

564 565 566 567 581A

GABBRO

666 629 626

539 540 707 522

FIGURE 25. K_2O/SiO_2 diagram for tectonite peridotite, transition zone, and cumulate gabbro, Canyon Mountain complex (after Coleman, 1977).

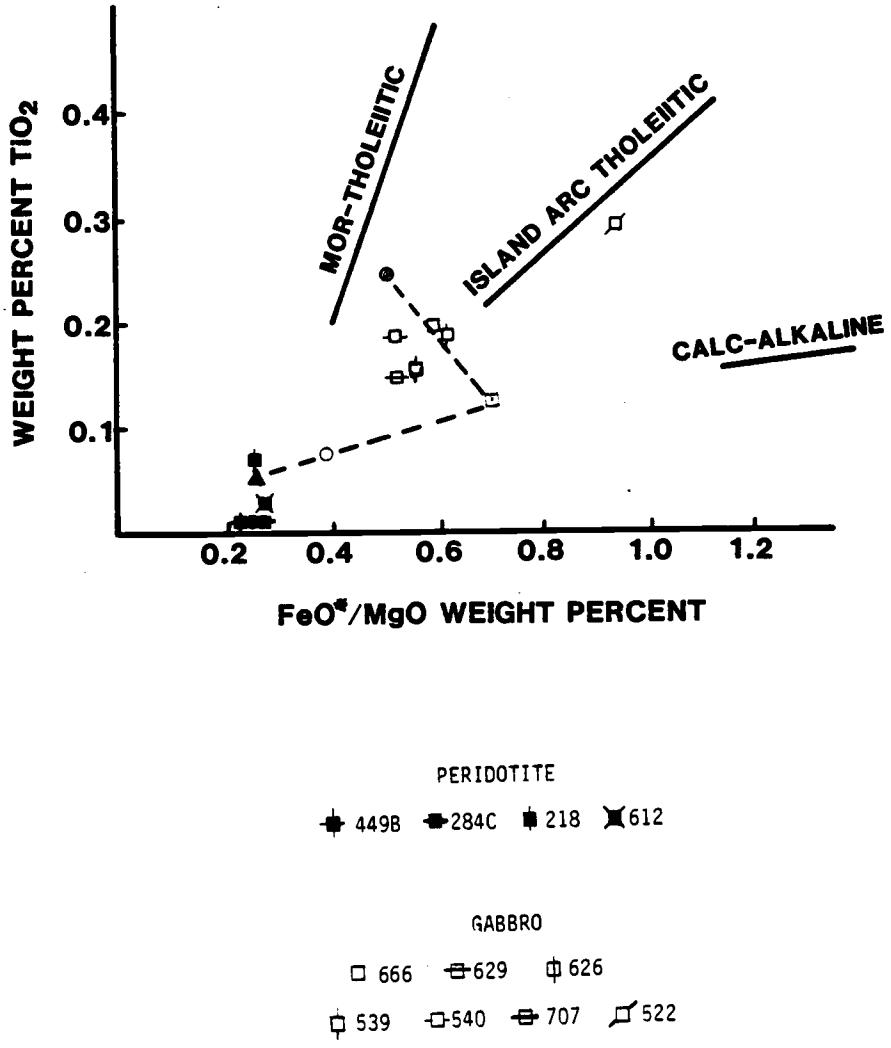

FIGURE 26. TiO_2:FeO*/MgO diagram for peridotite and gabbro of the Canyon Mountain complex.

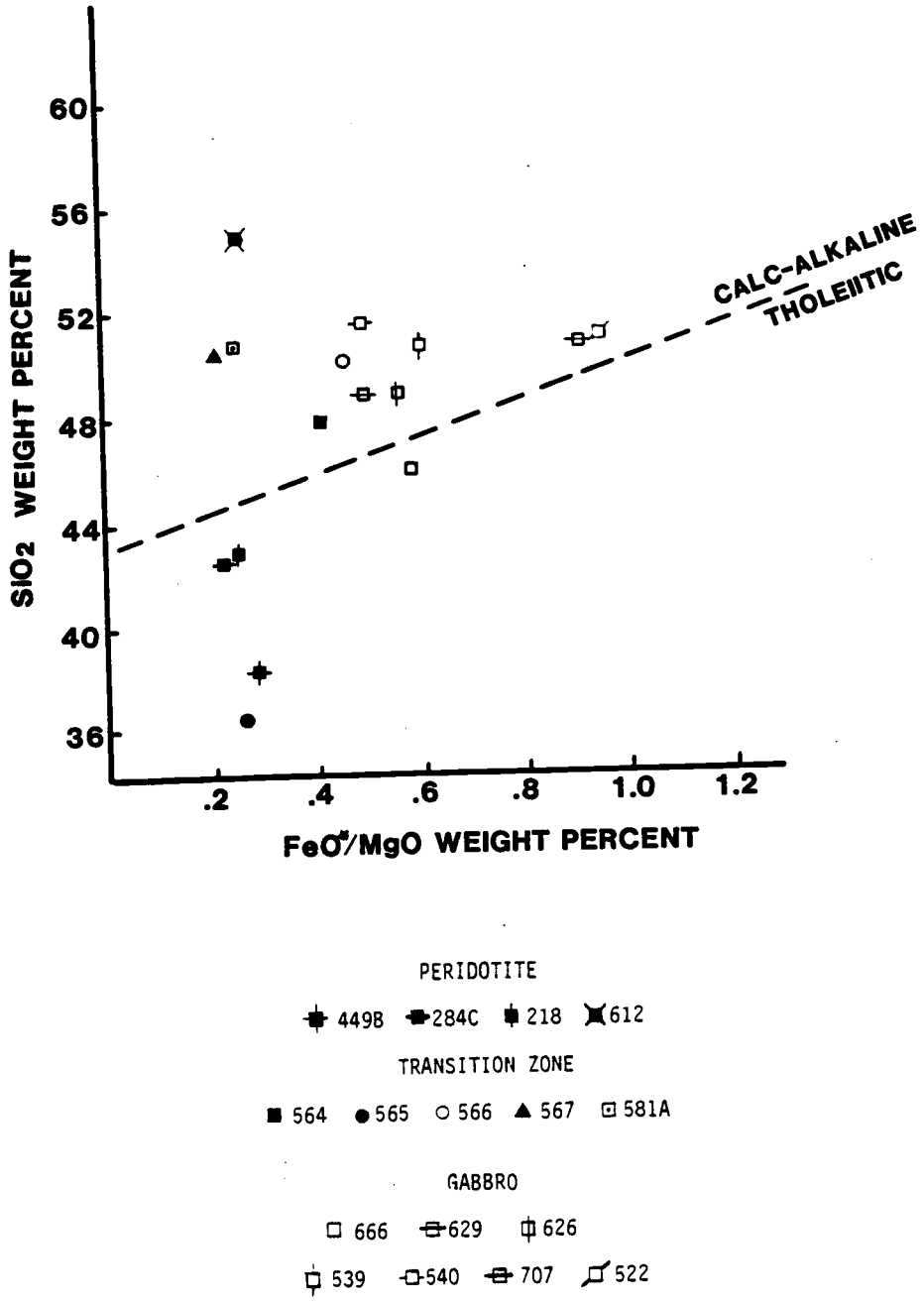

FIGURE 27. SiO_2:FeO*/MgO diagram for peridotite and gabbro of the Canyon Mountain complex.

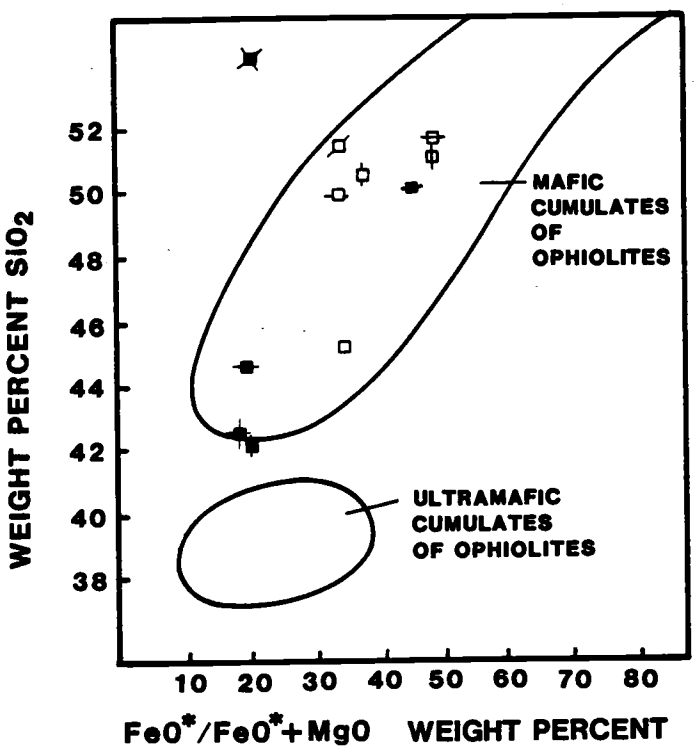

FIGURE 28. SiO_2:FeO*/FeO*+MgO diagram for tectonite peridotite and cumulate gabbro of the Canyon Mountain complex.

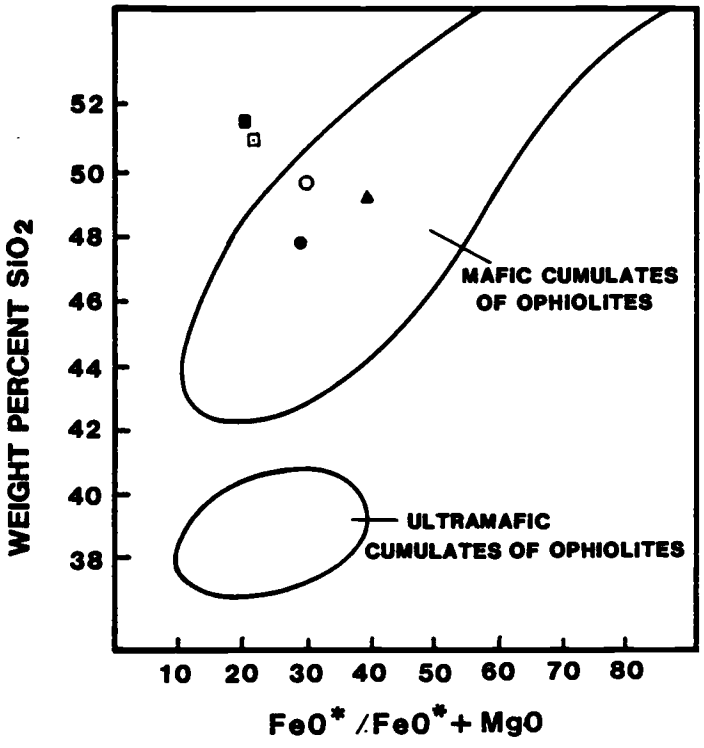

TRANSITION ZONE

■ 564 ▲ 567
● 565 ⊡ 581A
○ 566

FIGURE 29. SiO_2:FeO*/FeO*+MgO diagram for rocks of the transition zone of the Canyon Mountain complex.

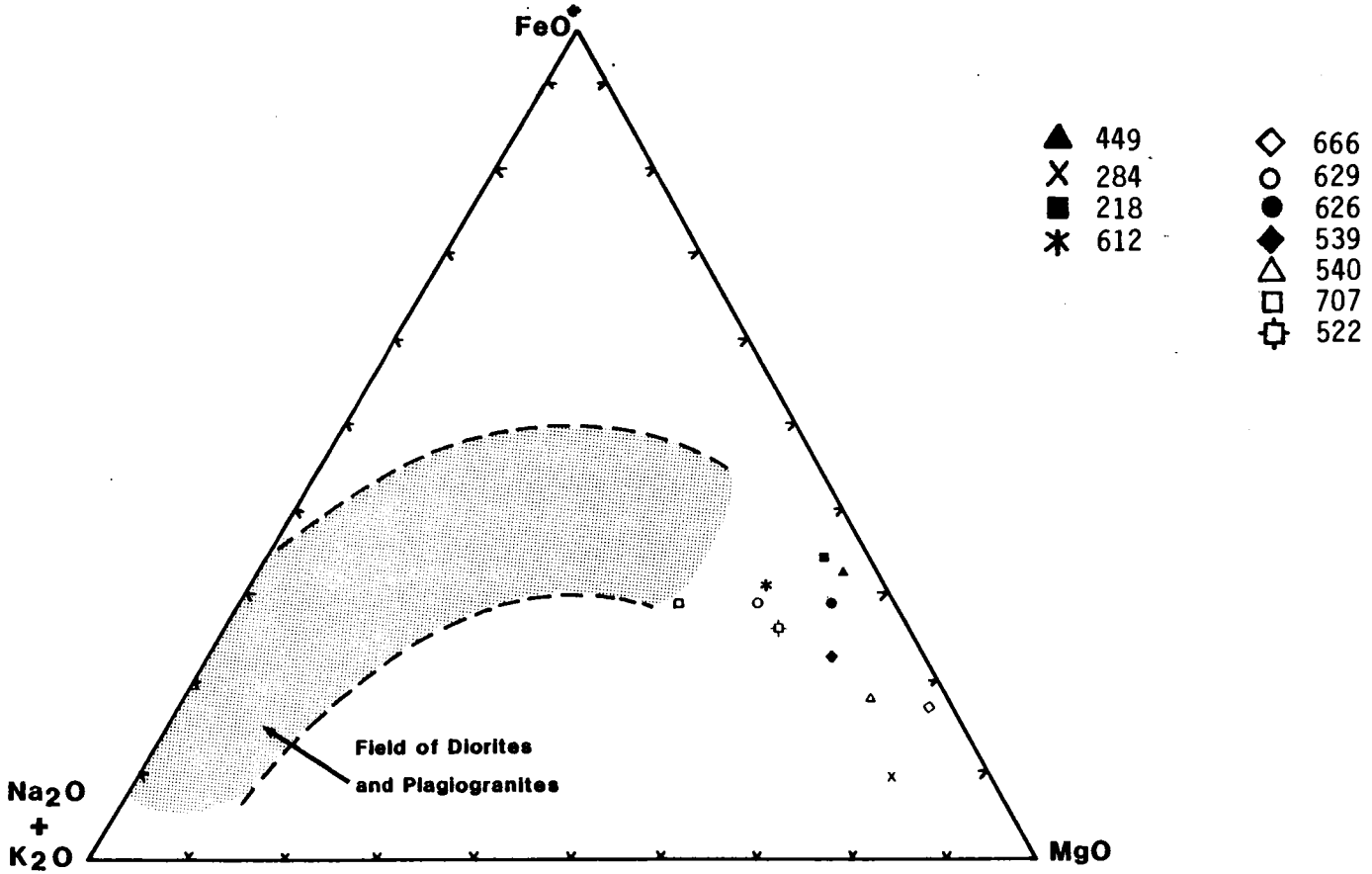

FIGURE 30. AFM diagram for gabbro and peridotite of the Canyon Mountain complex.

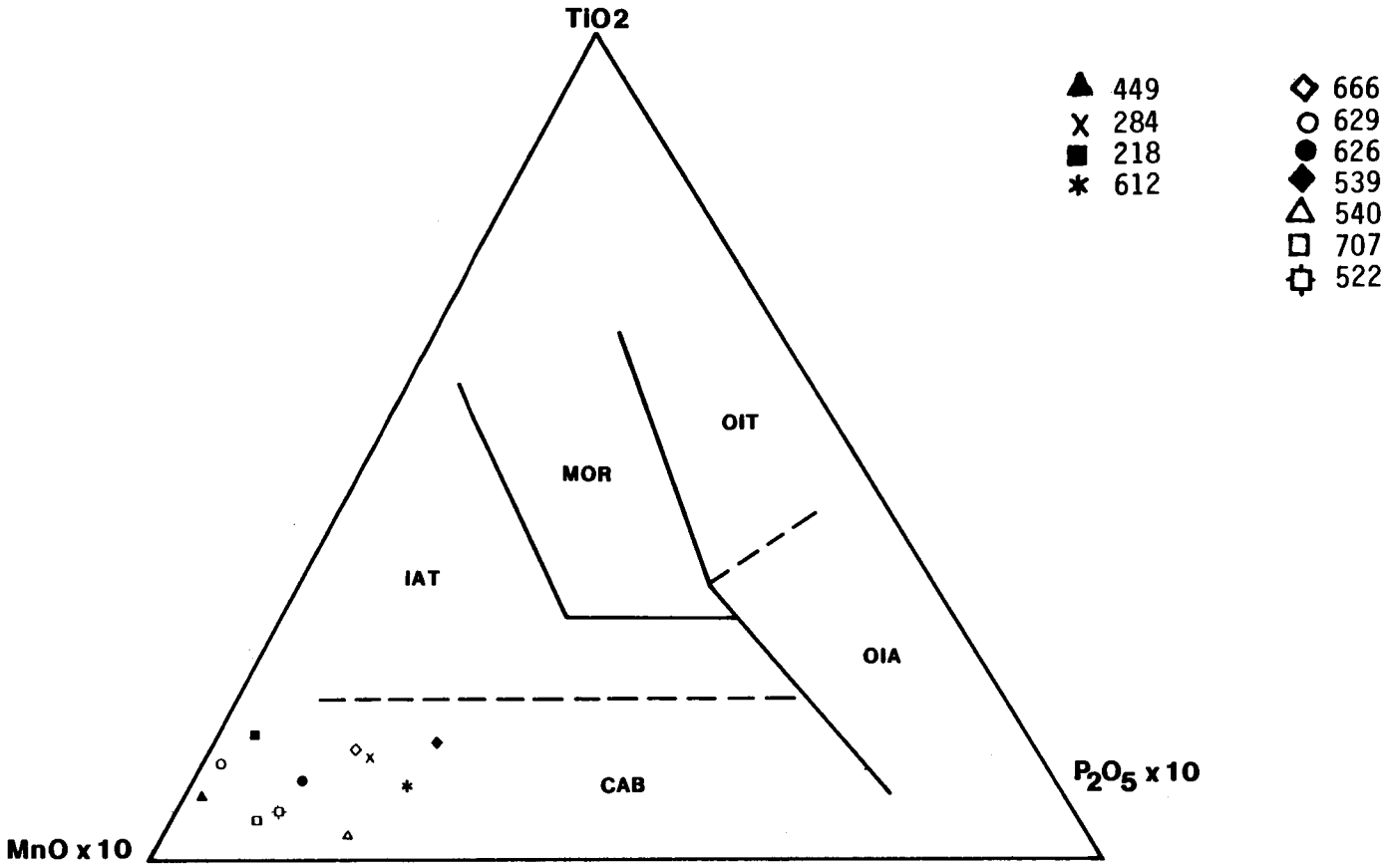

FIGURE 31. $MnO/TiO_2/P_2O_5$ for gabbro of the Canyon Mountain complex.

$MnO/TiO_2/P_2O_5$ relations of Canyon Mountain gabbroic samples (Figure 31) also clearly indicate calc-alkaline affinity for these rocks. Furthermore, SiO_2:(FeO*+MgO) ratios (Figure 27) for cumulate gabbros (with the exception of sample #666 of Gwynn Gulch) and transition zone gabbro plot in the calc-alkaline field.

Finally, the TiO_2:FeO*/MgO diagram discussed earlier (Figure 26) may also be utilized to distinguish ocean ridge tholeiite, island arc tholeiite, and calc alkaline trends (Coleman, 1977). On Figure 26, CMC gabbro falls on an IAT trend, harzburgites occur at the apex of MOR and IAT trends, and two evolved transition zone cumulates plot near the MOR trend. For a given SiO_2 content, Canyon Mountain complex gabbros are, as previously noted, quite low in TiO_2 compared to most ophiolites.

Summary of Major Element Geochemistry

1. Major oxide compositions of the peridotites are characteristic of depleted upper mantle rocks, with the exception of relative enrichment in K_2O for CMC peridotite.

2. Transition zone rocks have a high abundance of CaO which is probably a consequence of their high modal content of clinopyroxene and extremely calcic plagioclase. Although also relatively enriched in K_2O compared with other ophiolites, the transition zone rocks have more tholeiitic fractionation trends on AFM and SiO_2/FeO*:MgO and TiO_2/FeO*:MgO plots.

3. The fractionation trend of transition zone rocks on a $CaO/Al_2O_3/MgO$ diagram parallels, and is more Al_2O_3 and MgO enriched

than the CMC gabbro trend, indicating a more tholeiitic affinity for the transition zone than the gabbro.

4. The regular variation of major oxides with SiO_2 supports the CMC gabbro as being a single, fractionated magma. The primitive, parental composition, represented by the gabbro of Gwynn Gulch, is high in MgO, with tholeiitic ratios of FeO*, SiO_2, and alkalis. Progressive fractionates are more calc-alkaline. The CMC gabbros overall are K_2O-rich, TiO_2-depleted relative to other ophiolites. Most discriminant diagrams suggest island arc affinity for the gabbro.

5. Finally, irregularities in the variation of major oxides with SiO_2, especially for the transition zone, indicate that the CMC was periodically replenished by small quantities of primitive magma.

TRACE ELEMENT GEOCHEMISTRY OF PERIDOTITE AND GABBRO OF THE CANYON MOUNTAIN COMPLEX

Analyses for 14 trace elements (eight rare earth elements plus Ni, Cr, Co, Sc, Rb and Sr) were done by instrumental neutron activation (INAA) for 21 samples of the Canyon Mountain complex. Two tectonite harzburgites (296 and 110P) from the zone of infiltration, one lherzolite (284), four rocks of the Celebration Ridge transition zone (569, 574, 578, and 579), two gabbros from dikes within the peridotite (285, 110G), and 12 gabbros from throughout the CMC (664, 665, 666; 626, 629; 95, 531, 539, 540; 335, 713, 714, 721) were analyzed. Analyses are presented in Table 15.

Abundances of U, Th, Zr, Sb were below detectable limits in virtually all samples, reflecting low overall abundances of large ion lithophile (LIL) and incompatible elements in the Canyon Mountain complex.

Rare Earth Elements

Rare earth element (REE) patterns were determined for all analyzed samples. In some peridotites La and Nd were below detectible limits. Analytical precision for light rare earth elements (LREE) is ± 5-12 percent, and for heavy rare earth elements (HREE) of atomic number 64 or greater, analytical error is ± 7-23 percent. Analytical precision is better for more silicic, upper level gabbros which have greater overall REE abundances.

All analyzed gabbro and peridotite of the Canyon Mountain complex are depleted in LREE reflecting 1) a generally high

TABLE 15. Trace element analyses of rocks of the Canyon Mountain complex, in ppm.

	PERIDOTITE				TRANSITION ZONE			
	664	284	110P	296	574	578A	579A	569
La	.06	--	--	0.06	0.17	0.20	0.12	0.07
Ce	0.24	--	--	--	0.69	0.59	0.41	0.30
Nd	--	--	--	--	1.24	0.54	0.53	0.50
Sm	.17	0.01	0.06	0.35	0.69	0.28	0.13	0.31
Eu	.05	0.08	--	0.19	1.31	0.29	0.18	3.62
Tb	--	--	--	--	0.21	0.10	--	0.06
Yb	.23	0.09	--	0.41	0.97	0.40	0.20	0.41
Lu	.18	.03	0.03	0.12	0.16	0.09	0.06	0.04
Rb		--	--	--	--	1.7	--	--
Sr		44	--	450	--	--	84	--
Co		40	43	44	--	42	26	--
Sc		11	11	6	--	54	36	--
Ni		2800	2800	2750	--	100	50	--
Cr		3800	3700	5800	--	8000	3500	--

	DIKES			GWYNN GULCH GABBRO		BEAR SKULL RIMS		TABLE CAMP GABBRO			PINE CREEK MOUNTAIN GABBRO					
	110G	285	531	666	665	626	629	95	539	540	708	707	713	714	721	335
La	.06	.24	.02	0.08	0.17	0.06	0.06	0.09	0.07	0.08	0.04	0.20	.01	1.54	.44	.23
Ce	0.31	0.76	0.13	0.34	0.50	0.27	0.28	0.34	0.35	0.39	0.16	0.71	0.09	4.8	1.21	1.73
Nd	--	--	0.42	0.53	0.57	0.69	0.81	--	0.59	0.67	0.32	1.35	0.90	5.70	--	2.32
Sm	0.35	0.44	0.25	0.34	0.28	0.37	0.39	--	0.32	0.32	0.20	0.78	0.62	2.06	0.42	1.15
Eu	0.19	0.21	0.59	0.14	0.13	0.16	0.29	1.16	0.53	0.58	0.13	0.26	0.67	2.24	2.53	1.22
Tb	0.18	--	0.12	.06	--	--	0.14	--	--	0.21	0.08	0.18	--	0.42	--	
Yb	0.77	0.41	0.40	0.36	0.38	0.32	0.59	0.30	0.70	1.03	0.35	1.09	0.56	2.17	0.21	--
Lu	0.12	--	0.09	0.08	0.06	0.07	0.17	0.05	0.19	0.06	0.05	0.28	0.16	0.49	0.06	0.59
Rb	--	--	--					--	--		--	--		--		--
Sr	329	391	--	--				366			88			--		227
Co	25	20	33	90	30	--	42	30	--	35	31	38	--	21	--	15
Sc	40	34	25	24	26	--	40	24	--	25	44	44	--	40	--	55
Ni	370	385	100	300	265	--	200	190	--	90	20	20	--	15	--	100
Cr	1300	1100	1700	4850	4100	--	2700	--	--	2700	1300	1050	--	10	--	160
Hf				0.20	0.10		0.01			0.06	0.1	0.07	--	0.16	-	--
Ta				0.30	1.80	--	--0.0							0.01		
Th							0.03.				0.11	0.11				

modal abundance of pyroxene and 2) the overall primitive, unfractionated nature of the magma represented by these rocks.

Rare Earth Element Geochemistry of Peridotite

Two tectonite peridotites - a harzburgite (296) from the zone of infiltration and a lherzolite (284) which is adjacent to rare 0.5 mm-wide feldspathic veins, were analyzed for REE. Their REE patterns (Figure 32) are anomalous compared to concave-upward REE patterns reported in some ophiolites such as Samail and Point Sal. Both samples have La, Ce, and Nd values below detectable limits of 0.05 times chondrite for INAA in this study. They have pronounced positive Eu anomalies of, respectively, 2.2 and 1.0 times chondrite, and have HREE of 0.45 and 2.0 times chondrite. Their Eu and HREE are similar to cumulate troctolites reported by Gerlach (1980) for the Canyon Mountain complex and by other investigators elsewhere (Coleman, 1977). Extreme LREE depletion may be due simply to the overall LREE depletion seemingly characteristic of the CMC system. The substantial positive Eu anomaly in these rocks does not prove either their cumulate origin or a fertile nature, but rather simply indicates the presence of a calcic, unfractionated feldspathic component. The low abundance of REE, and LREE depletion of 284 is marked compared to fertile lherzolites such as Ronda (Menzies, et al., 1977a), and suggests the CMC rocks are depleted and incapable of yielding basaltic melt.

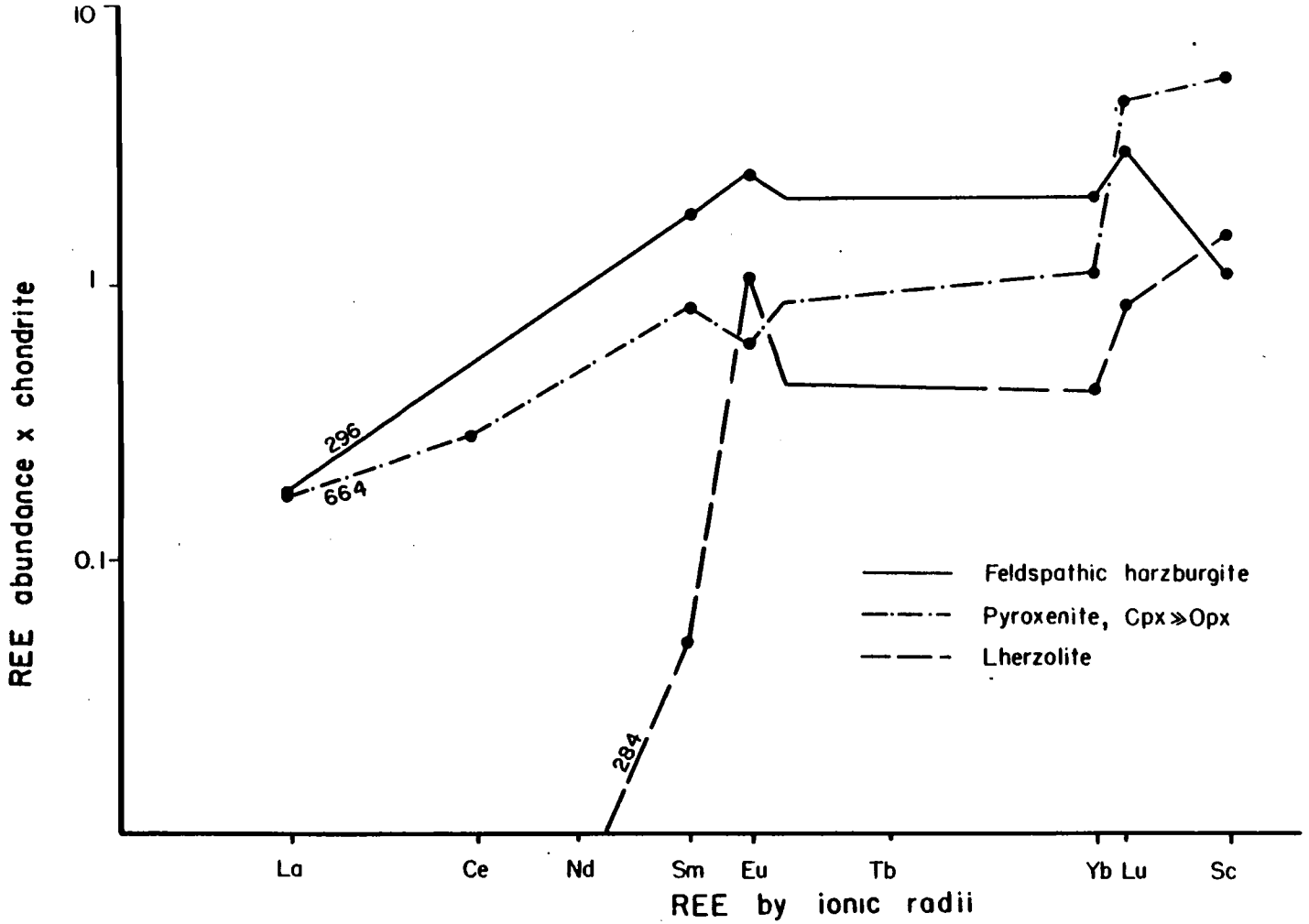

FIGURE 32. REE for peridotite of the Canyon Mountain complex.

Rare Earth Element Geochemistry of the Rocks of the Transition Zone

Rare earth element data from four rocks of the transition zone on Celebration Ridge (Ridge 2) (Figure 33) have depleted LREE (La = 0.3-0.8 x chondrite, La/Sm = 0.4-0.8), large positive Eu anomalies, and flat HREE. Samples 578 (melagabbro) and 579A (olivine websterite) from the summit of the ridge, have relatively flat patterns with slight (2.0-4.0 times chondritic) positive Eu anomalies. Sample 574, an olivine-orthopyroxene-clinopyroxene gabbro from the center of the ridge is more LREE depleted than the melagabbro, and has a very strong positive Eu anomaly, indicating accumulation of early plagioclase. These patterns suggest that continued fractionation occurred throughout the Celebration Ridge sequence, with probably a small influx of primitive melt into upper portions of the magma chamber to account for greater relative LREE depletion in 579 than either 578 or 574, and the low abundance of REE in rocks of the upper ridge.

Gabbro 569, from the basin west of Celebration Ridge, has the strongly depleted LREE, and large positive Eu anomaly characteristic of gabbroic rocks on Baldy Mountain near Table Camp. Its REE pattern crosses all three Celebration Ridge patterns. Hence the gabbros in Pine Creek west of Celebration Ridge are not part of the transition zone sequence and were probably intrusive into transition zone cumulates at an early stage of CMC history. The absence of tectonite fabric in the cumulate gabbros such as 569 indicates that they intruded the transition zone after its deformation.

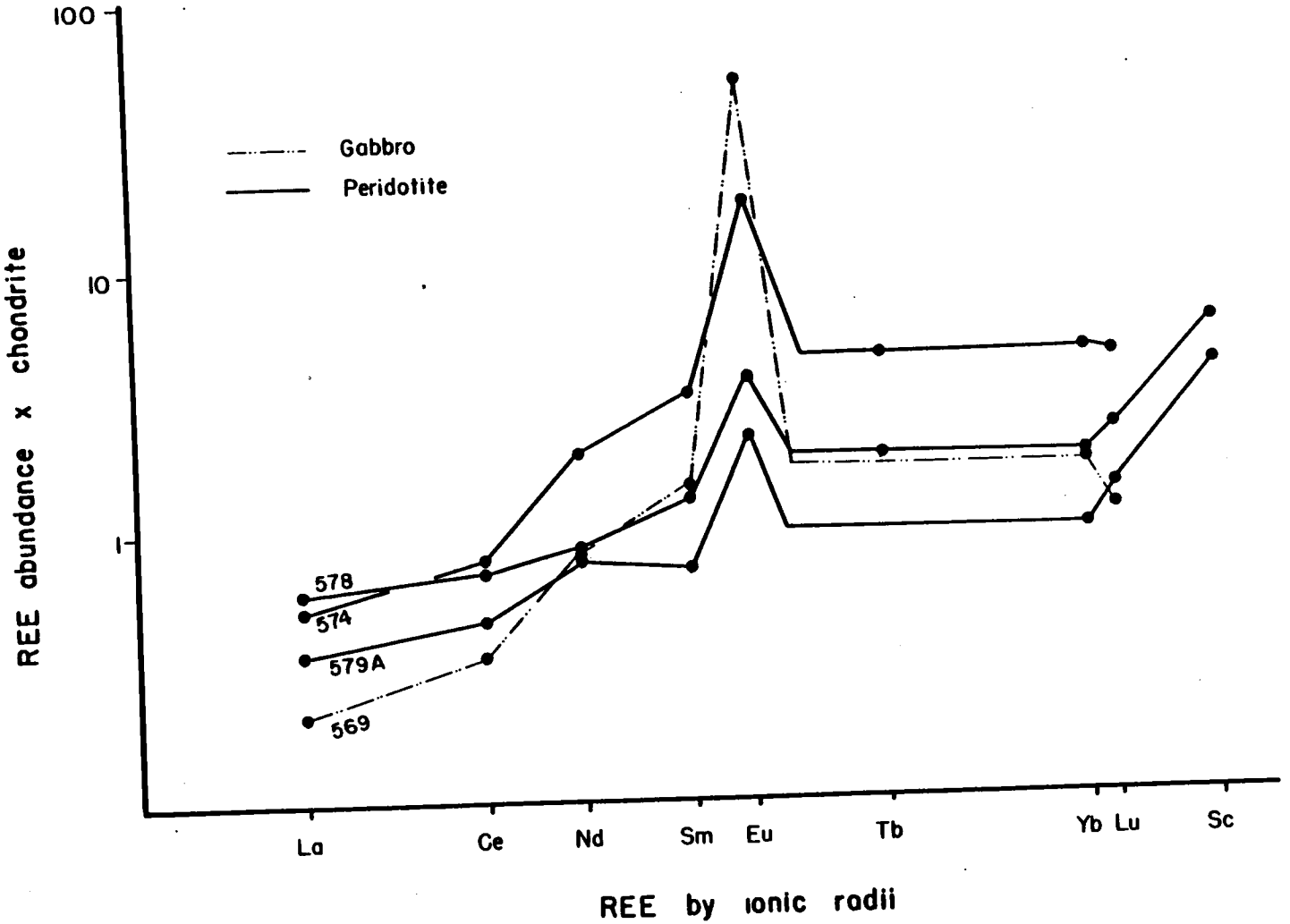

FIGURE 33. REE for rocks of the transition zone.

Rare Earth Element Geochemistry of Gabbro

Gabbro of the Canyon Mountain complex exhibits REE patterns which indicate protracted fractionation and accumulation, as well as influx of more primitive magma.

Gabbro from dikes in tectonite peridotite (110G, 285; Figure 34), from Gwynn Gulch (665, 666; Figure 35), and the gabbro of Bear Skull Rims (626, 629; Figure 36) is noteworthy for low overall REE abundance, extreme depletion of LREE, and flat patterns for HREE.

Abundance of REE in Gwynn Gulch gabbro varies from 0.20 to 2.0 x chondritic. This range is characteristic of primitive, undifferentiated melts of both MOR and IAT affinity (Hanson, 1980). Gabbro from the northwest side of Baldy Mountain which is interlayered with tectonite harzburgite and dunite (285), and gabbro dikes within tectonite harzburgite (531, 110G) have slightly greater REE abundances, with LREE-depleted patterns, flat HREE, and a slight positive Eu anomaly suggesting possible accumulation of plagioclase. The interlayered gabbro of northwest Baldy Mountain is slightly more HREE enriched than 531 and 110G dikes, reflecting a greater abundance of orthopyroxene.

Gabbro of Bear Skull Rims, mostly two-pyroxene gabbro with clinopyroxene predominant, displays REE patterns which are only slightly more evolved than the patterns of Gwynn Gulch and the dikes. Samples 626 (fresh) and 629 (slightly altered) have abundances of La = 0.2 x chondritic, and Lu = 2.0 x chondritic - very similar to gabbro discussed above. Both have slight positive

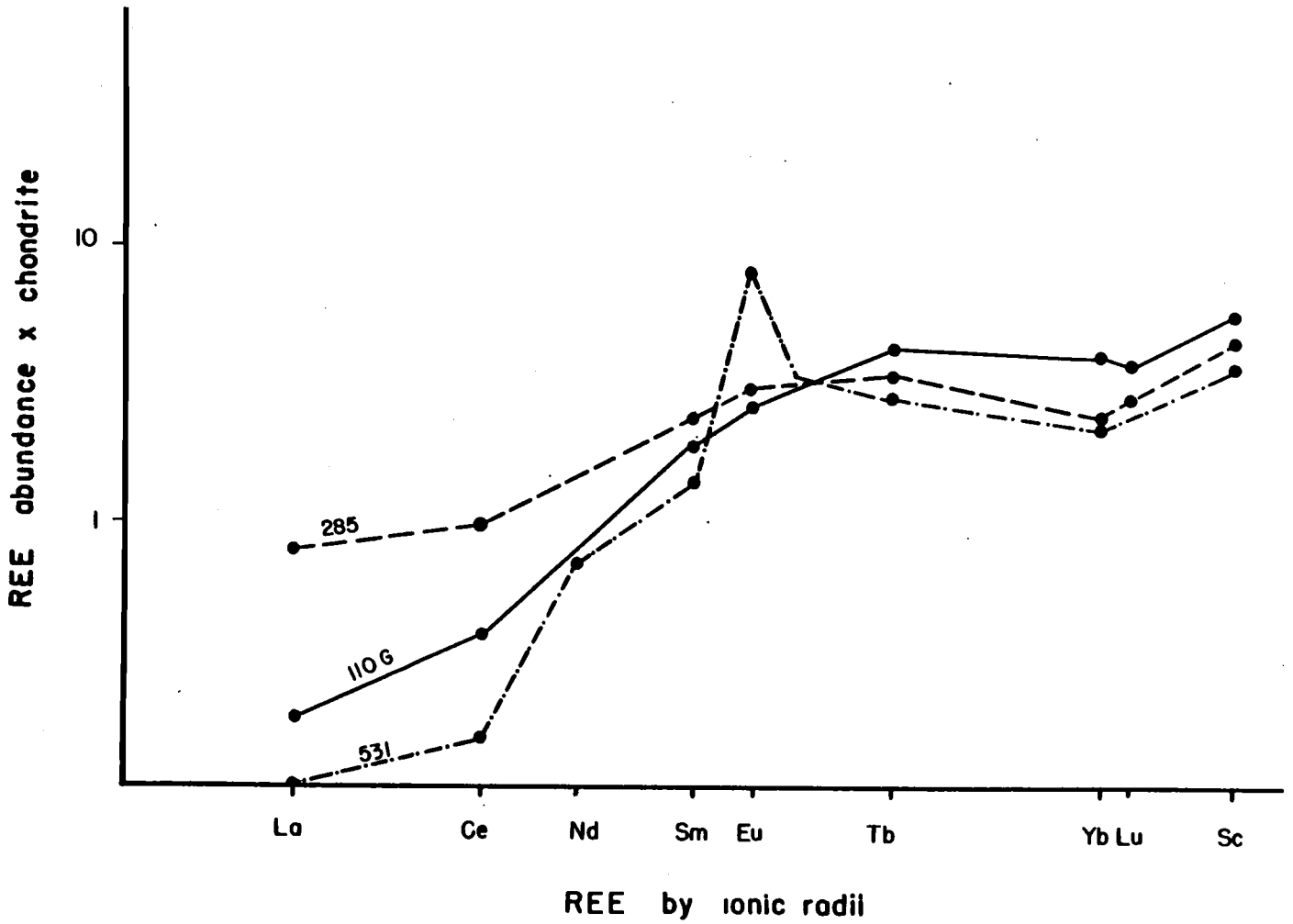

FIGURE 34. REE for gabbro dikes in harzburgite.

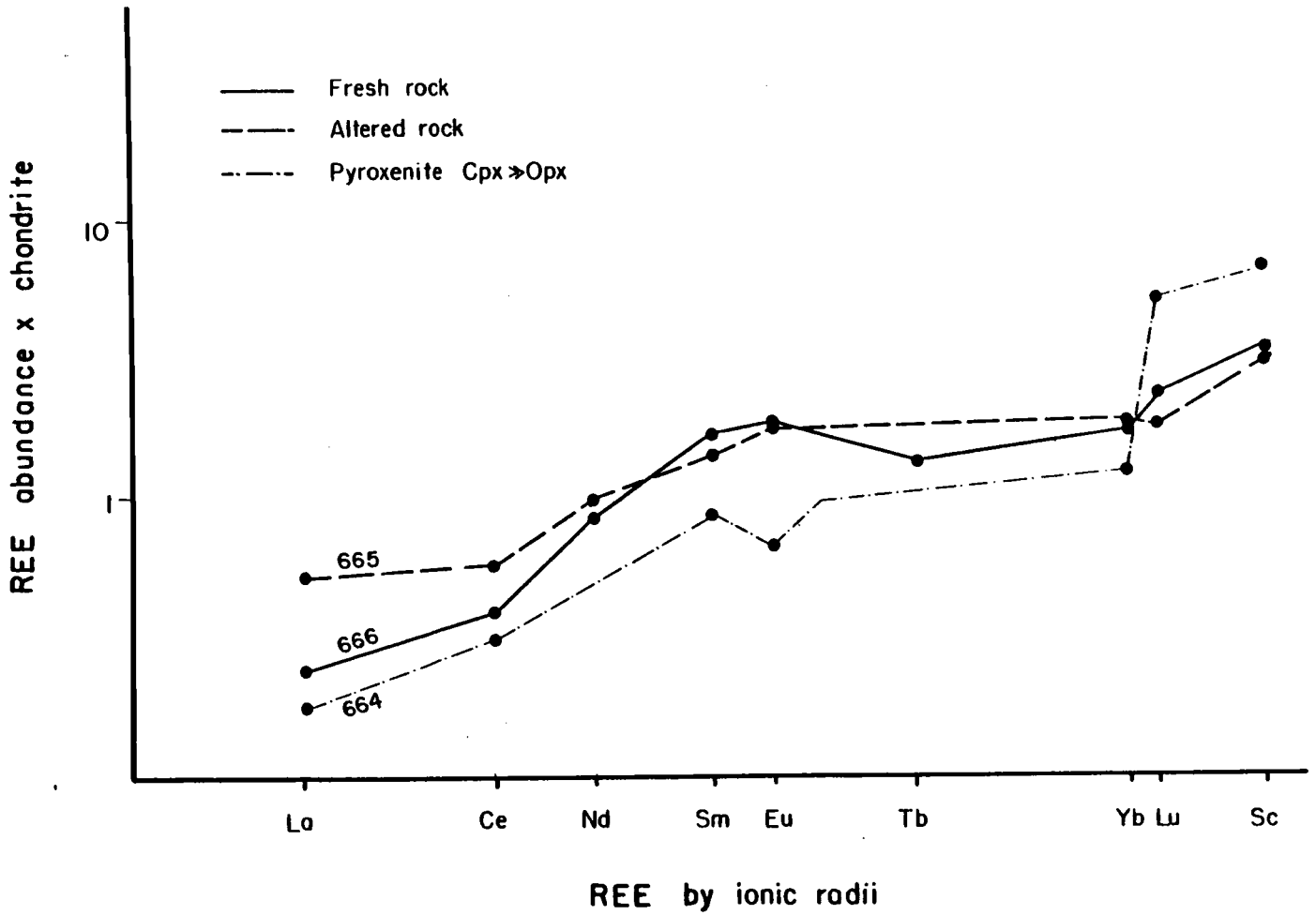

FIGURE 35. REE for gabbro of Gwynn Gulch.

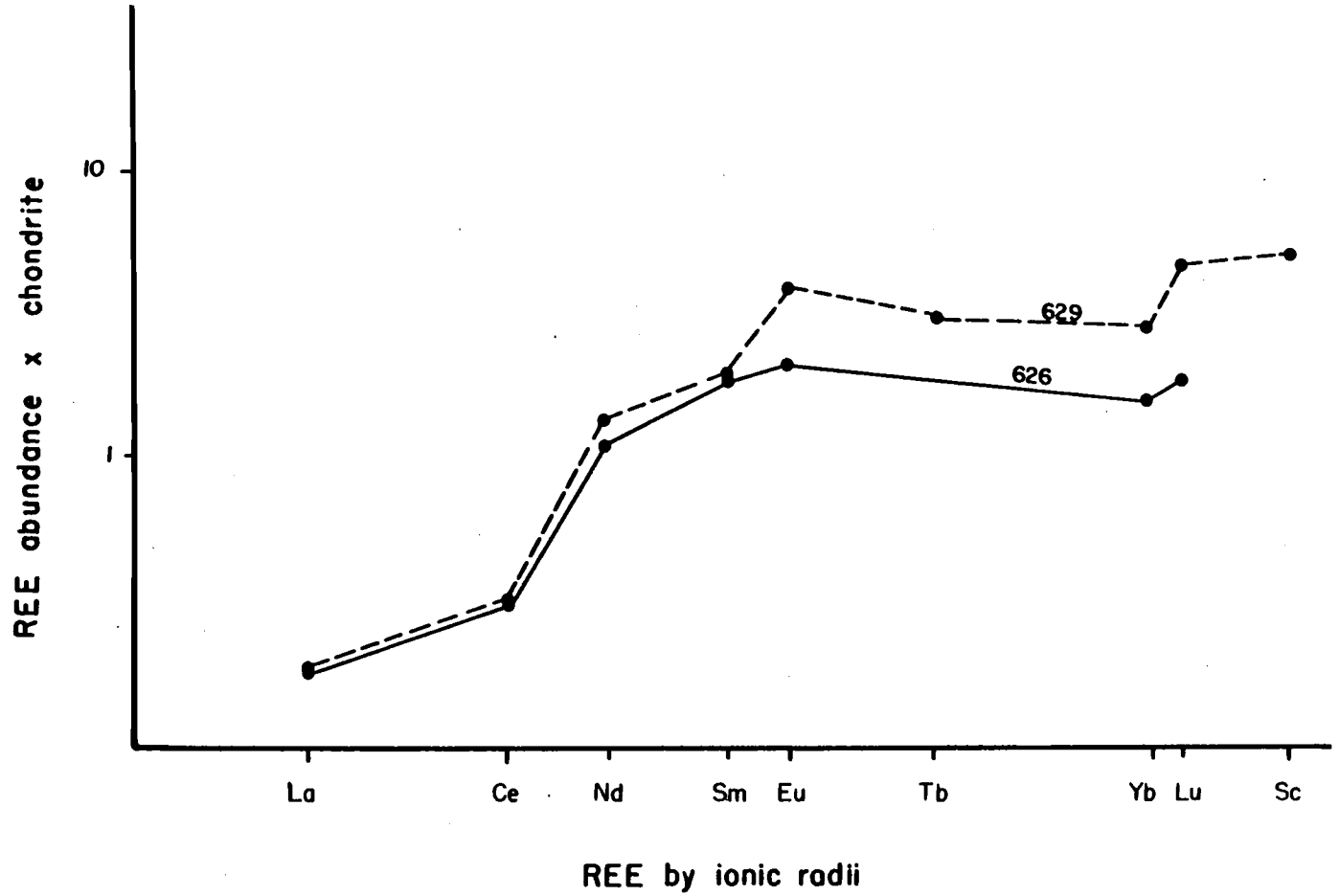

FIGURE 36. REE for gabbro of Bear Skull Rims.

Eu anomalies, suggesting that some plagioclase accumulated. These gabbros have adcumulate textures, are layered at a few localities (629) and are isotropic or slightly foliated elsewhere (626). The small positive Eu anomalies indicate cumulate processes were important; low LREE abundances show that magmas were not highly evolved.

Gabbro near Table Camp on the southeast side of Baldy Mountain (95, 539, 540) is olivine two-pyroxene gabbro with greater modal abundance of orthopyroxene than gabbro of Bear Skull Rims. Gabbro near Table Camp (Figure 37) is generally less depleted in LREE than Gwynn Gulch, Bear Skull Rim and dike gabbros, and has a strong positive Eu anomaly eight to 12 times chondritic. Just as the Bear Skull Rims gabbro, these rocks have adcumulate textures and a high modal abundance of very calcic plagioclase, which is reflected in the pronounced concentration of Eu.

Increasing overall REE abundances, increased La/Sm, and greater positive Eu anomalies are characteristic of upper level gabbro of Pine Creek Mountain (714) and Yellow Jacket Ridge (721) (Figure 38). REE are 1.5 to 12 times chondritic; abundances in 714 are greater than 721. Both have nearly flat patterns with La/Lu ratios of 0.75 with La/Sm of 0.65 and 0.80, respectively. Their Eu abundances are both about 12 x chondritic. With the exception of the large Eu anomaly, the overall patterns of these gabbros are flat. In these hypidiomorphic rocks, clinopyroxene is subordinate to orthopyroxene, plagioclase (An_{70}) is abundant, and olivine is absent. REE patterns reflect these modes. The greater LREE abundance indicates that the upper Pine Creek Mountain gabbro magma was more fractionated

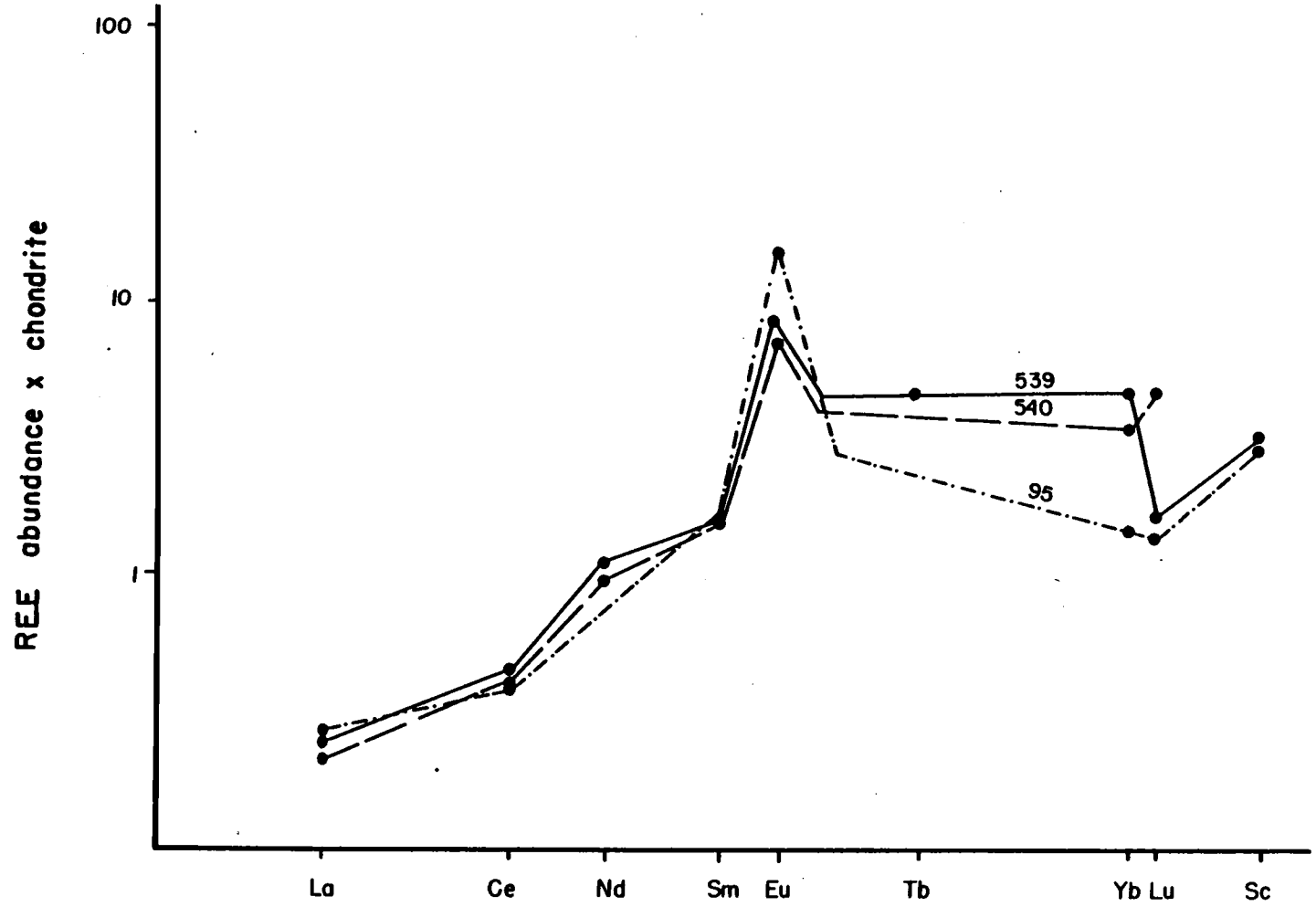

FIGURE 37. REE for gabbro of Table Camp.

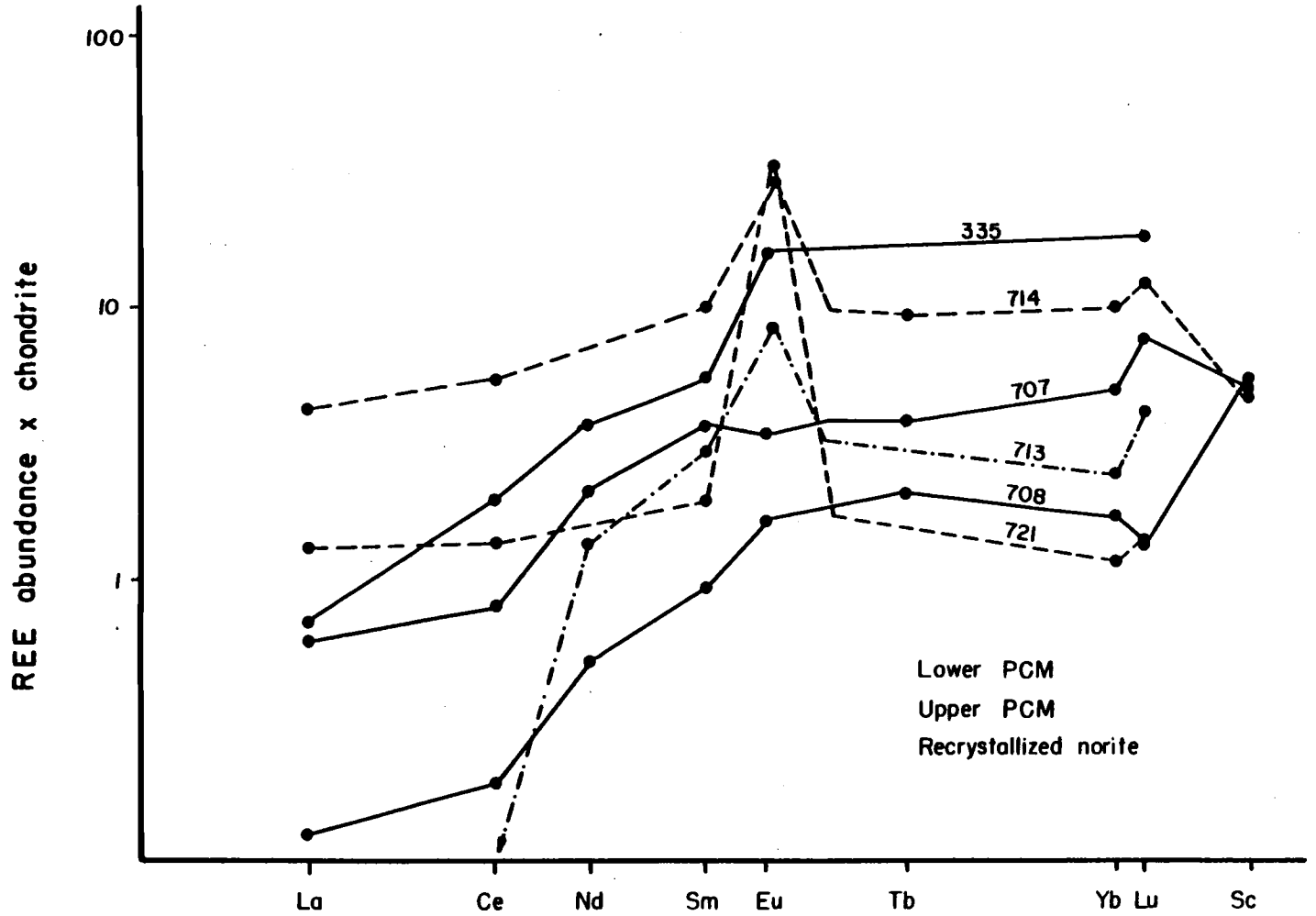

FIGURE 38. REE for Pine Creek Mountain and recrystallized gabbro.

than gabbro previously discussed which is stratigraphically lower. Substantial accumulation of plagioclase is suggested by the large Eu anomalies, especially in 721.

Sample 713, a layered hypersthene + augite gabbroic rock (norite) of Norton basin contains 17 modal percent poikiloblastic green-brown hornblende, and has been affected by hydrous recrystallization. Its rare earth element pattern is extremely depleted in LREE (La/Sm = 0.01, La = 0.05 times chondritic), and slightly enriched in HREE, with a significant positive Eu anomaly of eight times chondritic. The REE pattern suggests this rock is a product of pulses of primitive LREE depleted melt which mixed with more evolved, HREE enriched magmas in the upper chamber.

An alternative explanation for this pattern is mobilization and removal of LREE via metasomatism, rock hydration, and alteration, with eventual partial fusion of some gabbros to produce plagiogranite magma. However, REE are generally immobile in alteration processes at least to greenschist facies conditions (400°C +), and are usually enriched rather than depleted (Pallister and Knight, 1981). Other than growth of poikiloblasitic hornblende, which should increase LREE (K_D Ce melt/amphibole = 0.85 (Hanson, 1980)), alteration of 713 is not significantly greater than 714, or 721.

Sample 335 represents one of the most evolved gabbros of this study. It is a plagioclase (An_{65})-orthopyroxene, apatite and zircon bearing, isotropic gabbro from the northeast side of Pine Creek Mountain. Although it is markedly depleted in LREE

(La = 0.6 times chondrite), it has no Eu anomaly and strong (25 x chondrite) enrichment in HREE. The great abundance of HREE is probably due to the presence of zircon which has a high K_D for HREE. The absence of Eu anomaly reflects the lower An content of the plagioclase and results principally from precipitation of feldspars throughout earlier gabbro. Depletion in LREE, and consequent crossing REE patterns of this rock and other gabbros again indicate that fractionation was complicated by late injection of more primitive melt.

Comparison of REE Geochemistry to Other Ophiolites

Numerous studies of REE abundances and behavior in all components of ophiolites have been published (Figures 39, 40). Generally, the ultramafic rocks have very low REE abundances with concave upward patterns due to their depleted, residual nature (Coleman, 1977; Menzies, 1976; Jaques and Chappel, 1980). Cumulate gabbros are strongly depleted in LREE, may display positive Eu anomalies, and have overall REE abundances between 0.1 and 2.0 times chondrites. Upper level gabbros are not as LREE depleted, lack the pronounced positive Eu anomaly, and characteristically have abundances between two and seven times chondritic. Pillow lavas and sheeted dikes of "average" ocean ridge ophiolites plot in the range of ten times chondritic, with flat overall patterns, and plagiogranites have similar abundances but show a negative Eu anomaly.

More specifically, in the Point Sal ophiolite, Menzies, et al. (1977a) have shown that olivine-clinopyroxene gabbros are

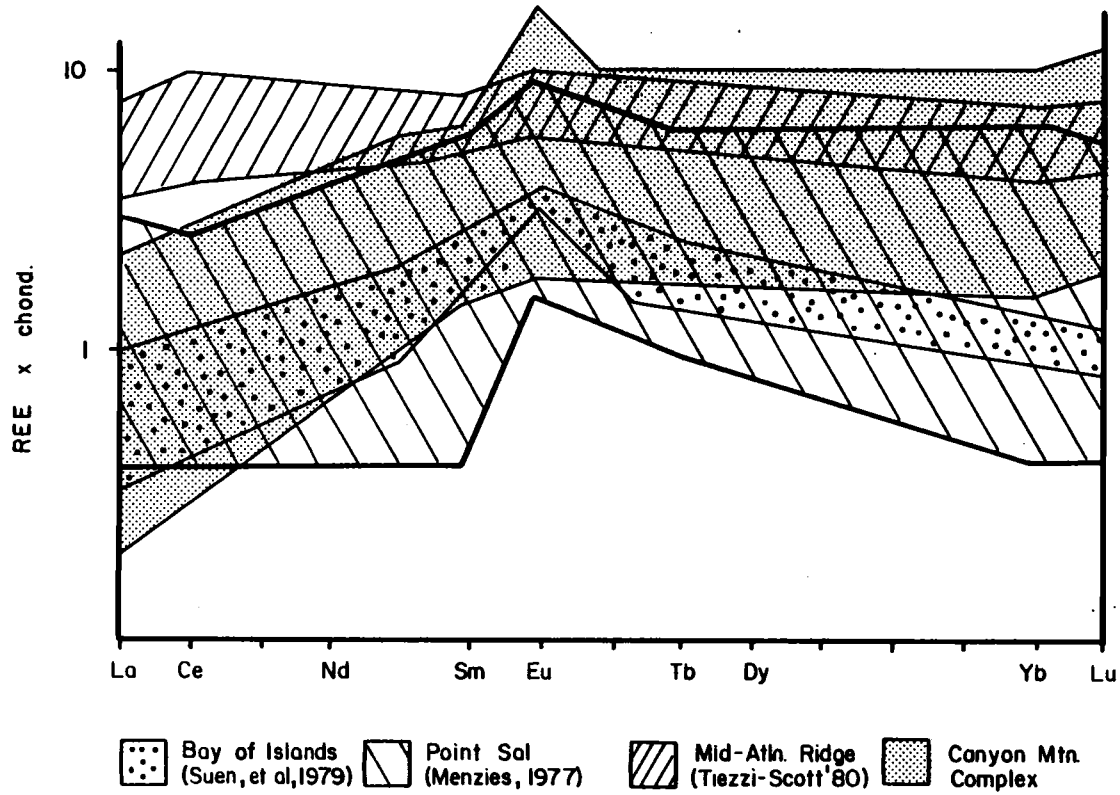

FIGURE 39. Range of REE in gabbro of ophiolites.

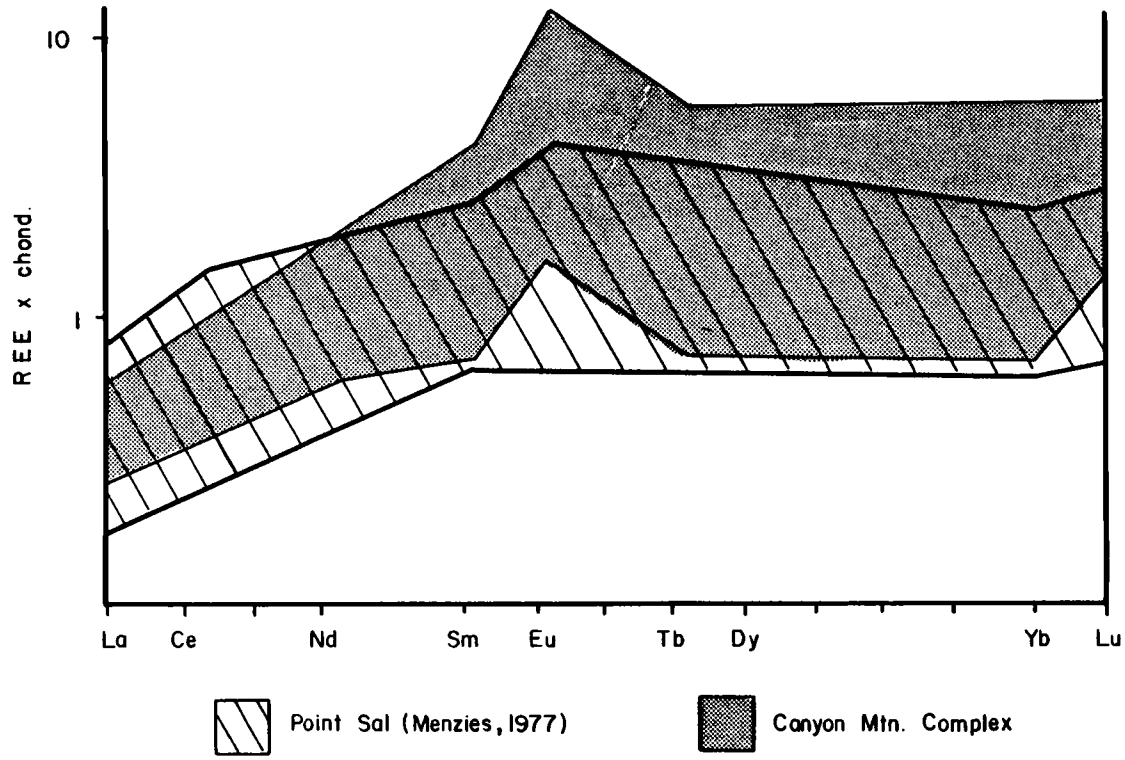

FIGURE 40. Range of REE in transition zone cumulates.

approximately 0.4 times chondritic in La, are slightly Eu enriched, and have flat HREE - a pattern which is similar to the Canyon Mountain complex. Upper level gabbros of Point Sal have total REE about the same as chondritic abundances, flat patterns, and positive Eu anomalies up to ten times chondritic. Because of the impossibility of differentiating LREE-enriched plagiogranite from strongly LREE depleted gabbro, Menzies invokes separate sources for silicic plutonic and extrusive components of ophiolites.

In the Samail ophiolite investigated by Pallister and Knight (1981), the tectonite harzburgite has "typical" V-shaped REE patterns, and cumulate gabbros are enriched in REE abundances by an order of magnitude (one to eight times chondritic) above Canyon Mountain complex gabbros although they are still strongly LREE depleted and have positive Eu anomalies. Diorites and plagiogranites of the Samail are similar to abundances and patterns of equivalent CMC rocks reported by Gerlach (1980).

REE patterns and progressions of units in the Canyon Mountain complex are similar to plutonic rocks (gabbros) from DSDP site 334 on the mid-Atlantic ridge (Dostol and Muecke, 1978), and to peridotites and gabbros of Troodos reported by Kay and Senechal (1976), although gabbro LREE is more strongly depleted in CMC rocks than other ophiolites. The REE most like Canyon Mountain are those of the Bay of Islands ophiolite, Newfoundland (Suen, et al., 1979). Gabbros in these rocks are severely depleted in both overall REE and LREE abundances. Most cumulate ophiolitic gabbros show marked

positive Eu anomalies, although few are as greatly Eu enriched as Canyon Mountain upper cumulate gabbro. The large anomalies of the CMC may be partly due to high CaO content of plagioclase in those rocks, and partly due to periodic influxes of fresh magma with renewal of Eu abundances. HREE enrichment of CMC gabbro compared to other ophiolites reflects the greater abundance of orthopyroxene in the Canyon Mountain complex.

Rb and Sr in Peridotite and Gabbro

Abundances of Rb are low in all CMC units analyzed, but are slightly higher than abundances in other ophiolites. Rb is between 15 and 20 ppm in gabbros, and below detectable limits in peridotites. The slight relative abundance of Rb may reflect the slightly greater amount of K_2O noted in CMC units. Sr is also more abundant than is common in ophiolites, 20 to 46 ppm in harzburgite, 67 to 107 ppm in primitive gabbro of Gwynn Gulch and veins in peridotite, and up to 391 ppm in more fractionated gabbro such as 713 and 714. This overall greater concentration is consistant with either the high CaO content of most CMC samples, or - especially in peridotite - infiltration of gabbroic melt and possible attendant metasomatism.

Cr and Ni in Peridotite and Gabbro

Abundances of both Cr and Ni are high throughout peridotite and gabbro of the Canyon Mountain complex. It is noteworthy that Cr-enrichment persists through the gabbro, and that most gabbro

contains at least 20 modal percent clinopyroxene. Clinopyroxene from gabbro in the upper transition zone (Table 7) contains as much as 0.25 weight percent Cr_2O_3, and comprises 20-35 percent of the rock. Orthopyroxene of the same samples contains as much as 0.77 weight percent Cr_2O_3 (Table 6) and comprises 15 to 18 percent of the rock. If these Cr_2O_3 abundances are characteristic, high Cr_2O_3 content of the transition zone and lower gabbros of the Canyon Mountain complex would be expected.

Nickel abundances are more consistent with values reported for other ophiolites, and generally reflect modal olivine or modal sulphide. Nickel-iron sulphide (pentlandite) in the upper transition zone helps account for up to 2800 ppm Ni in these rocks.

Cr and Ni show marked and logical variance through the lower stratigraphic succession of the CMC. Their variation with progressively evolved peridotite and gabbro is shown in Figures 41 and 42. Cr is enriched in pyroxenite and less abundant (but greater than 3000 ppm) in harzburgite and lherzolite samples. Its abundance increases abruptly in the pyroxene-rich cumulates of the transition zone, and declines slightly in gabbro dikes in the harzburgite. Cr increases again in the gabbro of Gwynn Gulch, then declines rapidly through the cumulate gabbro section.

Gabbroic dikes in Baldy Mountain (285, and 110G) have Ni abundances similar to the gabbro of Gwynn Gulch and may represent unfractionated magma related to Gwynn Gulch gabbro. Specimens 110G and 285, despite low Cr content have depleted LREE patterns and very low REE abundances also similar to gabbro of Gwynn Gulch.

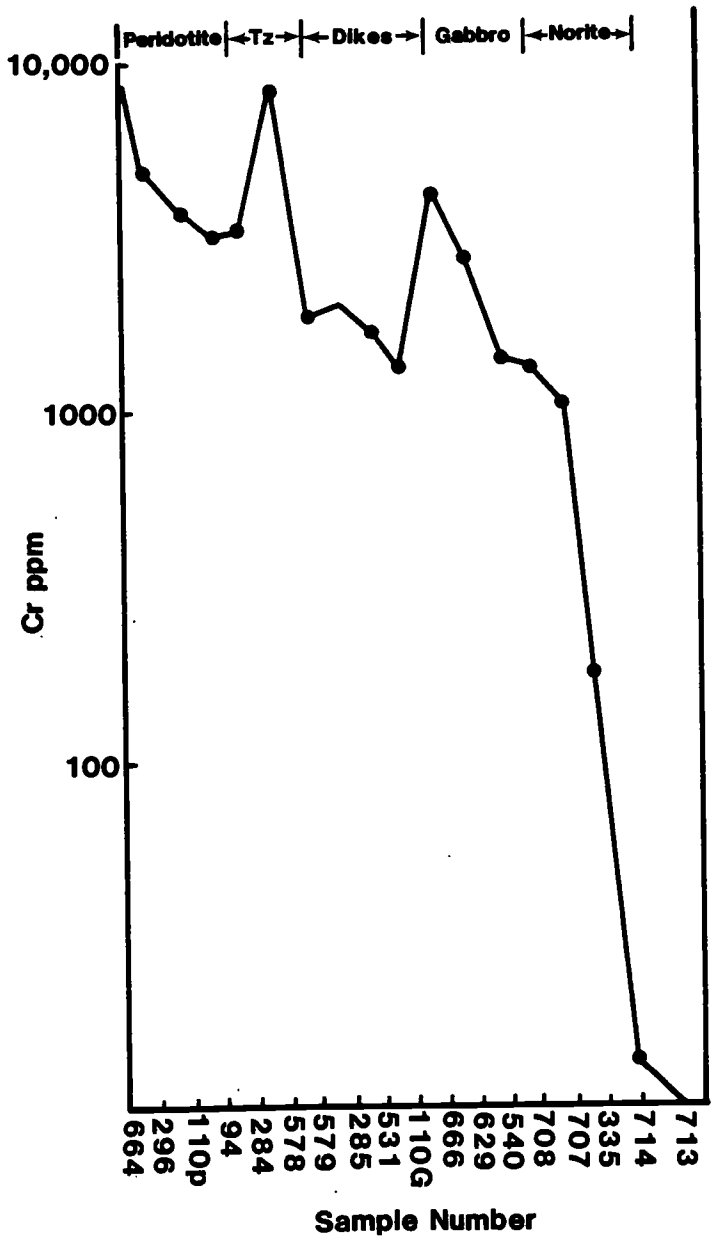

FIGURE 41. Cr varience with stratigraphy, peridotite and gabbro.

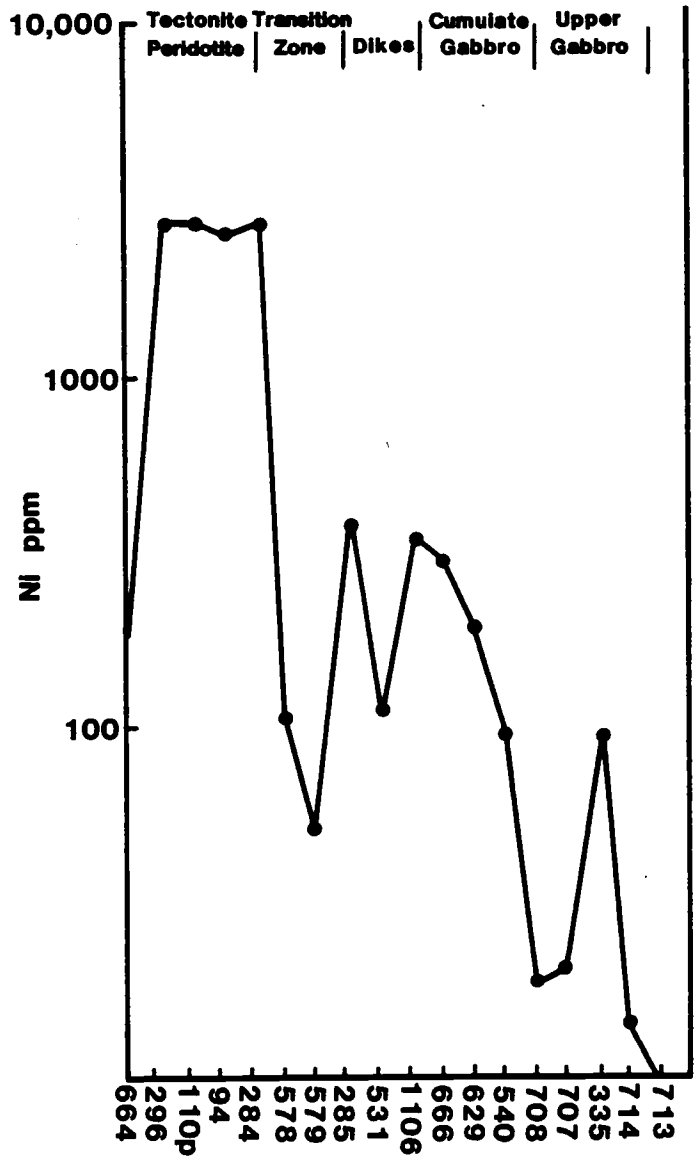

FIGURE 42. Ni varience with stratigraphy, peridotite and gabbro.

The low abundance of Cr may merely reflect low modal abundances of pyroxene in the dikes. The low abundance of Ni in sample 531, combined with a positive Eu anomaly, suggests it is a more plagioclase-rich rock.

Ni is greatly enriched in tectonite harzburgite, and generally decreases in abundance through the gabbro. As should be expected, its abundance in transition zone and lower gabbroic rocks is directly proportional to the amount of olivine present. Ni varies in the gabbro dikes as a function of mineralogy. Both 110G and 285 are high in Ni, and contain small amounts of modal olivine (Fo_{70}). Sample 531, which is low in nickel, contains no olivine. Ni decreases regularly through the gabbro, with the exception of 335. The abundance of both Cr and Ni in the gabbro of Gwynn Gulch, as well as in gabbro dikes within the harzburgite suggest that the dikes, and particularly the gabbro of Gwynn Gulch are relatively unfractionated and represent possible parental compositions for CMC gabbro. One dike sample (531) contains less Cr and Ni than other dikes and the Gwynn Gulch gabbro, and may present a more fractionated composition. Fractionation of some gabbroic magma during its rise through peridotite would not be unexpected.

Co and Sc in Peridotite and Gabbro

Co and Sc analyses of Canyon Mountain samples fall within the ranges characteristic of ophiolites and ocean-floor rocks. Abundances vary broadly, and are not as regular as Cr and Ni partly

due to alteration, and partly because Sc (in particular) is not partitioned into only early or late pyroxenes (Hanson, 1980), hence Sc abundance tends to change more stocastically than Cr, Ni, or even Co. Sc is slightly depleted in CMC peridotite (6-20 ppm) and increases in abundance in the upper gabbro (46-55 ppm). Co generally follows Ni, and is partitioned into olivine. Consequently, it is more abundant in peridotites (121 to 130 ppm) than in gabbro (28-37 ppm).

Summary of Trace Element Geochemistry

Trace element analyses of Canyon Mountain complex samples have focused on rare earth elements, but valuable information regarding the magmatic history and relations among units is provided also by Rb, Sr, Cr, Ni, Co, Sc. The data support the following conclusions:

1. Overall abundances and patterns of the Canyon Mountain complex peridotites and gabbro are compatible with similar rocks of other ophiolites. Peridotite within the zone of infiltration has large positive Eu anomalies, which suggest it has been affected by intrusion of gabbro.

2. Rocks of the transition zone are LREE depleted, slightly more enriched in HREE than the gabbro of Gwynn Gulch, and have positive Eu anomalies. Crossing patterns of some transition zone rocks' REE suggest that steady accumulation of these rocks was interrupted from time to time by the influx of unfractionated magma. The abundances of Cr, Ni, Sc, and Co vary and appear to be occasionally replenished. Thus REE and other trace elements indicate that fractionation occurs through the transition zone, but the rocks are not a simple sequence.

3. REE of the Canyon Mountain complex gabbro indicate progressive fractionation with occasional replenishment of LREE-depleted magma. Gabbro from dikes in harzburgite and from Gwynn Gulch have low abundances of REE, with

flat patterns for HREE and the greatest LREE depletions. Cr and Ni are significantly enriched in the gabbro of Gwynn Gulch. Less depletion in LREE, greater overall REE abundances, and increasing positive Eu anomalies indicate that the succeeding, higher gabbro represents progressive fractionation of the Gwynn Gulch gabbro. Cr and Ni decrease regularly upward through the gabbro and support the evidence provided by REE.

4. Low overall abundance of LREE in the CMC gabbro indicates that the gabbro was derived from a depleted source.

5. The REE patterns of the CMC gabbro fall close to, but do not completely overlap the field of REE calculated as sources for derivation of plagiogranite by partial melting of hydrated, altered gabbro calculated by Gerlach (1980) (Figure 60).

PETROGENESIS OF THE CANYON MOUNTAIN COMPLEX

Based upon lithology, mineralogy, and geochemistry, ophiolites are considered to be fragments of oceanic crust generated at mid-ocean ridge or marginal basin spreading centers. From the presentation and discussion of data earlier in this work it is apparent that there are substantial discrepancies between the Canyon Mountain complex and the "normal" ophiolite. The ultramafic and mafic parts of the CMC contain generally the sequence of lithologies which are common to other ophiolites, but there are differences in details of geochemistry and structure, and the occurrence of recrystallization.

The mineralogy and composition of the tectonite harzburgite of the Canyon Mountain complex indicate that it is thoroughly depleted, with very little fertile capacity. Field and textural considerations indicate that feldspar and much clinopyroxene of the zone of infiltration represent gabbroic magma which has passed through the harzburgite enroute to the overlying magma chamber, rather than partial melts of aboriginal fertile phases within the harzburgite. Accessory spinel of the harzburgite is high in Al_2O_3 whereas podiform chromitites contain higher Cr/Cr + Al ratios, suggesting that some podiform chromitites originated from a different source, did not crystallize contemporaneously with the enclosing harzburgite, or re-equilibrated with later liquids. Podiform chromitites which contain clinopyroxene and high-Al chromite most commonly occur within the zone of infiltration of gabbros. Hence it is suggested

that re-equilibration of some ore bodies with Ca-Al-rich liquid occurred. Re-equilibration of chromite has been noted in the Bushveld Intrusion (Cameron, 1979) where late fluids metasomatized stratiform ores and caused recrystallization. There is no systematic variation of accessory spinel composition with stratigraphic height in the harzburgite, nor any systematic variation in composition of any phase. Hence, the harzburgite probably does not represent a cumulate sequence, but instead is upper mantle tectonite which has undergone multiple deformations, metasomatic episodes, and intrusion. Strongly developed foliation and lineation, and the tectonite equigranular to mosaic fabric in the harzburgite also indicate an upper-mantle origin.

Structural mapping and petrologic analysis by Misseri and Boudier (pers. comm., 1982) indicate two diapiric structures in the Canyon Mountain complex, with a zone of flattened foliation between them. This conclusion is similar to the finding of Ave Lallemant (1976), who defined two separate diapiric structures in respectively, the east and west of the Canyon Mountain complex.

The zone of gabbro infiltration coincides with the area of flattened foliation between the two diapirs. The amount of gabbro and width of gabbro dikes increase toward the center of this zone. Layering and flow foliation in the wider dikes suggest that movement of partly crystallized magma occurred. However, large grain size and equigranular textures of most dikes indicate that final crystallization was slow and occurred in the absence of stress.

Within the zone of infiltration, gabbro probably occupies less than five percent of the overall volume. The absence of contact effects indicates that gabbro intruded peridotite when both were at elevated temperatures and probably within the plagioclase lherzolite stability field (Figure 43).

An alternative model for the genesis of gabbro in the zone of infiltration is partial melting of the harzburgite during its diapiric rise, and late squeezing of melt into the middle zone due to movement in the east and west diapiric masses. However, the textures and occurrence of gabbro veins do not favor this alternative. No trace of gabbro or of fertile phases other than clinopyroxene veins and layers is present outside the zone of infiltration.

Field relations shown on Plate 2 unequivocally demonstrate that where the contact between harzburgite and CMC gabbro is directly or nearly exposed it is irregular and characterized by apophyses of gabbro into the harzburgite. Contacts on the northeast side of Pine Creek (SE 1/4, sec. 14 and SW 1/4, sec. 13), near Table Camp (sec. 29) and the abundant dikes on the south side of Baldy Mountain (SW 1/4, sec. 19) all strongly suggest that the gabbro intruded harzburgite. Transition zone rocks are rare or absent in these locations. Their scarcity, especially near the center of the CMC may be due to greater influx of gabbro in this area, and a tendency for cumulates which resulted from fractionation to precipitate away from the principal upward flow. Near Gand Saddle (SE 1/4, sec. 15), along the west margin of the zone

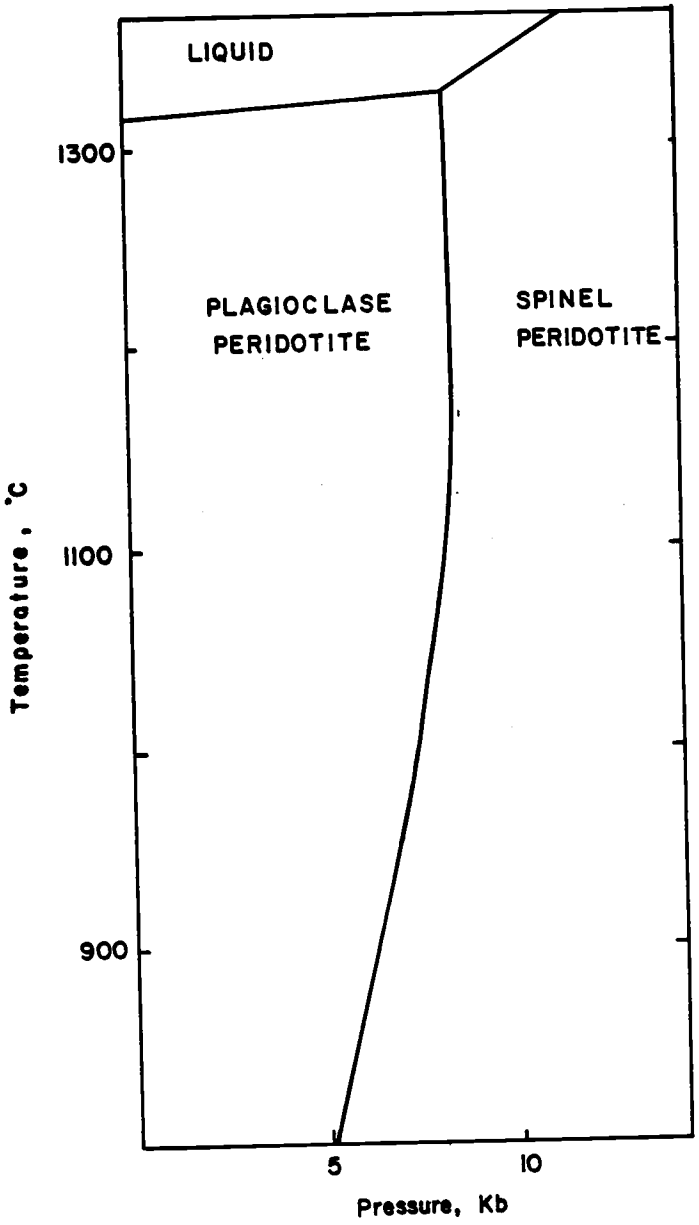

FIGURE 43. Peridotite stability in the system: MgO - Al_2O_3- SiO_2 - CaO (after Yoder, 1976).

of infiltration, gabbro, harzburgite, and transition zone contacts are complicated by deformation, but again are indicative of gabbro intrusion.

Although few contacts between the transition zone and the CMC gabbro are exposed, field relations shown on Plate 2 suggest that the gabbro is also intrusive into, and encloses some of the transition zone. Gabbro foliation on the west side of Ridge 4 is parallel to the contact with transition zone rocks, and nearly perpendicular to their foliation. Isolated inclusions of partly digested, strongly foliated gabbro occur on strike with other remnants of the transition zone in isotropic or discordant upper CMC gabbro. Noteable examples are in Norton basin (Ridge 6) and on Ridge 4. Inclusions of partly serpentinized ultramafics are found near the west summit of Canyon Mountain, to the south near Sheep Rock (NE 1/4, sec. 29) and on the west side of Norton basin (SW 1/4, sec. 22). Some of these rocks have been interpreted as channel fillings or localized cumulates (Himmelberg and Loney, 1980). However, their rarity and limited dimensions suggest that they may be intruded remnants or screens of transition zone cumulates.

The relation of the transition zone to the underlying harzburgite and overlying gabbro is difficult to resolve in the field because of poor exposure. Geochemical and petrographic relations are also not completely clear. Penetrative deformation of transition zone rocks is evident in outcrop and in thin section; deformation decreases upward through the sequence and toward the center

of the CMC. The thickness and extent of units, the amount of deformation, and the order of lithologies has no systematic variation from ridge to ridge, which suggests that during deposition of transition zone cumulates, local compositions and equilibria prevailed, and little circulation occurred in the transition zone cumulate pile. The lineated and foliated nature of these rocks may be related to early magmatic flow lamination, but because deformation affects and aligns mineral lattices, the texture must also in part be due to subsolidus plastic flow. Gabbro of the transition zone displays more folding and slump features than ultramafic layers, possibly due to its maintaining a more plastic or semi-solid condition at lower temperatures. The relatively large crystal size prevalent throughout the transition zone suggests slow cooling. The downward increase in deformation which parallels structure of the harzburgite indicates that late stresses on the harzburgite also affected the transition zone rocks, probably after their solidification. Gabbro structure is not as closely allied to the harzburgite as is structure of the transition zone rocks, suggesting that solidification of most gabbro probably occurred after harzburgite flow ceased and during or after consolidation of the transition zone.

Abrupt transitions between lithologies and lack of noteable phase grading in rocks of the transition zone suggest that either pressure changes or influxes of new magma were responsible for the lithologic variation in the rocks, and that a mechanism such as double-diffusive convection (Irvine, 1980) or in situ crystallization

(McBirney and Noyes, 1979) was responsible for continued crystal growth and final equilibration. If pressure change initiated the crystallization of different minerals in cumulate rocks, as has been postulated for precipitation of chromite in the Bushveld (Cameron, 1979), layers should be laterally extensive. However, transition zone layering rarely persists for more than tens of meters. Therefore, pressure changes cannot explain phase changes, and periodic influx of new magma must have occurred during development of the transition zone. Lack of lateral persistance of layers suggests that these injections were localized, and relatively minor.

Major and trace element geochemistry supports the magma injection concept for the transition zone. Methodical, uninterrupted, upward differentiation does not occur through the sequence, although overall trends show broad fractionation. Olivine websterite is both at the top and bottom of the zone, with little variation of mineral composition. Rocks from dunite to gabbro occur in-between. Similarly, although REE patterns of the transition zone sequence demonstrate increasing accumulation of plagioclase, crossing REE patterns (Figure 33) indicate mixing of more primitive magmas with slightly fractionated cumulates. Variation of Ni and Cr in rocks (Figures 41 and 42) and in minerals (Figure 8) also strongly suggest influx of primitive (picritic) magma. Both major and trace element data suggest that this magma was injected into a chamber which, overall continued to fractionate, but assimulated the influx of new magma readily. Cryptic variation of major oxides as well as minor and trace elements in the minerals

of the upper transition zone (Figures 7, 8 and 9) are further confirmation of the injection of primitive magmas.

Major element geochemistry indicates that some transition zone rocks may plot on an ocean-ridge tholeiitic trend although most plutonics and hypabyssal intrusives of the Canyon Mountain complex are calc-alkaline to island-arc tholeiite. These more tholeiitic rocks are gabbro. Their chemistry may be a function of decreased f_{O_2} and less magnetite fractionation, or they may be more FeO-rich. More detailed study of rocks such as the transition zone sequence which vary from arc tholeiite to ocean ridge tholeiite affinities may be helpful in determining how and why the two different trends occur.

Major and trace element compositions indicate that the composition of primitive Canyon Mountain complex gabbro (Gwynn Gulch gabbro) cannot be derived by fractional crystallization of gabbroic rocks of the transition zone. Rather, the Gwynn Gulch gabbro is parental to the main CMC gabbro sequence. Transition zone gabbro is enriched in TiO_2 and MnO, and although rather high in MgO, (17 percent) also contains 8-11 percent FeO*. REE of transition zone gabbro indicate substantial plagioclase accumulation and some fractionation, whereas gabbros of Gwynn Gulch and Bear Skull Rims have primitive, flat HREE without substantial positive or negative Eu anomalies. REE patterns of transition zone metacumulate gabbro are most similar to fractionated, upper gabbro and norite of Pine Creek Mountain, but transition zone rocks have lower overall REE abundances, and are more depleted in LREE. The transition

zone metacumulates cannot solely represent accumulation of minerals fractionated from CMC gabbro because calculated gabbro fractionate is plagioclase-olivine-orthopyroxene-rich (Table 19) whereas the transition zone is mostly olivine-clinopyroxene websterite or clinopyroxene-rich gabbro.

The transition zone is principally composed of cumulates from the fractionation of Canyon Mountain complex gabbro with small additions of Cr-enriched, LREE depleted, probably picritic magma. Gabbro fractionation sequences shown in Tables 16-18, and summarized in Table 19, yield an overall chemical composition similar to that expected as an average for rocks of the transition zone. However, the cumulates calculated are plagioclase-olivine-orthopyroxene rich with only about 15 percent clinopyroxene whereas the rocks of the transition zone are predominantly olivine-clinopyroxene compositions, with subordinate orthopyroxene, and less gabbro than ultramafic rocks. The calculated modal abundances do not agree well with the real rocks. The abundance of Cr-rich clinopyroxene in the transition zone, as well as reversals in cryptic variation presented in Figure 9 and discussed previously strongly support the addition of primitive magma during the crystallization of the transition zone cumulates.

Gabbro intruded and infiltrated the harzburgite and some of the transition zone enroute to the overlying magma chamber. The primitive magma composition is represented by olivine-two pyroxene gabbro of Gwynn Gulch which represents magma trapped in the harzburgite. This rock has strongly depleted LREE, no Eu anomaly,

Table 16. Fractionation of Gwynn Gulch Gabbro to Bear Skull Rims Gabbro.

	Parent: Gwynn Gulch #666	Calculated Bear Skull Rims	Actual BSR #629
SiO_2	47.40	49.77	48.68
Al_2O_3	12.10	17.68	18.59
TiO_2	0.20	0.13	0.15
FeO*	10.30	4.86	5.13
MnO	0.17	0.13	0.09
MgO	17.91	10.70	10.16
CaO	10.70	14.34	13.44
Na_2O	1.27	2.06	2.08
K_2O	0.07	0.1	0.06
TOTAL	100.00	100.00	100.00

Fractionated minerals: olivine (15%), orthopyroxene (12%), clinopyroxene (5%), plagioclase (3%), and Mg-rich spinel (4%).

Compositions of fractionate:

	olivine	opx	cpx	plag	spinel	TOTAL
SiO_2	39.90	55.00	54.00	45.20	--	41.58
Al_2O_3	0.01	0.23	0.50	36.10	--	2.94
TiO_2	0.00	0.04	0.10	--	--	0.01
FeO*	18.00	11.80	4.70	0.16	70.00	20.53
MnO	0.26	0.24	0.10	0.01	1.00	0.19
MgO	41.85	32.30	23.00	--	29.00	30.88
CaO	0.00	0.63	17.60	18.70	--	3.86
Na_2O	--	--	--	0.13	--	0.01
K_2O	--	--	--	--	--	--
TOTAL	100.00	100.00	100.00	100.00	100.00	100.00

Table 17. Fractionation of Bear Skull Rim Gabbro to Table Camp Gabbro.

	Parent: Calculated Bear Skull Rims	Calculated Table Camp	Actual TC Average
SiO_2	49.77	49.14	49.34
Al_2O_3	17.68	19.11	19.38
TiO_2	0.13	0.09	0.10
FeO*	5.13	5.08	5.12
MnO	0.13	0.08	0.09
MgO	10.70	9.11	9.61
CaO	14.30	14.95	14.16
Na_2O	2.06	2.31	2.24
K_2O	0.1	0.13	0.06
TOTAL	100.00	100.00	100.00

Fractionated minerals: orthopyroxene (5%), clinopyroxene (5%) plagioclase (3%).

Compositions of fractionate:

	orthopyroxene	clinopyroxene	plagioclase	TOTAL
SiO_2	55.00	53.50	53.00	53.92
Al_2O_3	--	0.50	30.10	7.18
TiO_2	0.05	0.10	--	0.04
FeO*	11.00	5.80	0.89	6.59
MnO	0.25	0.10	--	0.13
MgO	33.20	23.00	--	21.76
CaO	--	17.00	15.00	9.92
Na_2O	--	--	1.90	0.44
K_2O	--	--	--	--
TOTAL	100.00	100.00	100.00	100.00

Table 18. Fractionation of Bear Skull Rims Gabbro to Pine Creek Mountain Gabbro.

	Parent: Calculated Bear Skull Rims	Calculated PCM	Actual PCM # 707
SiO_2	49.77	50.29	50.58
Al_2O_3	17.68	16.57	16.64
TiO_2	0.13	0.54	0.19
FeO*	5.13	6.35	8.47
MnO	0.13	0.12	0.14
MgO	10.70	10.72	8.91
CaO	14.30	12.80	12.79
Na_2O	2.06	2.49	1.71
K_2O	0.10	0.12	0.06
TOTAL	100.00	100.00	99.49

Fractionated minerals: plagioclase (20%) and clinopyroxene (10%).

Compositions of fractionate:

	plagioclase	clinopyroxene	TOTAL
SiO_2	45.20	52.00	47.46
Al_2O_3	36.80	4.00	25.06
TiO_2	--	0.32	0.11
FeO*	0.10	3.80	1.33
MnO	--	0.10	0.03
MgO	--	23.00	7.67
CaO	18.20	15.20	17.20
Na_2O	1.00	1.00	1.07
K_2O	0.10	--	0.07
TOTAL	100.00	100.00	100.00

Table 19. Summary of gabbro fractionation.

Percent gabbro fractionated	50%	10%	40%	
Gabbro unit	GG → BSR	BSR → TC	BSR → PCM	OVERALL FRACTIONATE
SiO_2	41.6	53.9	47.5	45.2
Al_2O_3	2.9	7.2	25.1	12.2
TiO_2	0.0	0.0	0.1	0.0
FeO*	20.5	6.6	1.3	11.4
MnO	0.2	0.1	0.0	0.1
MgO	3.9	21.8	7.7	7.2
CaO	30.9	9.9	17.2	23.3
Na_2O	0.0	0.4	1.1	0.6
K_2O	0.0	0.0	0.0	0.0
TOTAL	100.0	100.0	100.0	100.0
Fractionate Mineralogy				
olivine	39%	--	--	21%
orthopyroxene	31	38	--	21
clinopyroxene	12	38	33	15
plagioclase	08	24	67	37
magnetite (spinel)	10	--	--	06
TOTAL	100	100	100	100

and flat HREE, with overall low REE abundances. It is high in both Ni and Cr. Major element plots of this gabbro are distinctive because it is more tholeiitic than most CMC gabbro, and it is the only rock which is intermediate between ultramafic transition zone and other gabbro compositions. The mineralogy of the gabbro of Gwynn Gulch indicates crystallization in the olivine-plagioclase, plagioclase lherzolite stability field, at probably no more than 5-6 kb pressure (Figure 43). The lineated and foliated structure of some of this gabbro suggests that it crystallized partly during diapiric rise of the intruded harzburgite. Precise determination of P/T conditions via geothermometry and geobarometry is very desirable, and would provide helpful suggestions regarding timing of gabbro infiltration.

The gabbro of Bear Skull Rims is also a rather primitive gabbro, although it is unmistakably calc-alkaline and contains no olivine. It is LREE depleted, with a small positive Eu anomaly, and slightly greater overall abundances of REE. Calculations summarized in Table 16 show that the gabbro of Bear Skull Rims may be derived from a liquid of Gwynn Gulch composition by fractionation of 15 percent olivine (Fo_{80}), 12 percent orthopyroxene (En_{77}), five percent clinopyroxene (diopside), four percent Mg-rich magnetite, and three percent plagioclase (An_{97}) at high P_{H_2O}.

The gabbro of Table Camp is very limited in exposure. It is an olivine-two pyroxene gabbro which probably crystallized from slightly fractionated Bear Skull Rims magma by subtraction of five percent

orthopyroxene (En_{77}), five percent clinopyroxene (diopside) and three percent plagioclase (An_{78}) under lower P_{H_2O} than BSR gabbro (Table 17).

The gabbro of Pine Creek Mountain is a still more fractionated gabbro to norite and quartz norite which occurs in uppermost levels of the Canyon Mountain complex gabbro. It contains localized concentrations of as much as ten percent iron-rich sulfide, which seems to be a late, immiscible liquid. Unlike upper gabbro of many ophiolites, the Pine Creek Mountain gabbro is commonly layered, in layers which persist for a few to several tens of meters. Mineralogy, major element, and trace element data all indicate that this is the most fractionated gabbro of the series.

At the base of the Pine Creek Mountain gabbro, some LREE-depleted, 1-4x chondrite gabbro (707-708) occurs. Upward, the gabbro-norite is enriched in all REE (10 x chondrite) and has nearly flat patterns with strong positive Eu anomalies. One evolved sample of Pine Creek Mountain gabbro (335) is HREE enriched and has slightly negative Eu anomalies. This rock contains zircon and quartz, as well as a high percentage of hypersthene. It is the only Eu-negative gabbro analyzed. The HREE enrichment is an expression of zircon.

Major and trace element data indicate that periodic influxes of primitive magma affected the upper gabbro, causing LREE depleted patterns and fluctuations in Ni, Cr, and other elements which cannot be explained by continued fractionation. Major element compositions of Pine Creek Mountain gabbro cannot be duplicated

via calculated fractionation of reasonable phases, although fractionation of ten percent clinopyroxene (diopside) and 20 percent plagioclase (An_{95}) from BSR liquid produce a reasonable approximation which is slightly high in MgO, and too low in FeO* (Table 18). Consequently, it is probable that the upper gabbro of the Canyon Mountain complex was affected by periodic influx of another magma also, and that influx of magma was an on-going process throughout the crystallization of the CMC.

Plagiogranites intrude and recrystallize the gabbro of the Canyon Mountain complex. Thermal modeling suggests that gabbro was solid, but at elevated temperatures near 600°C when intruded.

Calculation of possible plagiogranite sources by Gerlach (1980) based on trace element data indicated that partial melting of an altered gabbro was the most likely source for the CMC plagiogranite magmas. The abundance of REE in oceanic gabbro, as shown in Figure 60, is a much better fit for the hypothetical plagiogranite source than is the strongly LREE-depleted CMC gabbro.

Thus, it is proposed that the plagiogranite of the Canyon Mountain complex was derived from partial melting of lower oceanic crust into which the CMC was intruded, and that the plagiogranite was injected downward into the more solidified gabbro of the CMC. Tectonism or shearing may have opened avenues for its intrusion. The source of the diabase which is coeval with the plagiogranite is a fundamental enigma of ophiolites.

The tholeiitic to calc-alkaline composition of the CMC, the intrusive nature of the gabbro, both through harzburgite and into oceanic crust, the absence of well developed sheeted dikes, the dearth of mafic volcanics, and the abundance of keratophyres noted by Gerlach (1980), Thayer (1977), and many field observers, all indicate that the Canyon Mountain complex was not generated at an oceanic spreading center. Instead, it represents an ophiolitic sequence which formed in a non-extensional environment, and is proposed as a type example of a forearc ophiolite.

REGIONAL SETTING OF THE CANYON MOUNTAIN COMPLEX

The Canyon Mountain complex is at the southern boundary of a melange-like Permian to Triassic terrane which has been classified anew by nearly every geologist who has studied it (see Figure 44 and Plate 6). This group of rocks separates the Permian and Triassic Seven Devils arc to the north from the Triassic Huntington arc on the south, and is unconformably overlain by Triassic to Jurassic sediments and volcanics. It consists of a seemingly chaotic mixture of pillowed greenstones and cherts, silicic greenstones and wacke plus siliceous sediments, fragmented, disrupted ophiolites, and serpentinite matrix melanges which contain an admixture of all lithologies. Schistose rocks containing barroisitic amphiboles which indicate high to moderate pressures of metamorphism (five to seven kilobars) and moderate temperatures (300-350°C) occur sporadically through the melanges. The melanges represent traceable zones which crosscut the terrane on a northwest trend. The assemblage has been termed the Central Melange terrane (Dickinson, 1979), Oceanic terrane (Vallier and Brooks, 1977), and the Forearc terrane (Mullen, 1982).

A detailed discussion of all lithologies in the terrane is not appropriate for this work (see Brooks and Vallier, 1978, for details). However, to better understand the origin and tectonic setting of the Canyon Mountain complex, the petrology and geochemistry of greenstones and metagabbros are considered in some detail below, and a model is proposed for this terrane and its relation to the CMC.

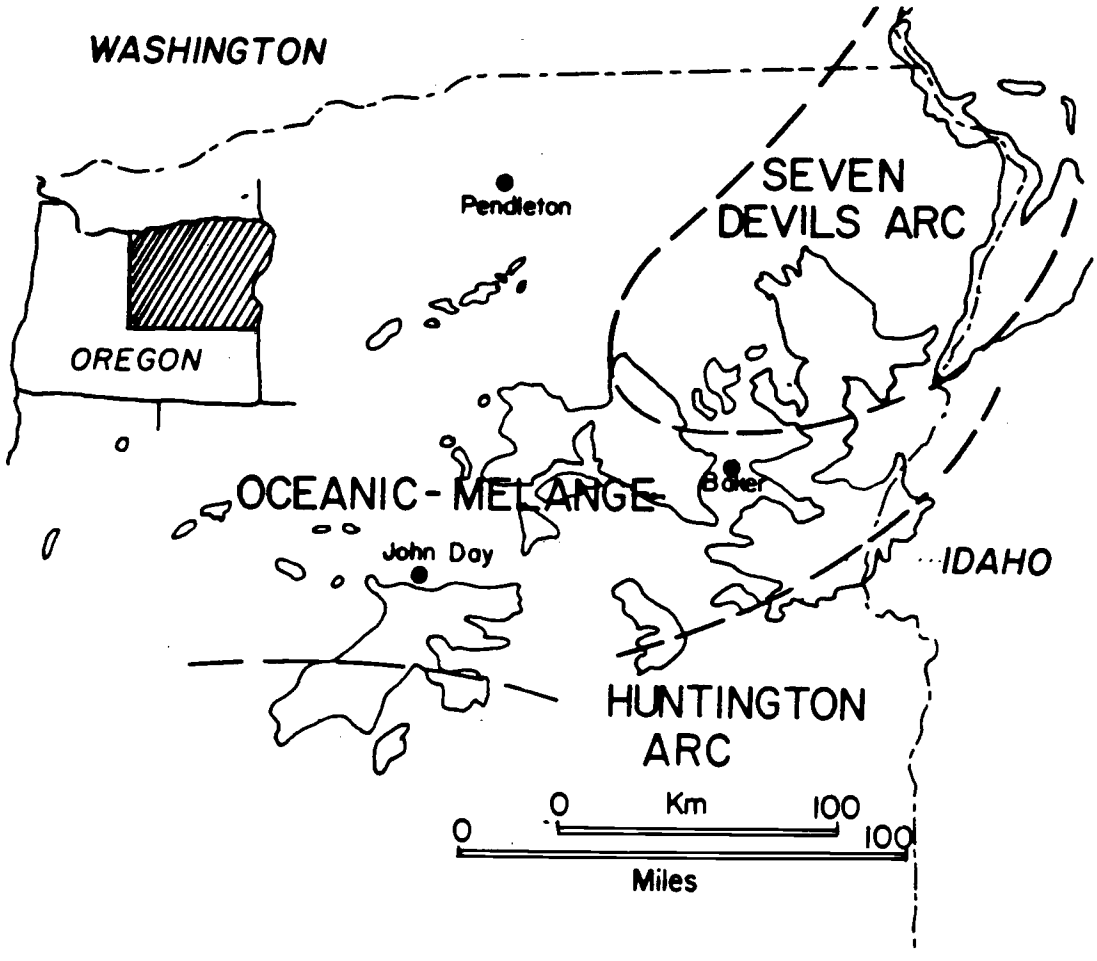

FIGURE 44. Permian and Triassic terranes of northeast Oregon.

Volcanic Greenstones and Associated Metasediments

Volcanic greenstones from ten localities within the forearc terrane were studied in detail. Sample locations are shown on Plate 6. Results of this study indicate that two distinct suites of greenstone occur in the oceanic/melange terrane: 1) alkalic greenstones usually associated with chert and 2) volcanic arc (island arc tholeiite to calc-alkaline) greenstones usually associated with coarser sediments as well as siliceous oozes. Only one greenstone of demonstratably mid-ocean ridge (MOR) affinity occurs in the group studied.

Field Relations and Petrography of Greenstones Associated with Chert

Pillowed greenstones from two, and possibly three localities are intercalated with chert of the Elkhorn Ridge Argillite, and contain relict titanaugite which is a titanium-rich clinopyroxene characteristic of alkalic basalts. Sample BRS-3, the most eastern location sampled, is from an outcrop on the west side of the Snake River near the site of Sturgill, Oregon. Pillows are discernable as one-half meter--diameter ovoids in dark olive-green greenstone. The rock is not appreciably sheared, but adjacent cherts are contorted in the style common throughout much Elkhorn Ridge Argillite.

In thin section these greenstones are ophitic to sub-ophitic. Titanaugite is markedly pleochroic, clear to pink-brown or violet brown and forms about 35 percent of the rock. It is subhedral to

anhedral, averages 0.5 mm in diameter, and is interstitial. Euhedral laths of plagioclase 0.25 to 0.75 mm long are mostly altered to albite. The groundmass is a mat of chlorite, quartz, fine acicular actinolite, sphene, and opaques.

The other alkalic greenstone, sample V-27 (Mullen, 1979), occurs near the center of the forearc terrane on the west and east sides of Olive Creek in the Greenhorn Mountains. In outcrop and road-cut it is olive green to grey-green, with 0.1 m to 1.0 m diameter pillows. It also is intercalated with Elkhorn Ridge Argillite chert, volcanic breccias, and very fine sedimentary breccias. As is true of the BRS-3 alkalic greenstones 150 kilometers east, exposure of this rock is limited.

In thin section, V-27 is ophitic, with about 30 percent pink to violet-brown titanaugite 0.1-0.4 mm in diameter. Plagioclase, 0.1-0.7 mm long, is partly altered to chlorite + albite, but relicts of An_{62} were detected with the microprobe. Possible pseudomorphs of olivine, now filled by nontronite and chlorite occur in one thin section. The groundmass is altered to chlorite, actinolite, and sphene.

The textures, mineralogy, and sedimentary association of these two greenstones are remarkably similar. Clinopyroxene is virtually unaltered and some relict plagioclase is preserved. One other greenstone (PH-76) which may contain very small amounts of titanaugite also occurs in association with cherts, although it is a "knocker" in serpentinite-matrix melange south of Mount Vernon near Pleasant Hill. The pervasive alteration of this rock precludes

optical confirmation of small relict patches of pyroxene with nearly clear to violet pleochroism as titanaugite. Microprobe analysis of this pyroxene has not yet been attempted. Confirmation of its apparently alkalic nature would mean that alkalic greenstones may be distributed across the width of the terrane.

A single sample of pillowed greenstone from serpentinite-matrix melange north of Mount Vernon (MV-48) contains 26.3 modal percent clear, subophitic to intergranular clinopyroxene. This greenstone has limestone overgrowths on pillows, and is associated with nearby knockers in the melange. Pyroxenes are unzoned and well-preserved. However, plagioclase laths are pervasively replaced by chlorite + albite, and many form glomeroporphyritic clusters. Olivine is pseudomorphed by iddingsite and nontronite. The groundmass is altered to chlorite, albite, quartz, and opaques. This sample resembles BRS-3 and V-27 in all respects (texture, alteration, and associated sediments) except clinopyroxene composition. The TiO_2 content of this non-pleochroic augite is too low for an alkalic rock.

Field Relations and Petrography of Other Greenstones

The remaining greenstones of the forearc terrane which were sampled and examined in detail are much different than BRS-3, V-27, and MV-48 with respect to deformation, appearance and association in the field, and texture in thin section, as well as relict clinopyroxene composition.

PR-82, a sample from the dam site of Phillips reservoir, ten kilometers east of Sumpter, is light olive green, and possibly

pillowed. Rim-like textures with parallel plagioclase were not found in thin-sections of outer parts of rounded greenstone. Outcrops of chert of the Elkhorn Ridge Argillite occur nearby, but greenstones are not intercalated with chert, and their relation to any sediments is obscure. In thin section there are no relict phases or pseudomorphs of mafic minerals. The entire rock is composed of chlorite, albite and magnetite and veins of epidote-albite. Although the rock is strongly sheared, barely visible plagioclase laths surrounded by chlorite, and thoroughly replaced by albite + chlorite + calcite suggest a clustered, glomeroporphyritic texture for the original rock.

Seventy-five kilometers southeast of Phillips Reservoir, light yellow-green to olive-green, sheared, greenstones associated with the Burnt River Schist occur along ridges south of the Burnt River near White Rock Gulch. The rocks contain excellent relicts of euhedral to subhedral clinopyroxene phenocrysts, 0.25 to 2.0 mm in diameter. Some relicts are partly recrystallized by stress, but optical zoning is preserved in others. Plagioclase - as both groundmass laths and some phenocrysts - is altered to albite and chlorite. Pumpellyite occurs in one thin section. Its relatively clear color suggests a high Al_2O_3 content and formation at high to moderate pressure. Although the original texture of the rock has been obscured by deformation, the prevalence of relict clinopyroxene phenocrysts and the appearance of some undeformed remnants strongly suggest an intergranular texture.

Twelve samples of greenstone were collected on the south and west sides of Dixie Butte, about 16 km northeast of Prairie City, and 95 km west of the Burnt River locations. These greenstones are intercalated with some wacke and fine conglomerates. Considerable variation in modal mineralogy and SiO_2 content is apparent even in outcrop. However, there is excellent preservation and little alteration of these greenstones (possibly Jr-Tr?), despite the nearby intrusion of a porphyritic, mineralized late Jurassic stock. Most greenstones are dark olive green to brown-green, and many contain hornblende and plagiocalse phenocrysts.

In thin section, it is apparent that these rocks are generally more silicic than other greenstones of the oceanic-melange terrane. Hornblende phenocrysts are pseudomorphed by actinolite and chlorite. Some mafic greenstones contain clinopyroxene which is well preserved, clear, with a 2V about 55°, suggestive of fairly high CaO content. Zoning is visible in some plagioclase, but most feldspar is altered to chlorite + actinolite + albite. Textures are trachytic for hornblende-bearing greenstone, and intergranular for those with pyroxene.

Very fine-grained, non-pillowed, yellow-green to olive-green greenstones, as well as some which are quite silicic, occur on the east and south flanks of Vinegar Hill in the Greenhorn Mountains. Actinolite, calcite, and chlorite replace most mafics. Clinopyroxene relicts are less than 0.1 mm in diameter and are widely dispersed in chlorite. This pyroxene comprises only about five percent of the rock. It is clear and non-pleochroic. Plagioclase

laths are only partly replaced by chlorite + albite; some relict andesine is present. Although the original texture of this rock is not well preserved, it most closely resembles an intergranular texture.

Implications of Field and Petrographic Data

Three lines of evidence cited above indicate that at least two suites of greenstones occur in the oceanic/melange terrane of northeast Oregon. First, the close association of four pillowed greenstones (BRS-3, V-27, MV-48, and PH-76) with chert and/or melange, and the absence of pillows and chert from association with the others suggests that these four may be from a different depositional and tectonic setting.

Second, TiO_2-rich pyroxene occurs in two and possibly three of these four greenstones.

Third, these greenstones have ophitic to sub-ophitic textures. The remaining greenstones are intersertal to porphyritic. This textural distinction is significant because it results from differences in the timing and sequence of crystallization in magmas. In the four chert/melange associated greenstones, only plagioclase crystallized early. Pyroxene is a late phase, and phenocrysts are virtually absent. However, in the remaining samples, the intergranular texture and presence of abundant clinopyroxene phenocrysts in some samples indicate that crystal growth and fractionation probably had evolved farther at the time of eruption. Although alteration has obscured the origin of magnetite, both plagioclase and

clinopyroxene fractionated from this melt with clinopyroxene probably the earliest to form. This fractionation sequence is characteristic of island arcs. In contrast, the chert-associated greenstones, which contain euhedral pseudomorphs of olivine, probably fractionated in the sequence olivine-plagioclase-clinopyroxene, a sequence more typical of magmas following the tholeiitic, iron-enrichment pattern of ocean ridge basaltic magmas, and the alkalic rocks of intraplate regions.

Major Element Geochemistry of Greenstones

Major element geochemistry of 17 greenstone samples was done by Professor Peter Hooper at Washington State University. Results of these analyses are given in Table 20. Norms are given in Table 20 and also shown graphically in Figure 45.

Analyzed greenstones vary from 46.1 to 57.1 percent SiO_2. Most are the equivalent of basalt to basaltic andesite. Those greenstones which contain, or possibly contain, titanaugite (V-27, BRS-3, and PH-76) are lowest in SiO_2 (46.1 to 47.5%). The remaining 14 samples vary between 50-57% SiO_2, are relatively low in TiO_2 and high in Al_2O_3. Only NF-64, a light-colored greenstone from the North Fork of the John Day is sufficiently enriched with Na_2O to qualify as a spilite. All other samples analyzed have CaO/Na_2O ratios which plot well within the non-spilite field of Amstutz (Figure 46).

The CIPW norms of all analyzed rocks were calculated. The samples which contain titanaugite are olivine or nepheline normative, with the exception of BRS-3, which is strongly quartz normative.

Table 20. Major Element Analyses of Greenstones

	PH-76	MV-48	MV48A	DXB-17	DXB-19	DXB-20	V252	MP-64	MP-65	BR-49	BR-52	BR-59	BR-59A
SiO_2	47.5	52.2	51.6	55.4	53.4	53.6	57.1	55.0	53.3	51.2	53.4	52.3	56.4
Al_2O_3	22.0	16.0	16.2	21.5	17.5	18.1	16.0	21.6	18.8	18.6	16.4	17.7	16.4
TiO_2	1.1	1.5	1.4	1.0	1.5	1.3	1.1	0.9	0.9	0.7	0.9	0.8	0.9
Fe_2O_3	4.5	5.0	5.5	3.2	5.4	3.8	5.3	3.9	4.4	4.1	4.6	4.2	4.2
FeO	5.1	5.8	6.3	3.6	6.2	4.4	6.0	4.5	5.1	4.7	5.5	4.8	4.8
MnO	0.16	0.16	0.14	0.11	0.26	0.18	0.18	0.11	0.17	0.25	0.18	0.13	0.14
CaO	11.9	7.8	8.3	7.8	6.4	7.8	6.9	4.9	8.3	11.2	8.7	9.8	6.9
MgO	3.6	6.2	6.1	3.0	5.4	5.9	3.5	3.9	4.7	5.8	5.8	6.6	5.7
K_2O	0.01	1.57	1.07	0.54	0.54	1.43	0.02	0.06	0.32	0.01	0.02	0.02	0.03
Na_2O	3.5	3.3	3.0	3.3	2.8	2.8	3.3	4.6	3.4	3.2	3.7	3.2	4.1
P_2O_5	0.13	0.16	0.16	0.18	0.26	0.36	0.13	0.11	0.13	0.11	0.09	0.09	0.08
CIPW NORMS													
Q	--	2.3	4.0	11.8	11.5	6.4	16.7	10.1	6.5	2.1	5.1	3.9	8.9
Or	0.06	9.3	6.3	3.1	3.1	8.4	--	0.3	1.8	0.05	0.1	--	0.1
Ab	28.7	27.9	25.3	28.4	23.9	23.8	28.2	39.0	29.1	26.9	29.3	27.5	34.9
An	44.1	24.2	27.3	37.3	30.2	32.5	28.7	23.9	35.2	35.5	25.9	33.9	26.2
C	--	--	--	2.0	1.25	--	--	5.3	--	--	--	--	--
Di	11.7	10.8	10.3	--	--	3.4	4.0	--	4.8	15.3	5.2	11.3	6.0
Hy	7.4	14.6	15.3	10.1	18.3	16.6	11.7	13.5	13.8	12.2	26.2	15.5	15.4
Ol	--	--	--	--	--	--	--	--	--	--	--	--	--
Ne	0.9	--	--	--	--	--	--	--	--	--	--	--	--
Mt	6.5	7.3	8.0		8.5	5.8	7.7	5.7	6.4	5.8	6.2	6.1	6.1
Il	2.1	2.9	2.8		2.9	2.5	2.1	1.7	1.8	1.4	1.6	1.5	1.7
Ap	0.3	0.3	0.3		0.6	0.8	0.03	0.2	0.1	0.3	0.1	0.2	0.2

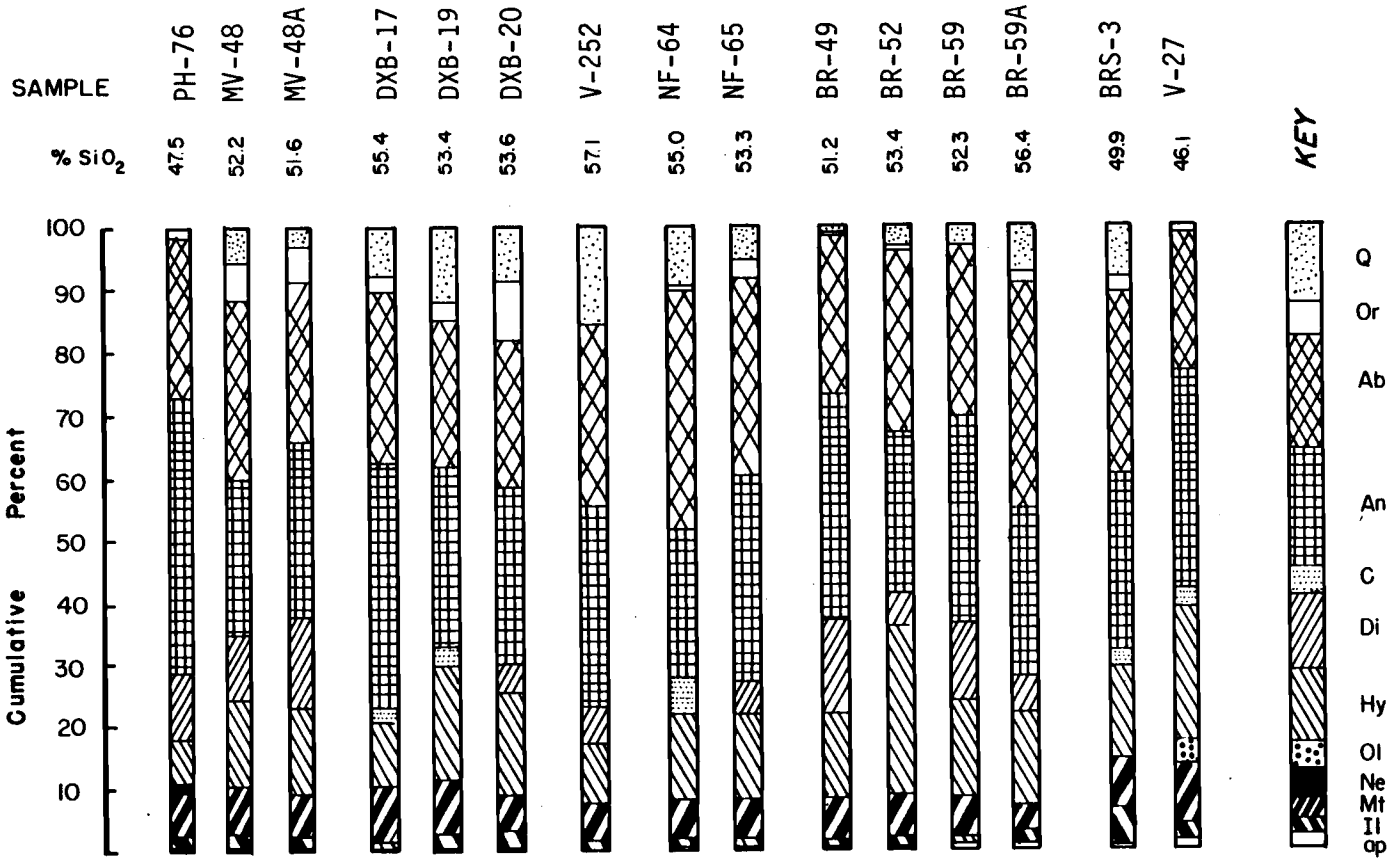

FIGURE 45. Normative compositions of NE Oregon greenstones.

Three contain corundum in the norm: two from Dixie Butte, and NF-64. Hence the assemblage is generally enriched in silica and aluminum. Hypersthene occurs in all norms indicating some iron enrichment.

The low degree of spilitization of most analyzed northeast Oregon greenstones is demonstrated by Figure 46. On this Na_2O/CaO plot most samples are in the non-spilite field. The relatively low mobilization of Na_2O indicates that other major element plots such as AFM are probably valid.

On an AFM plot, most greenstones are on a calc-alkaline trend (Figure 47). Exceptions are the andesitic sample from the Burnt River, and two titanaugite-bearing samples which plot in a range intermediate between calc-alkaline and tholeiitic.

In order to better utilize the major element data, a plot of $MnO/TiO_2/P_2O_5$ was developed which can discriminate among five plate-tectonic environments: Ocean-island tholeiite (OIT), ocean-island alkalic (OIA), mid-ocean ridge (MOR), island arc tholeiite (IAT), and calc-alkaline (CAB) for rocks of basaltic to basaltic andesite composition (46-54% SiO_2) (Mullen, 1983). This discriminant diagram is applicable to greenstones and ophiolitic rocks, providing they are not extremely spilitized. The marked absence of spilitization in the northeast Oregon greenstones allows their application to the plot (Figure 48). Most samples in this study plot in the island arc tholeiite field. Exceptions are BRS-3, a titanaugite-bearing greenstone, which plots in the ocean-island alkalic field; V-27, also a titanaugite greenstone, which plots in the MOR field; and MV samples, which plot in the MOR field.

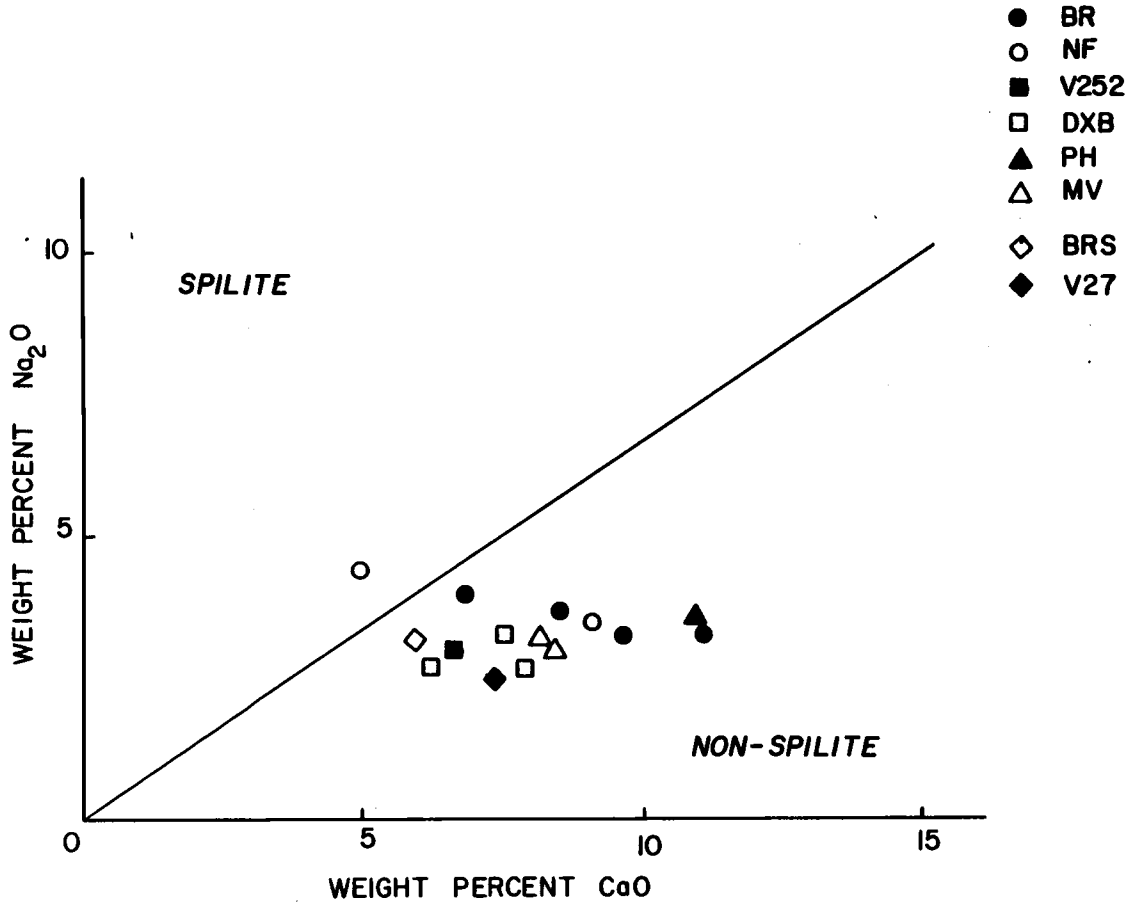

FIGURE 46. CaO-Na_2O relations in northeast Oregon greenstones.

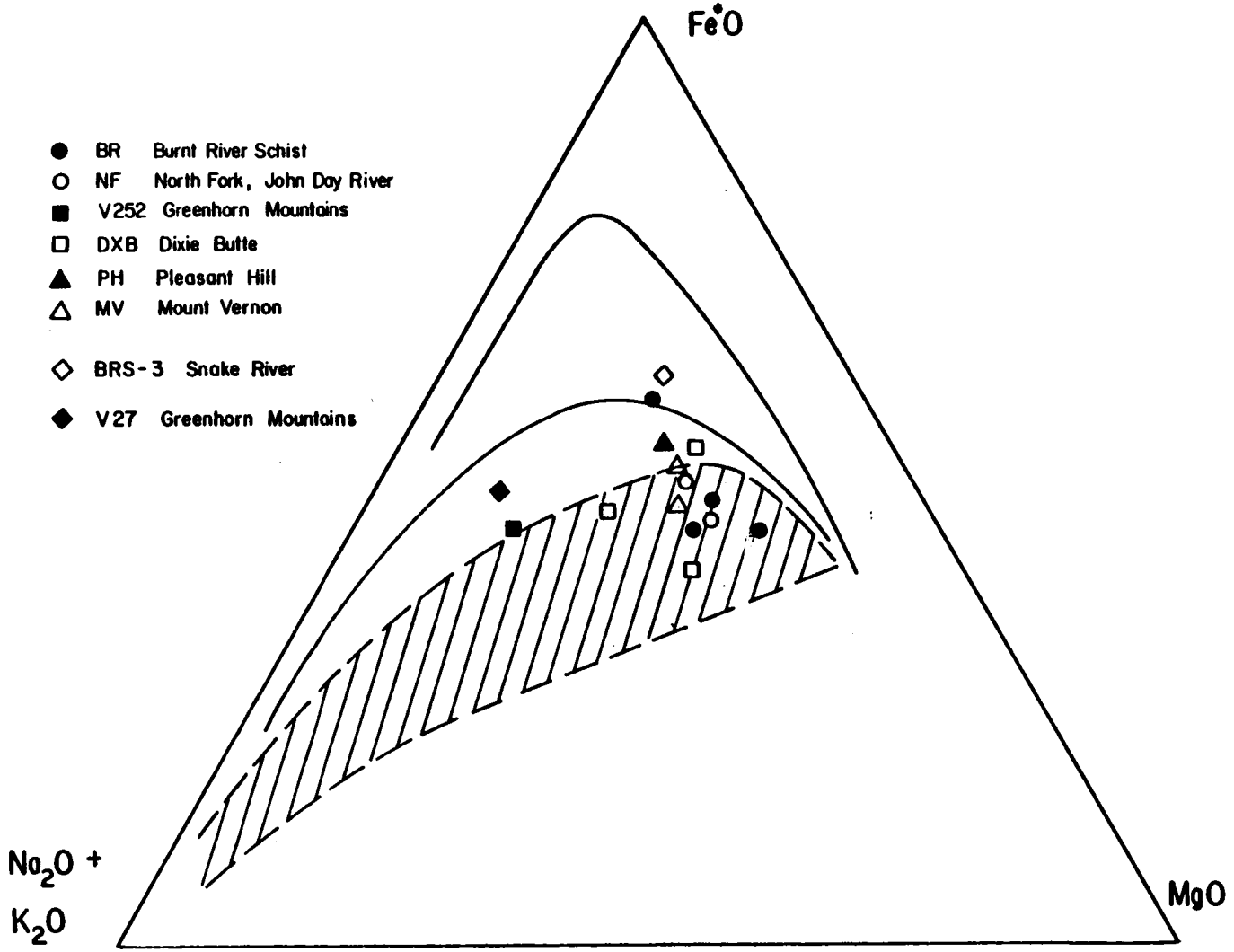

FIGURE 47. AFM diagram, northeast Oregon greenstones.

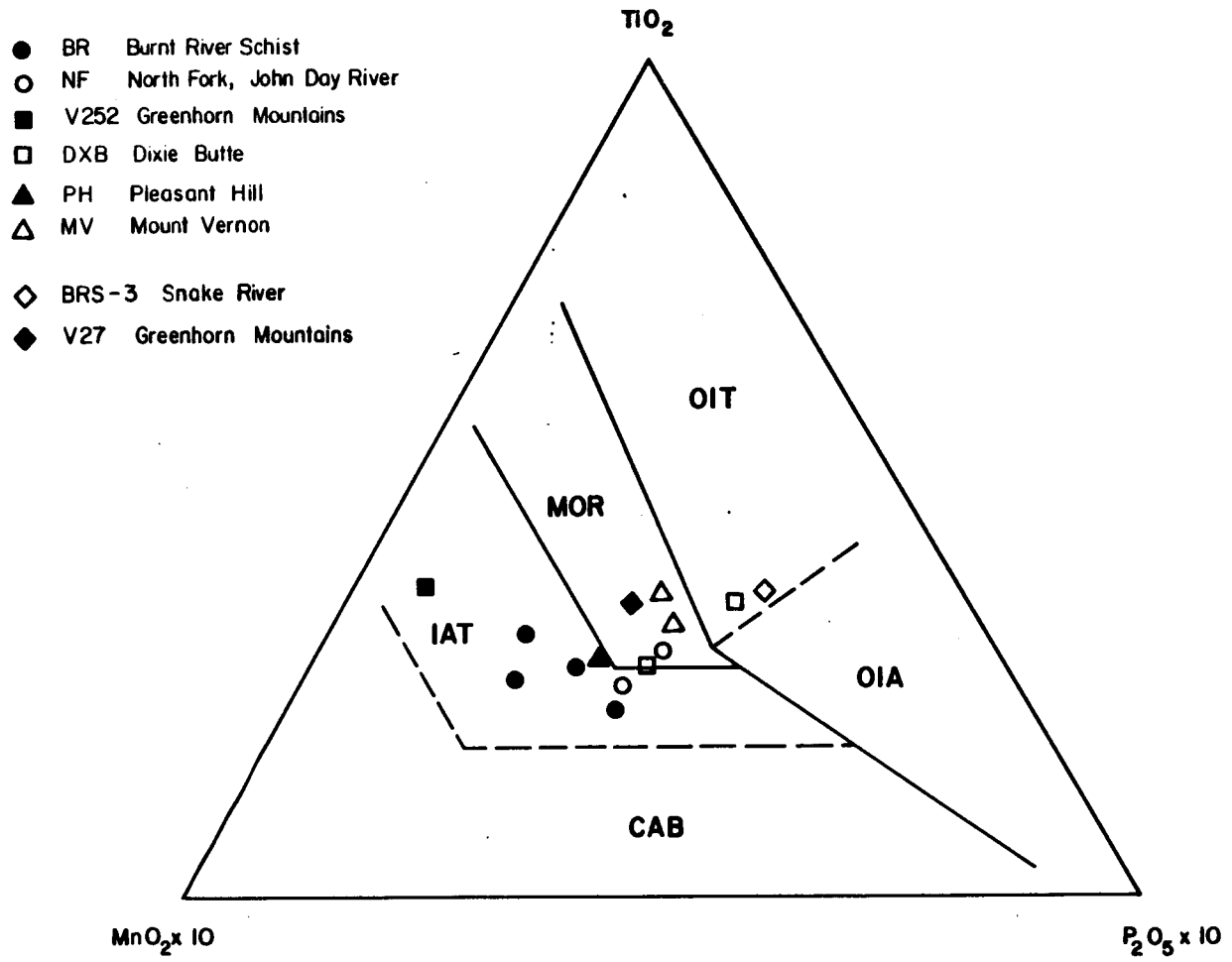

FIGURE 48. $MnO/TiO_2/P_2O_5$ for northeast Oregon greenstones.

In conclusion, the major element chemistry of the greenstones indicates that:

1) Titanaugite-bearing rocks are slightly undersaturated in SiO_2, high in TiO_2 and P_2O_5, are generally distinct from the other samples, and probably represent alkalic basalts.

2) The remaining greenstones are high in Al_2O_3 and P_2O_5 relative to MOR and plot on a calc-alkaline differentiation trend. Their major element chemistry is similar to island arc rocks, with the exception of MV-48 and MV-48A, which resemble MOR.

3) With one exception, the greenstones are NOT spilites.

Trace Element Geochemistry of Greenstones

Seven greenstones were analyzed for rare earth elements (La, Ce, Nd, Sm, Eu, Tb, Y, and Lu) and for Sc, Hf, Ta, and Th *via* instrumental neutron activation analysis (INAA). Data are given in Table 21.

Rare Earth Elements

Rare earth elements are generally considered immobile under conditions of greenschist facies metamorphism, although some workers have reported increased abundance of LREE in spilitized rocks (Hellman and Henderson, 1977).

Rare earth elements analyses are given in Table 21 and plotted in Figure 49. The six greenstones which do not contain titanaugite have nearly flat patterns, 8-20 x chondrite, with slight negative Eu anomalies. Their abundances and patterns are nearly identical, which is quite remarkable considering the broad dispersion of localities

Table 21. Trace Element Abundances in Northeast Oregon Greenstones.

	BR-52	DXB-16	MV-47	NF-65	V-252	V-27
La	2.79	7.15	3.33	2.62	4.83	6.38
Nd	2.6	6.0	4.4	8.9	8.3	--
Sm	2.18	2.71	2.64	2.99	2.66	4.43
Eu	0.17	0.77	0.62	0.60	0.70	1.23
Yb	2.76	2.31	2.95	2.89	2.95	3.31
Lu	0.49	0.48	0.77	0.58	0.68	0.71
Sc	41	40	43	37	41	44
Hf	1.40	0.16	--	2.28	1.62	2.94
Ta	0.06	0.04	--	0.09	0.04	0.29
Th	--	1.03	--	0.26	1.33	0.18

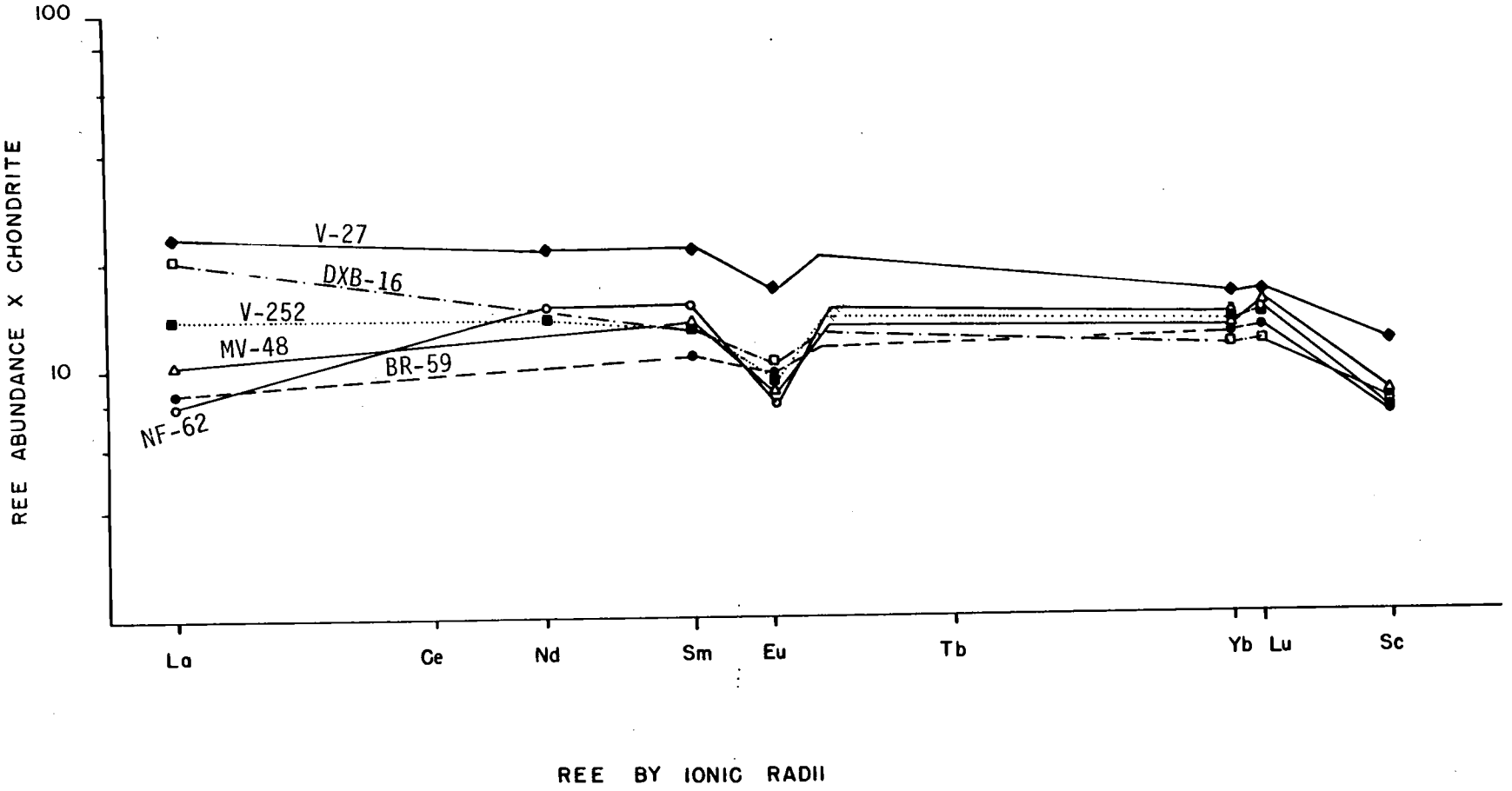

FIGURE 49. REE of northeast Oregon greenstones.

and range of SiO_2 contents (46-51 percent). REE of these greenstones overlap patterns of both primitive island arc tholeiites (IAT) and mid-ocean ridge basalts (MORB), but are most similar to MORB.

The pronounced negative Eu anomaly, overall abundance (8-20 x chondritic), and flat pattern of most samples are characteristic of some mid-ocean ridge basalts and diabases of ophiolites. Only one greenstone from the group classified as arc-related on the basis of pyroxene compositions and major element chemistry (DXB-16) has a pattern which is anomalous for MORB. This greenstone is slightly LREE enriched (La = 20 x chond; La/Sm = 8) with a small negative Eu anomaly, and flat HREE. Such a pattern should be expected from this rock because it is high in SiO_2 (51 percent) and more differentiated than basaltic greenstones.

The REE pattern of these rocks also overlaps the field for IAT. However, a marked negative Eu anomaly, and depletion in LREE is very rare in IAT because plagioclase and clinopyroxene do not fractionate in as great a quantity as in MORB liquids (Thorpe, 1982; Mullen, 1983).

The two greenstones (V-27, BRS-3) which contain titanaugite and plot mostly in alkalic or intraplate basalt fields based upon major element analyses and pyroxene compositions are LREE enriched and have negative Eu anomalies. These patterns are compatable with basalt from several environments: ocean island tholeiite, ocean island alkalic, and basalts from transform faults. However, for basalts

of equivalently low SiO_2 (47 percent), alkalic basalts of ocean islands have patterns compatible with those of the two greenstones.

Hf/Ta/Th

Hf-Ta-Th are high charged ionic elements which are relatively immobile during a greenschist alteration (Wood et al., 1980).

Wood et al. (1980) have shown that a ternary plot of Hf x 3/ Ta/Th can discriminate among basalts from destructive plate margins as well as N-MORB, E-MORB, and alkalic basalts. Hf-Ta-Th data were obtained for four greenstones of basaltic affinity (Figure 50).

Three greenstones (NF-65, DXB-16, and BR-59) plot within the field for basalts of destructive plate margins. V-27, an alkalic greenstone from the Greenhorn Mountains, plots in the field for N-MORB.

Relict Clinopyroxenes of Greenstones

Many workers in recent years, including Nesbitt and Pearce (1977), and Garcia (1978), recognized that relict minerals -- especially clinopyroxene -- in altered greenstones could be utilized to determine the original geochemical type of the host rock. Although there has been some debate about the element mobility within the "relict" phases (Moody, pers. comm., 1977), generally the composition of a relatively unaltered mineral is more reliable than major and even trace element data from whole rocks (Hellman and Henderson, 1977). Major problems in using relict minerals as

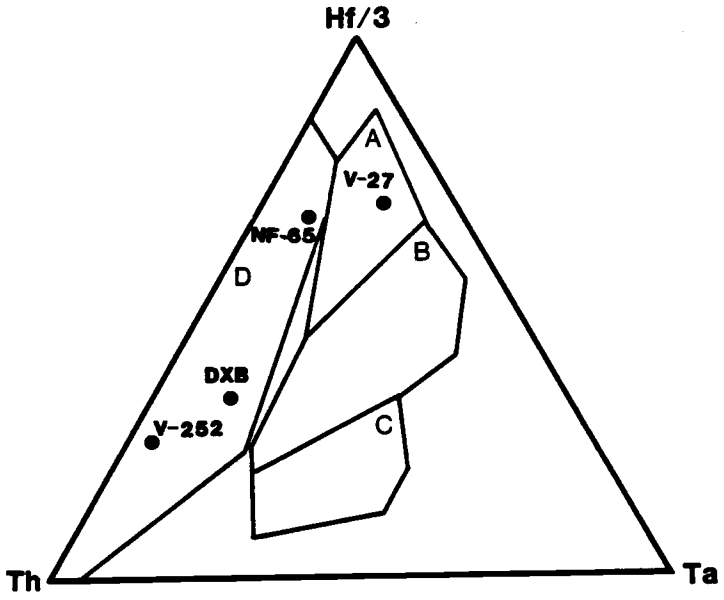

A = N MORB
B = E MORB
C = WPB
D = Destructive Margins

V-27 Alkalic greenstone, Greenhorn Mts.
NF-65 greenstone-North Fork John Day R.
DXB Dixie Butte greenstone
V-252 Greenhorn greenstone

FIGURE 50. Hf/Ta/Th diagram - N.E. Oregon greenstones.

indicators of original geochemistry, however, are that they are generally rare, and they require careful analysis with the electron microprobe to avoid possible altered zones. Relicts were not present in all samples collected and utilized in this study. However, they occur in sufficient quality and quantity to allow correlation of results from pyroxene compositions with major element whole rock geochemistry and the small amount of trace element data available.

Greenstones from six localities contain relict clinopyroxene: V-27 and BRS-3 contain relict titanaugite; BR-59, BR-61, MV-48, V-252 and P-1 (also from the Greenhorns, but not shown on the map, Plate 6) contain clear green augite. One additional sample (PH-76) may contain very fine grained and rare relicts of titanaugite, but the mineral composition has not yet been confirmed via probe analyses. Pyroxene compositions are given in Tables 22-29.

Titanaugite compositions in V-27 and BRS-3 are very similar (Table 22). Both contain three to four percent TiO_2, with low MgO and high CaO contents. They are low in SiO_2 and characteristically average about six percent Al_2O_3. Clinopyroxenes plot inside fields for within-plate alkali basalt on all plots of tectonic provenance versus composition. (They are peralkaline in nature, plotting near the top of the pyroxene quadrilateral due to high CaO content.) Figures 52-54 show plots of pyroxene compositions and tectonic environments.

Interpretation of the remaining pyroxene compositions is not so straightforward. They are generally low in TiO_2 relative to the titanaugites, but contain more TiO_2 than many arc basalts. They

TABLE 22. Relict clinopyroxene compositions of alkalic greenstones.

	V-27A					BRS										
SiO_2	45.3	44.5	46.1	44.6	46.6	46.2	46.9	46.1	43.9	43.7	44.6	44.8	45.0	47.8	46.7	48.3
TiO_2	3.5	4.6	3.4	4.1	3.3	3.7	2.8	3.6	4.5	4.4	4.4	4.1	3.9	2.4	3.5	2.4
Al_2O_3	5.4	6.9	6.2	5.9	6.3	5.4	5.0	5.9	6.2	5.5	6.1	5.9	5.8	4.3	5.1	4.1
Fe 0*	13.2	13.6	12.3	13.5	11.4	12.5	12.1	11.7	11.6	12.3	11.6	11.9	12.3	12.9	12.2	12.5
Cr_2O_3	0.6	0.2	0.1	0.0	0.0	0.0	0.0	0.1	0.0	0.0	0.0	0.1	0.0	0.0	0.0	0.0
MnO	0.3	0.3	0.2	0.3	0.2	0.3	0.3	0.2	0.2	0.2	0.3	0.2	0.3	0.3	0.3	0.3
MgO	9.9	9.2	10.0	9.5	8.8	10.9	11.3	11.5	10.8	10.4	10.2	10.3	10.7	10.8	10.9	11.3
CaO	21.0	21.2	21.6	21.4	20.1	20.7	20.7	21.1	21.0	21.6	21.6	21.1	21.4	20.3	20.7	20.0
Na_2O	0.6	0.7	0.6	0.7	0.8	0.5	0.5	0.5	0.5	0.5	0.5	0.5	0.5	0.4	0.4	0.4
K_2O	0.0	0.0	0.0	0.0	0.0	0.0	0.0	0.2	0.01	0.0	0.0	0.0	0.0	0.C	0.0	0.0
Total	99.4%	101.1	100.5	100.0	97.7	100.3	99.8	100.6	98.8	98.8	99.5	99.1	100.1	99.4	99.7	99.4
No. ions																
Si	1.75	1.70	1.75	1.72		1.76	1.79	1.75	1.70	1.71	1.72	1.73	1.73	1.84	1.79	1.84
Ti	0.10	0.13	0.10	0.12		0.11	0.08	0.10	0.13	0.13	0.13	0.12	0.11	0.07	0.10	0.07
Al	0.25	0.31	0.28	0.27		0.24	0.23	0.26	0.28	0.26	0.27	0.27	0.26	0.20	0.23	0.18
Fe	0.43	0.44	0.39	0.57		0.40	0.38	0.37	0.38	0.40	0.38	0.39	0.40	0.42	0.39	0.40
Mn	0.01	0.01	0.01	0.02		0.01	0.01	0.01	.01	0.01	.01	0.01	0.01	0.01	0.01	0.10
Mg	0.58	0.52	0.57	0.87		0.62	0.65	0.65	0.63	0.61	0.59	0.60	0.66	0.62	0.62	0.65
Ca	0.87	0.87	0.88	0.56		0.85	0.85	0.86	0.87	0.90	0.89	0.87	0.84	0.84	0.85	0.82
Na	0.05	0.05	0.05	0.68		0.04	0.4	0.04	0.04	0.04	0.04	0.03	0.03	0.03	0.03	0.31
K	0.02	0.00	0.00	0.00		0.00	0.01	0.00	0.00	0.00	0.00	0.0C	0.00	0.00	0.01	0.02
Fe	.23	.24	.21	.29		.21	.20	.20	.20	.21	.20	.21	.21	.22	.21	.21
Mg	.31	.28	.31	.44		.33	.35	.35	.34	.32	.32	.32	.35	.33	.33	.35
Ca	.46	.48	.48	.28		.45	.45	.46	.46	.47	.48	.47	.44	.45	.46	.45

Table 23. Relict Clinopyroxene Compositions, MV-48.

	1	2	3	4	5	6	7
SiO_2	52.20	50.58	49.89	51.34	50.54	51.67	50.87
TiO_2	0.63	0.92	1.04	0.80	0.79	0.66	0.71
Al_2O_3	3.76	3.73	3.70	4.01	3.82	3.74	3.94
FeO	6.63	8.98	9.36	6.81	7.17	6.82	6.46
MnO	0.18	0.24	0.22	0.17	0.16	0.17	0.16
MgO	16.90	17.44	15.74	17.56	16.96	17.02	16.65
CaO	19.12	16.79	17.60	17.93	19.12	19.00	20.13
Na_2O	0.37	0.32	0.31	0.32	0.29	0.29	0.30
Cr_2O_3	0.40	0.29	0.02	0.34	0.14	.37	0.38
NiO	0.01	0.00	0.02	0.00	0.00	.00	0.00
Σ	100.18	99.01	97.91	99.28	98.96	99.74	99.61
Si	1.907	1.882	1.887	1.890	1.879	1.899	1.878
Ti	0.017	.025	0.029	0.022	0.022	.018	0.019
Al	0.162	.163	0.164	0.174	0.167	.161	0.171
Fe	0.202	.279	0.296	0.209	0.222	.209	0.199
Mn	0.005	.007	0.007	0.005	0.005	.005	0.004
Mg	0.920	.968	0.888	0.964	0.940	.932	0.912
Ca	0.748	.669	0.713	0.707	0.762	.748	0.796
Na	0.025	.022	0.023	0.022	0.020	.020	0.021
Cr	0.011	.000	0.000	0.010	0.003	.010	0.011
Ni	0.000	.000	0.000	0.000	0.000	.000	0.000
Σ	4.002	4.021	4.011	4.006	4.024	4.006	4.021
Fe	.11	.15	.16	.11	.12	.11	.10
Mg	.49	.51	.47	.51	.49	.49	.48
Ca	.41	.35	.38	.38	.40	.40	.42

TABLE 24. Relict clinopyroxene compositions of MV-48A

	1	2	3	4	5	6	7	8	9	10	11	12	13	14
SiO_2	51.33	49.02	53.58	51.17	52.08	52.33	52.27	53.78	51.19	51.26	50.88	49.91	50.25	48.59
TiO_2	.94	1.21	0.46	0.84	0.86	0.47	0.81	0.73	0.82	0.80	1.13	1.18	0.93	1.46
Al_2O_3	3.61	4.50	2.01	4.14	3.94	3.15	4.34	3.97	4.05	3.84	4.26	3.77	3.78	3.62
FeO	6.41	7.93	7.82	6.40	7.20	5.51	6.82	7.79	6.46	5.86	7.99	9.95	7.03	12.08
MnO	0.14	0.16	0.23	0.15	0.21	0.12	0.12	0.15	0.14	0.17	0.22	0.23	0.15	0.19
MgO	17.60	16.56	19.52	16.51	17.06	17.25	17.31	17.70	17.10	17.00	16.32	15.98	16.91	12.58
CaO	19.18	18.09	16.86	19.41	19.15	19.95	19.16	17.60	19.37	19.86	18.31	17.34	19.04	17.84
Na_2O	0.25	0.30	0.22	0.28	0.27	0.28	0.25	0.27	0.30	0.30	0.27	0.34	0.32	0.38
Cr_2O_3	0.10	0.00	0.43	0.39	0.15	0.55	0.05	0.15	0.22	0.66	0.00	0.00	0.10	0.00
NiO	0.04	0.06	0.00	0.00	0.00	0.00	0.13	0.03	0.08	0.14	0.00	0.06	0.09	0.09
Σ	99.11	97.85	100.74	99.28	100.91	99.62	101.24	102.70	99.74	99.90	99.37	98.75	98.595	96.85
Si	1.896	1.85	1.941	1.888	1.893	1.918	1.889	1.920	1.882	1.882	1.883	1.876	1.876	1.88
Ti	0.026	0.03	0.012	0.023	0.023	0.012	0.002	0.019	0.022	0.02	0.031	0.033	0.024	0.042
Al	0.157	0.19	0.085	0.179	0.168	0.136	0.184	0.166	0.175	0.17	0.185	0.167	.166	0.165
Fe	0.198	0.25	0.236	0.197	0.218	0.168	0.206	0.232	0.198	0.18	0.247	0.312	.219	.392
Mn	0.004	0.005	0.007	0.004	0.006	0.003	0.008	0.004	0.004	0.01	0.006	0.007	.004	.006
Mg	0.942	0.931	1.054	0.908	0.924	0.942	0.933	0.942	0.397	0.93	0.901	0.895	.94	.729
Ca	0.759	0.731	0.654	0.767	0.746	0.783	0.741	0.673	0.763	0.78	0.726	0.698	.761	.743
Na	0.018	0.021	0.015	0.020	0.019	0.019	0.017	0.018	0.021	0.02	0.018	0.024	.023	.029
Cr	0.002	0.000	0.001	0.011	0.004	0.015	0.001	0.004	0.006	0.02	0.000	0.000	.003	.000
Ni	0.001	0.00T	0.000	0.000	0.000	0.000	0.003	0.000	0.002	0.01	0.000	0.001	.002	.002
	4.006	4.026	4.010	4.002	4.006	4.002	4.004	3.984	4.015	4.013	4.001	4.018	4.025	4.000
Fe	.10	.13	.12	.11	.12	.09	.11	.13	.10	.10	.13	.16	.11	.21
Mg	.50	.49	.54	.49	.49	.50	.50	.51	.49	.49	.48	.47	.49	.39
Ca	.40	.38	.34	.40	.40	.41	.39	.36	.40	.41	.39	.37	.40	.40

TABLE 25. Relict clinopyroxene compositions, BR-52

					Px 1A	Px 2	Px 2A	Px 2B	Px 3	Px 4	Px 4A	Core	———	Rim
SiO_2	53.99	53.46	52.23	53.28	53.04	51.65	52.62	51.19	53.43	52.47	52.09	53.70	52.95	52.46
TiO_2	0.24	.26	.31	.26	0.29	0.41	0.42	0.56	0.19	0.35	.33	.23	0.33	0.31
Al_2O_3	1.68	1.67	2.19	2.34	2.73	3.89	3.47	3.33	1.90	2.93	3.13	1.87	3.39	2.91
FeO*	6.07	5.34	5.69	6.08	5.99	6.70	6.06	6.20	6.01	5.04	4.42	5.74	6.07	6.17
MnO	0.15	0.12	0.13	0.20	0.13	0.10	0.11	0.12	0.13	0.15	0.13	0.13	0.12	0.16
MgO	18.91	19.03	18.14	18.29	18.25	17.07	17.42	16.59	19.12	18.12	17.46	19.17	17.03	18.55
CaO	18.09	18.73	19.83	17.95	18.46	19.21	19.54	19.54	18.49	18.96	20.50	17.62	19.30	18.46
Na_2O	0.14	0.14	0.19	0.17	0.19	0.32	0.18	0.24	0.17	0.19	0.22	.17	0.17	0.23
Cr_2O_3	0.04	0.24	0.09	0.10	0.16	0.03	0.99	0.00	0.06	0.32	0.57	.12	0.19	0.16
NiO	0.06	0.16	0.03	0.11	0.08	0.00	0.27	0.04	0.09	0.04	0.05	.07	0.05	0.12
Σ	99.38	99.00	98.82	98.69	99.35	99.40	99.96	97.79	99.61	98.62	99.15	98.82	99.62	99.52
Si	1.97	1.959	1.931	1.959	1.941	1.902	1.920	1.915	1.95	1.931	1.914	1.967	1.936	1.922
Ti	0.006	.007	0.008	0.007	0.007	.011	0.011	0.015	.005	0.009	.009	.006	.009	.003
Al	.072	.071	0.095	0.101	0.117	.169	0.149	0.146	.081	0.127	.135	.08-	0.146	.125
Fe	.185	.163	0.175	0.186	0.183	.206	0.185	0.194	0.183	0.155	.145	.175	0.185	.189
Mn	.004	.003	0.003	0.006	0.004	.003	0.003	0.003	.004	0.004	.003	.003	0.003	.004
Mg	1.03	1.040	0.999	1.002	0.996	.937	0.947	0.925	1.040	0.994	.957	1.046	0.928	1.013
Ca	0.707	0.735	0.785	0.707	0.724	.758	0.764	0.783	0.723	0.747	.807	0.691	0.756	0.724
Na	0.009	0.010	0.014	0.011	0.013	.023	0.013	0.017	0.012	0.013	.015	0.011	0.012	0.016
Cr	0.001	.006	0.002	0.003	0.004	.000	0.002	0.000	0.001	.009	.016	0.003	0.005	0.004
Ni	0.001	.000	0.001	0.000	0.002	.000	0.000	0.001	0.002	.001	.001	0.002	0.001	0.003
	3.990	3.944	4.018	3.987	3.996	4.013	3.998	4.004	4.007	3.997	4.008	3.990	3.985	4.012
Fe	.10	.08	.09	.10	.10	.11	.10	.10	.09	.08	.08	.09	.10	.10
Mg	.54	.54	.51	.53	.52	.49	.50	.49	.53	.52	.50	.55	.50	.53
Ca	.37	.38	.40	.37	.38	.40	.40	.41	.37	.39	.42	.36	.40	.38

Table 26. Relict Clinopyroxene Compositions, BR-61.

	1	2	3	4	5	6	7
SiO_2	52.84	53.89	52.50	52.71	52.37	51.58	51.64
TiO_2	0.31	0.23	0.31	0.27	0.31	0.26	0.26
Al_2O_3	2.75	3.03	2.90	2.62	2.64	3.00	2.07
FeO	4.12	4.24	4.24	4.57	4.81	3.95	4.29
MnO	0.11	0.12	0.11	0.14	0.10	0.10	0.01
MgO	17.84	18.62	18.01	18.17	18.69	17.35	17.55
CaO	20.54	20.37	20.55	19.95	20.22	20.08	20.53
NaO	0.25	0.21	0.19	0.19	0.20	0.22	0.49
Cr_2O_3	0.56	0.47	0.47	0.32	0.81	0.85	0.27
NiO	0.00	0.03	0.38	0.13	0.13	0.04	0.01
Σ	99.31	101.21	99.32	99.05	99.77	97.45	97.20
Si	1.932	1.930	1.922	1.934	1.914	1.923	1.936
Ti	0.008	0.006	0.008	0.007	.008	0.007	0.007
al	0.118	0.127	0.125	0.113	.113	0.132	0.091
Fe	0.125	0.126	0.129	0.140	.146	0.123	0.134
Mn	0.003	0.003	0.003	0.004	.002	0.003	0.003
Mg	0.972	0.994	0.983	0.993	1.018	0.964	0.98
Ca	0.804	0.781	0.806	0.784	0.791	0.802	0.824
Na	0.017	0.014	0.013	0.013	0.014	0.015	0.035
Cr	0.016	0.013	0.013	0.009	0.008	0.025	0.008
Ni	0.000	0.000	0.001	0.003	0.003	0.001	0.000
	4.000	4.000	4.007	4.004	4.023	3.998	4.024
Fe	.07	.07	.07	.07	.07	.07	.07
Mg	.51	.52	.51	.52	.52	.51	.51
Ca	.42	.41	.42	.41	.40	.42	.42

Table 27. Relict Clinopyroxene Composition of V-252

	GROUNDMASS	PHENOCRYST				
	V-252-1	RIM	INT	CORE	INT	RIM
SiO_2	48.8	50.7	50.0	50.6	50.1	50.2
TiO_2	0.9	0.9	0.6	0.9	0.7	0.9
Al_2O_3	2.8	3.9	2.9	4.5	4.2	3.9
FeO*	18.4	12.7	12.9	13.0	13.3	12.7
Cr_2O_3	0.0	0.0	0.0	0.0	0.0	0.0
MnO	0.5	0.3	0.5	0.4	0.4	10.3
MgO	9.0	14.1	14.4	14.2	13.8	14.1
CaO	15.8	17.6	16.5	17.6	17.5	17.6
Na_2O	1.6	0.3	0.2	0.2	0.3	0.2
K_2O	0.0	0.1	0.0	0.0	0.0	0.2
Total	97.9	97.5	97.9	101.5	100.2	100.0
No. Ions						
Si		3.90	3.83	3.75	3.76	3.77
Ti		0.06	0.04	0.05	0.04	0.05
Al		0.24	0.26	0.39	0.37	0.35
Fe		0.80	0.83	0.80	0.84	0.80
Mn		0.03	0.03	0.02	0.02	0.02
Mg		1.45	1.65	1.57	1.54	1.57
Ca		1.43	1.35	1.40	1.41	1.42
Na		0.05	0.04	0.03	0.04	0.04
K		0.00	0.00	0.003	0.00	0.00
Fe		.22	.22	.21	.22	.21
Mg		.39	.43	.42	.41	.41
Ca		.39	.35	.37	.37	.37

Table 28. Relict Plagioclase of DXB-20.

	1	2	3
SiO_2	52.89	57.53	55.43
TiO_2	0.06	0.02	0.09
Al_2O_3	30.65	26.41	28.95
FeO	0.68	0.36	0.51
MnO	0.02	0.03	0.03
MgO	0.14	0.02	0.04
CaO	11.43	7.00	10.13
NaO	4.16	6.31	5.24
Cr_2O_3	0.03	0.00	0.00
NiO	0.00	0.00	0.00
	100.03	97.67	100.42
An	59	36	45

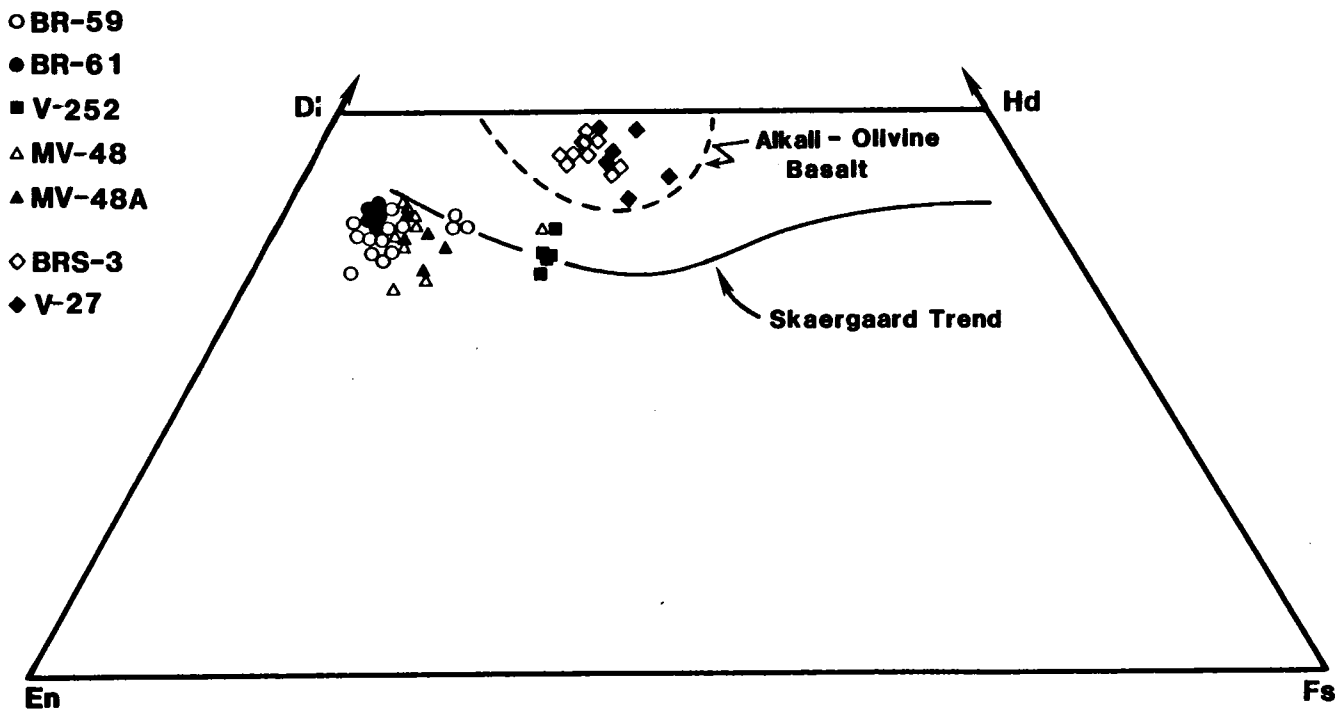

FIGURE 51. Clinopyroxenes of northeast Oregon greenstones.

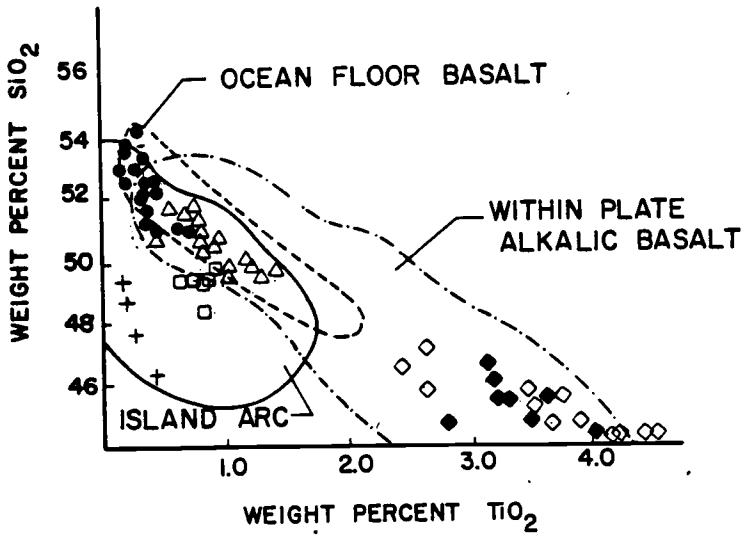

●	BR-52, BR-61	Burnt River Schist sheared greenstones
□	V-252	Greenhorn Mountains massive greenstone
+	P-1	Greenhorn Mountains dike in peridotite
△	MV-48, MV-48A	Mount Vernon pillowed greenstones
◇	BRS-3	Snake River pillowed greenstone
◆	V-27	Greenhorn Mountains pillowed greenstone

FIGURE 52. SiO_2-TiO_2 in clinopyroxenes from northeast Oregon greenstones.

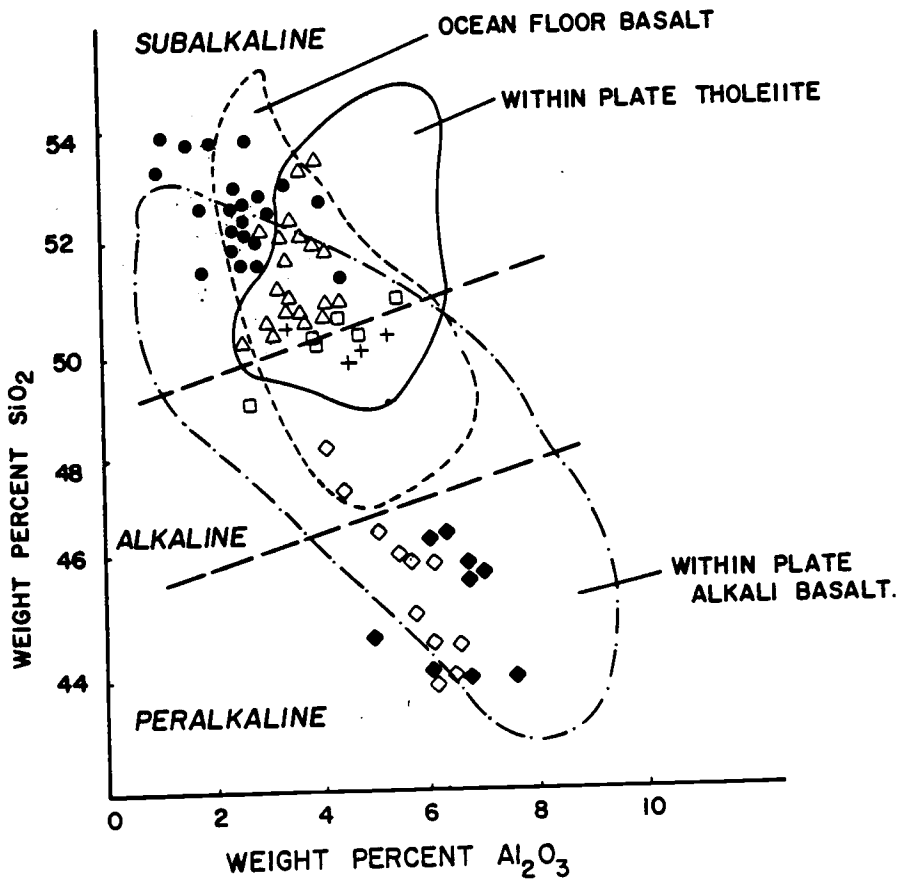

●	BR-52, BR-61	Burnt River Schist sheared greenstones
□	V-252	Greenhorn Mountains massive greenstone
+	P-1	Greenhorn Mountains dike in peridotite
△	MV-48, MV-48A	Mount Vernon pillowed greenstones
◇	BRS-3	Snake River pillowed greenstone
◆	V-27	Greenhorn Mountains pillowed greenstone

FIGURE 53. SiO_2-Al_2O_3 in clinopyroxenes from northeast Oregon greenstones.

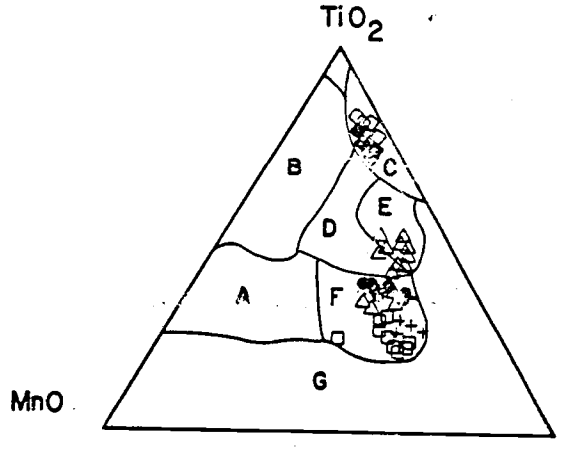

A VOLCANIC ARC BASALT
B OCEAN FLOOR BASALT
C WITHIN PLATE ALKALI BASALT
D ALL BASALTS
E VAB + WPA + WPT
F VAB + WPA
G WITHIN PLATE THOLEIITES

● BR-52, BR-61	Burnt River Schist sheared greenstones
□ V-252	Greenhorn Mountains massive greenstone
+ P-1	Greenhorn Mountains dike in peridotite
△ MV-48, MV-48A	Mount Vernon pillowed greenstones
◇ BRS-3	Snake River pillowed greenstone
◆ V-27	Greenhorn Mountains pillowed greenstone

FIGURE 54. $MnO/TiO_2/Na_2O$ in clinopyroxenes from northeast Oregon greenstones.

range widely from 46 to 54 percent in SiO_2 content. On an SiO_2/TiO_2 plot (Figure 52) they fall into an area which is within both volcanic arc basalt and MOR compositions. They contain less Al_2O_3 than the titanaugites, and are clearly subalkaline. However, on an Al_2O_3/SiO_2 plot (Figure 53) they fall into fields for ocean floor basalt AND within-plate tholeiite. The relation which most clearly delineates the nature of these augites is the ternary plot of MnO/TiO_2/Na_2O of Nesbitt and Pearce (Figure 54). On this diagram, these pyroxenes fall into areas of, respectively, volcanic arc basalts and within-plate alkalics, and plot near the apex OPPOSITE from the ocean floor basalt field. The high SiO_2/Al_2O_3 ratio of these basalts indicate that they are clearly subalkaline in nature, probably tholeiitic, and not characteristic of alkalic basalts. Hence, the within-plate alkali possibility of the plot can be eliminated, and volcanic arc basalts remain,--an origin which is possible based on other clinopyroxene compositional plots as well.

Summary: Igneous Association and Origin of Volcanic Greenstones

Textural, mineralogical, and geochemical data are compatible with the following conclusions regarding greenstone origins:

1) Pillowed greenstones closely associated with cherts at two and possibly three localities represent alkalic basalts: BRS-3 from the Snake River, V-27 from the north side of the Greenhorns, and possibly PH-76 from the melange south of Mount Vernon. Major element

compositions strongly suggest that these are alkalic basalts; mineral chemistry of relict pyroxenes permits no other alternative.

2) The remaining samples have a broad range of compositions, but are all quartz normative, and probably represent tholeiites. However, they plot on a calc-alkaline trend as is unequivocally shown on ternary plots of $MnO/TiO_2/Na_2O$. The pyroxenes are almost all subalkaline, and again, the majority of these rocks represent tholeiites or fairly silicic calc-alkaline rocks.

Hence, two distinct varieties of basaltic rock are represented in the greenstones of the oceanic/melange terrane: 1) alkalic basalts and 2) island arc tholeiites and calc-alkaline basalts to basaltic andesites. Two samples may represent N-MORB mid-ocean ridge basalt. A mixture of these rock types may most reasonably be expected to occur in a region where the oceanic and arc regimes overlap, such as a forearc. For a detailed description of the lithologies and geology of a modern forearc, the reader is referred to Bloomer and Hawkins (in press) and to Karig and Ranken (in press). Forearcs are essentially a mixture of two regimes--oceanic and nascent island arc. Hence they contain representative rocks of both, and in addition are intruded by diapiric serpentinites which penetrate the oceanic crust upon which the arc is constructed. True oceanic crust is uncommon in arc regions. This

puzzling absence may be due to extrusion of forearc basalts and consequent masking of the oceanic component, or it may be due to a process not yet recognized. Nevertheless, it is evident that most components of a coherent forearc are present in the area discussed, and its interpretation as a forearc is consistant with data presently available.

Peridotite and Gabbro of the Forearc Terrane

Fragments of plutonic ophiolitic rocks, principally gabbro, occur throughout the oceanic/melange terrane. They vary in dimension from meter-sized knockers in serpentinite matrix to masses of several square kilometers. These rocks are usually strongly deformed and altered. Some gabbro (North Fork, John Day River) is so strongly sheared that its phaneritic character is virtually obliterated. Other gabbro, especially south-southeast of Olive Lake in the Greenhorn Mountains, has been transformed into flaser gneiss. Virtually no plutonic fragment in the forearc terrane has escaped noteable deformation.

No stratigraphic coherency can be found within slivers of the dismembered ophiolite. Ophiolitic rock-types are usually mixed into a 'melange'. Some gabbro is layered, and rare layered ultramafic rocks occur near the town of Greenhorn. However, petrofabric study indicated that these rocks do not have a tectonite fabric, but rather, a rotational shear fabric (M80b). Hence, if they were tectonites, equivalent to the transition zone of the Canyon Mountain

Table 29. Major element analyses of plutonic ophiolitic rocks.

	M42	M46	M208	M213	M240
SiO_2	49.27	51.55	45.87	48.19	43.63
TiO_2	0.29	0.21	0.32	0.22	0.46
Al_2O_3	18.92	19.90	12.53	20.13	17.63
FeO*	7.78	5.97	8.54	5.32	9.00
MnO	na	na	na	na	na
MgO	6.57	6.40	14.40	7.90	12.72
CaO	15.62	15.10	15.95	17.35	15.80
Na_2O	0.61	0.58	0.21	0.61	0.41
K_2O	0.09	0.11	0.06	0.05	0.05
TOTAL	99.15	99.82	97.88	99.77	99.70

complex, later recrystallization has overprinted the upper mantle fabric.

The gabbro and peridotite are strongly altered. Olivine and orthopyroxene appear to be absent from gabbro throughout the terrane. Clinopyroxene is altered to uralitic hornblende or actinolite. Plagioclase is commonly chloritized. Although clinopyroxenite has largely retained its mineralogy and structure, peridotites containing olivine and orthopyroxene are extensively serpentinized and commonly grade into sheared serpentinite which may serve as melange matrix.

Major Element Variation of Gabbro

Major element data for metagabbros of the oceanic/melange terrane in the Greenhorn Mountains are given in Table 30, and indicate that they are tholeiitic, but are equivocal about their arc or oceanic origin. The gabbros plot on a strongly tholeiitic trend on an AFM diagram, in contrast to the Canyon Mountain complex calc-alkaline trend (Figure 55). On TiO/FeO*:MgO, diagram (Figure 56), the oceanic/melange gabbros plot in both calc-alkaline and tholeiitic fields: M208 and M240 are tholeiitic and fall on a MOR-trend, whereas M46 and M213 are island arc tholeiites, and plot along a trend similar to the Canyon Mountain complex.

Rare Earth Elements in Peridotite and Gabbro

Trace element analyses were made for one gabbro and one peridotite of the melange. The gabbro, M46, has a flat REE pattern, 4-7 x chondritic, slightly LREE depleted, with a small positive Eu

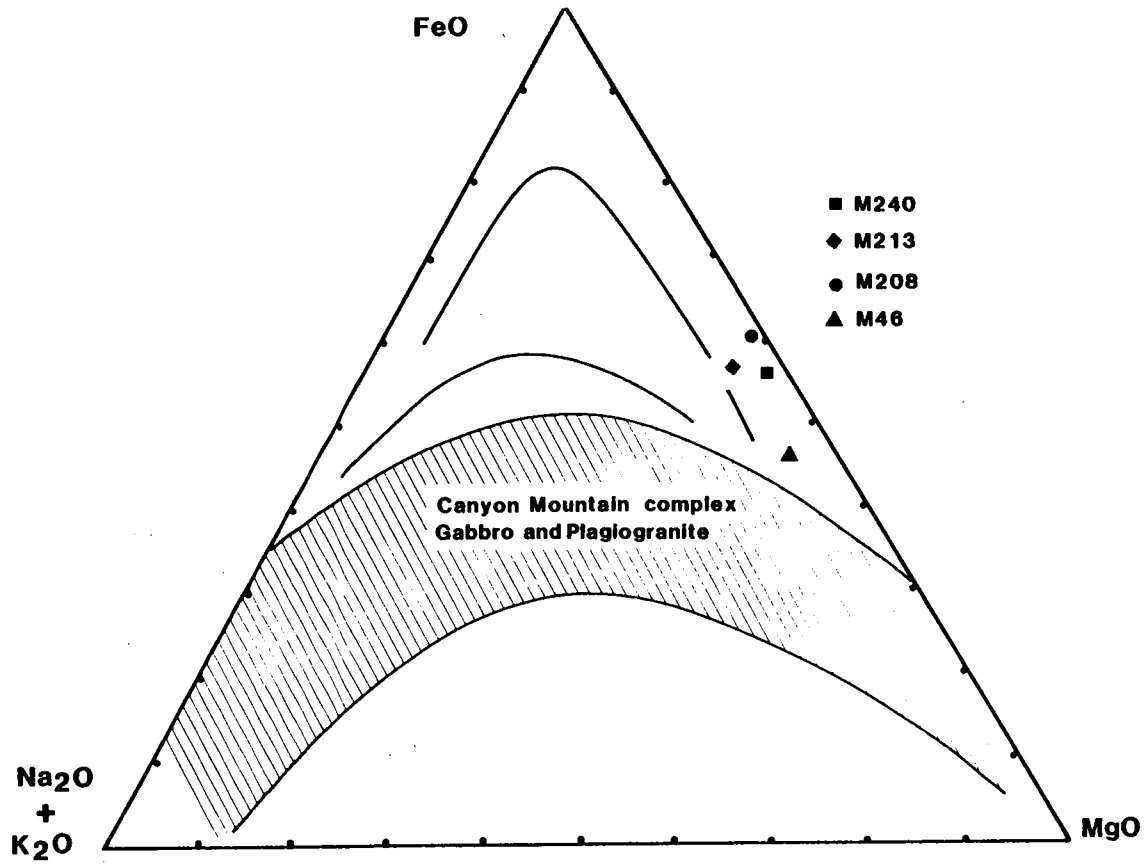

FIGURE 55. AFM diagram of gabbros of the forearc terrane.

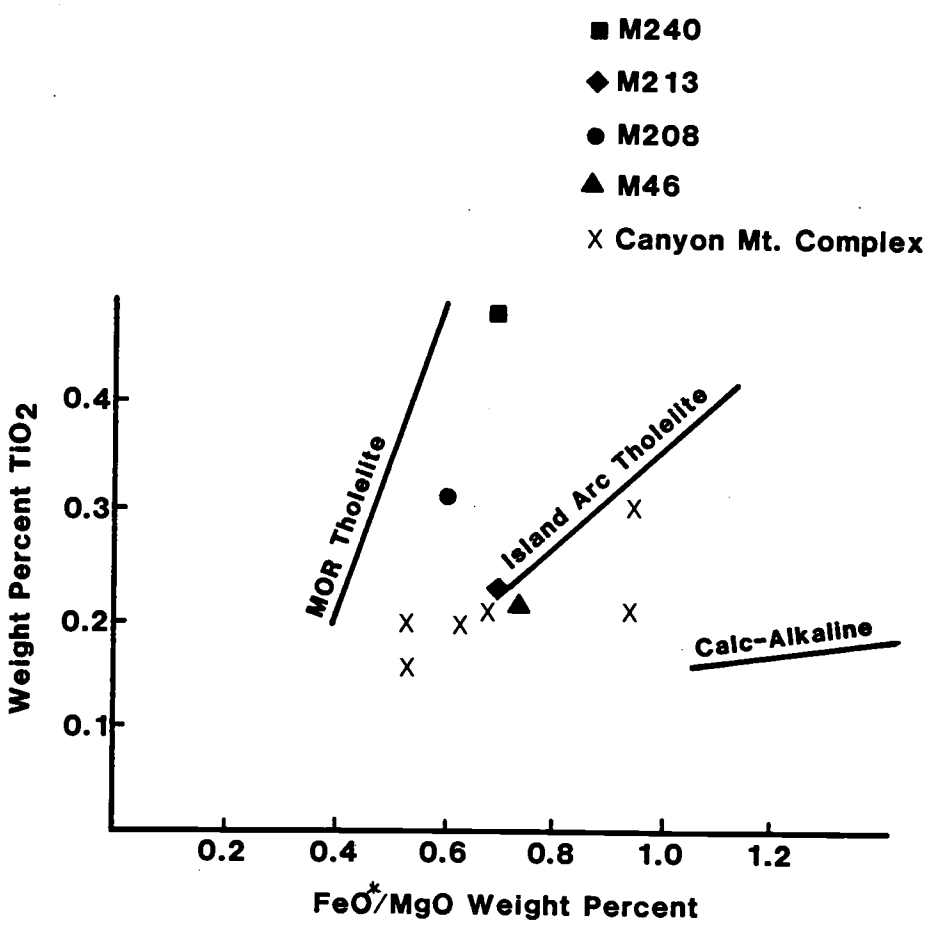

FIGURE 56. $TiO_2/FeO^*:MgO$ diagram for gabbro of the forearc terrane.

TABLE 30. Relict clinopyroxenes of plutonic ophiolitic rocks.

	M-42 (Cumulate)							M-42 (Cumulate)						
	Rim	Int	Int	Core	Int	Int	Rim	Rim	Core	Rim	Mis	CPX		
SiO_2	50.6	49.6	48.9	47.3	47.9	51.8	49.3	48.7	50.0	51.5	49.5	49.9	49.7	48.8
TiO_2	0.7	0.6	0.3	0.6	0.7	0.3	0.6	0.5	0.7	0.5	0.8	0.9	0.8	0.8
Al_2O_3	5.2	4.9	5.2	7.8	6.3	3.9	6.2	4.6	5.2	4.0	1.8	5.4	5.8	6.9
FeO*	9.1	7.5	8.3	12.5	8.6	8.0	10.6	8.1	8.5	8.7	12.0	8.4	8.3	9.4
Cr_2O_3	.0	0.0	0.0	0.0	0.3	0.0	0.0	0.0	0.0	0.0	0.0	0.0	0.0	0.0
MnO	0.3	0.3	0.3	0.3	0.3	0.3	0.3	0.3	0.3	0.3	0.4	0.3	0.3	0.3
MgO	13.4	13.4	12.6	13.7	13.5	13.5	13.1	13.2	12.9	13.6	12.9	12.8	12.9	12.7
CaO	21.0	22.0	22.1	16.5	22.3	21.5	19.2	22.0	22.5	22.0	22.3	21.6	22.3	20.5
Na_2O	0.4	0.5	0.4	0.4	0.4	0.3	0.4	0.4	0.4	0.5	0.5	0.5	0.4	0.5
K_2O	0.0	0.0	0.0	0.0	0.0	0.0	0.0	0.0	0.0	0.0	0.0	0.0	0.0	0.0
TOTAL	100.7	98.9	98.2	99.1	100.0	99.6	99.6	97.9	100.5	101.1	100.2	99.9	100.6	100.1
Sum														
Si	1.87	1.87	1.86	1.79	1.80	1.93	1.85	1.86	1.86	1.90	1.88	1.86		1.82
Ti	0.02	0.02	0.01	0.02	0.02	0.01	0.02	0.01	0.02	0.01	0.02	0.02		0.02
Al	0.23	0.22	0.23	0.35	0.28	0.17	0.27	0.21	0.23	0.17	0.08	0.24		0.31
Fe	0.28	0.24	0.26	0.90	0.27	0.25	0.33	0.26	0.26	0.27	0.38	0.26		0.29
Mn	0.00	0.01	0.01	0.01	0.01	0.01	0.08	0.01	0.01	0.01	0.01	0.01		0.01
Mg	0.74	0.75	0.71	0.77	0.75	0.75	0.73	0.75	0.72	0.75	0.74	0.71		0.71
Ca	0.83	0.89	0.90	0.67	0.90	0.86	0.77	0.90	0.89	0.87	0.91	0.86		0.82
Na	0.04	0.04	0.03	0.03	0.03	0.02	0.03	0.03	0.03	0.04	0.04	0.04		0.04
K	0.01	0.00	0.00	0.00	0.00	0.00	0.001	0.00	0.00	0.00	0.00	0.00		0.00
Fe	.15	.13	.14	.22	.14	.13	.18	.14	.14	.14	.19	.14		.17
Mg	.40	.40	.38	.42	.39	.40	.40	.39	.39	.40	.36	.39		.39
Ca	.45	.47	.48	.36	.47	.46	.42	.47	.47	.46	.45	.47		.45

	M-46 (Mafic Gabbro)				Layered Ultramafic			M-91	Rim	Core	Rim	Olivine - M-91			
					M-80b3										
S_iO_2	47.9	46.4	47.5	54.8	53.4	53.0	52.8	54.9	53.8	54.2	54.5	40.6	40.6	40.1	40.5
T_iO_2	0.8	0.7	1.4	0.1	0.1	0.01	0.20	0.22	0.18	0.21	0.10	0.11	0.03	0.08	0.04
Al_2O_3	11.6	10.8	8.6	2.0	3.1	4.7	4.3	1.48	1.7	1.2	1.5	0.03	0.00	0.03	0.04
FeO	12.2	11.7	11.7	8.3	2.9	2.1	3.2	2.0	2.4	2.1	1.9	12.2	14.8	12.5	14.3
Cr_2O_3	0.03	0.03	0.10	0.02	0.33	0.13	0.48	0.14	0.17	0.17	0.17	0.0	0.0	0.03	0.00
MnO	0.2	0.3	0.2	0.20	0.1	0.11	0.10	0.04	0.10	0.08	0.10	0.8	0.20	0.6	0.4
MgO	14.7	13.7	14.6	17.5	15.7	18.2	15.7	17.0	16.7	16.7	17.0	45.9	44.1	46.0	44.72
CaO	11.6	12.4	12.0	14.5	23.6	21.0	24.2	24.7	23.7	23.7	24.0	0.0	0.0	0.0	0.0
Na_2O	1.7	2.1	1.9	0.44	0.07	0.01	0.09	0.07	0.08	0.06	0.02	0.0	0.0	0.0	0.0
K_2O	0.04	0.06	0.20	0.00	0.01	0.00	0.00	0.00	0.02	0.01	0.01	0.0	0.0	0.0	0.0
Total	99.9	98.1	98.1	98.0	99.2	99.2	101.0	100.5	98.8	99.0	99.2	99.6	99.7	100.3	100.0
Sum	3.50	3.51	3.60	4.00	3.91	3.84	3.81					Fo_{89}	Fo_{85}	Fo_{90}	Fo_{84}
Si	3.50	3.51	3.59	4.00	3.91	3.84	3.81	3.96	3.95	3.96	3.97				
Ti	3.04	0.04	0.08	0.01	0.01	0.001	0.01	0.01	0.01	0.01	0.01				
Al	1.00	0.96	0.76	0.18	0.27	0.40	0.37	0.13	0.15	0.14	0.13				
Fe	3.75	0.74	0.74	0.52	0.17	0.13	0.19	0.12	0.15	0.13	0.11				
Mn	3.014	0.02	0.01	0.01	0.01	0.01	0.01	0.00	0.01	0.01	0.01				
Mg	1.60	1.55	1.64	0.55	1.71	1.96	1.69	1.83	1.83	1.82	1.85				
Ca	3.91	1.00	0.97	0.70	1.85	1.63	1.87	1.91	1.86	1.86	1.87				
Na	3.24	0.31	0.29	0.063	0.01	0.00	0.01	0.01	0.01	0.01	0.01				
K	3.00	0.01	0.02	0.00	0.00	0.00	0.00	0.00	0.002	0.00	0.01				
Cr	3.02	0.00	0.01	0.001	0.019	0.01	0.03	0.01	0.01	0.01	0.01				
Fe	.23	.22	.22	.29	.05	.03	.05	.03	.04	.04	.03				
Mg	.49	.47	.49	.31	.46	.53	.45	.47	.48	.48	.48				
Ca	.28	.30	.29	.40	.50	.44	.50	.49	.48	.48	.49				

anomaly, and is very similar to REE of oceanic cumulate gabbro reported by Tiezzi and Scott (1980) (Figure 58). This gabbro, as are most gabbros in the melange, is uralized and altered. Its major element data suggest island arc affinities. However, alteration may have affected the FeO*/MgO ratio upon which the determination of affinity is largely based. REE are less subject to mobilization during alteration, and hence may be a more reliable guide to the character of the unaltered rock. The peridotite (M91) is strongly serpentinized clinopyroxene-rich harzburgite which has been partly recrystallized and metasomatized by a tonalite which intrudes it. Its REE enrichment may partly be related to the adjacent intrusion, but may also relate to high modal percent of clinopyroxene (and probably orthopyroxene).

Relict Clinopyroxenes of Peridotite and Gabbro

Clinopyroxenes of the melange gabbro plot in a broad scatter on the pyroxene quadrilateral (Figure 59). The relict clinopyroxene of M46 plots in the augite field. It is low in Cr_2O_3 and CaO, and is enriched in Al_2O_3 and TiO_2 relative to most CMC gabbroic clinopyroxenes. On pyroxene discriminant diagrams, the M46 gabbro plots in alkaline or island arc fields, rather than in the oceanic field.

Gabbro M42, a less altered cumulate of the oceanic/melange terrane, Greenhorn Mountains, contains well-preserved relict clinopyroxene. The pyroxenes are zoned but the zonation may be due to alteration rather than original igneous compositional variation, as less mobile oxides (TiO_2, Cr_2O_3, MnO) vary little, whereas more

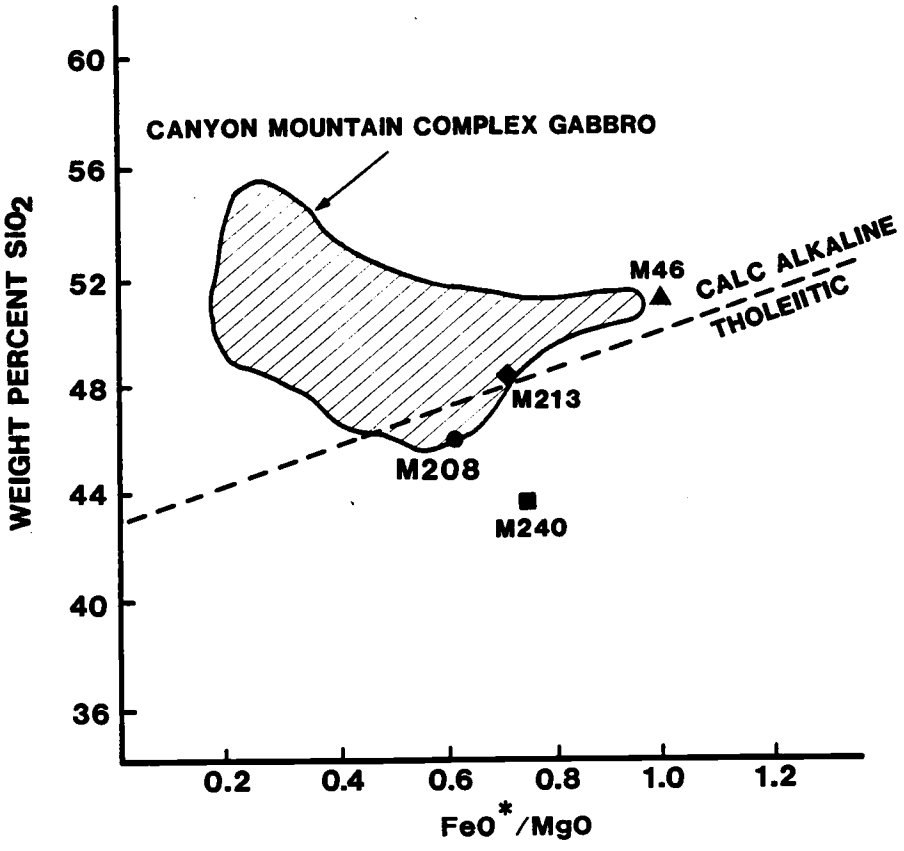

FIGURE 57. SiO_2:FeO*/MgO diagram for gabbros of the forearc terrane.

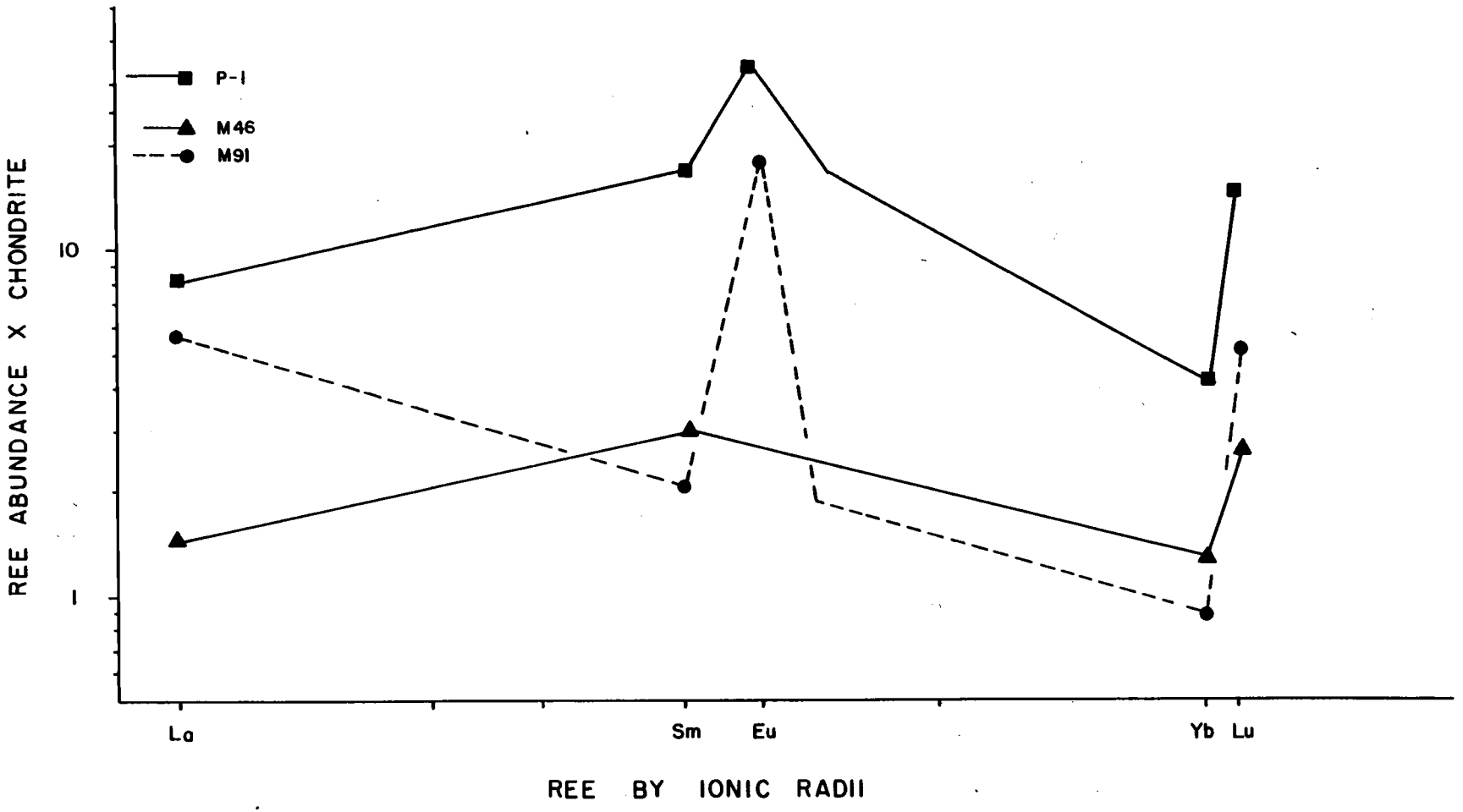

FIGURE 58. REE of plutonic rocks of the forearc terrane.

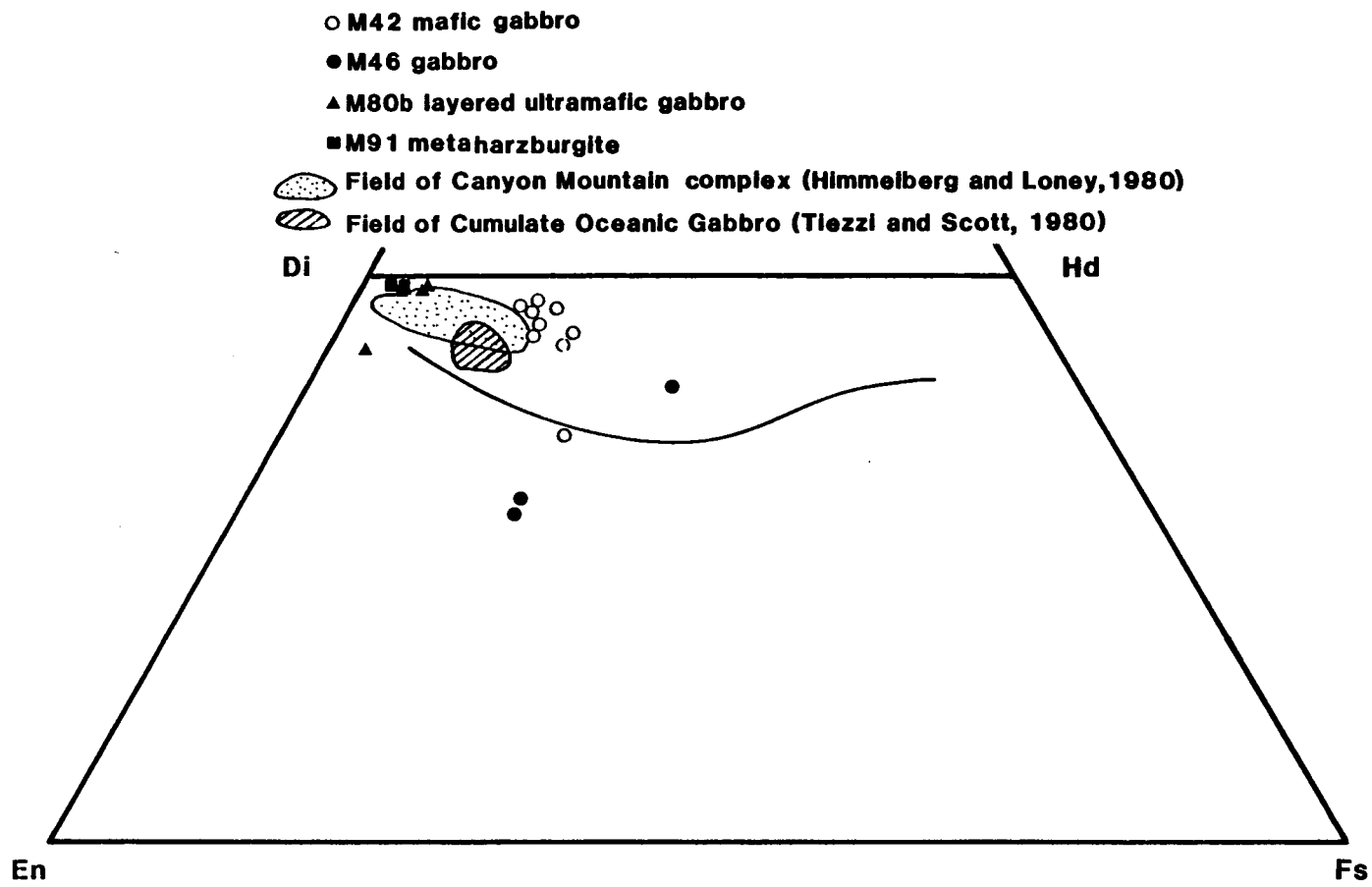

FIGURE 59. Pyroxene quadrilateral for clinopyroxenes in gabbro and peridotite of the forearc terrane.

mobile components (CaO, MgO) vary about 15 percent within the grain. M42 clinopyroxenes plot in a tight cluster on the pyroxene quadrilateral, slightly more iron-enriched than CMC. Generally, their SiO_2/Al_2O_3 and SiO_2/TiO_2 ratios are characteristic of island arc tholeiitic to sub-alkalic rocks.

In addition to the gabbro samples, clinopyroxenes of two ultramafic rocks from the melange were analyzed. M80b is a layered ultramafic which may be analogous to the CMC transition zone, although petrofabric analysis indicates only rotational deformation rather than a tectonite fabric. Clinopyroxenes from M91 were also analyzed. As shown on the pyroxene quadrilateral (Figure 59), clinopyroxene of both rocks is slightly more calcic than clinopyroxenes of the Canyon Mountain complex analyzed by Himmelberg and Loney (1980). As in the CMC, the clinopyroxenes of layered rocks contain more Cr_2O_3 and Al_2O_3 than the metaharzburgite, and are less enriched in MgO and TiO_2. Olivine in M91 is Fo_{84-90}, slightly less magnesian than olivine of the Canyon Mountain complex.

In summary, the metagabbro and peridotite of the oceanic/melange terrane analyzed for this study may have diverse origins. Two megagabbros, M213 and M46 have tholeiitic, MORB major element trends, although their chemistry may be somewhat affected by alteration. Clinopyroxenes of M46 plot in arc and alkalic fields, but the scatter of their compositions around the Skaergaard trend on the pyroxene quadrilateral suggests alteration of a MOR tholeiite. Hence, M46 may represent a fragment of ocean-ridge gabbro within melange. The

flat, MOR-like rare-earth element pattern of M46 is also strongly indicative of ocean-ridge affinity.

The remaining gabbros and peridotites are more arc-like in their chemistry and mineralogy. Their clinopyroxene compositions straddle, and plot on the same trend as, the Canyon Mountain complex clinopyroxenes. Major element analyses are low in TiO_2, Al_2O_3 enriched, although they show much stronger iron enrichment than the CMC. These rocks most probably represent fragments of early island arc basement, similar in origin to the Canyon Mountain complex.

Nature of the Terrane

The terrane which surrounds the Canyon Mountain complex contains all the petrologic elements of present-day forearc regions (Bloomer and Hawkins, in press; Karig and Ranken, in press). These include: 1) arc tholeiites, 2) alkalic rocks which may represent seamounts or transform basalts, 3) MORB tholeiites, 4) fragments of oceanic ophiolite, 5) serpentinite melanges and diapiric serpentinites, and 6) possible fragments of arc basement. The Permian and Triassic metasediments associated with this terrane are diverse, and are also characteristic of forearc settings.

No other petrotectonic environment presently defined contains this assemblage. Large ocean basins, as far as known, do not contain calc-alkaline rocks. Back arc basins seem to lack alkalic basalts. The overall scale of the terrane is similar to modern forearc regions. Distances of approximately 150 to 175 km are

common for the distance from trench to the main, magmatic arc. Measured NW-SE, the distance from rocks of Huntington arc affinity to the probable northeasterly trace of the Mitchell blueschists near Heppner is 150 km. The Canyon Mountain complex is situated approximately midway between the trend of the Mitchell blueschists and the Seven Devils arc. Thus the interpretation of the CMC as a forearc ophiolite, and the surrounding terrane as a relatively coherent forearc, is in keeping with both tectonic and petrologic surroundings.

THE ORIGIN OF THE CANYON MOUNTAIN COMPLEX AND ITS RELATION TO THE FOREARC TERRANE

The Canyon Mountain complex is an arc-related ophiolitic sequence which consists of tectonite peridotite overlain by transition zone "metacumulates" which show varying amounts of deformation, and gabbro which intrudes through and overlies both lower units.

The following observations, discussed previously, are pertinent to the origin of the Canyon Mountain complex:

1. Textural and field evidence strongly suggests that gabbroic mamga did not originate by partial melting of the Canyon Mountain complex harzburgite, but had a different source and intruded the harzburgite along the zone between two rising diapirs of peridotite. Gabbro in narrow, early veins and dikes has primitive REE patterns similar to those of wider, probably later dikes.
2. Structural studies by Misseri and Boudier (in prep.) indicate two diapiric structures in the Canyon Mountain harzburgite, with an area of flattened foliation in the middle. This zone of flattened foliation coincides with the zone of infiltration.
3. No feldspathic harzburgite was observed outside of the zone of infiltration.
4. The rocks of the transition zone are not uniformly deformed. Those at east and west ends of the CMC, and those closest to the harzburgite, have the

strongest fabric.

5. Transition zone metacumulates are crosscut and intruded by isotropic gabbro.
6. Transition zone major element trends are slightly more tholeiitic than gabbro trends, implying possible influx of magma from a different source as well as accumulation of early gabbro precipitates. Both transition zone and gabbro contain more K_2O than is common in other ophiolites.
7. Periodic influxes of picritic or primitive magma occurred throughout crystallization of the transition zone, and also during crystallization of gabbro - noteably of the Pine Creek Mountain gabbro.
8. The major element composition of the calculated fractionate is that of an iron-rich melagabbro, which again agrees with the probable average composition of transition zone rocks. However, minor and trace element data for both minerals and whole rocks require addition of relatively small amounts of LREE-depleted, Cr and Ni enriched magma to the transition zone during its crystallization. Volumetric and time considerations, as well as evidence for contribution from primitive magma, indicate that the transition zone did not accumulate solely by crystallization from Canyon Mountain complex gabbro.

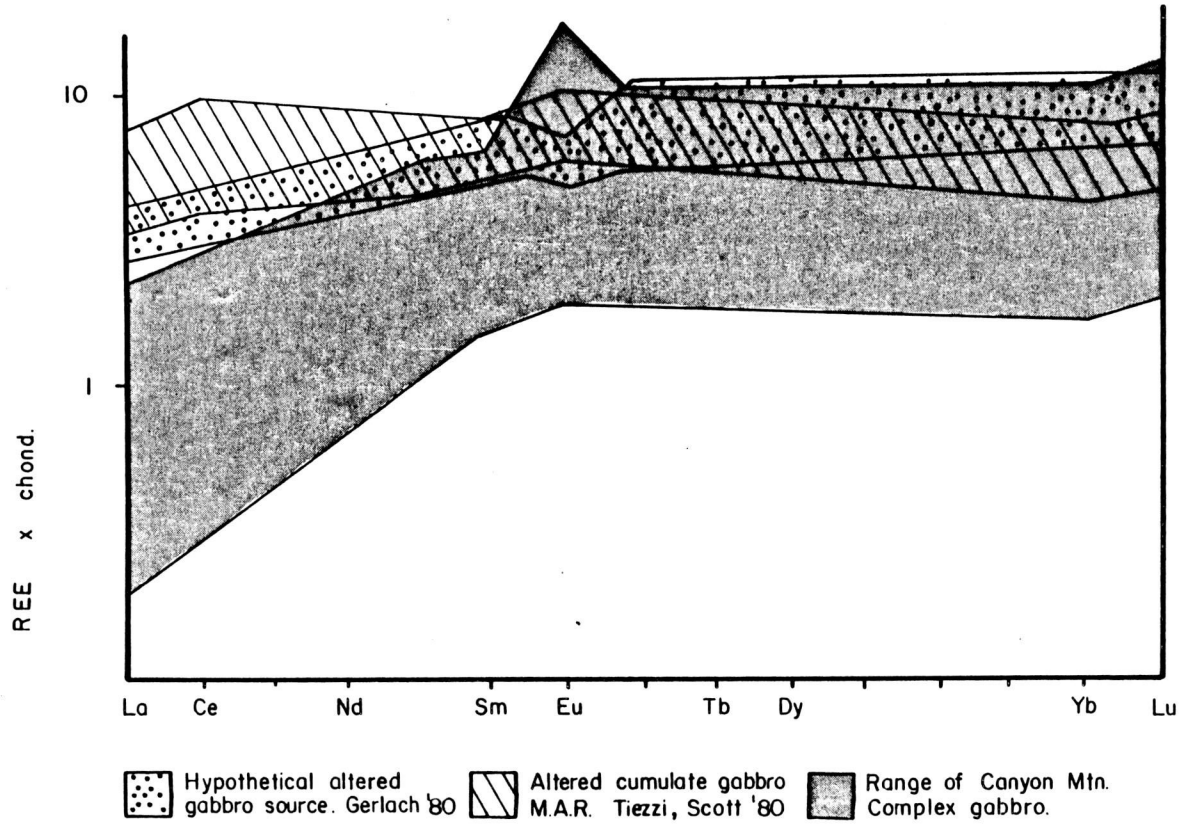

FIGURE 60. REE models for plagiogranite source rocks.

For example, assuming that Bear Skull Rims gabbro is 40% of the total gabbro, and Pine Creek Mountain represents the remainder, the calculated fractionate would yield a rock with 19.2 percent olivine, 15.4 percent orthopyroxene, 23.1 percent clinopyroxene, 5.0 percent magnetite, and 37.3 percent plagioclase. Overall, this composition is similar to the average for transition zone rocks, but contains more orthopyroxene.

9. The intrusion of gabbro into peridotite which was at elevated temperatures ($\approx$ 800°C?) is supported by: a) lack of chilling, b) no reaction or thermal metamorphism of the peridotite and c) rodingization of the gabbro.
10. Gabbro of the Canyon Mountain complex contains abundant orthopyroxene and compositional layering throughout the stratigraphic section.
11. Lastly, the upper levels of the Canyon Mountain complex gabbro were intruded and partly fused by the coeval intrusion of plagiogranite and diabase dikes and sills.

The observations noted above, and other data presented and discussed in this thesis lead to the following major conclusions regarding the origin of the Canyon Mountain complex.

1. The harzburgite was emplaced as rising diapirs. Gabbro intrudes through the peridotite in the area between principal diapiric structures. Gabbro intrusion occurred during and after harzburgite deformation.

2. The gabbro and most of the transition zone are not genetically related to the harzburgite, but intruded through it and crystallized in a chamber above the harzburgite. Remnants of primitive gabbroic magma which fed the CMC gabbro are present in pods and dikes within the zone of infiltration in the harzburgite.
3. The zone of infiltration served as a conduit for gabbro magma of almost uniform composition probably for long duration.
4. The transition zone is mostly cumulates of fractionating gabbro and was also periodically replenished by Cr, Ni, MgO enriched magmas, probably similar to primitive gabbro. Portions of the transition zone are intruded and enclosed by CMC gabbro.
5. The Canyon Mountain complex gabbro is a single differentiated sequence. The olivine two-pyroxene parent, the gabbro of Gwynn Gulch, is represented by the pods and dikes within the harzburgite. It is tholeiitic, with low TiO_2, slightly enriched K_2O relative to other ophiolites, and high MgO. Its REE pattern is very LREE depleted, with no Eu anomaly and flat HREE, and low overall REE abundances. This magma fractionated mostly olivine and orthopyroxene, with small amounts of clinopyroxene, plagioclase, and magnetite at high P_{H_2O} to yield a more calc-alkaline

rock, the gabbro of Bear Skull Rims. The BSR gabbro is a clinopyroxene rich rock with subordinate orthopyroxene and no olivine. It is the principal gabbro stratigraphically above the CMC harzburgite and transition zone and represents about half the volume of gabbro in the CMC. REE for samples of this lithology are LREE depleted, HREE flat, and show a slight positive Eu anomaly. The BSR magma fractionated principally by precipitation of clinopyroxene and plagioclase to yield the orthopyroxene-rich gabbro and norite of the Pine Creek Mountain (PCM) gabbro. The PCM gabbro is the upper-most unit examined in detail for this thesis. It varies from LREE depleted to flat LREE, and has substantial positive Eu anomalies. REE patterns cross, indicating a complex magmatic history for the upper gabbro unit. The norites were probably replenished by more primitive gabbro magma. A small amount of the BSR gabbro also fractionated under less hydrous conditions to produce an olivine-bearing gabbro with more evolved REE and substantial positive Eu anomaly which is similar to much transition zone gabbro. Overall, the CMC gabbro is enriched in Cr, K_2O, and orthopyroxene compared to other ophiolitic gabbros, suggesting an origin by partial melting of a clinopyroxene-rich depleted source under hydrous conditions with K_2O added to the system by metasomatism.

The Canyon Mountain complex was intruded into altered oceanic crust. Some oceanic crust was partially fused by the high temperature, relatively anhydrous gabbroic magma, and formed plagiogranites. REE data shown in Figure 60 and calculated by Gerlach (1980) indicate that partial fusion of oceanic crust is a better and more likely source for the plagiogranite than either fractionation of CMC gabbro or partial melting of altered CMC gabbro.

The plagiogranite magma intruded the lower, solidified and slightly cooled (600°C) CMC gabbro, causing recrystallization and dehydration. Diabase intruded the gabbro and upper harzburgite at the same time, and is chilled against the gabbro. Source of the diabase is not known. Its chilled margins, and the fact that it pinches out downward into the gabbro just as the albite granite does suggests that the diabase is not directly part of the CMC magma.

Thus, the Canyon Mountain complex is, as Thayer (1977) recognized, composed of a variety of magmas of different origins.

In the 1948 symposium on the Origin of Granite, Bowen succintly stated: "Look as one will at the rocks, he cannot see them in the process of formation." This is as true of Canyon Mountain and present-day petrology as it was for Bowen and H. H.

Read. The following discussion and model for the origin of the Canyon Mountain complex is based upon experimental petrology and our current geochemical, geophysical, and plate tectonic understanding of island arc systems. However, it is still constrained by Bowen's observation.

Numerous geochemical criteria indicate that the CMC gabbro is associated with a calc-alkaline island arc setting as inferred from its calc-alkaline major element trends, its high abundance of K_2O, and relatively low TiO_2 content. Hence the CMC may be considered an intrusion of gabbroic magmas through a rising diapir in early island arc crust (Figure 61). High K_2O has been shown to be characteristic of early rocks in the Marianas, and may signal early arc magmas (Meijer and Reagan, 1983).

The importance of the anomalously high content of orthopyroxene in CMC gabbro should not be overlooked. Kushiro and Yoder (1969) found that under dry conditions $MgSiO_3$ melts congruently and under hydrous conditions melts to Fo plus SiO_2-oversaturated liquid. Mantle peridotite partially melted under hydrous conditions such as an island arc should yield more silicious magmas than mantle peridotite melted under dry conditions such as a mid-ocean ridge. Thus, the presence of orthopyroxene throughout the CMC gabbro sequence suggests an origin by partial melting in a more hydrous environment - such as an island arc.

The following sequential model for the Canyon Mountain complex incorporates all points discussed and reiterated above. The model is illustrated in Figure 61.

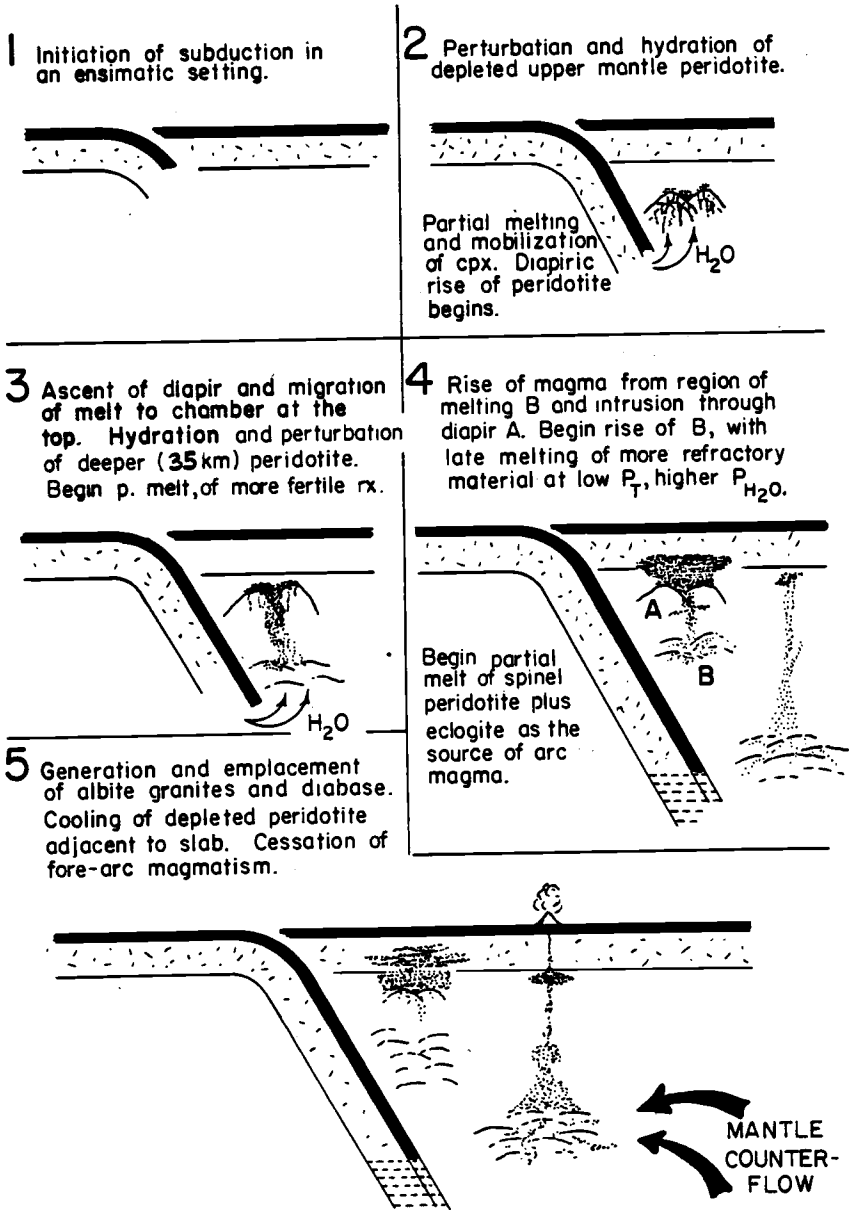

FIGURE 61. Schematic model for the origin of the CMC and forearc terrane.

Table 31. A classification of ophiolites.

Island Arc	Oceanic
Diapiric Peridotite	Horizontal Structure in Peridotite.
OPX in Early Gabbro	OPX Absent or Rare in Early Gabbro.
Sheeted Sills. Coeval Diabase & Plagiogranite	Sheeted Dikes Feed Pillow Lavas.
Abundant Plagiogranite	Little Plagiogranite
High K_2O/SiO_2	Low K_2O/SiO_2
Low TiO_2/SiO_2	High TiO_2/SiO_2
Calc-Alkaline Gabbro	Tholeiitic Gabbro

Initiation of subduction in an ensimatic settling must have occurred at least by early Permian. At a half-spreading rate of 4 cm/year, the downgoing, hydrated oceanic slab would reach 50 km depth in 5 million years.

Perturbation of upper mantle peridotite occurred throughout descent of the slab's leading edge. Mostly depleted harzburgite began to rise from a depth of about 20-25 km. Adiabatic rise, plus the addition of water from the downgoing slab resulted in partial melting of the remaining fertile components within this peridotite. Partial melts of the diapir contained little or no plagioclase, although there might have been minor contribution of alkalis (such as K_2O) from the down-going slab. This melting event yielded clinopyroxene and/or orthopyroxene veins initially parallel to, and later crosscutting foliation. These early partial melts rose to the top of the ascending diapir and formed magma pockets of the lower transition zone which crystallized as the diapir rose. The rocks resulting from the early melts thus developed a fabric similar to their parent peridotite. These rocks - now of the lower transition zone - are high in CaO, low in Al_2O_3, and have a high modal content of clino and orthopyroxene which reflects the principal mode of origin - partial melting of clinopyroxene at low pressure and high P_{H_2O}.

Perturbation and hydration of less depleted peridotite at depths of 30-35 km, and probable diapiric rise of this deeper peridotite resulted in greater percent of partial melting and the generation of a tholeiitic to silicic calc-alkaline magma, with overall low abundances of REE and depleted LREE. This

gabbroic magma may have fractionated slightly enroute to the "surface", although Gwynn Gulch gabbro shows little evidence of fractionation.

Primitive gabbro from this less depleted peridotite intruded through the depleted peridotite diapirs above. Intrusion occurred during and after diapiric rise, and was confined principally to the zone between diapirs. Gabbro and transition zone rocks resulting from gabbro fractionation which crystallized prior to the cessation of rise would develop a tectonite fabric, parallel with that of the host peridotite. Gabbro which intruded through the diapirs, or after rise had stopped as well as the later transition zone cumulates, would lack the tectonite overprint. Some gabbro of the transition zone may be early gabbro from the second melting event which was mixed with picritic to melagabbro liquids of the first diapir. Similarly, late injections of picritic magma into the upper, Pine Creek Mountain gabbro might originate from late, additional melting of the now-more-depleted second diapir. An important consideration for this model of magma generation in forearc regions is that because continued subduction will cool the mantle adjacent to the downgoing slab, and thus terminate partial melts from this region, no long-term, steady-state source is present, and forearc magmatism will eventually cease as the geothermal gradient around the newly developed subduction zone decreases with time.

Partial melting of overlying hydrated oceanic crust and probable in-mixing of upper late fractionate of the gabbro occurred only after solidification and cooling of cumulates, and is

related to the appearance of mafic dikes. Magma from both plagiogranite and mafic dikes was injected downward and also spread laterally, parallel to gabbro layering. This process appreciably contributed to the thickening of forearc crust and thinning of overlying oceanic crust.

A fundamental problem of island arcs (Bloomer, pers. comm., 1982) is the apparent absence of oceanic crust as basement. They seem to be constructed directly on island arc material. A process of crustal thickening by partial melting, mixing, and injection into oceanic gabbro and basalt might account for the seeming disappearance of oceanic rocks in island arc regions.

The Canyon Mountain complex represents nascent island arc crust which probably did not vent a significant quantity of volcanics. However, other arc-related ophiolite fragments throughout northeast Oregon represent probably similar magma chambers which may have vented island arc volcanic rocks of the type found in the forearc terrane, rather than simply melting island arc crust. The occurrence of greenstones and gabbros of oceanic affinity within the forearc terrane suggests that <u>all</u> oceanic crust is not destroyed in forearcs.

Based upon the data and interpretations in this thesis, it is apparent that there are ophiolites and ophiolites. Unlike granites and granites, there is no gradation between them. The oceanic, "common" ophiolite, such as Oman or Bay of Islands originates in a tensional environment, at a constructional ocean ridge or spreading

center. The forearc type of ophiolite such as the Canyon Mountain complex, originates in early stages of arc development, in the compressional environment of a destructive margin. It is composed of a limited supply of magma from sequential, but restricted, melting events. Unlike the oceanic type, a forearc ophiolite does not receive an unlimited supply of basaltic magma.

The two types are distinct in many other respects, including the absence or presence of orthopyroxene, the abundance of K_2O and Na_2O, the presence of dikes versus sills, the abundance of plagiogranite, the major and minor element petrologic trends, and the field association with only chert, or with wacke, conglomerates, and shales. These ophiolite subtypes are superficially similar, but differ in significant details. Oceanic and forearc ophiolites are categorized in Table 30.

Ophiolites are key windows to magmatic and related tectonic processes. The recognition of ophiolite subtypes should further the study of these complex assemblages, and their continuing investigation should yield a better comprehension of ocean ridges and island arcs. Diligent research in concert with new techniques and a finer distinction among ophiolite subtypes will lead to the resolution of long-standing petrotectonic questions as well as problems yet unconceived. The study of the Canyon Mountain complex is but one step on the journey.

BIBLIOGRAPHY

Amstutz, G. C., 1974. Spilites and Spilitic Rocks. New York, Springer-Verlag, 482 p.

Arai, S., 1980. Dunite-harzburgite-chromite complexes as refractory residue in the Sangun-Yamaguchi zone, western Japan. Jour. Petrol., V. 21, p. 141-165.

Atkins, F. B., 1969. Pyroxenes of the Bushveld intrusion, South Africa. Jour. Petrol., V. 10, p. 222-249.

Ave Lallemant,H. G., 1976. Structure of the Canyon Mountain (Oregon) ophiolite complex and its implication for seafloor spreading. Geol. Soc. America Spec. Paper 173, 49 p.

Bloomer, S. and Hawkins, J., in press. Gabbroic and ultramafic rocks from the Mariana Trench: an island arc ophiolite. In Hayes, ed., The tectonic and geologic evolution of Southeast Asian Seas and Islands, J. Am. Geophys. Union Monograph 27.

Boudier, F., and Nicholas, A., 1977. Structural controls on partial melting in the Lanzo peridotite. in Dick, HJB, ed., Magma Genesis. Ore. Dept. Geol., Min. Ind. Bull. 96. p. 63-78.

Boudier, F., and Coleman, R. G., 1981. Cross section through the peridotite of the Samail ophiolite, southeastern Oman mountains. Jour. Geophys. Res., V. 86, p. 2573-2592.

Brooks, H. C., and Vallier, T. L., 1978. Mesozoic rocks and tectonic evolution of eastern Oregon and western Idaho: In Howell, D. G. and McDougal, K. A. (eds), Pacific Section Soc. Econ. Paleont. and Mineral., Pacific Coast Paleogeog. Symp. 2, p. 133-145.

Cameron, E. N., 1969. Post cumulus changes in the eastern Bushveld complex. Am. Mineral., V. 54, p. 754-779.

Cameron, W. E., 1978. The lower zone of the eastern Bushveld complex in Olifant's River trough. Jour. Petrol., V. 19, p. 437-462.

Cameron, W. E., Nisbet, E. G., and Dietrich, V. J., 1979. Boninites, komatiites, and ophiolitic basalts. Nature, V. 280, p. 550-553.

Capedri, S. and Venturelli, G., 1979. Clinopyroxene compositions of ophiolitic metabasalts in the Mediterranean area. Earth and Planet. Sci. Lett., V. 43, p. 61-73.

Cassard, D., Nicholas, A., Rabinovitch, M., Moutte, J., LeBlanc, M., and Printzhofer, A. 1981. Structural classification of chromite pods in southern New Caledonia. Econ. Geol. V. 76, p. 805-831.

Church, W. R., and Ricco, L., 1977. Fractionation trends in the Bay of Islands ophiolite of Newfoundland: Polycyclic cumulate sequences in ophiolites and their classification. Can. Jour. Earth Sci., V. 14, p. 1156-1165.

Church, W. R., and Coish, R. A., 1976. Oceanic versus island arc origin of ophiolites. Earth Planet. Sci. Lett., V. 31, p. 8-14.

Clarke, S. P. Jr. 1966. Handbook of Physical Constants. Geol. Soc. Am. Memior 97. 587p.

Coleman, R. G., 1977. Ophiolites. Springer-Verlag, New York, 229 p.

_____, 1981. Tectonic setting for ophiolite obduction in Oman. J. Geophysical Res. V. 86, p. 2497-2508.

Corrigan, G. M., 1982. Cooling rate studies of rocks from two basic dykes. Mineral. Mag., V. 46, p. 387-394.

Den Tex, E., 1969. Origin of ultramafic rocks, their tectonic setting and history. Tectonophysics, V. 7, p. 457-488.

Dick, H.J.B. 1977. Partial melting in the Josephine peridotite, I. The effect on mineral composition and its consequences for geothermometry and geobarometry. Am. Jour. Sci., V. 277, p. 801-832.

Dickey, J. S., Jr., 1970. Partial fusion products in alpine-type peridotites: Serrania de la Ronda and other examples. Spec. Paper 3, Min. Soc. America, p. 33-49.

_____, 1975. A hypothesis of origin for podiform chromite deposits. Geochim. Cosmochim. Acta, V. 39, p. 1061-1074.

Dickinson, W. R., 1979. Mesozoic forearc basin in central Oregon. Geology, V. 7, p. 166-170.

Dostol, J. and Muecke, G. K., 1978. Trace element geochemistry of the peridotite-gabbro-basalt suite, from DSDP Leg 37. Earth Planet. Sci. Lett., V. 40, p. 415-422.

Dungan, M. A. and Ave Lallemant, H. G., 1977. Formation of small dunite bodies by metasomatic transformation of harzburgite in the Canyon Mountain ophiolite, northeast Oregon. In Dick, H.J.B., ed., Magma Genesis. Proceedings of the A.G.U. Chapman Conf. on Partial Melting in the Earth's Mantle. Ore. Dept. Geol. Mineral Ind. Bull. 96, p. 109-128.

Elthon, D., Casey, J. F., and Komor, S., 1982. Mineral chemistry of ultramafic cumulates from the North Arm massif of the Bay of Islands ophiolite: Evidence for high pressure fractionation of oceanic basalts. Jour. Geophys. Res., V. 87, p. 8717-8734.

Garcia, M. O., 1978. Criteria for identification of ancient volcanic arcs. Earth Sci. Rev., V. 14, p. 147-165.

Gerlach, D., 1980. Petrology and geochemistry of plagiogranite and related basic rocks of the Canyon Mountain ophiolite, Oregon. MS Thesis, unpub., Rice University. 198 p.

Gerlach, D. C., Ave Lallemant, H. G., and Leeman, W. P., 1981a. An island arc origin for the Canyon Mountain ophiolite complex, eastern Oregon, U.S.A. Earth Planet. Sci. Lett., V. 53, p. 255-265.

Gerlach, D. C., Leeman, W. P., and Ave Lallemant, H. G., 1981b. Petrology and geochemistry of plagiogranite in the Canyon Mountain ophiolite, Oregon. Contrib. Mineral. Petrol., V. 77, p. 82-92.

Greenbaum, D., 1977. The chromitiferous rocks of the Troodos ophiolite complex, Cyprus. Econ. Geol., V. 72, p. 1175-1194.

Gueguen, Yves, and Nicholas, Adolphe, 1980. Deformation of mantle rocks. Ann. Review Earth Planet. Sci., V. 8, p. 119-144.

Hanson, G. N., 1980. Rare earth elements in petrogenetic studies of igneous systems. Ann. Review Earth Planet. Sci., V. 8, p. 371-406.

Hawkins, J. W., and Evans, C. A. (in press). Geology of the Zambales Range, Luzon, Philippine Islands: Ophiolite derived from an island arc-back arc basin pair. In Hayes, ed., The tectonic and geologic evolution of southeast Asian Seas and islands: Part 2. Am. Geophys. Union Monograph 27.

Hellman, P. L., and Henderson, P., 1977. Are rare earth elements mobile during spilitization? Nature, V. 267, p. 38-40.

Himmelberg, G. H., and Loney, R. A., 1980. Petrology of ultramafic and gabbroic rocks of the Canyon Mountain ophiolite, Oregon. Am. Jour. Sci., V. 280A, p. 232-268.

Hopson, C. A., 1976. Sheeted sill complexes in ophiolites: Their occurrence, and tectonic significance. EOS, V. 57, p. 1026.

Hopson, C. A., and Frano, C. J., 1977. Igneous history of the Point Sal ophiolite, Southern California. In Coleman, R. G. and Irwin, W. P., eds. North American Ophiolites. Ore. Dept. Geol. Mineral Ind. Bull. 95, p. 161-183.

Irvine, T. N., 1965. Chromian spinel as a petrogenetic indicator, Part 1, theory. Can. Jour. Earth Sci., V. 2, p. 648-672.

_____, 1967. Chromian spinel as a petrogenetic indicator, Part 2, petrologic applications. Can. Jour. Earth Sci., V. 4, p. 71-103.

Irvine, T. N., 1980. Magmatic infiltration metasomatism, double-diffusive convection, fractional crystallization, and adcumulus growth in the Muskox intrusion and other layered intrustions. In Hargraves, ed. Physics of Magmatic Processes. Princeton Univ. Press, p. 325-384.

Jackson, E. D., 1969. Chemical variation in co-existing chromite and olivine in chromite zones of the Stillwater complex. In Wilson, H.B.D., ed., Magmatic Ore Deposits, Econ. Geology Monograph, p. 41-71.

Jackson, E. D., and Thayer, T. P., 1972. Some criteria for distinguishing between stratiform, concentric, and alpine peridotite-gabbro complexes. Int. Geol. Cong. 24th Series. Sect. 2, p. 289-296.

Jaeger, J. C., 1957. The temperature in the neighborhood of a cooling intrusive sheet. Am. Journ. Sci., V. 255, p. 306-318.

Jan, M. Q., and Howie, R. A., 1981. The mineralogy and geochemistry of metamorphosed basic and ultrabasic rocks of the Jijal complex, Kohistan, N.W. Pakistan. Jour. Petrol., V. 22, p. 85-126.

Jaques, A. L., 1981. Petrology and petrogenesis of cumulate peridotites and gabbro from the Marum ophiolite complex, northern Papua, New Guinea. Jour. Petrol., V. 22, p. 1-40.

Jaques, A.L., and Chappel, B. W., 1980. Petrology and trace element geochemistry of the Papuan ultramafic belt. Contrib. Mineral. Petrol., V. 75, p. 55-70.

Jorgenson, D. B., 1979. Textural banding in igneous rocks: An example from SW Oregon. Am. Mineral., V. 64, p. 527-530.

Karig, D., and Ranken, B. in press. Marine geology of the forearc region, southern Mariana Island Arc. In Hayes, Ed. The Tectonic and Geologic evolution of Southeast Asian Seas and Islands; 2. American Geophys. Union, Monograph 27.

Kay, R. W. and Senechal, R. G., 1976. The rare earth geochemistry of the Troodos ophiolitic complex. Jour. Geophys. Res., V. 81, p. 964-970.

Kushiro, I., 1969. The system forsterite-diopside-silica with and without water at high pressures. Am. Jour. Sci., V. 267A, p. 269-294.

Kushiro, I., and Yoder, H., 1969. Melting of forsterite and enstatite at high pressures under hydrous conditions. Carnegie Inst. Washington Yearb. 67, p. 153-158.

Lago, B. L., Rabinowicz, M. and Nicholas, A., 1982. Podiform chromite ore bodies: A genetic model. Jour. Petrol., V. 23, p. 103-125.

Malpas, J., 1978. Magma generation in the upper mantle: Field evidence from ophiolite suites and application to the generation of oceanic lithosphere. Philos. Trans. R. Soc. London, Ser. A., V. 288, p. 527-546.

Mathews, D. W., 1976. Post cumulus disruption of the Lilloise intrusive, East Greenland. Geol. Mag., V. 113, p. 287-296.

McBirney, A. R., and Noyes, R. M., 1979. Crystallization and layering in the Skaergaard Intrusion. J. Petrol., V. 20, p. 487-554.

Meijer, A., and Reagan, M., 1983. Origin of K_2O-SiO_2 trends in volcanoes of the Mariana arc. Geology, V. 11, p. 67-71.

Menzies, M. A., 1976. Rare earth element geochemistry of fused alpine and ophiolitic lherzolites: Constraints on basalt genesis. I: Orthis, Lanzo and Troodos. Geochim. Cosmochim. Acta., V. 40, p. 645-656.

Menzies, M. A., Blanchard, D., Brannon, J., and Korotev, R., 1977a. Rare earth and trace element geochemisty of a fragment of Jurassic seafloor, Point Sal, California. Geochim. Cosmochim. Acta., V. 41, p. 1419-1430.

Menzies, M. A., Blanchard, D., and Jacobs, J., 1977b. Rare earth and trace element geochemistry of metabasalts from the Point Sal ophiolite, California. Earth Planet. Sci. Lett., V. 37, p. 203-215.

Moore, A. C., 1973. Studies of igneous and tectonic textures and layering in rocks of the Gosse Pile Intrusion, central Australia. Jour. Petrol., V. 14, p. 49-79.

Moores, E. M., 1969. Petrology and structure of the Vourinous ophiolitic complex, northern Greece. Geol. Soc. America Spec. Paper 118, p. 1-74.

Morse, S. A., 1969. The Kiglapait layered intrusion, Labrador. Geol. Soc. America Memoir, V. 112. 204 p.

Moutte, Jacques, 1982. Chromite deposits of the Tiebaghi ultramafic massif, New Caledonia. Econ. Geol., V. 77, p. 576-591.

Mullen, E. D., 1979a. Alkalic pillowed greenstones, Greenhorn Mountains, Northeast Oregon. Geol. Soc. America, Abstr. W. programs, V. 11, p. 109.

_____, 1979b. Temperature-pressure progression in high-pressure Permo-Triassic metamorphic rocks of northeast Oregon. EOS, V. 51, p. 70.

_____, 1982. Permian and Triassic forearc terrane of the Blue Mountains, northeast Oregon. Geol. Soc. America Abstr. W. program, V. 14, p. 573.

_____, 1983. $MnO/TiO_2/P_2O_5$: A minor element discriminant for basaltic rocks of oceanic environments and its implications for petrogenesis. Earth Planet. Sci. Lett., V. 62, p. 53-62.

Nesbitt, E. G., and Pearce J., 1977. Clinopyroxene composition in mafic lavas from different tectonic settings. Contr. Mineral. Petrol., V. 63, p. 149-160.

Nicholas, A., Boudier, F., and Bouchez, J. L., 1980. Interpretation of peridotite structures from ophiolites and oceanic environments. Am. Jour. Sci., V. 280A, p. 192-210.

Nicholas, A., and Le Pichon, X., 1980. Plastic deformation in oceanic crust and upper mantle. Earth Planet. Sci. Lett., V. 46, p. 397-406.

Nicholas, A., and Jackson, M., 1982. High temperature dikes in peridotites: Origin by hydraulic fracturing. Jour. Petrol., V. 23, p. 568-582.

O'Hara, M. J., 1968. The bearing of phase equilibria studies on the origin and evolution of basic and ultrabasic rocks. Earth Sci. Rev., V. 4, p. 69-133.

_____, 1977. Geochemical evolution during fractional crystallization of a periodically refilled magma chamber. Nature, V. 266, p. 503-507.

Pallister, J., 1981. Structure of the sheeted dike complex of the Samail ophiolite near Imbra, Oman. Jour. Geophys. Res., V. 86, p. 2661-2672.

Pallister, J., and Hopson, C. A., 1981. Samail ophiolite plutonic suite: Field relations, phase variation, cryptic variation and layering, and a model of a spreading ridge magma chamber. Jour. Geophys. Res., V. 86, p. 2593-2644.

Pallister, J., and Knight, R. J., 1981. Rare earth element geochemistry of the Samail ophiolite near Imbra, Oman. Jour. Geophys. Res., V. 86, p. 2673-2697.

Pankhurst, R. J., 1977. Open system crystal fractionation of a periodically refilled magma chamber. Nature, V. 268, p. 36-38.

Pearce, T. H., Gorman, B. E., and Birkett, T. C., 1977. The relationship between major element chemistry and tectonic environment of basic and intermediate volcanic rocks. Earth Planet. Sci. Lett., V. 36, p. 121-132.

Presnell, D. C., and Helsley, C. E., 1982. Diapirism of depleted peridotite - a model for the origin of hotspots. Phys. Earth Planet. Inst., V. 29, p. 148-160.

Presnall, D.C., Dixon, S., Dixon, J., O'Donnell, T., Brenner, N., Schrock, R., and Dycus, D., 1978. Liquid phase relations on the join diopside-forsterite-anorthite from 1 atm. to 20 kbar: Their bearing on the generation and crystallization of basaltic magma. Contrib. Mineral. Petrol., V. 78, p. 203-220.

Quick, J. E., 1981. The origin and significance of large, tabular dunite bodies in the Trinity Peridotite, northern California. Contrib. Mineral. Petrol., V. 78, p. 413-422.

Schnetzler, C. C., and Phillpots, T. A., 1970. Partition coefficients of rare-earth elements between igneous matrix material and rock-forming mineral phenocrysts. Geochim. Cosmochim. Acta., V. 34, p. 331-338.

Simpkin, T., and Smith, J. V., 1970. Minor element distribution in olivine. Jour. Geology, V. 78, p. 304-325.

Smewing, J. D., 1981. Mixing characteristics and compositional differences in mantle-derived melts beneath spreading ridges: Evidence from cyclically layered rocks in the ophiolite of North Oman. Jour. Geophys. Res., V. 86, p. 2645-2660.

Smewing, J. D., and Potts, P. W., 1976. Rare earth abundances in basalts and metabasalts from the Troodos massif, Cyprus. Cont. Mineral. Petrol., V. 57, p. 245-258.

Steinman, G., 1927. Die ophiolithischen Zonen in dem Mediterranen kettengebirge. 14th Int. Geol. Cong. Madrid., V. 2, p. 638-667.

Stern, C., 1979. Open and closed system igneous fractionation within two Chilean ophiolites and the tectonic implication. Contrib. Mineral. Petrol., V. 68, p. 243-258.

Strong, D. F., and Malpas, J., 1975. The sheeted dike layer of the Betts Cove ophiolite complex does not represent spreading: Further discussions. Can. Jour. Earth Sci., V. 12, p. 894-896.

Suen, C. J., Frey, F. A., and Malpas, J., 1979. Bay of Islands ophiolite suite, Newfoundland: Petrologic and geochemical characteristics with emphasis on rare earth element geochemistry. Earth Planet. Sci. Lett., V. 45, p. 337-348.

Sun, S-S., and Nesbitt, R. W., 1978. Geochemical regularities and genetic significance of ophiolitic basalts. Geology, V. 6, p. 689-693.

Thayer, T. P., 1940. Chromite deposits of Grant County, Oregon: A preliminary report. U. S. Geol. Survey Bull. 922D. 113 p.

_____, 1963a. Flow layering in alpine peridotite-gabbro complexes. Mineral. Soc. America Spec. Paper 1, p. 55-61.

_____, 1963b. The Canyon Mountain complex, Oregon, and the alpine mafic magma stem. U. S. Geol. Survey, Prof. Paper 475C, article 81, p. C82-C85.

_____, 1964. Principal features and origin of podiform chromite deposits, and some observations on the Guleman-Soridağ district, Turkey. Econ. Geol., V. 59, p. 1497-1524.

_____, 1969. Gravity differentiation and magmatic reemplacement of podiform chrome deposits. Econ. Geol. Monograph 4, p. 132-146.

_____, 1970. Chromite segregations as petrogenetic indicators. In Visser, D.J.L. and Von Gruenewald, G., ed. Symposium on the Bushveld igneous complex, and other layered intrustions. Geol. Soc. South Africa Spec. Pub. 1, p. 380-390.

_____, 1972. Gabbro and epidiorite versus granulite and amphibolite: A problem in the ophiolite assemblage. VI. Conferencia Geologica del Caribe, Margarita, Venezuela, p. 315-320.

_____, 1976. Metallogenic contrasts in the plutonic and volcanic rocks of the ophiolite assemblage. Geol. Assoc. Canada Spec. Paper No. 14, p. 211-219.

_____, 1977. The Canyon Mountain complex, Oregon and some problems of ophiolites. In Coleman, R. G. and Irwin, W. P., eds. North American Ophiolites. Oregon Dept. Geol. Mineral. Ind. Bull. 95, p. 93-105.

Thayer, T. P., and Brown, C. E., 1968. Geologic map of the Aldrich Mountain Quadrangle, Grant Co. Oregon, U. S. Geol. Survey Quadrangle Map, GQ 438.

Thayer, T. P., and Himmelberg, G. R., 1968. Rock succession in the alpine-type mafic complex of Canyon Mountain, Oregon. 23rd Int. Geol. Cong., Vol. 1, p. 175 186.

Thy, P., and Esbensen, K. H., 1982. Origin of fine-grained granular rocks in layered intrusions. Geol. Mag., V. 119, p. 405-412.

Tiezzi, L. J., and Scott, R. B., 1980. Crystal fractionation in a cumulate gabbro, mid-Atlantic ridge, 26°N. Jour. Geophys. Res., V. 85, p. 5454-5488.

Ulmer, G. C., 1969. Experimental investigations of chrome spinels. Econ. Geol. Monograph 4, p. 114-131.

Vernon, R. H., 1970. Comparative grain-boundary studies of some basic and ultra-basic granulites. Scot. Jour. Geol., V. 6, p. 337-351.

Waff, H., and Holdren, G. R., Jr., 1981. The nature of grain boundaries in dunite and lherzolite xenoliths: Implications for magma transport in refractory upper mantle material. Jour. Geophys. Res., V. 86, p. 3677-3683.

Wager, L. R., and Brown, G. M., 1966. Layered Igneous Rocks. Freeman, N.Y., 588 p.

Wager, L. R., Brown, G. M., and Wadsworth, W. J., 1960. Types of igneous cumualtes. Jour. Petrol., V. 1, p. 73-85.

Wood, D. A., Joron, J. L., and Treuil, M., 1979. A re-appraisal of the usage of trace elements to classify and discriminate between magma series erupted in different tectonic settings. Earth Planet. Sci. Lett., V. 45, p. 326-336.

Wyllie, P. J., 1979. Magmas and volatile components. Am. Mineral. V. 64, p. 469-500.

Yoder, H. S., 1976. Generation of basaltic magma. U. S. National Acad. Sci., Washington, 265 pp.

Yoder, H.S. and Tilley, C.E., 1962. Origin of basalt magmas: an experimental study of natural and synthetic rock systems. J. Petrol., V. 3, p.342-532.

APPENDIX 1
DEFINITION OF "OPHIOLITE" BY THE 1972 PENROSE CONFERENCE PARTICIPANTS (GEOTIMES, V.17, p. 25)

"Ophiolite", as used by those present at the GSA Penrose Conference on ophiolites, refers to a distinctive assemblage of mafic to ultramafic rocks. It should not be used as a rock name or as a lithologic unit in mapping. In a completely developed ophiolite the rock types occur in the following sequence, starting from the bottom and working up:

1) Ultramafic complex, consisting of variable proportions of harzburgite, lherzolite, and dunite, usually with a metamorphic tectonic fabric (more or less serpentinized).
2) Gabbroic complex, ordinarily with cumulus textures commonly containing cumulus peridotites and pyroxenites, and usually less deformed than the ultramafic complex.
3) Mafic sheeted dike complex.
4) Mafic volcanic complex, commonly pillowed.

Associated rock types include 1) an overlying sedimentary section typically including ribbon cherts, thin shale interbeds, and minor limestones; 2) podiform bodies of chromite generally associated with dunite; 3) sodic felsic intrusive and extrusive rocks.

Faulted contacts between mappable units are common. Whole sections may be missing. An ophiolite may be incomplete, dismembered, or metamorphosed, in which case it should be called a partial, dismembered, or metamorphosed ophiolite. Although ophiolite generally is interpreted to be oceanic crust and upper mantle, the use of the term should be independent of its supposed origin.

APPENDIX 2: FIELD METHODS AND THE SETTING OF THE CANYON MOUNTAIN COMPLEX

Field Methods

Twenty-one weeks were devoted to field work on the Canyon Mountain complex during the summers of 1980 and 1981. Mapping and field studies concentrated on gabbro and peridotite north of the Strawberry Range summit. Petrologic field work by the writer was conducted concurrently with structural mapping by Boudier and Misseri during three weeks in 1980, and also three weeks in 1981. Petrologic mapping was recorded on a base map at 1:12,000 scale for most of the complex (Plate 2) and 1:6000 scale for Celebration Ridge (Plate 3), Norton basin (Plate 4) and Canyon Mountain (Plate 5). The elevation of all map locations was established on the basis of aneroid altimeter readings to within at least ± 30 feet. Pace and compass methods were used on large scale maps where precision in location was desirable.

Samples discussed in detail and/or analyzed are a small but representative selection of the 650 specimens collected. Analyzed rocks (see Plate 2 for locations) were chosen principally from the east half of the mapped area where exposure is better and the infiltration zone, transition zone, recrystallized zone, and gabbro are all better defined and more extensive. Three hundred and twenty six thin sections of Canyon Mountain complex rocks were examined in order to define the lithologic units shown on Plates 1 and 2. In addition, sixty thin sections of greenstones and

gabbros of the forearc terrane were studied in order to choose the best possible specimens for microprobe and whole-rock analyses.

Setting of the Canyon Mountain Complex

The Canyon Mountain complex comprises the western third of the southernmost range in the Blue Mountain geomorphic province. The CMC has an areal extent of approximately 150 square kilometers, and is mostly included in the Malheur National Forest. A narrow, two-to-five kilometer wide strip along the ridge-crest is presently incorporated in the Strawberry Wilderness Area.

The Canyon Mountain complex "massif" rises southward within a horizontal distance of 4-6 kilometers from the serpentinized harzburgite at 4000 feet elevation along the John Day Fault to the east-west trending ridge crest at 7400 to 8010 feet elevation. The maximum total relief of the area studied is about 4,000 feet.

Harzburgite is exposed in the north of the complex on north-south ridges with somewhat muted relief. Juniper, lodgepole, and some yellow pine persist to elevations of approximately 6100 feet on these broad ridges. Above 6500 feet, most notably on Baldy Mountain, trees are absent on harzburgite.

Gabbroic rocks, both of transition zone in the east, and the CMC gabbro in the west commence at elevations of about 6000 feet on the main ridge. Below 7000 feet, some slopes on gabbro or gabbro regolith, are heavily forested. Especially noteworthy are strands of yellow pine, and mixed spruce, fir, and tamarack along Norton

Creek from 5200 to 6100 feet, and dense fir and lodgepole pine along upper Dog Creek. Yew groves persist to 6500 feet in upper Norton Creek.

The higher portions of north-south ridges, the north face of the main ridge crest, and the north face of Baldy Mountain have been glaciated. Well polished, steep, unvegetated slopes with excellent exposure of gabbro occur within the Dog Creek cirque in the central part of the area, in Norton basin, and in similar, but less well developed basins at the head of Pine Creek. The ridge crest, and rocks to elevations as low as approximately 6000 feet on the south and west sides of the Canyon Mountain complex offer excellent exposures. White bark pine, limber pine, and several severely stunted yellow pine grow along the barren ridge crest. The most prolific form of vegetation associated with the gabbro, however, is lichen, which grows in profusion over many large, smooth, outcrops at all elevations.

APPENDIX 3. ANALYTICAL METHODS

The samples summarized in Appendix 4 were analyzed by a variety of techniques which are described below.

Petrography

Thin sections of 326 Canyon Mountain complex samples were examined. Modal analyses tabulated in the text were made by counting 1500 to 2000 points on a mechanical stage using a Leitz monocular student model petrographic microscope. Samples mentioned in the text, but not tabulated were checked with a 500 point count.

Mineral 2V was estimated by examination of optic axis and Bxa figures. Plagioclase compositions, except where specified as microprobe analyses, were determined by the Michele-Levy method.

X-ray Fluorescence - Major Oxides

Major oxide analyses were done by Dr. Peter Hooper at Washington State University. Samples were broken by hammer and crushed into small chips in an aluminum plated jaw crusher. Approximately 30 gms of chips were hand picked, to avoid weathered surfaces and possible small slivers of steel or aluminum, and placed in a swing-mill (shatter box) where they were ground for six minutes. This provided a fine, even grained powder which is an essential prerequisite to the production of homogeneous samples. A normal ballmill was inadequate for this purpose

Seven grams of lithium tetraborate ($Li_2B_4O_7$) and 3.5 grams of the rock powder were thoroughly mixed in a plastic jar on a spex

ball-mill and then fused in graphite crucibles for five minutes at 1000°C. When cooled, the Li-tetraborate beads dropped out of their crucibles and their lower surfaces were ground with fine silicon carbide powder. The samples were analyzed after rinsing.

The flat surface of the bead was irradiated in a Philips P.W. 1410 manual spectrometer with a chromium target tube. The recorded count rate for each element was related to the calibration curve derived from the count rate of eight analyzed basalts supplied by T. L. Wright and D. A. Swanson of the U. S. Geological Survey. The raw oxide values are corrected for absorption and normalized on a volatile free basis with Fe_2O_3 assumed to be 2.00 percent.

PRECISION AND ACCURACY OF THE ANALYSES

Many factors influence the reliability and overall accuracy of the oxide values obtained. Of these, the most important are:

1. Instrumental Precision. By this is meant the ability to repeat the same count rate from the machine every time the same Li-tetraborate bead is measured.
2. Total Precision. This term includes both instrumental precision and the homogeneity of the Li-tetraborate beads. It is best tested by making many beads from the same rock sample and measuring the variations between the beads for each oxide.
3. Bias. This is the difference between two sets of analyses run at different times and is due to

differences in the measured calibration curve. It has only been found significant when different standard samples are used in calibration. All analyses in this report used the same eight standard beads.

4. Sample Inhomogeneity. The size of the sample crushed for analysis (20 grams) is large enough to give a statistically homogeneous sample of fine, even grained rocks. It is inadequate, however, to provide a homogeneous sample of the coarsely porphyritic flows where the proportion of large plagioclase phenocrysts clearly varies from one part of the flow to another and from one sample to another.
5. Haphazard Errors. Under this heading are included small instrumental malfunctions which can occur without detection on rare occasions and simple human errors. Normally extraordinary values or poor totals allow such errors to be detected.

The importance of these potential sources of error can be estimated with decreasing accuracy from 1 to 5.

Instrumental precision was routinely recorded by repeat measurement of a single bead every tenth sample or so throughout an analytical run.

Despite the satisfactory precision revealed in these tests, a small minority of analyses resulted in poor totals between 95 and 102 prior to normalization. Rare totals outside these limits were discarded. The poor totals may imply errors not recorded in the precision tests; they are most prevalent in the feldsparphyric samples and can be shown to be related to the grain size of the powdered rock before fusion. Coarser than normal powders gave higher than normal totals. Some settling of rock powder may occur during the fusion process.

Nevertheless, a small error remains. Two beads made from the same rock sample, one with a pre-normalization total of 95 and another with a pre-normalization total of 102, do not normalize to quite the same values. The bead with the higher pre-normalization total will, after normalization, show marginally higher SiO_2 and Al_2O_3 values than the other bead. The other oxides are the reverse of this. The difference is very consistent and a "summation correction" has been made on the computer to account for it. The reason for this small discrepancy may be that plagioclase feldspar is taken into solution by the Li-tetraborate flux a little more slowly than the other components in the rock powder and hence settles a little more towards the bottom during the fusion process. This would be exaggerated as the grain size of the powder increased.

INAA - Trace Elements

Instrumental neutron activation analysis (INAA) was utilized for trace element determination. Ten to twenty gram rock samples were chipped from specimens, washed in dilute HCl, crushed, homogenized, ground, and re-homogenized in ceramic grinders. Approximately 0.3 grams of resulting powder was obtained as a split from the homogenized sample, placed into small polyvials, sealed, placed into larger 2 dram polyvials, and irradiated for 6 hours at 1 MW in the rotating rack of the Oregon State University Radiation Center TRIGA reactor.

Samples were counted 6-12 days after irradiation, for 10,000 seconds each on an ND 2200 Ge-Li detector. Standards used were CRB - a Columbia River Basalt used as an "in house" standard, from the same location as U.S.G.S. BCR, and U.S.G.S. standard PCC1. Accuracies were checked by replicate analyses of unknowns, by analyses of standard as unknown, and by multiple counts of the same sample. Elements determined in first count were: Na, K, La, Nd, Sm, Eu, Yb, and Lu. For some samples Ce was determined from first count data. Most samples were counted for a second, longer time, 40-47 days after activation to determine longer-lived nucleides. Counts were for 20,000 to 40,000 seconds, and determined Hf, Ta, Th, Co, Ni, Cr, Rb, Sr, Ce, and Tb. Analytical precision for rare earth elements (La-Lu) was within ± 10% for most samples, with largest errors for Ce, Nd, and Tb, and greatest precision for La and Sm.

Sr and Rb determinations contain errors of up to 75%. Co, Cr, and Ni similarly contain possible large errors of up to 40%. Values for Na_2O, K_2O, and FeO* determined by INAA agreed within 0.5 percent with values determined by XRF. Hf, Ta, Th values for greenstones contain possible errors of up to 30 percent.

Mineral Analyses: Electron Microprobe

Mineral compositions for eight to ten major and minor oxides were determined with the Applied Research Laboratory (ARL) electron microprobe at the University of Oregon. Samples to be analyzed were mounted on 1-inch round glass slides and polished to a smooth surface. Prepared slides were carbon-coated with a 30-35 nm film by evaporation of two carbon rods at 50 Δmp current under high vacuum conditions.

Oxide standards were run on minerals or glasses of known composition. Wavelength dispersive analyses were conducted for all microprobe data presented in this dissertation. The instrument was operated at 15 kV, 50 ma, with sample current of 0.05 μA. Spot size was approximately 10 μ for all analyses. Data were analyzed by an on-line microcomputer which corrected results by the Bence-Albe method, and presented weight percentage and cation percent for each analysis.

APPENDIX 4. SUMMARY OF ANALYZED SAMPLES

Type of data presented for each sample given by:

(P): Modal analysis, point count of 2,000 points.

(M): Major element whole rock via XRF-WDS.

(T): Trace element, whole rock via INAA.

(E): Electron microprobe, WDS of selected minerals.

Minerals listed in order of abundance, and abbreviated as:

ol	olivine	hb	primary amphibole
opx	orthopyroxene	am	secondary amphibole
cpx	clinopyroxene	sp	lizardite, chrysotile
pl	plagioclase	mt	magnetite
ch	chrome spinel	s	sulfide
ap	apatite	hg	hydrogrossular

CANYON MOUNTAIN COMPLEX

Note: Section number followed by W denotes T.14S; R.32E; section number followed by E denotes T.14S, R.33E.

USGS 7 1/2' quadrangle sheet designated as follows:

JD = John Day, CM = Canyon Mountain, CC = Castle Creek, PCM = Pine Creek Mountain.

74. Podiform chromitite, Haggard and New Mine. El. 5350, NW 1/4, NE 1/4, sec. 16W, CM Cumulate. ol, ch. (E)

82. Podiform chromitite, Ward Mine (CMCW). El. 4500, NW 1/2, SE 1/2, sec. 5 W, J.D. Cumulate. ol, ch, sp. (P)

90. Podiform chromitite, Chambers mine. El. 6570, SE 1/4, SE 1/4, sec. 13W., PCM Cumulate. ol, ch, cpx, opx.

95. Table Camp gabbro. NE of Table Camp. El. 7180, NE 1/4, NE 1/4, sec. 30 E. PCM Deformed cumulate. Pl, cpx, opx, ol, hb, ap. (T)

110G. Gabbro dike in harzburgite. El. 5300, NE 1/4, SE 1/4, sec. 12 W. PCM Adcumulate? Pl, hg, cpx, am. (P) (T)

110P. Tectonite harzburgite, dike host rock, Zone B. El. 5300, NE 1/4, SE 1/4, sec. 12 W. PCM sp, opx, ol, (hg?) (P) (T)

149. Podiform chromitite, lower pit, Ray Mine. El. 7230, NE 1/4, NE 1/4, sec. 20 E. PCM Cumulate. ch, opx, cpx, ol, sp. (E)

169. Podiform chromitite, upper pit, Ray Mine. El. 7265, NE 1/4, NE 1/4, sec. 20 E. PCM Cumulate. ch, opx, cpx, sp. (E)

218. Feldspathic lherzolite, zone A. W. side of Pine Creek. El. 5250. NW 1/4, SW 1/4, sec. 14 W. PCM Tectonite. ol, opx, sp, cpx, hg, pl (M)

284. Lherzolite. East border, zone A, east side, Little Indian Creek. El. 5650. NE 1/4, SE 1/4, sec. 17 E. PCM Tectonite. ol, opx, cpx. (P) (M) (T)

285C. Layered gabbro, from broad apophysis into harzburgite, SW side Baldy Mountain. Sample from more leucocritic band. El 6000. NW 1/4, NW 1/4, sec. 24 W. PCM Adcumulate, pl, cpx, hg, opx, am. (M) (T)

286. Podiform chromitite, Bald Eagle mine, SW side, Baldy Mountain. El. 6030. NW 1/4, NW 1/4, sec. 24 W. PCM Cumulate. ch, sp, cpx. E

296. Feldspathic harzburgite. Zone C. E. side Pine Creek. El. 5190. SE 1/4, SW 1/4, sec. 12 W. PCM Tectonite. ol, opx, sp, am, hg, pl. (P) (M) (T)

335. Pine Creek Mountain gabbro. Upper gabbro. El. 7340. SE 1/4, NE 1/4, sec. 31 E. PCM Cumulate. pl, opx, cpx, ap, s. (P) (T)

410. Podiform chromitite, Haggard and New Mine, upper pit. El 5420. NW 1/4, NE 1/4, sec. 16 W. PCM Cumulate. ch, sp, ol. (E)

449B. Tectonite harzburgite, vein host rock, zone A, east side Pine Creek. El. 4880. NE 1/4, NE 1/4, sec. 14 W. PCM sp, ol, opx. (P) (M) (T)

522. Pine Creek Mountain gabbro, W. side Pine Creek. El. 5400. NW 1/4, NE 1/4, sec. 23 W. PCM. Deformed cumulate. pl, cpx, opx, ol, hb, hg, am. (M)

531. Gabbro dike 35 cm wide S. side Baldy Mountain. El. 6500. SE 1/4, SW 1/4, sec. 19 E. PCM. Adcumulate, with flow banding. pl, cpx, hg, opx. (P) (T)

539. Table camp gabbro. South side, Baldy Mountain. El. 7150. NE 1/4, NE 1/4, sec. 30 E. PCM Deformed adcumulate. pl, cpx, opx, ol, hb, hg, am, mt, s. (P) (M) (T)

540. Table Camp gabbro. South side, Baldy Mountain. El. 7040. NE 1/4, NE 1/4, sec. 30 E. PCM Deformed adcumulate. pl, cpx, opx, ol, hb, hg, am, mt. (P) (M) (T)

563. Dunite. N. end Celebration Ridge. El. 6750. NW 1/4, NW 1/4, sec. 30 E. PCM Tectonite-cumulate. sp, ol, ch. (P) (M)

564. Olivine-clinopyroxenite. N. end, Celebration Ridge. El. 6800. NW 1/4, NW 1/4, sec. 30 E. PCM Tectonite cumulate. cpx, ol, opx, sp. (P) (M)

565. Gabbro layer. N. end, Celebration Ridge. El. 6800. NW 1/4, NW 1/4, sec. 30 E. PCM Tectonite cumulate. cpx, ol, opx, sp. (P) (M)

566. Wehrlite. From banded outcrop. N. end Celebration Ridge. El. 6790. SW 1/4, NW 1/4, sec. 30 E. PCM Tectonite to tectonite-cumulate. cpx, ol, opx, sp, am, mt. (P) (M)

567. Gabbro, central Celebration Ridge. El. 6850. Faintly layered. SW 1/4, NW 1/4, sec. 30 E. PCM Cumulate. pl, cpx, hg, am, mt, ap. (P) (M)

569. Gabbro, central Celebration Ridge. El. 6800. Coarse to fine grained, faintly layered. SW 1/4, NW 1/4, sec. 30 E. PCM Cumulate. pl, cpx, hg, am. (P) (M) (T)

574. Gabbro, basin west of Celebration Ridge. El. 7000. SW 1/4, SW 1/4, sec. 30 E. pl, opx, cpx, am. (M) (T)

578A. Gabbro, upper Celebration Ridge. El. 7680. NW 1/4, NW 1/4, sec. 31 E. PCM pl, opx, cpx, am, mt, s. (M)

579A. Olivine websterite, upper Celebration Ridge. El. 7780. NW 1/4, NW 1/4, sec. 31 E. PCM Cumulate. cpx, ol, opx, hb, sp, am. (P) (E)

579B. Melagabbro, upper Celebration Ridge. El. 7780. NW 1/4, NW 1/4, sec. 31 E. PCM Cumulate. pl, opx, cpx, ol, hb, am, sp, s. (P) (E)

579C. Melagabbro, upper Celebration Ridge. El. 7780. NW 1/4, NW 1/4, sec. 31 E. PCM Cumulate. pl, opx, cpx, ol, hb, sp. (P) (E)

579D. Olivine websterite, upper Celebration Ridge. El. 7780. NW 1/4, NW 1/4, sec. 31 E. PCM Cumulate. cpx, ol, opx, hb, sp, am. (P) (E)

581A. Olivine websterite, upper Celebration Ridge. El. 7230. SE 1/4, SW 1/4, sec. 30 E. PCM Tectonite-cumulate. sp, cpx, ol. (M)

612. Feldspathic harzburgite, E. side, Pine Creek. El. 4300. NW 1/4, SE 1/4, sec. 1 W. CC Tectonite. sp, ol, hg, pl, am. (M)

626. Bear Skull Rim gabbro, faintly layered, W. side Pine Creek. El. 6450. NE 1/4, NE 1/4, sec. 23 W. PCM Cumulate. pl, cpx, am, mt. (P) (M) (T)

629. Bear Skull Rim gabbro, E. side Pine Creek. El. 5580. SE 1/4, SE 1/4, sec. 14 E. PCM Cumulate. pl, cpx, hg, am, mt. (P) (M) (T)

664. Websterite, Gwynn Gulch. El. 4570. W. side Gwynn Creek. SW 1/4, NW 1/4, sec. 7 E. PCM Cumulate. cpx, opx, ol, am, mt. (P) (M) (T)

665. Gwynn Gulch gabbro. El. 4530. W. bank Gwynn Creek. SW 1/4, NW 1/4, sec. 7 E. PCM Adcumulate. pl, cpx, hg, opx, am, ol. (P) (M) (T)

666. Gwynn Gulch gabbro. El. 4520. W. bank Gwynn Creek. SW 1/4, NW 1/4, sec. 7 E. PCM Adcumulate. pl, cpx, opx, ol, am. (P) (M) (T)

707. Pine Creek Mountain gabbro, Summit, Pine Creek Mountain. El. 7910. SE 1/4, NE 1/4, sec. 36 E. PCM Heteradcumulate. pl, opx, cpx, am, hg, s. (P) (M) (T)

708. Pine Creek Mountain gabbro. El. 7620. SE 1/4, NE 1/4, sec. 36 E. PCM Heteradcumulate. pl, opx, cpx, am, hg, x. (P) (M) (T)

713. Recrystallized poikiloblastic gabbro, Norton Basin. El. 7400. PCM SW 1/4, NE 1/4, sec. 27 W. pl, am, cpx, hg, opx, s. (P) (T)

714. Recrystallized norite, upper level Pine Creek Mountain gabbro. PCM El. 7020. SW 1/4, NW 1/4, sec. 32 E. pl, opx, am, cpx, s. (P) (T)

721. Norite, Yellow Jacket Ridge. El. 7220. SW 1/4, NW 1/4, sec. 26 W. PCM pl, opx, cpx, am. (P) (T)

GREENSTONE AND DISMEMBERED OPHIOLITE

BR-49. Basaltic greenstone, Burnt River Schist, head of White Rock Gulch quadrangle. El. 5440', SE 1/4 sec. 15, T. 12S; R. 41 E. French Gulch 7 1/2'. Relict cpx phenocrysts in sheared, intergranular matrix. Pl, chlorite, cpx, pumpellyite. (M)

BR-52. Basaltic greenstone, Burnt River Schist. El. 5450', 1/2 mile W. lf #49. SW 1/4 sec. 15, T. 12S; R. 41 E. French Gulch 7 1/2 ' quadrangle. Relict cpx phenocrysts in sheared, subophitic to intergranular groundmass. Pl, chlorite, cpx. (M) (E)

BR-59. Basaltic greenstone, Burnt River Schist. El. 4900,' 1/2 mile W. #52. NE 1/4 sec. 21, T. 12 S; R. 41 E. French Gulch 7 1/2' quadrangle. Intergranular. Pl, chlorite, cpx. (M)

BR-61. Basaltic greenstone, Burnt River Schist. El. 4820, 1.3 miles SW #59. SW 1/4 sec. 21 T. 12 S; R. 41 E. French Gulch 7 1/2' quadrangle. Intergranular, with relict cpx phenocrysts. Pl, cpx, chlorite. (E)

BRS-3. Pillowed basaltic greenstone intercalated with Elkhorn Ridge Argillite. Near Sturgill, W. side, Snake River, on Richland-Snake River road. El. 2400'. NW 1/4, sec. 5, T. 15 N., R. 6 W. Mineral 15' quadrangle. Ophitic texture; titanaugite. Pl, cpx , chlorite. (M) (E)

DXB-17. Porphyritic, andesitic greenstone, W. side Dixie Butte. El. 6000', NW 1/4 sec. 8, T. 11 S; R. 34 E. Bates 15' quadrangle. Trachytic. Pl, chl. (M) (E)

DXB-19. Andesitic greenstone, W. side Dixie Butte. El. 5760. NW 1/4 sec. 7, T. 11 S; R. 34 E. Faintly trachytic. Bates 15' quadrangle. Chl, pl. (M)

DXB-20. Andesitic greenstone, W. side Dixie Butte. El. 4680. NW 1/4, sec. 12, T. 11 S; R. 34 E. Bates 15' quadrangle. Trachytic. Chl, pl. (M)

M80b. Layered ultramafic. Irish Gulch, Greenhorn Mountains. El. 6150. SW 1/4 sec. 3, T. 10 S; R. 35 E. Greenhorn 7 1/2' quadrangle. Cumulate. Sp, cpx , ol, hg. (E)

M42. Cumulate gabbro, Ben Harrison Peak, Greenhorn Mountains. El. 7540, SE 1/4 sec. 34, T. 10 S; R. 34 E. Bates 15'. Cumulate. cpx, pl, hg, chlorite. (M) (E)

M46. Cumulate gabbro, near Olive Lake, Greenhorn Mountains. El. 7050, SE 1/4 sec. 27, T. 10 S; R. 34 E. Desolation Butte 15' quadrangle. Cumulate. cpx, pl, hg, chlorite. (M) (E)

M91. Serpentinized tectonite harzburgite fragment, Ben Harrison peak, Greenhorn Mountains. El. 7400, SE 1/4 sec. 34, T. 10 S; R. 34 E. Bates 15' quadrangle. sp, cpx, ol, am. (E)

M242. Cumulate gabbro, head of Granite Boulder Creek, Greenhorn Mountains. El. 5620, NW 1/4 sec. 18, T. 10 S; R. 34 E. Bates 15' quadrangle. Pl, chlorite, cpx. (E)

MV-47, MV-48, and MV-48A. Pillowed basaltic greenstone, from serpentinite matrix melange, 2.9 miles N. of Mount Vernon, Oregon. Mount Vernon 7 1/2' quadrangle. El. 3400. NW 1/4, sec. 13, T. 13 S; R. 30 E. Intergranular relict clinopyroxene. cpx, chlorite, plagioclase. (M) (T) (E)

NF-64. Andesitic greenstone, North Fork of the John Day River. Sec. 12, T. 8 S; R. 34 E. Desolation Butte 15' quadrangle. El. 4800. N. side, John Day River. Chlorite, pl. (M)

NF-65. Basaltic greenstone, North Fork, John Day River. Sec. 14, T. 8 S; R. 34 E. Desolation Butte 15' quadrangle. El. 4950, N. side, John Day River. Chlorite, pl, s. (M)

PH-76. "Pillowed"(?) basaltic greenstone, from serpentinite matrix melange, 3.5 miles south of Mount Vernon, Oregon, near Pleasant Hill townsite, Aldrich Mountain Road. chlorite, alb, cpx?? (M)

PR-82. "pillowed" basaltic greenstone, Phillips Reservoir, near Sumpter, Oregon.

V-27, V-27A. Pillowed basaltic greenstone, E. side, Olive Creek, Greenhorn Mountains. El. 5420. SW 1/4, NW 1/4, sec. 2, T. 10 S; R. 35 E. Greenhorn 7 1/2' quadrangle, Titan-augite, plagioclase, chlorite. (M) (T) (E)

V-252. Basaltic greenstone, head of Snow Creek, Greenhorn Mountains. El. 6260, NW 1/4, sec. 16, T. 10 S; R. 35 E., Greenhorn 7 1/2' quadrangle. Chlorite, pl, cpx. (M) (T) (E)